Investigation into the early steps of the *Daphniphyllum* alkaloid biosynthetic pathway

Barbara Anna Radzikowska

Doctor of Philosophy

University of York

Biology

September 2024

Abstract

Plants produce a range of secondary metabolites which give them an evolutionary advantage, for example by providing defence against herbivores. *Daphniphyllum* alkaloids are a class of complex bioactive secondary metabolites found in *Daphniphyllum* sp. which have been used in traditional Chinese Medicine, but knowledge about bioactivities of *Daphniphyllum* alkaloids is limited due their scarcity and challenge of isolation. Their biosynthetic pathway is hypothesised to start with squalene, which is sequentially oxidised to squalene-27,28-diol and squalene-27,28-dial, followed by the introduction of a nitrogen atom, which initiates a cyclisation reaction and formation of a scaffold.

In chapter 2, we synthesised squalene-27,28-diol over eight steps with an overall yield of 2%. This represents the first synthesis of this hypothesised precursor. In chapter 3, we aimed to characterise a range of *Daphniphyllum* alkaloids isolated from *D. macropodum*. We successfully isolated and characterised eight known *Daphniphyllum* alkaloids and one not previously reported alkaloid – 7-hydroxydaphnilongeranin D.

In chapter 4, we investigated the role of squalene and squalene-27,28-diol in the early steps of the biosynthesis in tissue extracts. The results supported role of squalene as a precursor. However, we were not able to identify accumulation of non-alkaloid modified squalene intermediates, nor did feeding of squalene-27,28-diol show significant impact on alkaloid content. This indicates that squalene-27,28-diol might not be a direct precursor. In chapter 5, we studied the origin of nitrogen in *Daphniphyllum* alkaloids and detected non-specific labelling of alkaloids when ^{15}N amino acids were fed to the hydroponic seedlings. This is the first demonstration of ^{15}N incorporation into *Daphniphyllum* alkaloids, however, the origin of nitrogen in the scaffold remains unclear.

Overall, this work resulted in the successful synthesis of the hypothesised precursor, isolation of several *Daphniphyllum* alkaloids from multiple skeletal families, and an increased understanding of the early steps of the biosynthetic pathway.

Declaration

I declare that this thesis is a presentation of original work and represents my own work, unless otherwise stated. This work has not previously been presented for a degree or other qualification at this University or elsewhere. All sources are acknowledged as references.

All research carried out within this thesis was completed by the author except for the work listed below:

- *Daphniphyllum* plants were looked after in collaboration with the University of York Horticulture Team and Dr Danielle Taylor
- HPLC purification of *Daphniphyllum* alkaloids (**3.1** and **3.4**) was carried out in collaboration with Dr Swen Langer
- The initial data processing and peak picking of ^{15}N-labelled features in the Orbitrap LC-MS analysis presented in chapter 5 was carried out by Dr Tony Larson

Acknowledgments

Firstly, I would like to thank both my supervisors Benjy Lichman and Will Unsworth for the opportunity to work on this fascinating project, the support and encouragements. And to the BBSRC White Rose DTP studentship for funding this project.

I also need to thank the technical staff at University of York, Heather Fish and Matt Davy at the NMR Centre, Lee Duff for keeping things running smoothly in D block, Swen Langer and Martina Conti at the Technology Facility for all the help and advice with Orbitraps. Special thanks to Tony Larson for all the support with data analysis. I would like to thank Yorkshire Arboretum and Castle Howard for access to *Daphniphyllum* plants and University of York Horticulture Department for taking such a good care of them and keeping them alive.

To all the members of the WPU and POB groups, both past and present, I really enjoyed working alongside you in the Chemistry Department. A particular thanks to James Donald and Ryan Epton for all the help and coffee breaks.

To all the members of the Lichman group, you have really made a transition from Chemistry to Biology really smooth and kept answering all my questions. Particular thanks to the members of the *Daphniphyllum* group, Kaouthar Eljounaidi, Danielle Taylor and Sandesh Swamidatta.

To the boardgame and pub quiz team, Matt Gill, Ryan Barker, Aparna Sinha and Matt Davy. You have brought so much joy and fun into my life. It was always a pleasure. Special thanks go to Aparna and Matt for making me feel like I can do it, proofreading, helping with formatting and most importantly feeding me.

To my parents, I truly would not be who I am if it wasn't for your support, encouragement and love. Finally, to my partner, Douglas Teale, a special thank you, you always supported me, and made me laugh, especially during those last few months, it would have been so much harder without you.

Table of Contents

List of figures

List of tables

List of abbreviations

Ac	acetyl
APCI	Atmospheric Pressure Chemical Ioniosation
Aq.	aqueous
BBN	9-borabicyclo[3.3.1]nonane
br	broad
^{o}C	Celsius
Calc.	calculated
CoA	coenzyme A
Conc.	concentration
Conv.	conversion
COSY	correlation spectroscopy
d	doublet
DBU	1,8-diazabicycloundec-7-ene
DCM	dichloromethane
dd	doublet of doublets
DEPT	Distortionless Enhancement by Polarisation Transfer
DFT	density functional theory
DIBAL	diisobutylaluminium hydride
DMF	N,N-dimethylformamide
DMP	Dess-Martin periodinane
DMS	dimethyl sulfide
DMSO	dimethyl sulfoxide
Dppf	1,1'-bis(diphenylphosphino)ferrocene
EIC	Extracted ion chromatogram
Equiv	equivalent(s)
ESI	Electrospray ionisation
EWG	electron withdrawing grup
FAD	flavin adenine dinucleotide

FT-IR	Fourier-Transform Infrared Spectroscopy
GNPS	Global Natural Product Social Molecular Networking
h	hour(s)
HMBC	Heteronuclear Multiple Bond Correlation
HPLC	High Performance Liquid Chromatography
HRMS	High Resolution Mass Spectrometry
HMQC	Heteronuclear Multiple Quantum Coherence
HWE	Horner-Wadsworth-Emmons
Hz	Hertz
IC_{50}	half maximal inhibitory concentration
J	coupling constant
KHMDS	potassium bis(trimethylsilyl)amide
LC-MS	Liquid Chromatography Mass Spectrometry
LDA	lithium diisopropylamide
LiHMDS	lithium bis(trimethylsilyl)amide
M	molar
m	multiplet
m/z	mass-to-charge-ratio
MEP	methylerythritol phosphate
MHz	megahertz
min	minute
MS	mass spectrometry
MS/MS	tandem mass spectrometry
MT	methyl transferase
MVA	mevalonate
NADPH	nicotinamide adenine dinucleotide phosphate
nd	not determined
NMR	Nuclear Magnetic Resonance
NOESY	Nuclear Overhauser Effect Spectroscopy

ppm	parts per million
R	general carbon-based organic group
R_f	retention factor
p	pentet
rt	room temperature
q	quartet
s	singlet
SAM	S-adenosylmethionine
Sat	saturated
S_N2	bimolecular nucleophilic substitution
TBAF	tetrabutylammonium fluoride
TBS	tert-butyldimethylsilyl
Temp	temperature
TFA	trifluoroacetic acid
THF	Tetrahydrofuran
TIC	Total ion chromatogram
TIPS	triisopropylsilyl
TLC	thin layer chromatography
TMS	trimethylsilyl
t_R	retention time
UHPLC	Ultra High-Performance Liquid Chromatography
UV	Ultraviolet
δ	chemical shift

1 Introduction

1.1 Alkaloids

1.1.1. Alkaloid types

Plants produce a range of compounds which can be considered primary and secondary metabolites. Primary metabolites, for example sugars and amino acids are involved in essential functions such as growth, development and reproduction (Ishiai et al., 2016; Chen et al., 2018; Maeda, 2019). Secondary metabolites are not directly involved in those functions and so are not essential for survival but provide advantages needed for survival, for example they can act for defence or attract pollinators. Secondary metabolites include alkaloids, terpenes and polyketides amongst others. Alkaloids are a class of secondary metabolites containing at least one nitrogen atom, typically a primary, secondary or tertiary amine (Lichman, 2021; Parthasarathy et al., 2021).

Alkaloids can be generally sub-divided into true alkaloids and pseudoalkaloids based on the origin of the nitrogen atom. In the true alkaloids, nitrogen originates from an amino acid, which also forms part of the alkaloid skeleton.

1.1.2. Pseudoalkaloids

Pseudoalkaloids are a group of alkaloids in which the nitrogen atom is incorporated at a late stage of the biosynthesis and nitrogen is introduced via a transamination reaction (Dewick, 2011). Nitrogen can also be introduced via an amino acid, but its structure is not retained in the skeleton of pseudoalkaloids, instead pseudoalkaloids often derive from terpenoids or steroids.

1.1.3. General alkaloid biosynthesis

True alkaloids contain a nitrogen atom which is derived from an amino acid and forms part of the skeleton of the molecule (Dewick, 2011). Alkaloids are often classified into diverse categories: indole, tropane, imidazole, quinoline, and quinolizidine amongst others, based on the biosynthetic precursor and their skeletons containing various heterocyclic rings systems (Figure 1.1). Indole alkaloids include akuammicine **1.1** isolated from the plant *Picralima nitida* (Shittu et al., 2010). Tropane alkaloids, for example scopolamine **1.2** from *Solanaceae* sp., possess tropane ring system and can be biosynthesised from ornithine or arginine, (Kohnen-Johannsen and Kayser, 2019). Imizadole alkaloids such as dolichotheline **1.3** in *Dolichothele sphaerica* originate from L-histidine. Indole alkaloids can be rearranged to quinoline alkaloids such as quinine **1.4** from *Cinchona* trees (Trenti et al., 2021). Quinolizidine alkaloids include lupin **1.5** isolated from *Lupinus* sp. (Mancinotti, Frick and Geu-Flores, 2022).

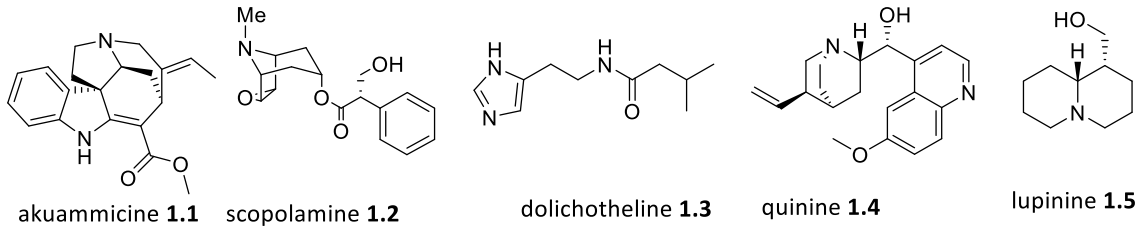

*Figure 1.1 Example of alkaloids: akuammicine **1.1**, scopolamine **1.2**, dolichotheline **1.3**, quinine **1.4** and lupinine **1.5**.*

A typical biosynthesis of alkaloids includes the following steps (Scheme 1.1): production of an amine precursor, reaction with an aldehyde precursor, formation of an iminium cation and a "scaffold-forming" Mannich-like reaction (Lichman, 2021). The scaffold forming step is the first step committed to the pathway followed by oxidations and decorating the scaffold, for example acetylation.

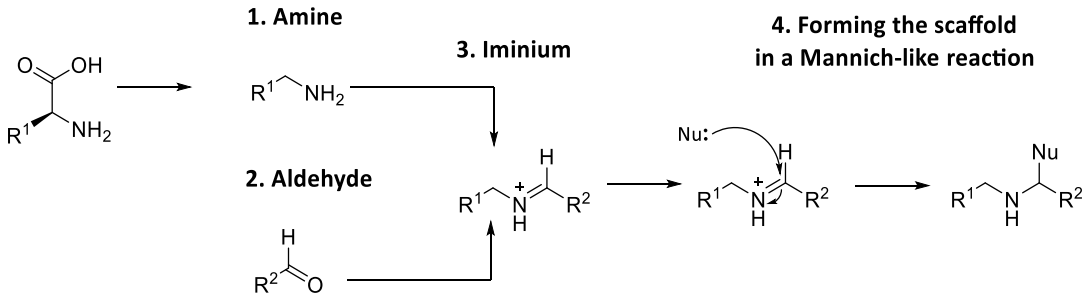

Scheme 1.1 Main steps in a typical alkaloid biosynthesis.

In alkaloids, nitrogen comes from an amino acid. In plants, primary amino acids are ubiquitous and are needed for various roles such as primary metabolism, plant growth and stress response (Ishiai et al., 2016; Chen et al., 2018; Maeda, 2019). An aldehyde needs to be produced in high quantity to react with an amine precursor. The origin of an aldehyde is dependent on the type of an alkaloid and can include amino aldehydes and amino acids. An iminium cation can be formed by a reversible condensation of an amine with an aldehyde. Iminium cation can be formed spontaneously or in an enzyme catalysed reaction (Scheme 1.2) (Scheller et al., 2015; Aleku et al., 2017). All the steps of iminium formation are reversible. The reaction is quenched in a Mannich-like reaction in which an iminium reacts with a nucleophile which forms the scaffold on an alkaloid.

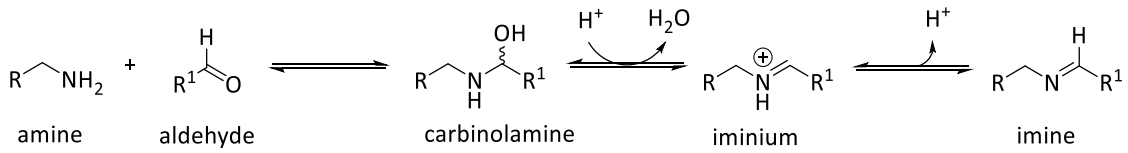

Scheme 1.2 Mechanism of an iminium formation.

1.1.4. Terpene-alkaloids

Terpene alkaloids are a class of natural products combining characteristics of terpenes and alkaloids. They can be characterised based on the number of isoprene units present in the skeleton. Monoterpenoid alkaloids contain two isoprene units (10 carbon atoms), for example actinidine **1.6** from *Actinidia polygama* (Horodysky, Waller and Eisenbraun, 1969) (Figure 1.2), sesquiterpenoid alkaloids such as alkaloid such as dendrobine **1.7**, have three isoprene units, diterpenoid alkaloids contain four isoprene units, for example aconite **1.8** isolated from *Aconite* species, commonly known as monkshood, and lastly triterpenoid alkaloids contain six isoprene units and include solanine **1.9**, steroidal glycoalkaloids from *Solanum* sp. (Ripperger, 1998; Grzech et al., 2024) or yuzurimine **1.10** a *Daphniphyllum* alkaloid from *Daphniphyllum* sp. (Sakurai et al., 1967).

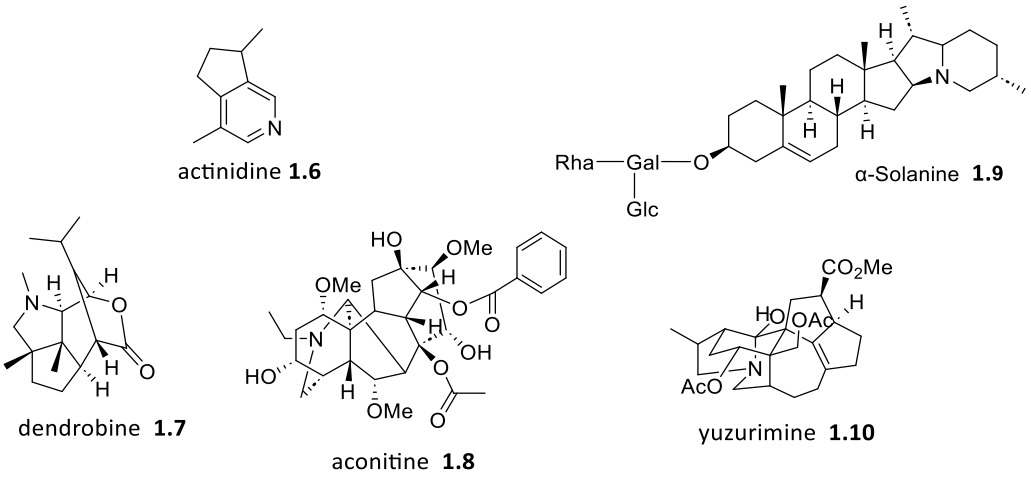

*Figure 1.2 Examples of different types of terpenoid alkaloids, from the left actinidine **1.6**, dendrobine **1.7**, aconitine **1.8**, solanine **1.9** and yuzurimine **1.10**.*

Like terpene biosynthesis, the prenyl units are initially linked together to form chains of varying lengths which then undergo cyclisation and Wagner-Meerwein rearrangements. The functionalisation of the molecules is done by subsequent oxidations, further rearrangements and introduction of the nitrogen. Introduction of the nitrogen makes the molecule a terpenoid alkaloid. Nitrogen atom is introduced, often in the form of ethylamine, methylamine or β-aminoethanol (Cherney and Baran, 2011). The introduction of the nitrogen can occur at any stage of the skeleton formation, i.e. before,

during or after cyclisation step. Dimethylallyl pyrophosphates (DMAPP) and isopentenyl diphosphate (IPP) are the main precursor towards terpenes and terpenoid alkaloids. Both can be produced in the mevalonate (MVA) or methylerythritol phosphate (MEP) pathways (Scheme 1.3) (Huang et al., 2022).

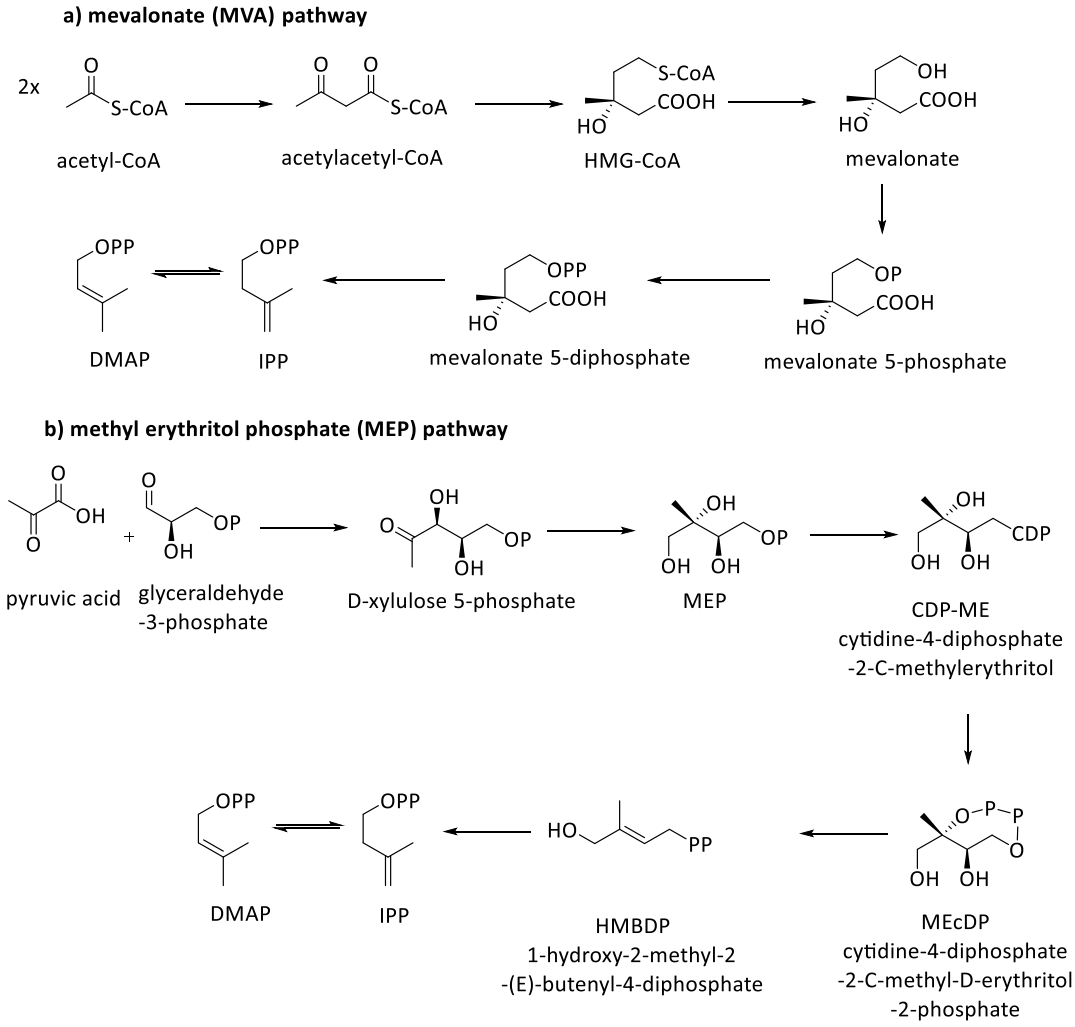

Scheme 1.3 a) MVA and b) MEP pathways involved in terpenoid biosynthesis adapted from (Huang et al., 2022).

Steroid alkaloids such as cyclopamine **1.14**, from *Veratrum californicum* (Turner et al., 2019), are biosynthesised from squalene **1.11** (Scheme 1.4). Squalene **1.11**, as proposed by Augustin et al. undergoes oxidations and cyclisation to form 22-hydroxycholesterol-26-al **1.12**. Then, in a transamination reaction, nitrogen is transferred from γ-aminobutyric acid to form forming 22-hydroxy-26-aminocholesterol **1.13**. Finally, following further oxidation, skeletal rearrangements and instruction of a nitrogen to form cyclopamine **1.14**. (Augustin et al., 2015) .

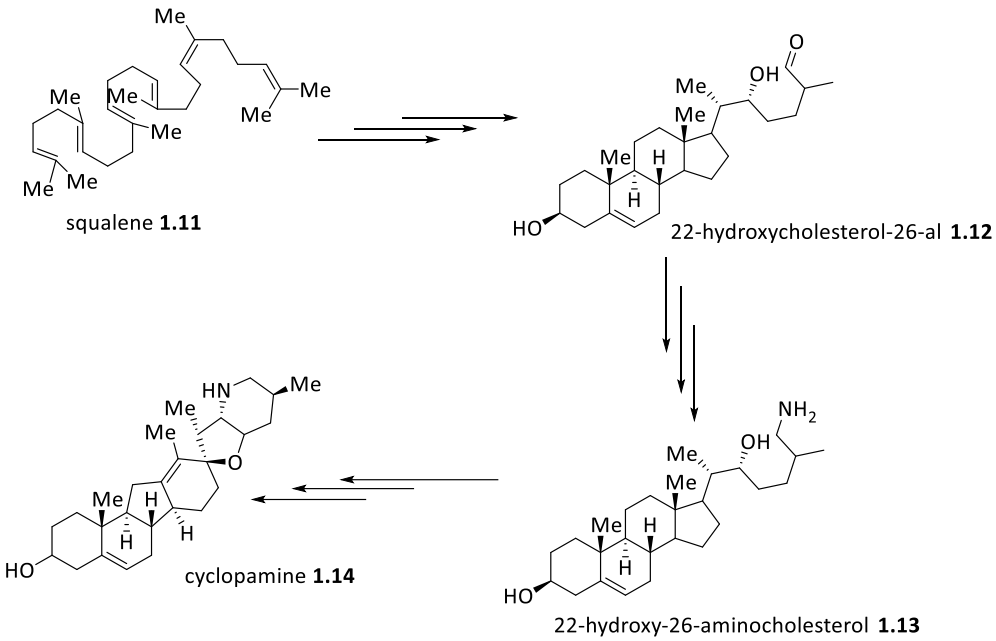

*Scheme 1.4 Biosynthesis of steroid alkaloid cyclopamine **1.14** as proposed by Augustin et al.*

1.1.5. Biosynthesis of alkaloids

The biosynthesis of alkaloids is a highly specialised process involving numerous enzymatic reactions converting primary metabolites into complex compounds. Alkaloids are known for their diverse bioactivities and are produced by plants as a response to various biotic and abiotic stresses caused by conditions such as drought, salinity, wounding or high temperatures. Indeed, there are examples of abiotic stress affecting levels of accumulation of alkaloids in plant species. For example, drought stress was showed to affect the levels of quinolizidine alkaloids in *Lupinus angustifolius* (Christiansen et al., 1997).

Huge structural diversity within alkaloids contributes to their wide range of different bioactive properties. Alkaloids can act as defence against pests, fungi, bacteria and herbivores amongst others (Bhambhani, Kondhare and Giri, 2021). Alkaloids derived from aromatic amino acids such as indole alkaloids exhibit antiherbivore activities and various types of alkaloids would have different modes of action affecting different physiological processes (War et al., 2019). Plants producing alkaloids such as strychnine and atropine are poisonous to predators by attacking central nervous system and affecting neurotransmission which can lead to death. Other alkaloids like capsaicin can have allelopathic effects on plants of *Capsicum* species and support germination of the seeds (Barchenger and Bosland, 2016).

There are multiple enzymatic conversions responsible for the biosynthesis of the alkaloids. Those can involve hydroxylation, oxidation, methylation and cyclisation. The biosynthesis is determined by set of genes encoding enzymes that catalyse the pathway reactions. The genes can be organised in biosynthetic gene clusters which can co-express allowing for their discovery.

Biosynthetic gene clusters are less frequently observed in plants than in bacteria or fungi but they are found more and more often with many genomes being sequenced now (Smit and Lichman, 2022). Plant biosynthetic pathways can be dispersed across the

genome due to gene duplications and horizontal gene transfers making them more difficult to identify. Biosynthetic gene cluster can be defined to contain at least three non-homologous genes of distinct evolutionary origin adjacent to one another in the genome which contribute to a specific biosynthetic pathway (Nützmann and Osbourn, 2014). Some of the known biosynthetic gene clusters include those encoding biosynthesis of noscapine in *Papaver somniferum* (Winzer et al., 2012), avenacin in oat *Avena* spp. (Qi et al., 2004) and phytocassane cluster in rice *Oryza saltiva* (Wilderman et al., 2004).

Alkaloid biosynthesis often occurs in specific plant tissue or specialised plant cell types (Lichman, 2021). In some species, the biosynthesis is localised to specific organs such as root, leaves or seeds, sometimes in response to environmental conditions. In opium poppy, although benzylisoquinoline alkaloids accumulate in the lacifers, they are biosynthesised in the competent cells of the phloem (Bird, Franceschi and Facchini, 2003). And the pyrrolozidine alkaloids of *Senecio vulgaris* are biosynthesised in the roots from which they are translocated via phloem to the shoots (Witte, Ehmke and Hartmann, 1990). The pathways may also be specific to tissues, for example in *Catharanthus roseus* there are leaf and root specific pathways (Scheme 1.5): in the leaves tabersonine **1.15** is converted into vindoline **1.16** whilst in the roots it is converted into lochnericine **1.17** (Amor Stander et al., 2020).

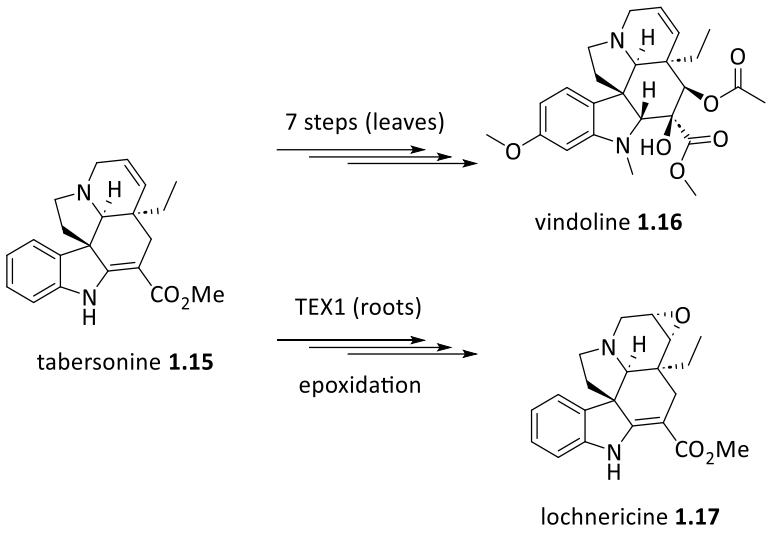

Scheme 1.5 Leaf and root specific pathway in Catharanthus roseus.

1.2 *Daphniphyllum* alkaloids

1.2.1 *Daphniphyllum*

The family Daphniphyllaceae contains a single genus *Daphniphyllum*, within which there are 34 species originating from South East Asia (Tang et al., 2012). The plants are evergreen trees or shrubs, with new leaves appearing early in the summer before the old leaves gradually fall. In Japan this behaviour gave the genus another name "yuzuriha" which broadly translates "to give away". Plants from this genus are dioecious which means that there are separate male and female plants, and they are wind pollinated with the seeds dispersed by birds (Yoichi et al., 2023).

Extracts of bark and leaves have been used in the traditional Chinese medicine to treat asthma and various ailments. Nowadays, the extract of *D. calycinum* is a main component of a Chinese patented drug Fengliao-Changweikang, which is used to treat bowel disease (Zhang et al., 2012).

1.2.2 *Daphniphyllum alkaloids*

The medicinal properties of *Daphniphyllum* sp. are thought to be caused by the presence of the class of complex alkaloids containing fused polycyclic rings. To the best of our knowledge, they have only been isolated from the genus *Daphniphyllum*, hence why this class of alkaloids is known as *Daphniphyllum* alkaloids. In 1909, the first *Daphniphyllum* alkaloid was isolated by Yagi in an attempt to identify natural products responsible for the bioactivity (Wu et al., 2013). Today it is thought it was an unseparated mixture of alkaloids (Heathcock, 1992). In the 1960s the structures of the first *Daphniphyllum* alkaloids – daphniphylline **1.18** and yuzurimine **1.10** – were elucidated and fully characterised (Irikawa et al., 1968). Today, over 330 different *Daphniphyllum* alkaloids, which can be grouped into 35 skeletal families, have been isolated and reported (Figure 1.3) (Chattopadhyay and Hanessian, 2017).

Daphniphyllum alkaloids exhibit a range of anticancer, antioxidant and vasorelaxant properties (Wu et al., 2013). For example, daphnilongeridine exhibited cytotoxicity against cancer cell lines with IC_{50} values between 2.4 and 9.7 μM (Zhang et al., 2009a) and daphmacromines A–J showed pesticide activities against brine shrimp (*Artemia salina*) with the corrected lethality between 41.00 and 70.90% (Cao et al., 2012). Deoxyyuzurimine **1.66** and yuzurimine C showed corrected lethality values of 81.81 and 80.56%, respectively (Cao et al., 2012). Daphtedinine C showed potent insecticidal effect against *Plutella xylostella* and *Heliothis virescens* (Wu et al., 2013)**.** *D. calycinum* is known to be toxic and it was found that deoxycalyciphylline B was the cause of hepatoxicity of that plant (Zhang et al., 2012).

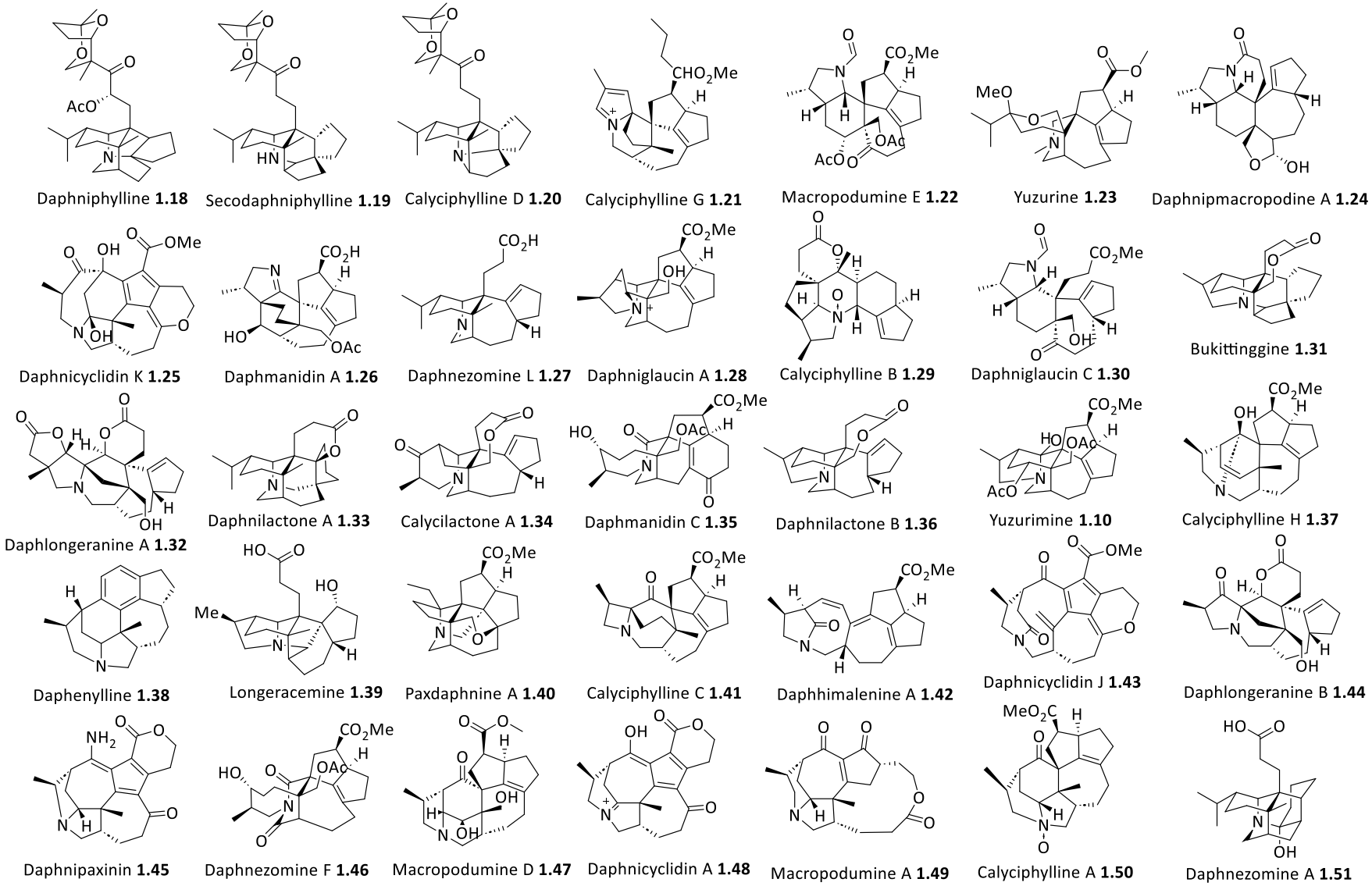

Figure 1.3 Skeletal families of Daphniphyllum alkaloids (Chattopadhyay and Hanessian, 2017).

1.2.3 *Daphniphyllum alkaloid subtypes*

The class of *Daphniphyllum* alkaloids contains high diversity of skeletons and are isobaric. To simplify the classification, the 35 skeletal classes can be categorised into subtypes based on the number of carbons within the core skeleton (Figure 1.4). Daphniphylline **1.18** and secodaphniphylline **1.19** have 30 or 32 carbons and can be called C30 alkaloids. The loss of C8 moiety (represented by the blue fragment) would lead to the formation of C22 alkaloids which can be divided into subtypes further. Compounds containing a hydroxypentalene moiety (two fused five-membered rings in red) were called C22A types and C22 alkaloids missing this moiety were called C22B and were represented by daphnilactone B **1.36** and daphnezomine L **1.27** types (Eljounaidi et al., 2024). It is important to remember that this classification is a simplification and there are number of different skeletal types that do not fit this classification. They include C22 alkaloids of daphnicyclidin type and, for example, daphnezomine A **1.53** – an alkaloid of a molecular formula of $C_{22}H_{35}NO_2$ which belongs to the secodaphniphylline type but is missing a C8 moiety. Those compounds will be called 'C22' unless specified otherwise.

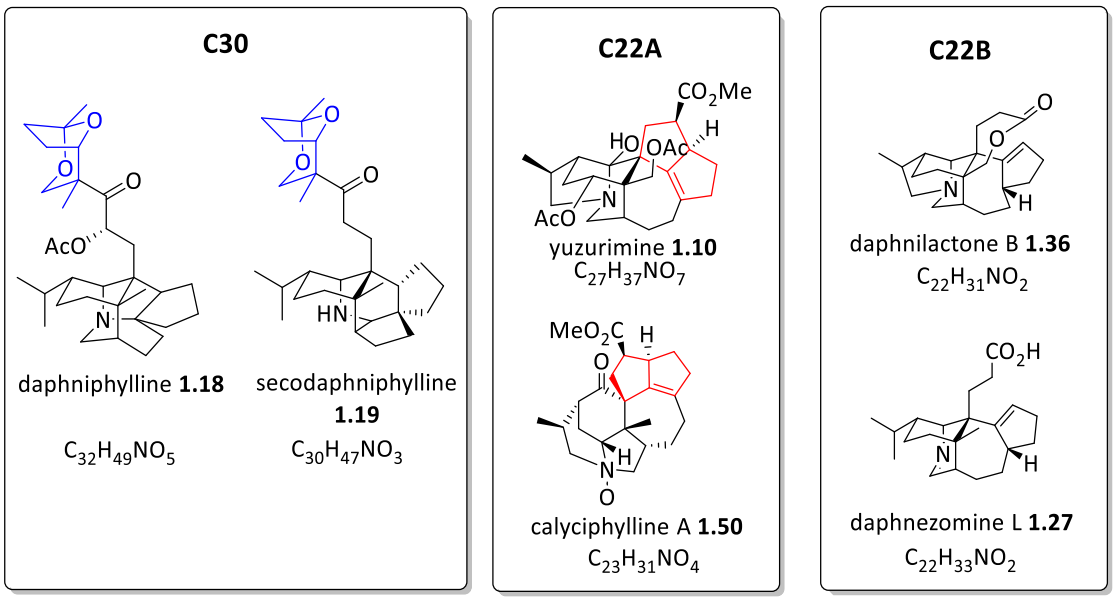

Figure 1.4 Daphniphyllum alkaloids. Representative Daphniphyllum *alkaloids, classified by carbon skeleton: C30 (blue highlighting C8 fragment lost in C22 compounds; C22A (presence of hexahydropentalene ring in red), C22B (absence of hexahydropentalene ring).*

1.2.3.1 Secodaphniphylline type alkaloids

Secodaphniphylline **1.19**, methyl homosecodaphniphyllate **1.52** and daphnezomine M **1.53** (Figure 1.5) are the examples of secodaphniphylline type alkaloids with structures confirmed by X-ray crystallography (Toda, Hirata and Yamamura, 1972). Based on the biomimetic studies, it is hypothesised that secodaphniphylline type alkaloids appear at the start of the *Daphniphyllum* alkaloid biosynthetic pathway (Heathcock, 1996).

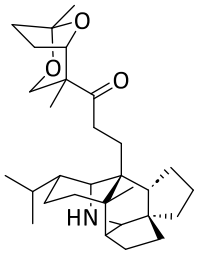

secodaphniphylline **1.19**
$C_{32}H_{47}NO_3$

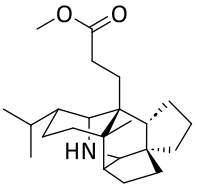

methyl homosecodaphniphyllate **1.52**
$C_{23}H_{37}NO_2$

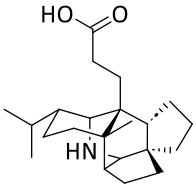

daphnezomine M **1.53**
$C_{22}H_{35}NO_2$

Figure 1.5 Structures of secodaphniphylline type alkaloids.

1.2.3.2 Daphniphylline type alkaloids

Daphniphylline type alkaloids form a large class of *Daphniphyllum* alkaloids containing either 30 or 32 carbons. Major compounds belonging to this class are daphniphylline **1.18**, codaphniphylline **1.54** and daphmacrine **1.55**. An example of a related compound lacking the C8 moiety is methyl homodaphniphyllate **1.56** which can be considered to be a C22 subtype (Figure 1.6).

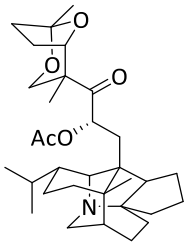

daphniphylline **1.18**
$C_{32}H_{49}NO_5$

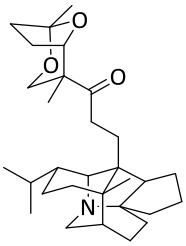

codaphniphylline **1.54**
$C_{30}H_{47}NO_3$

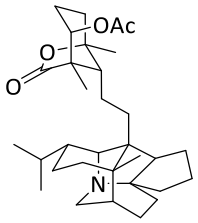

daphmacrine **1.55**
$C_{32}H_{49}NO_4$

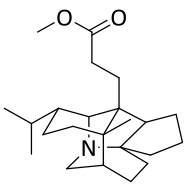

methyl homo-daphniphyllate **1.56**
$C_{32}H_{37}NO_2$

Figure 1.6 Structures of daphniphylline type alkaloids.

A plausible biosynthesis of daphniphylline type skeleton involves a conversion of secodaphniphylline type skeleton (Scheme 1.6). It was proposed that the nitrogen atom on secodaphniphylline type skeleton **1.57** is first oxidised to **1.58** which allows for the ring opening and skeleton rearrangement to daphniphylline type skeleton via a proposed intermediate **1.60** (Ruggeri and Heathcock, 1989; Heathcock et al., 1992b).

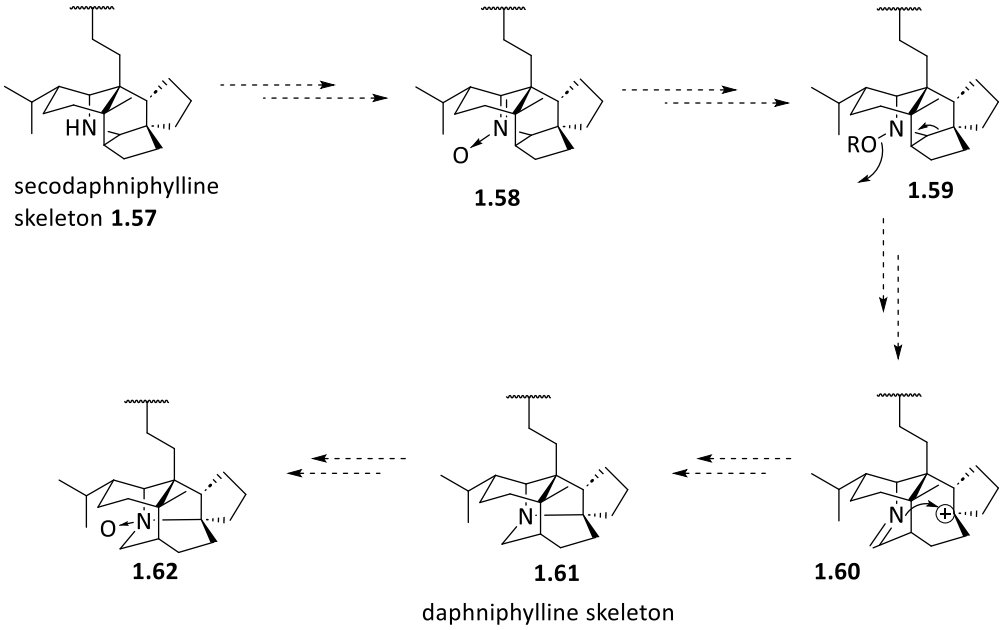

Scheme 1.6 Proposed biosynthesis of daphniphylline type alkaloids (Morita and Kobayashi, 2007)

1.2.3.3 Daphnilactone A and B type alkaloids

Daphnilactone B **1.36** was isolated from fruits of *D. teijsmanni, D. macropodum* and *D. macropodum* var. *humile* and with daphnilactone A **1.32** gave the name to daphnilactone class of *Daphniphyllum* alkaloids (Figure 1.7) (Sasaki and Hirata, 1972; Niwa et al., 1972; Toda et al., 1974). Daphnilactone B type alkaloids are hypothesised intermediates in the pathway and are an example of C22B alkaloid subtype (Eljounaidi et al., 2024). Daphnezomine I was the first example of an N-oxide daphnilactone B type alkaloid (Morita, Yoshida and Kobayashi, 2000). Daphnilactone A **1.33** is one of the alkaloids that does not fit into the simplified types of C30 and C22 as it has 23 carbons in its skeleton.

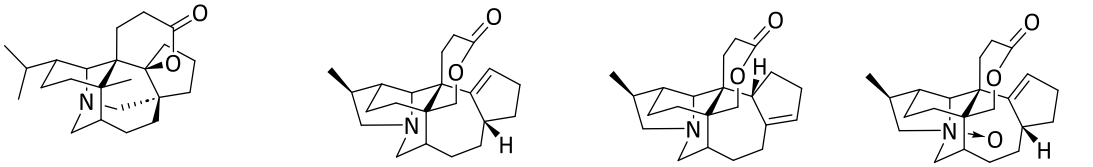

daphnilactone A **1.33** $C_{23}H_{35}NO_2$ | daphnilactone B **1.36** $C_{22}H_{31}NO_2$ | isodaphnilactone B **1.63** $C_{22}H_{31}NO_2$ | daphnezomine I **1.64** $C_{22}H_{31}NO_2$

Figure 1.7 Examples of daphnilactone A and daphnilactone B types.

The hypothetical unsaturated amine **1.65** was proposed to be an intermediate between methyl homodaphniphyllate **1.56** (daphniphylline type) and daphnilactone A **1.33** (Scheme 1.7) (Ruggeri, McClure and Heathcock, 1989; Heathcock, Ruggeri and McClure, 1992).

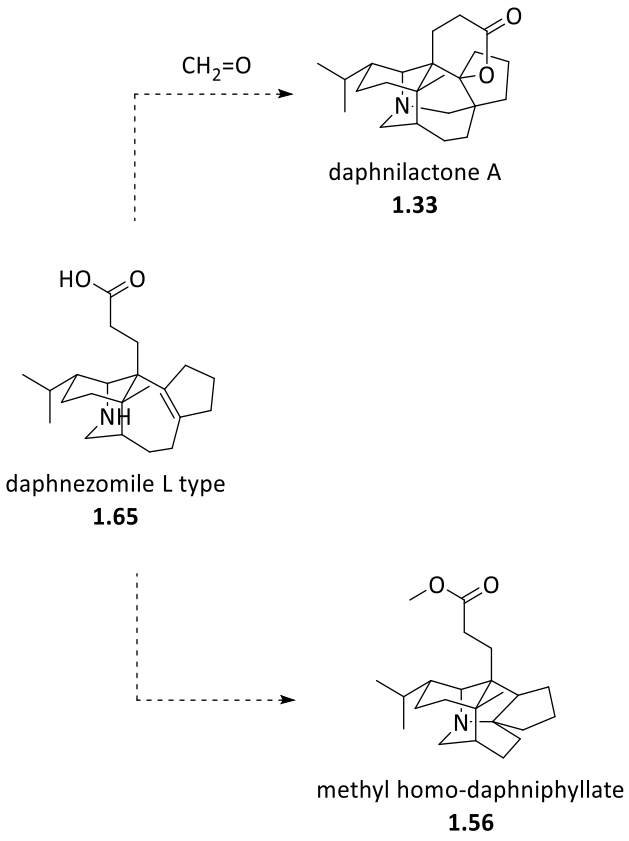

*Scheme 1.7 Proposed biosynthetic steps to methyl homodaphniphyllate **1.56** and daphnilactone A **1.33*** (Heathcock, 1996).

1.2.3.4 Yuzurimine type alkaloids

Yuzurimine **1.10** was isolated in 1967 from the bark and leaves from *D. macropodum* (Sakurai et al., 1967). Since then, tens of yuzurimine type alkaloids have been reported. The other examples of yuzurimine type alkaloids include deoxyyuzurimine **1.66**, N-oxide alkaloid daphnijsmine **1.67** and yuzurimine C **1.68** (Figure 1.8).

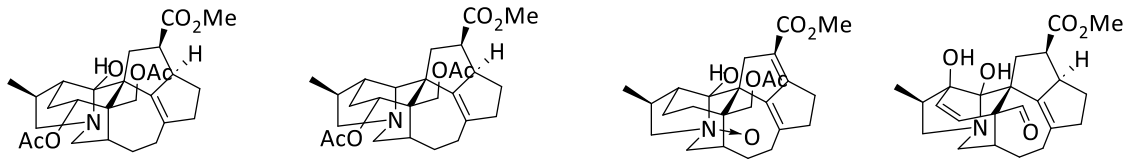

yuzurimine **1.10** $C_{27}H_{37}NO_7$

deoxyyuzurimine **1.66** $C_{27}H_{37}NO_6$

daphnijsmine **1.67** $C_{25}H_{33}NO_6$

yuzurimine C **1.68** $C_{23}H_{29}NO_5$

Figure 1.8 Examples of structures of yuzurimine type alkaloids.

The biosynthetic pathway towards yuzurimine type was proposed by Morita and Kobayashi (Morita and Kobayashi, 2007) and is presented below in Scheme 1.8. Yuzurimine was proposed to be produced in two ways, both starting from secodaphniphylline type skeleton **1.69**. Then yuzurimine can be formed via a ring opened intermediate **1.74** or alternatively it might be formed through daphnezomine G **1.72**, a daphnezomine F type alkaloid. Curiously, the proposed pathway contains intermediates **1.70** and **1.73**, both possessing a double bond in the isoprenyl group. The proposal for those intermediates likely comes from the early biomimetic studies with ammonia which resulted in a similar structure. Nevertheless, further studies showed that the double bond is not necessarily formed, this will be further discussed in section 1.1.1. This might mean that the early steps might need to be updated in the future. Still, the skeletal types are likely to follow the same order.

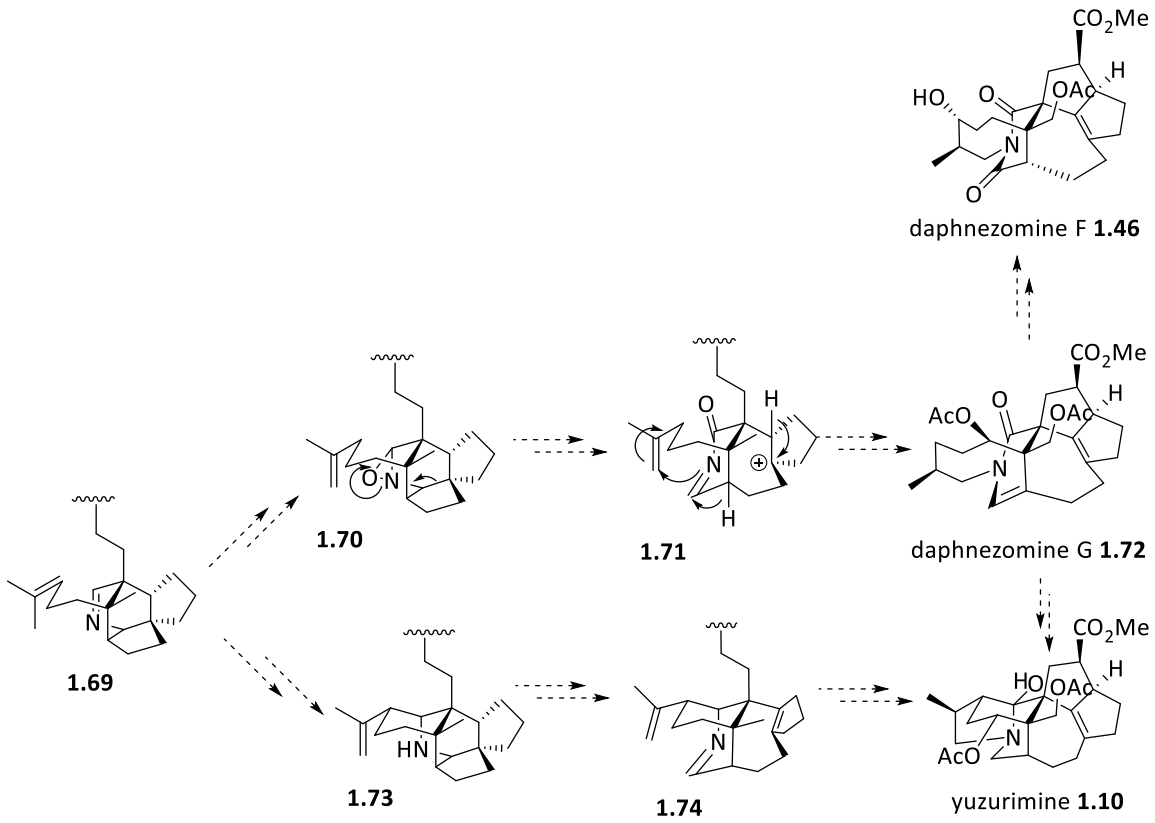

*Scheme 1.8 The hypothesised biosynthesis of daphnezomine F **1.46**, G **1.72** and yuzurimine **1.10** as proposed by Morita and Kobayashi* (Morita and Kobayashi, 2007).

1.2.3.5 Calyciphylline A-type

Calyciphylline A **1.50** was isolated from the leaves of *D. calycinum* (Morita and Kobayashi, 2003) and due to its novel skeleton, containing a fused-hexacyclic ring system, this type was named calyciphylline A type with examples presented in Figure 1.9. These alkaloids are structurally related to yuzurimine type, and many of calyciphylline A type alkaloids possess the same fused hydroxypentalene moiety, i.e. calyciphylline A **1.50** and himalenine C **1.75**, thus calyciphylline A also belong to C22A subtype. There are also alkaloids in calyciphylline A type that do not possess this moiety, for example daphenylline **1.38**, isolated from fruits of *D. longracemosum* (Zhang et al., 2009b).

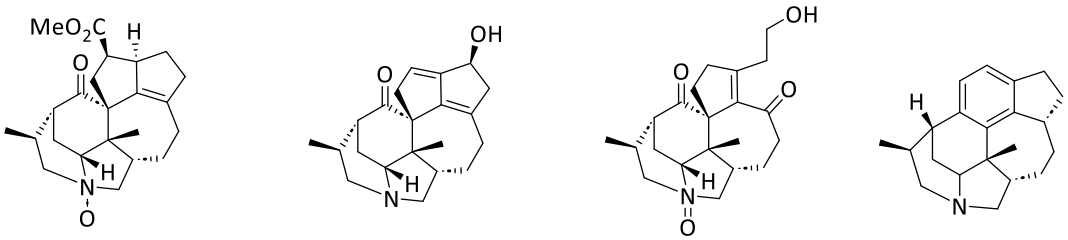

calyciphylline A **1.50** $C_{23}H_{31}NO_4$ | himalenine C **1.75** $C_{21}H_{27}NO_2$ | daphhimalenine D **1.76** $C_{21}H_{29}NO_4$ | daphenylline **1.38** $C_{21}H_{27}N$

Figure 1.9 Examples of alkaloids belonging to calyciphylline A type.

Morita and Kobayashi proposed a pathway towards calyciphylline A and daphnicyclidin type alkaloids (Scheme 1.9) (Morita and Kobayashi, 2003). They suggested that yuzurimine type alkaloids, such as yuzurimine A **1.76** or macrodaphniphyllamine **1.77** could be derived from a common intermediate **1.69** as described previously. Subsequently, **1.73** undergoes a ring expansion to form an intermediate **1.75** (similarly as in scheme 1.7) which, following skeletal rearrangements can lead to calyciphylline A type alkaloids such as daphniglaucin D **1.79** and calyciphylline A **1.50**. These alkaloids can then undergo further skeletal rearrangements to yield daphnicyclidin type alkaloids such as daphnicyclidin A **1.48**.

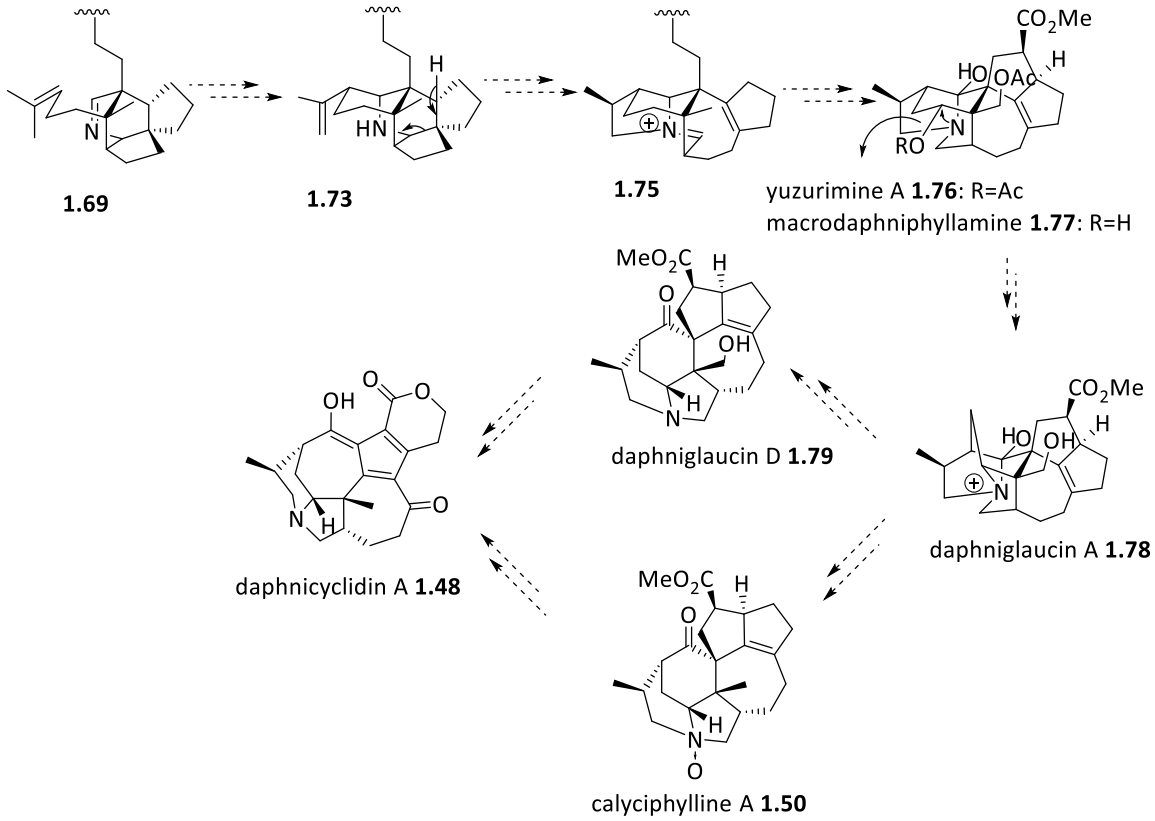

*Scheme 1.9 Proposed biosynthetic pathway towards calyciphylline A **1.50** and daphnicyclidin A **1.48** adopted from* (Morita and Kobayashi, 2003).

1.2.3.6 Daphnezomine type

Daphnezomines A **1.51** and B **1.80** are the sole members of this type of *Daphniphyllum* alkaloids containing an aza-adamantane core with an amino ketal bridge (Figure 1.10) (Morita, Yoshida and Kobayashi, 1999).

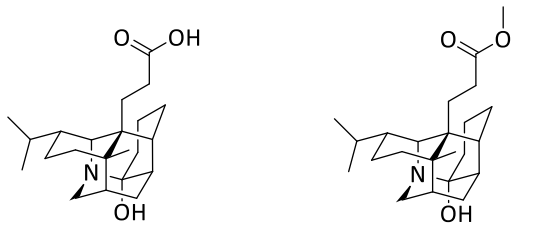

Daphnezomine A **1.51**
$C_{22}H_{35}NO_3$

Daphnezomine B **1.80**
$C_{23}H_{37}NO_3$

*Figure 1.10 Structures of daphnezomine A **1.51** and daphnezomine B **1.80**.*

It was also proposed that daphnezomine L **1.65** might be an intermediate to daphnezomine A **1.51** and B **1.80** (Scheme 1.10). An intermediate **1.82** if then formed following oxidation (epoxidation) which leads to a ring expansion, then through skeletal rearrangement daphnezomines A **1.51** and B **1.80** might be formed (Morita, Yoshida and Kobayashi, 1999)

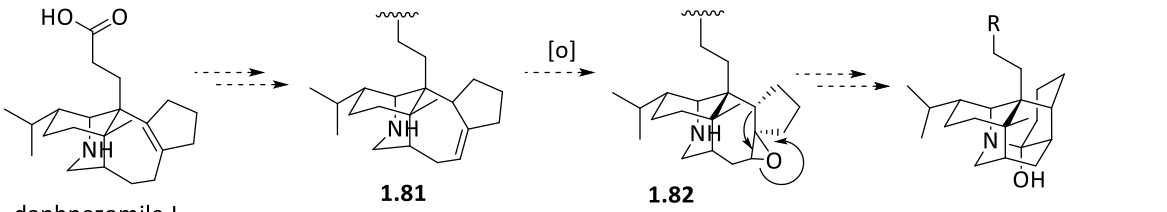

daphnezomile L
1.65

1.81

1.82

Daphnezomine A **1.51**: R = CO_2H
Daphnezomine B **1.80**: R = CO_2Me

Scheme 1.10 Proposed biosynthetic pathway towards daphnezomine B adapted from (Morita, Yoshida and Kobayashi, 1999).

1.2.4 *Basis behind biosynthetic hypothesis*

The early attempt at understanding the origin of *Daphniphyllum* alkaloids was reported in the 1973. In the experiment, to the branches of *Daphniphyllum macropodum* were fed ^{14}C and ^{3}H-labelled DL-mevalonic acid and isolated labelled and inseparable then mixture of labelled daphniphylline **1.18** and codaphniphylline **1.54** (Scheme 1.11). Based on the degradation studies it was suggested that daphniphylline **1.18** and codaphniphylline **1.54** must be produced from six molecules of mevalonic acid and a squalene-like intermediate (Haruki, Yoshimasa and Suzuki, 1973; Suzuki et al., 1973).

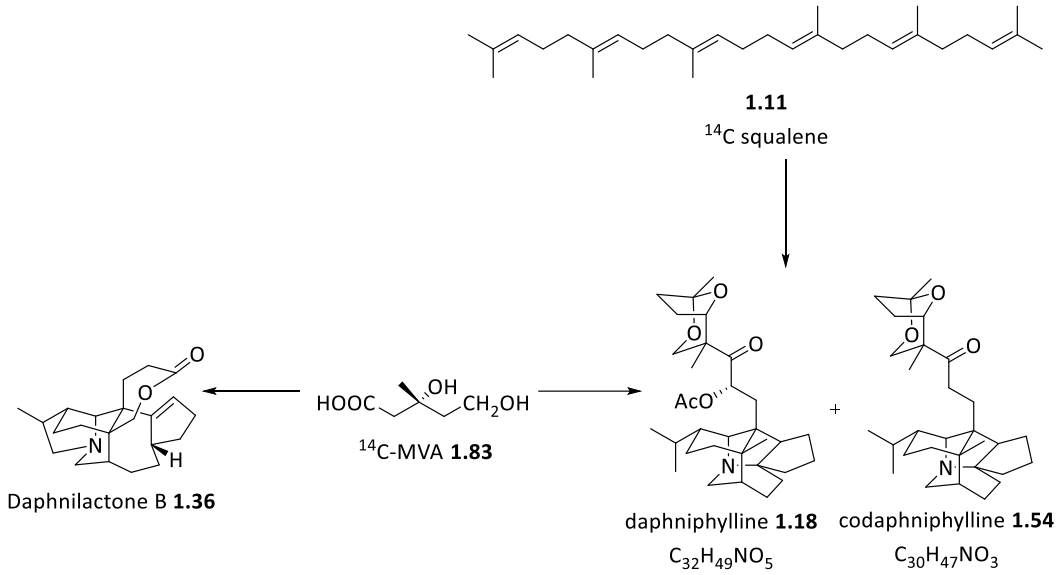

*Scheme 1.11 Representation of the feeding experiments with ^{14}C labelled mevalonic acid and ^{13}C-squalene which resulted in isolation of ^{14}C labelled daphniphylline **1.18**, codaphniphylline **1.54** and daphnilactone B **1.36*** (Haruki, Yoshimasa and Suzuki, 1973; Suzuki et al., 1973).

In a more recent experiment, hydroponic seedlings of *D. macropodum* were fed stable isotope labelled substrates – $^{13}C_6$-glucose and 2-$^{13}C_6$-mevalactone. The results supported previous experiments showing incorporation in *Daphniphyllum* alkaloids and showed that the pathway starts with C30 alkaloids via C22B and ends with C22A alkaloids. It also indicated that *Daphniphyllum* alkaloids are synthesised across multiple tissues with no need for transport between different tissues, although likely there is transport between different cell types within the tissue (Eljounaidi et al., 2024).

1.2.5 *First total synthesis of Daphniphyllum alkaloids*

In the 1980s Heathcock's group attempted the total synthesis of a *Daphniphyllum* alkaloid. Methyl homodaphniphyllate **1.56** was chosen as one of the simplest *Daphniphyllum* alkaloids and it was assumed that since daphniphylline **1.18** is one of the most wide-spread and abundant alkaloids in *D. macropodum*, daphniphylline skeleton must be an important intermediate in the pathway. Methyl homodaphniphyllate **1.56** was the first *Daphniphyllum* alkaloid to be synthesised (Heathcock et al., 1986).Later it was proposed that secodaphniphylline type alkaloids would precede daphniphylline types (Scheme 1.12). Thus, an unsaturated amine **1.84** was proposed as an intermediate between secodaphniphylline and daphniphylline-type alkaloids (Heathcock, 1996).

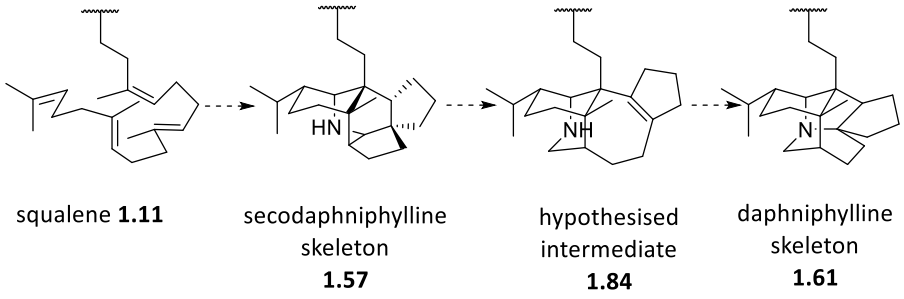

Scheme 1.12 A proposed order of skeletal rearrangement in Daphniphyllum *alkaloid biosynthetic pathway.*

A new synthetic plan was devised, using a biomimetic approach, with the secodaphniphylline type alkaloid: methyl homosecodaphniphyllate **1.52** chosen as the target. Biomimetic synthesis of natural products involves designing a synthetic pathway that mimics natural biosynthetic processes. Unlike total synthesis, a biomimetic pathway typically employs simpler precursor, mild conditions and cascade reactions to achieve high efficiency and selectivity is in fewer steps.

Therefore, the retrosynthetic strategy towards methyl homosecodaphniphyllate **1.52** aimed to minimise unnecessary functional groups and retain squalene-like skeleton for as long as possible, closely following its hypothesised biosynthetic pathway.

The synthesis started with three simple building blocks (Scheme 1.13). To the lithium enolate of **1.85**, unsaturated ester **1.86**, and homo-geranyl iodide **1.87** were added which resulted in the formation of compound **1.88**. This coupled product **1.88** was then converted into lactone **1.89**, followed by a reduction with lithium aluminium hydride to form diol **1.90**. Diol **1.90** was then oxidised in a Swern oxidation to afford a methylene chloride solution of dialdehyde **1.91,** to which gaseous ammonia was added. This resulted in the formation of the secodaphniphylline skeleton in good yield. The isopropenyl double bond, which is not present in *Daphniphyllum* alkaloids, was hydrogenated, and this also cleaved the benzyl ether group. In the final steps, Jones oxidation and Fischer esterification steps were performed, enabling methyl homosecodaphniphyllate **1.52** to be obtained in 48% overall yield.

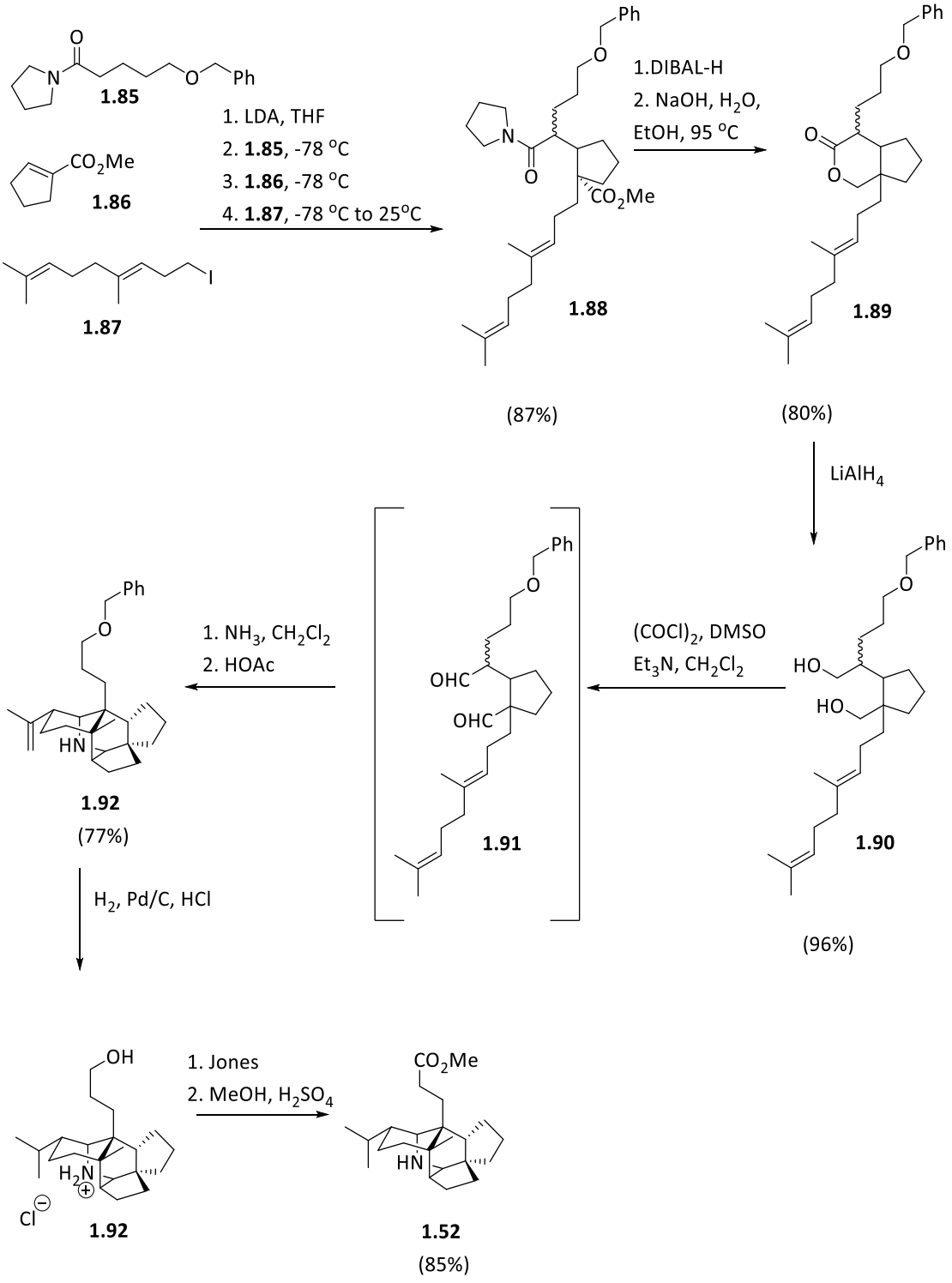

Scheme 1.13 Total synthesis of a secodaphniphylline type alkaloid as reported by (Heathcock, Ruggeri and McClure, 1992).

1.2.6 *Biomimetic synthesis of Daphniphyllum alkaloids*

Next, the group decided to follow a route that used more biologically relevant precursors in a biomimetic approach. A linear dialdehyde **1.93** was synthesised and allowed to react with ammonia (Scheme 1.14). Both stereoisomers formed a so called "proto-daphniphylline **1.94**" in fairly low yield, but remarkably, the secodaphniphylline skeleton was formed, although it had an additional double bond at the isopropyl group (i.e. an isopropenyl group) compared to the natural products.

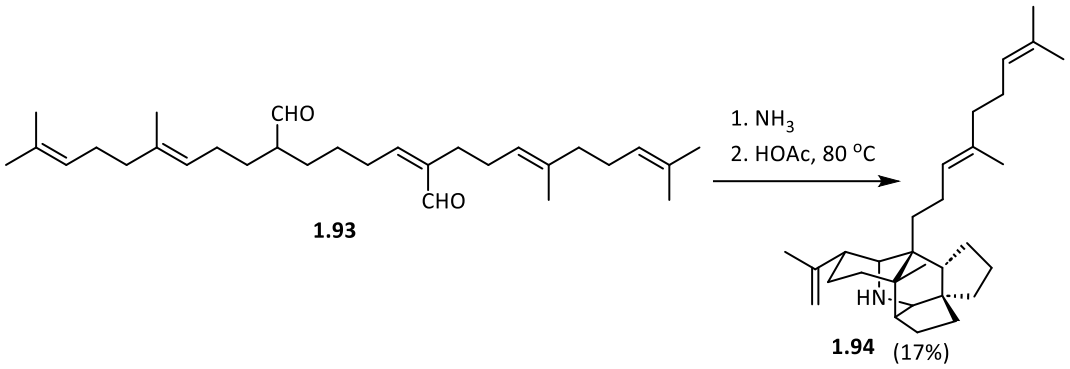

*Scheme 1.14 Synthesis of "proto-daphniphylline **1.94**" using ammonia* (Heathcock, 1996).

1.2.7 *Proposal for biosynthesis of* Daphniphyllum *alkaloids*

Based on the remarkable biomimetic formation of the secodaphniphylline skeleton in mild conditions, a biosynthetic route towards *Daphniphyllum* alkaloids was proposed (Scheme 1.15). Firstly, squalene **1.11** is oxidised to dialdehyde **1.96**, which would condense with an amino acid or a primary amine resulting in imine **1.98**. The next proposed step is a prototopic rearrangement to form enamine **1.100.** The steps from **1.96** to **1.00** are equivalent to a reductive amination. Then, **1.100** cyclises to form **1.102** and rearranges into **1.105**. **1.105** was then proposed to be converted into **1.69** in a Diels-Alder reaction, then and into **1.94** via ene-like cyclisation. Thus, the skeleton of secodaphniphylline **1.94** would be formed, although it contains an isopropenyl group which true *Daphniphyllum* alkaloids do not have (Heathcock et al., 1992b; Heathcock, 1996). Therefore, despite the impressive formation of a seco-daphniphylline-like skeleton from a linear precursor, the biosynthetic proposal ultimately led to an "incorrect" structure. Alternative mechanisms will be explored to propose the formation of a true *Daphniphyllum* alkaloid skeleton.

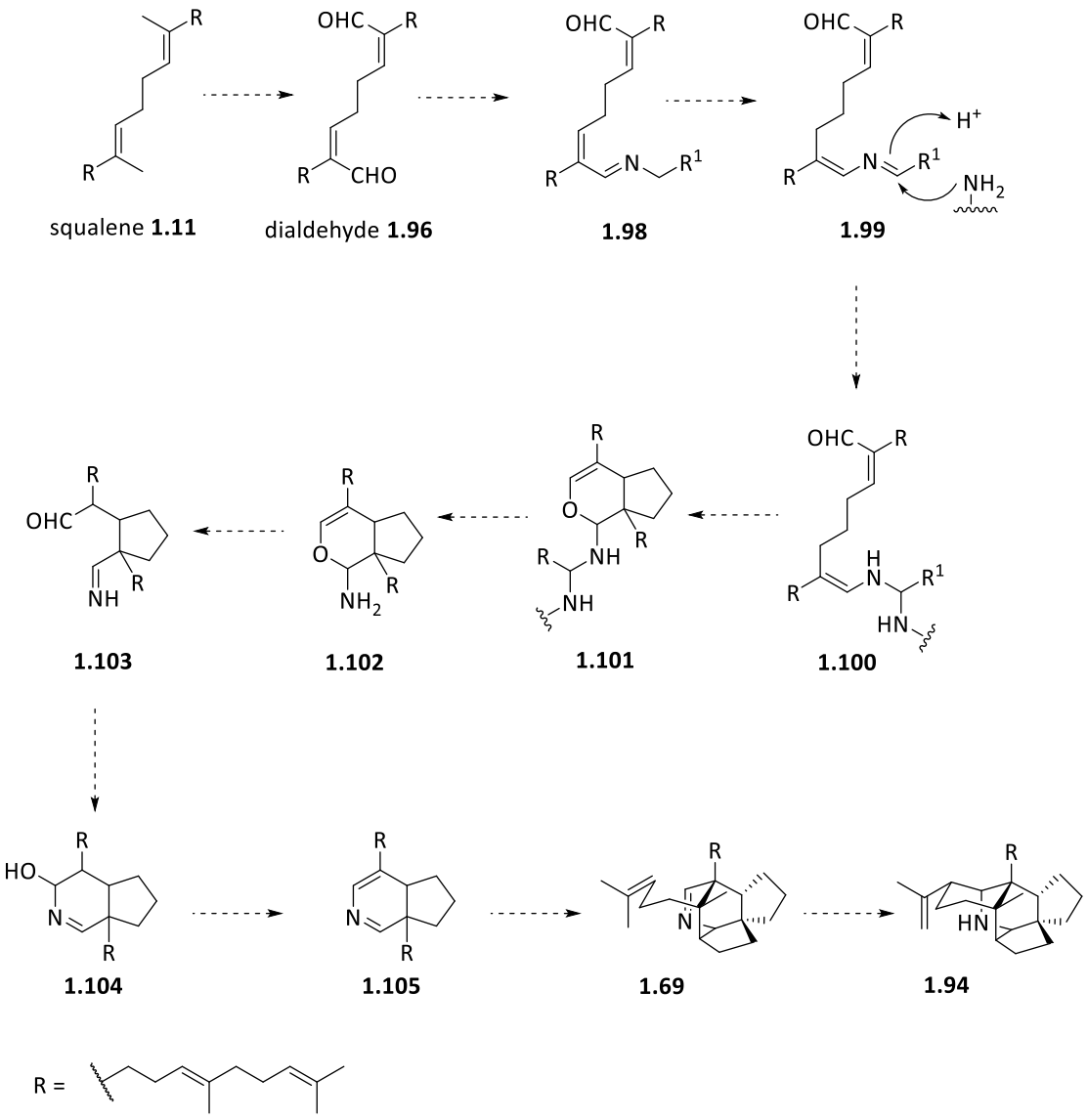

Scheme 1.15 Mechanism of the formation of secodaphniphylline skeleton as proposed by (Heathcock et al., 1992b).

Interestingly, the dialdehyde **1.93** formed a true secodaphniphylline skeleton when it reacted with methylamine as shown in Scheme 1.16 (Heathcock, 1996). The choice to try methylamine was not made deliberately, rather this experiment was done originally due to a mistake with a mis-labelled reagent bottle! Remarkably, the isopropenyl double bond present in **1.94** was absent in the product **1.95**, where it was saturated. This suggests that the reactions with these two amines must follow different mechanisms.

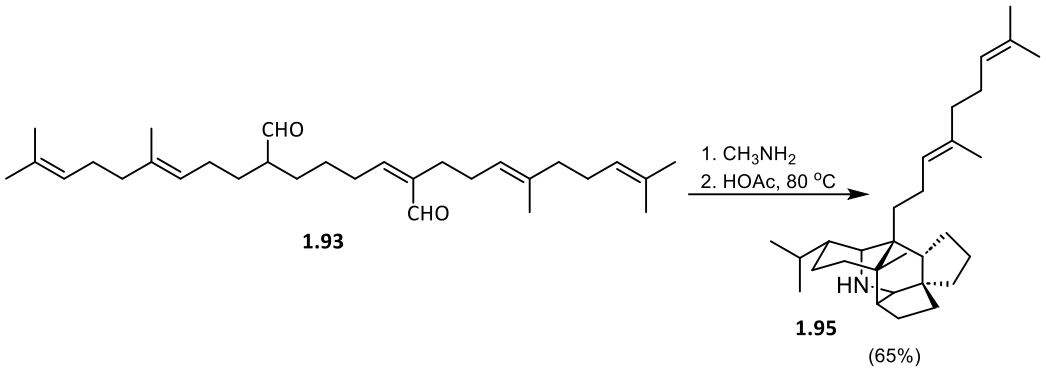

*Scheme 1.16 Synthesis of "proto-daphniphylline **1.95**" using methylamine* (Heathcock, 1996).

Also, the lack of isopropenyl group in *Daphniphyllum* alkaloids suggests that cyclisation with methylamine is more relevant to their biosynthesis than cyclisation with ammonia (Heathcock, 1996). Thus, a source of nitrogen in those natural products might be an amino acid. However, the question of where exactly the nitrogen comes from remains unanswered, and while the reaction proceeds under the laboratory conditions used by Heathcock et al, it might not react in the same way inside the plant cell.

Of additional note, both reactions to form **1.94** and **1.95** are fully diastereoselective. *Daphniphyllum* alkaloids are complex structures containing multiple stereocenters and their chirality is a key feature of their skeleton. Enzymes can play a role in stereocontrol by stabilising transition states and directing the biosynthesis towards one stereoisomer over another. Since a lab-based reaction produced a single diastereoisomer, it suggests that in nature it is possible that an enzyme is not required to shape the intermediate in the polycycle forming step. Nevertheless, *Daphniphyllum* alkaloids are found as single enantiomers and so there must be enzymatic control of the stereocenters at some point in the biosynthetic pathway, even if not at the cyclisation step.

It is remarkable how changing a reagent from ammonia to methylamine would affect the yields and the final products in such drastic way. In fact, the reaction yields improved when methylamine was used, albeit affording a different product. The mechanism of the reaction between dialdehyde **1.93** and methylamine was proposed by Tantillo and presented in Scheme 1.17 although it did not attempt to explain the biosynthetic steps (Tantillo, 2016). Here, **1.106** is formed first, before reacting with methylamine which

would result in forming a cation **1.107**. The next step involves a concerted ene reaction, as proposed before. Crucially, in this mechanism there is a methyl group on the nitrogen which allows for the hydride migration and cyclisation of **1.108** (though the steps could also occur with a methylene group on the nitrogen instead of the methyl). In the final step, the true secodaphniphylline skeleton **1.95** is formed via hydrolysis of **1.109**. However, the starting point in the proposal, dialdehyde **1.93** is a reduced form of dialdehyde **1.96** and so this mechanism does not explain the reduction which needs to happen first.

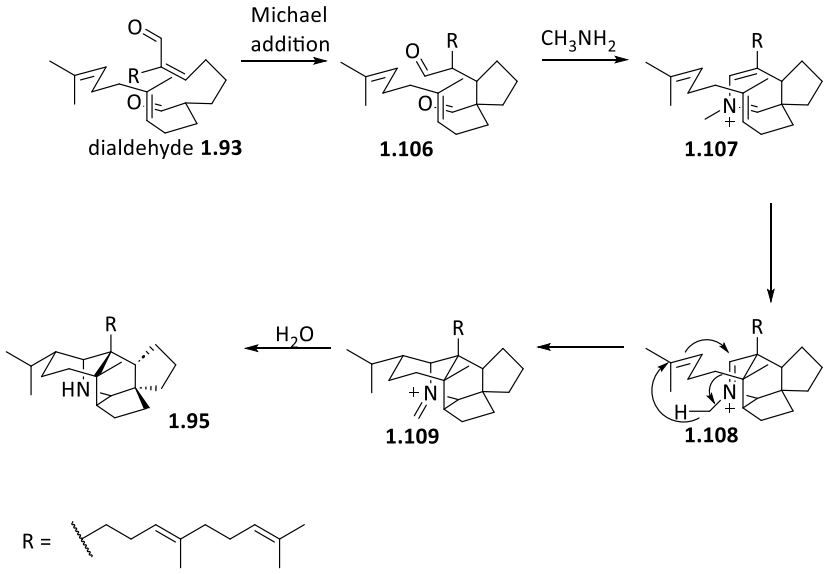

Scheme 1.17 Proposed mechanism of the formation of secodaphniphylline type skeleton as proposed by (Tantillo, 2016).

There are several ways this could be achieved (Scheme 1.18). The nitrogen could be introduced to dialdehyde **1.96** via Heathcock's proposed transamination-like process to obtain **1.100** followed by cyclisation to **1.105.** However, as the nitrogen lacks a methylene group to allow hydride transfer, the product is the incorrect isopropenyl form – "proto-daphniphylline **1.94**" as presented in Scheme 1.15. Alternatively, dialdehyde **1.96** needs to undergo an enzymatic reduction to form dialdehyde **1.93** which could cyclise into **1.106**. This would allow for the introduction of a nitrogen atom through a condensation with an amino acid or an amine forming an iminium ion **1.110**, followed by steps that yield the true secodaphniphylline skeleton with the isopropyl group **1.95**.

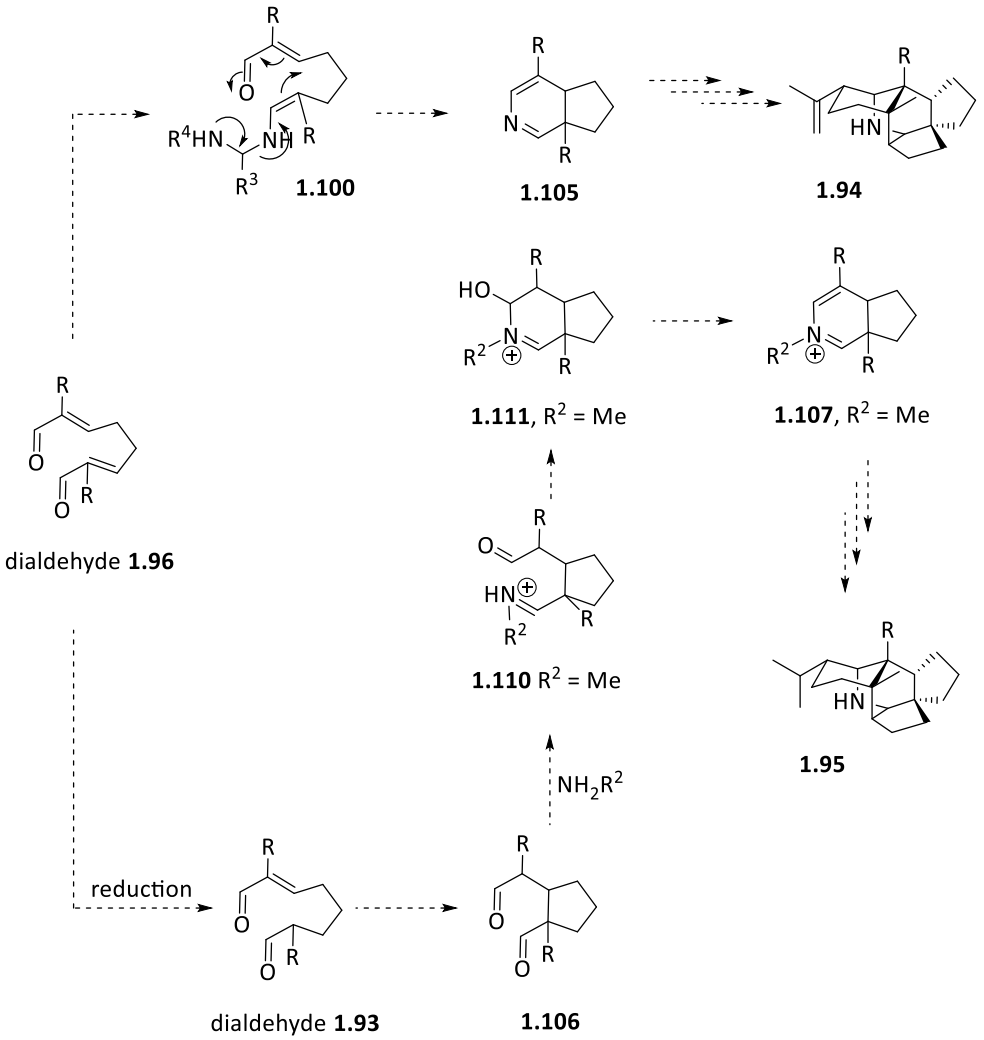

*Scheme 1.18 Proposed steps to "proto-daphniphylline **1.94** and **1.95**".*

It is worth noting that both dialdehydes **1.93** and **1.96** can form the expected scaffolds, although they require different mechanisms to achieve it. Instead, the mechanism of the reaction depends on the type of amine used. It was shown that a reaction with ammonia will yield an "incorrect" **1.94** while a reaction with an alkyl amine or an amino acid would result in the formation of an expected scaffold of **1.95** as it allows for a hydride shift as shown in Scheme 1.17.

Therefore, the true scaffold formation step needs a reduction, introduction of a nitrogen, and an N-methylene group during cyclisation. Introducing the nitrogen via Heathcock's proposed transamination-like process would miss the N-methylene and result in an isopropenyl group as presented in Scheme 1.15 and Scheme 1.18. Consequently, an intermediate, like reduced dialdehyde **1.93** is needed for the efficient

reaction to proceed because it can condense directly with an amino acid or N-R equivalent which is required for the reduced isopropyl group. Alternatively, to achieve a similar isopropyl product, following transamination, further modifications of the nitrogen could occur (i.e. methylation) to insert the required N-methylene.

In summary, the hypothetical pathway towards *Daphniphyllum* alkaloids can be simplified as shown in Scheme 1.19. It starts with sequential oxidation of squalene **1.11** to diol **1.97** and dialdehyde **1.96** followed by steps of reduction, introduction of a nitrogen, and an N-methylene equivalent, resulting in cyclisation leading to the formation of secodaphniphylline type alkaloids. Further modifications and skeletal rearrangements will produce a range of different skeletal families within this class.

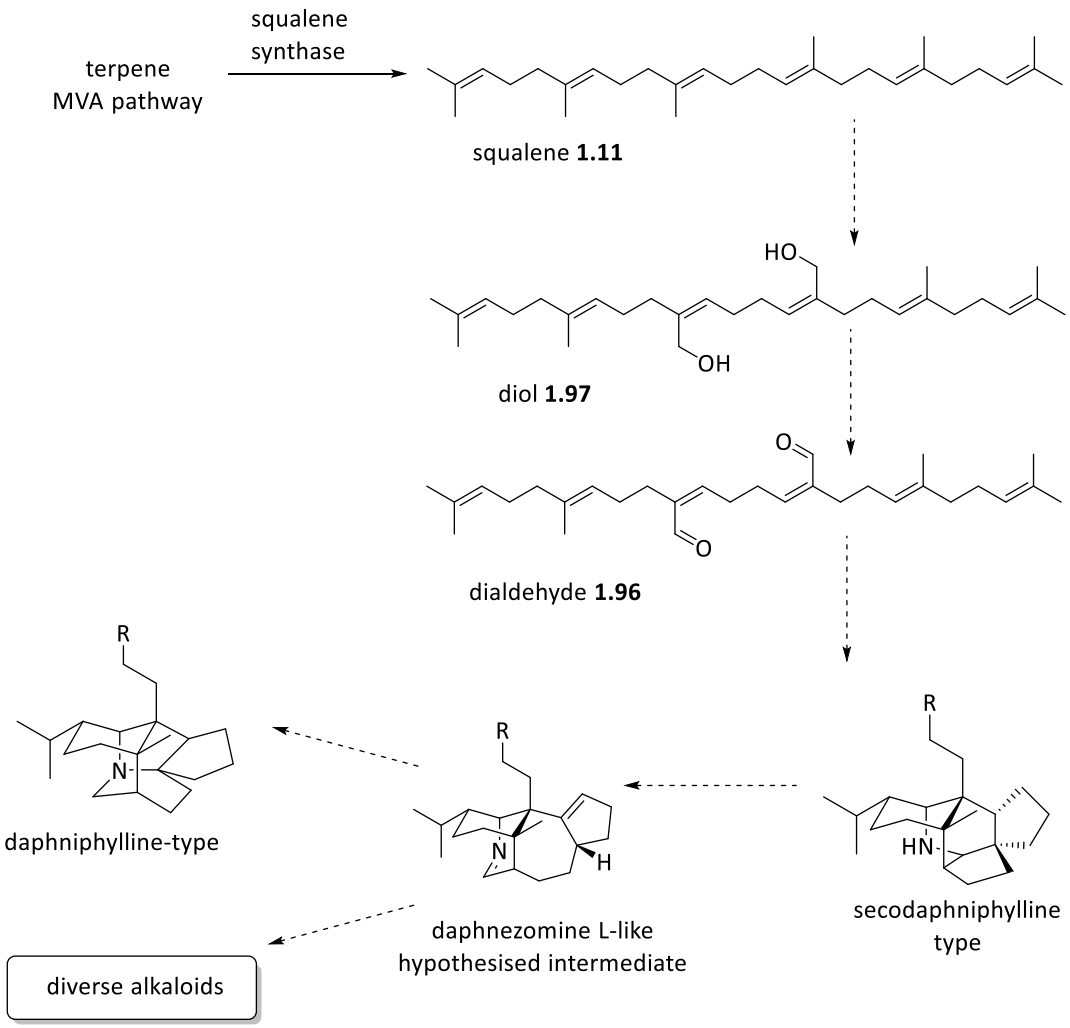

Scheme 1.19 Hypothetical biosynthetic pathway towards Daphniphyllum alkaloids.

While the hypothesis (Scheme 1.19) appears sound and is accepted by the scientific community, the presumed precursors – dialdehyde **1.96** and diol **1.97** – have never been synthesised and the hypothesis has never been tested *in planta*. Also, details of the origin of the nitrogen atom, the site of biosynthesis, and the order of the biosynthetic pathway remain unknown.

1.3 Project Aims

The goal of this project was to gain insight into the early steps of *Daphniphyllum* alkaloids biosynthetic pathway, specifically scaffold forming steps. *Daphniphyllum* alkaloids represent structurally diverse and biologically interesting class of natural products. These alkaloids exhibit a range of pharmacological properties including anticancer, antioxidant, antifungal and vasorelaxant making them a promising target for drug discovery. Although over 330 *Daphniphyllum* alkaloids have been identified and reported, their biosynthesis, particularly the scaffold-forming steps and the origin of the nitrogen within the skeleton, remains not well understood.

To answer questions about the biosynthetic pathway, this study will explore different strategies: synthesis of the hypothesised precursor (chapter 2), isolation of *Daphniphyllum* alkaloids (chapter 3), feeding of substrates to the plant tissue extracts (chapter 4) and investigation into the origin of nitrogen in the skeleton by feeding experiments with isotope-labelled substrates (chapter 5).

Daphniphyllum alkaloids are hypothesised to form by an oxidation of squalene **1.11** to diol **1.97**, dialdehyde **1.96** and subsequent rearrangements. Therefore, in chapter 2, we will focus on the synthesis of diol **1.97** in order to test the hypothesis and gain insight into the first step of the biosynthetic pathway.

In chapter 3, we will aim to isolate *Daphniphyllum* alkaloids from tissues of *D. macropodum* using liquid chromatography – mass spectrometry (LC-MS) to analyse plant tissue and high-performance liquid chromatography (HPLC) to separate and purify alkaloids from the extracts. The alkaloids were then characterised by high resolution mass spectrometry and 1D and 2D nuclear magnetic resonance (NMR) spectroscopy. Characterisation of the isolated alkaloids will provide access to standards, allow us to compare MS^2 fragmentation patterns of different skeletons, and provide substrates for feeding experiments as well as aid gene discovery.

In chapter 4, LCMS analysis of plant tissue extracts will be conducted to test the hypothesis for the biosynthetic pathway. The substrates: squalene **1.11** and synthesised diol **1.97** will be fed to different plant tissue extracts to explore their effect on the metabolite content. High-resolution mass spectrometry will be used to confirm the presence of *Daphniphyllum* alkaloids and determine their molecular formulas. This approach will help to trace the biosynthetic origin of *Daphniphyllum* alkaloids in different tissues as well as investigate the role of the hypothesised precursor diol **1.97** in the pathway.

Finally, in chapter 5 we will investigate the source of nitrogen in the skeleton of *Daphniphyllum* alkaloids. Although previous studies have proposed that nitrogen can be introduced by a spontaneous condensation between an amino acid and an aldehyde, the hypothesis was never tested in planta nor proposed whether it was amino acid specific. To address this, we will use ^{15}N-labelled amino acids as substrates, feeding them into the media of hydroponic seedlings as well as incorporating them into the tissue extract experiments. This part of the study will seek to determine the role and specificity of amino acids in the biosynthetic pathway, thus providing insight into the enzymatic processes involved in alkaloid formation.

Through those aims, this study will contribute towards deeper understanding of *Daphniphyllum* alkaloid biosynthesis. By investigating the first steps of the biosynthetic pathway, isolating standards and investigating the role of the precursors and nitrogen source, we hope to improve our knowledge of this unique class of compounds.

2 Synthesis of diol

2.1 Introduction

2.1.1 *The importance of the hypothesised precursor*

Diol **1.97** dialdehyde **1.96** are hypothesised precursors in the *Daphniphyllum* alkaloid biosynthetic pathway. The hypothetical pathway is distinctive, deviating from the established steroid and terpenoid alkaloid pathways, in which squalene **1.11** is typically oxidised to 2,3-oxidosqualene. Previous studies, particularly biomimetic studies (Heathcock, 1996) showed that dialdehyde **1.93** reacts with methylamine to yield a secodaphniphylline-type skeleton Scheme 2.1 as described in detail in chapter 1 section 1.2.7.

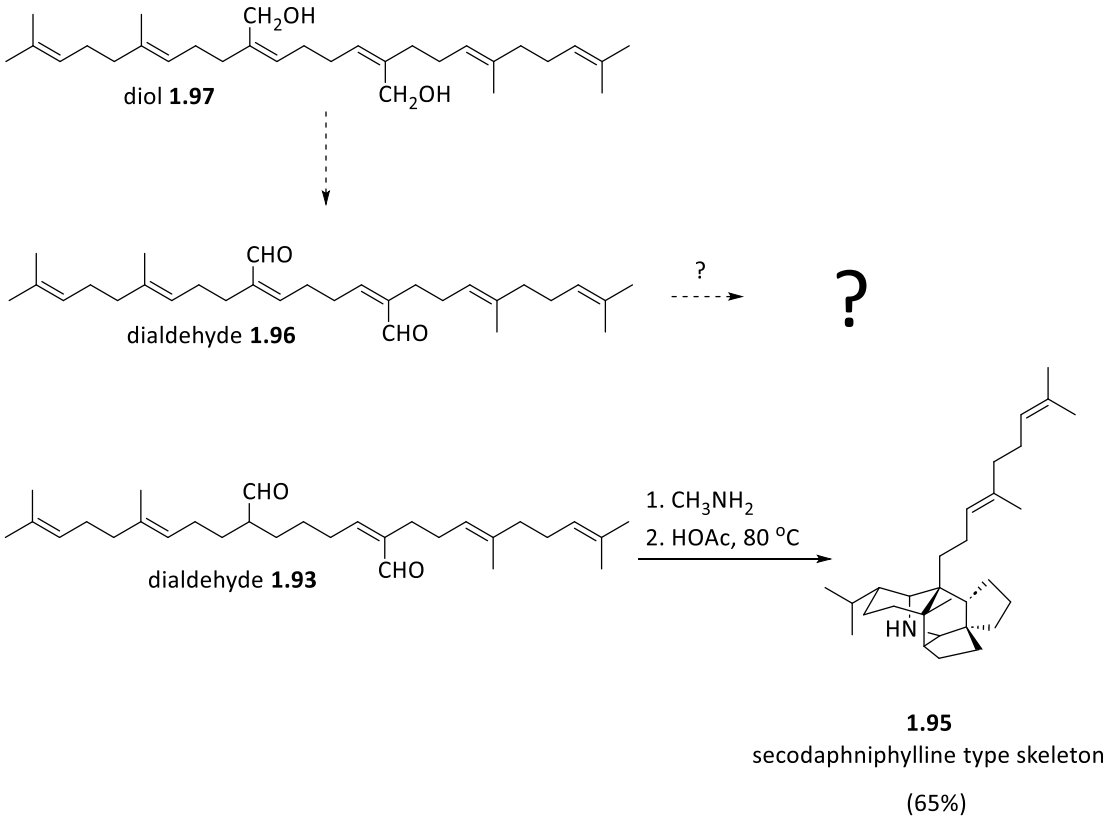

Scheme 2.1 Scheme representing a biomimetic reaction towards secodaphniphylline skeleton (Heathcock, 1996).

The hypothetical biosynthetic pathway towards *Daphniphyllum* alkaloids has not been validated *in planta*, and the synthesis of diol **1.97** has never been achieved. Furthermore, critical questions remain unanswered regarding the initial scaffold-forming steps of the *Daphniphyllum* alkaloid pathway. What is the true precursor? How is nitrogen incorporated into the structure? Are these steps spontaneous or enzymatically driven? Is the pathway tissue-specific?

The work described in this chapter outlines the synthesis of the hypothesised precursor diol **1.97**. We have explored various synthetic approaches with multiple retrosynthetic strategies to yield a successful synthesis of the diol **1.97** as well as addressing challenges such as the symmetry of the molecule and controlling the stereochemistry.

2.1.2 *Synthetic approaches*

Background on the major reactions that feature in the subsequent synthetic work in this chapter is included in the sections below.

2.1.2.1 Wittig reaction

The Wittig reaction is a reaction between a triphenyl phosphonium ylide – sometimes known as a Wittig reagent – and an aldehyde or a ketone, which are converted into alkenes. The stereochemistry of the product is influenced by the stability of the phosphonium ylid. Methylenetriphenylphosphorane is an ylide that is usually prepared in situ by deprotonation of methyltriphenylphosphonium bromide with a strong base (Scheme 2.2). The Wittig reagent replaces oxygen in an aldehyde or ketone with a methylene group. The side product of this reaction is triphenylphosphine oxide.

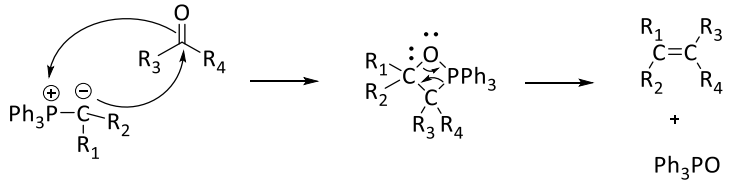

Scheme 2.2 Mechanism of the Wittig reaction.

2.1.2.2 Horner–Wadsworth–Emmons olefination

Horner–Wadsworth–Emmons reaction works similarly to the Wittig reaction. While in the Wittig reaction phosphonium ylid is used, in the Horner-Wadsworth-Emmons olefination phosphonate ester-stabilised carbanions are used instead. To obtain an *E*-stereoisomer, the phosphonate esters used are deprotonated with a strong base to form a stabilised anion, which subsequently reacts with an aldehyde to produce an alkene, usually with high *E*-selectivity (Scheme 2.3). In this reaction, as all of the steps leading to alkene formation are usually reversible, which favours formation of the more thermodynamically stable *E*-stereoisomer for steric reasons.

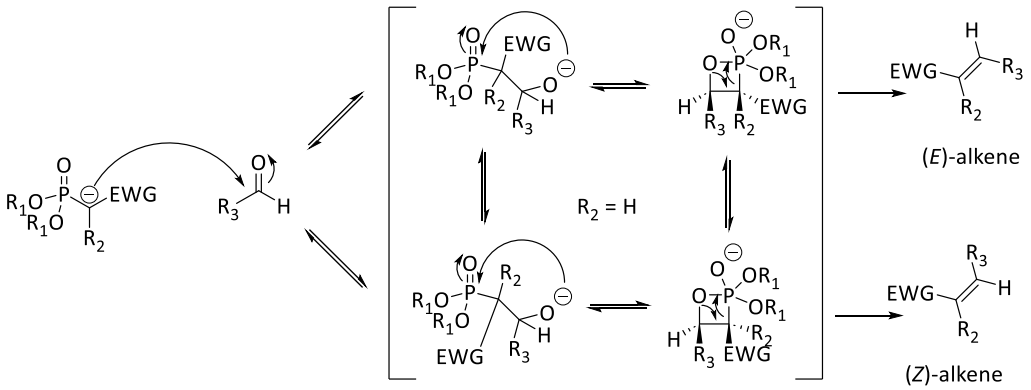

Scheme 2.3 Mechanism of Horner–Wadsworth–Emmons olefination.

2.1.2.3 Still Gennari reaction

A variation of HWE reaction was developed which predominantly gives Z-alkenes (Still and Gennari, 1983). This method involves the use of phosphonate esters with electron withdrawing groups, most commonly the trifluoroethyl group. This method was then further modified for the synthesis of vinyl bromide products, specifically (*E*)-α-bromoacrylates. This resulted in the development of a novel reagent bis(2,2,2-trifluorethyl)bromophonoacetate **2.3** which was prepared from bis(2,2,2-trifluorethyl)phonoacetate **2.1** (Scheme 2.4) (Tago and Kogen, 2000b). The procedure to prepare bis(2,2,2-trifluorethyl)bromophonoacetate was adopted from (McKenna and Khawli, 1986), however the products included a mixture of an over-reduced product **2.1**, unreacted **2.2** and the desired product **2.3**. This necessitated separation and the overall yield was low (35%).

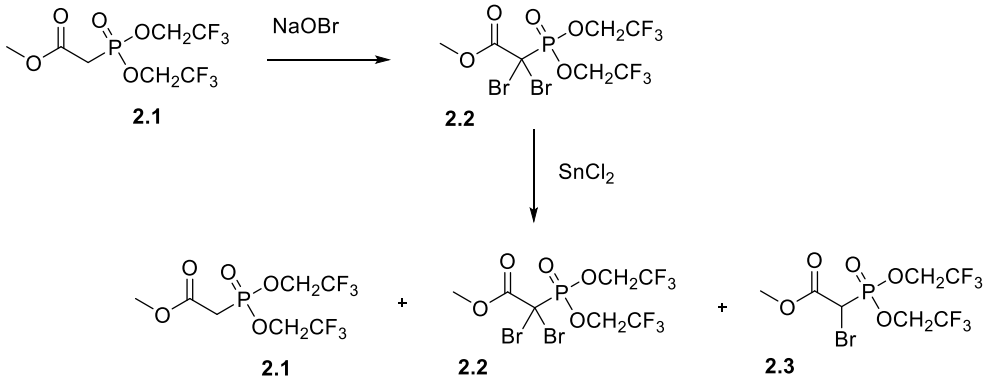

*Scheme 2.4 Bromination of Still-Gennari reagent **2.1**.*

To improve the synthesis of (*E*)-α-bromoacrylates, the procedure was further modified as a one-pot procedure for the preparation of (*E*)-α-bromo-α,β-unsaturated esters. Firstly, the one-pot reaction involved modification of a previously published procedure (Wadsworth and Emmons, 1961) in which a phosphonate anion was halogenated in situ, followed by an addition of an aldehyde or ketone to yield a vinylic halide **2.5**. The product **2.5** was formed as a mixture of *Z*- and *E*-isomers Scheme 2.5. The same group also further modified the procedure for use on ethyl bis(trifluoroethyl)phosphonoacetate **2.6** (Qing and Zhang, 2001).

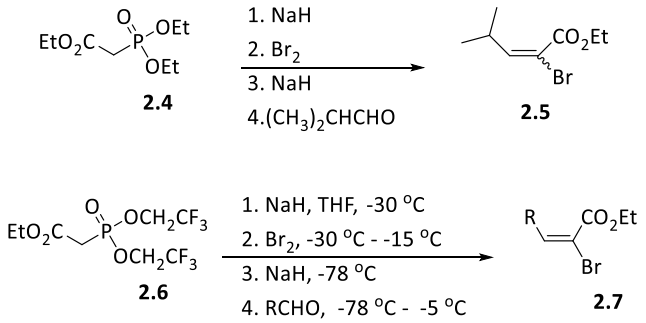

Scheme 2.5 Literature one pot synthesis of (E)-α-bromo-α,β-unsaturated esters

The mechanism for the synthesis of vinyl bromide **2.9** is summarised below (Scheme 2.6). Ethyl bis(trifluoroethyl)phosphonoacetate **2.6** is reacted in a one pot reaction with sodium hydride to generate the phosphonate anion **2.7**. The addition of bromine and sodium hydride then generates **2.8** following bromination and subsequent

deprotonation, which is then reacted with aldehydes to yield (E)-α-bromo-α,β-unsaturated ester **2.9** with high stereoselectivity (Qing and Zhang, 2001).

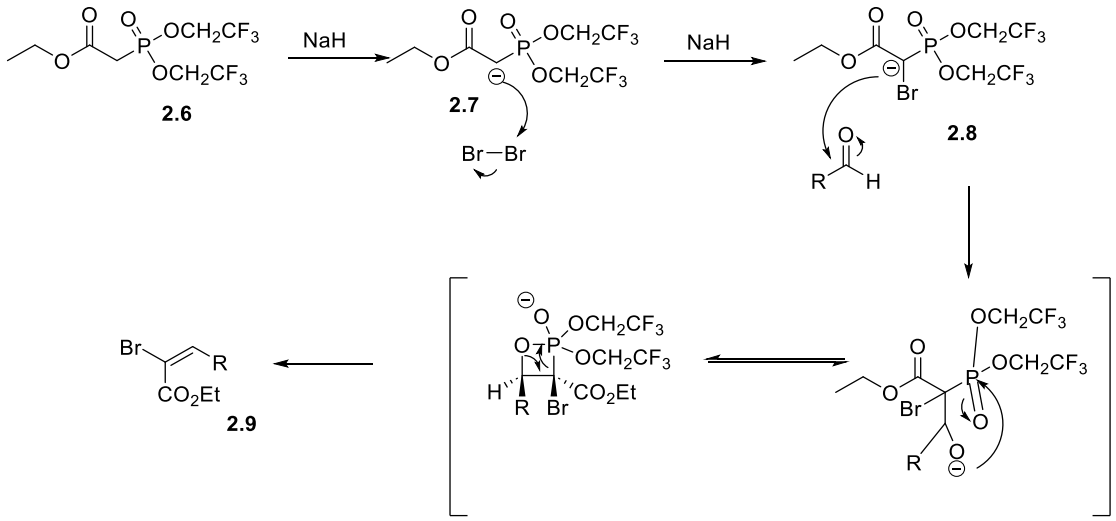

Scheme 2.6 Mechanism of one pot Still-Gennari HWE reaction resulting in (E)-α-bromo-α,β-unsaturated ester2 ***2.9****.*

2.1.2.4 Suzuki-Miyaura cross-coupling

The Suzuki-Miyaura cross-coupling is a well-known catalytic reaction used to form carbon-carbon bonds. In this reaction an organoborane (usually an boronic acid or boronic ester), is coupled with an aryl or vinyl halide catalysed by a palladium catalyst and a base (Miyaura and Suzuki, 1995). A typical Suzuki-Miyaura catalytic cycle has three major steps: oxidative addition, transmetallation and reductive elimination (Scheme 2.7).

First, the active palladium species LnPd(0) is reacts with the aryl or vinyl halide by insertion into the carbon halide bond, to form an organopalladium complex. This is known as the oxidative addition step, and during it palladium(0) is oxidised to palladium(II). Then, in the transmetallation step, which is usually promoted by the addition of base, the other carbon group being coupled is transferred from the organoboron – to form a new palladium complex. Finally, in the reductive elimination step, the C–C bonded product is formed, while palladium(0) catalyst is regenerated, which closes the catalytic cycle (Matos and Soderquist, 1998; Amatore, Jutand and Le Duc, 2011; Smith et al., 1994). Suzuki-Miyaura cross-coupling reactions sometimes need

much optimisation since there are multiple elements in the catalytic cycle which need to be coordinated together.

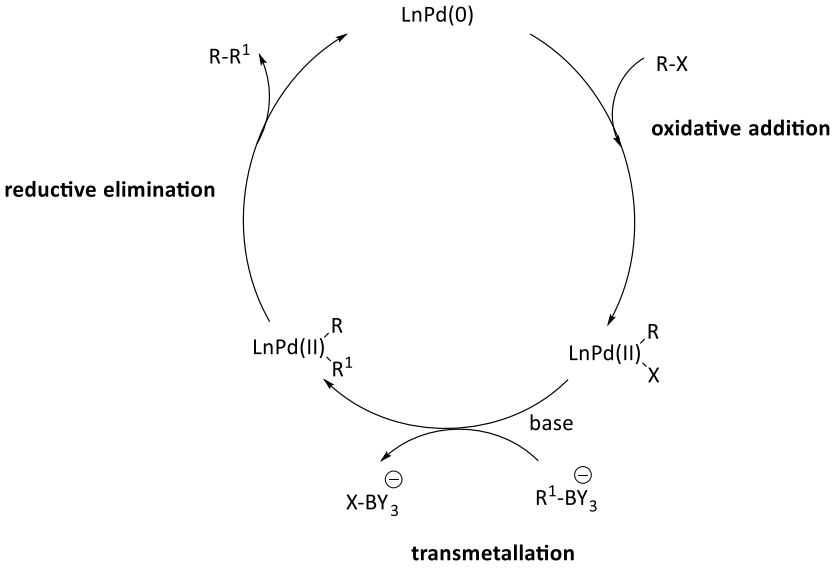

Scheme 2.7 Catalytic cycle of Suzuki cross-coupling, R and R_1 = H, aryl, alkene, alkyne; X = halide.

2.1.3 *Aims*

Elucidation of the biosynthetic pathway of *Daphniphyllum* alkaloids will allow us to gain access to complex bioactive structures in this pathway that do not appear in high abundance in nature. Currently we are unable to isolate them on the high scale due to the slow growth of the plant, low accumulation and the complexity of the extracted mixture of alkaloids. Additionally, through understanding of the biosynthetic pathway we will gain access to the novel enzymatic space that *Daphniphyllum* genus has created.

The goal of this work described in this chapter is to develop a synthetic pathway towards the hypothesised precursor in *Daphniphyllum* alkaloids biosynthetic pathway – diol **1.97**. Having access to the hypothesised precursor **1.97** will allow us to test the hypothetical biosynthetic pathway.

2.2 Synthesis of the hypothesised precursor

This chapter reviews the various strategies explored towards the synthesis of diol **1.97**. NMR spectra can be found in the Appendix 8.1.

2.2.1 *First attempt using Horner–Wadsworth–Emmons reaction and Suzuki cross-coupling*

In search of inspiration, we examined the literature to find the successful synthesis of similar compounds. At that time, an elegant synthesis of plaunotol via Suzuki cross-coupling was found (Tago and Kogen, 2000a). Plaunotol is a diterpenoid alcohol isolated from the leaves of the plant *Croton stellatopilosus* (plaunoi). The biosynthetic pathway has already been solved, with the main difference being that in squalene isoprenyl units are connected “head to tail”, which produces the characteristic structure of squalene. The final biosynthetic step to form plaunotol is proposed to be the hydroxylation of the methyl group, similarly to the proposed oxidation of diol **1.97**.

Based on this precedent, a strategy was proposed, as presented in Scheme 2.8. The target molecule diol **1.97** can be obtained by DIBAL-H reduction of diester **2.10**. The diester **2.10** could be produced by a Suzuki cross-coupling between a vinyl bromide **2.11** and an alkene **2.12**. The alkene **2.12** can be prepared from geraniol **2.18** which undergoes first an oxidation and then a Wittig reaction. Indeed, a route to alkene **2.12** has already been published. The route to the vinyl bromide **2.11** was more complex. Initially, it would be prepared from brominated Still-Gennari reagent **2.14** and aldehyde **2.13**. Still-Gennari reagent **2.14** is commercially available. An aldehyde **2.13** would be prepared from an alkene **2.12** and a vinyl bromide **2.15** with a protective group in a Suzuki cross-coupling. An appropriate deprotection or deprotection and oxidation would yield an aldehyde **2.13**. Finally, a protected aldehyde **2.15** would be produced by a Still-Gennari reaction between a Still-Gennari reagent **2.14** and an aldehyde containing four carbons and a protective group which would yield a second aldehyde.

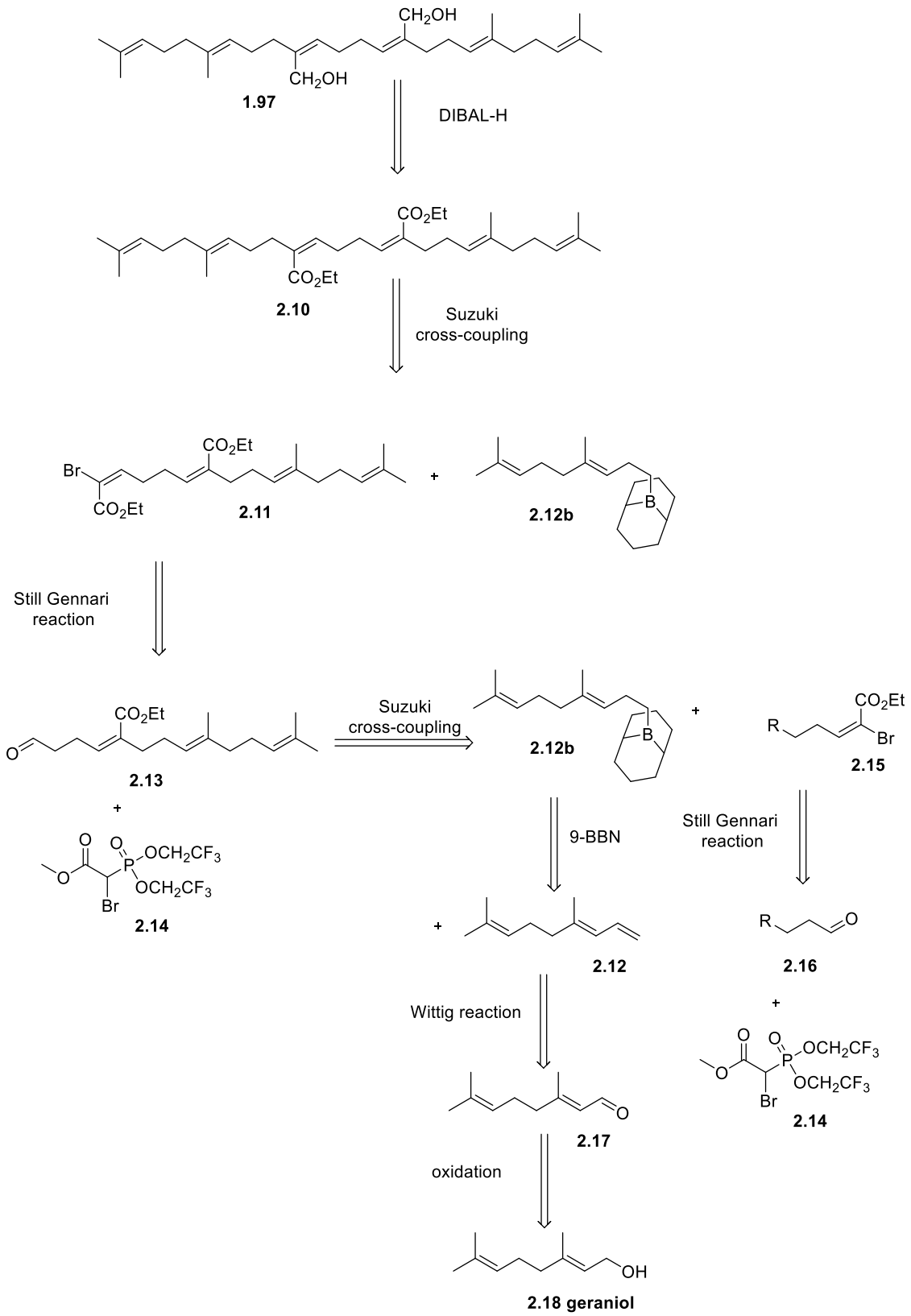

*Scheme 2.8 Retrosynthetic approach to diol **1.97** using Still Gennari and Suzuki cross-coupling reactions.*

2.2.1.1 Synthesis of the vinyl bromide 2.15.

To synthesise the vinyl bromide **2.15,** we followed a previously published one-pot procedure (Qing and Zhang, 2001), with a range of different aldehydes explored. Initially, we chose an aldehyde with a *tert*-butyldimethylsilyl protective group **2.19** (Scheme 2.9). Using the one pot method, the product **2.20** was produced at a low yield of 17% with the E:Z ratio of 8:1 (Figure 2.1).

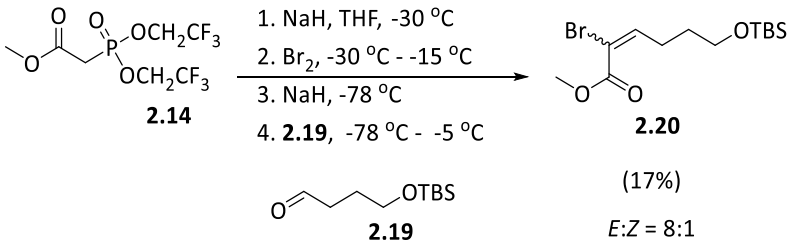

*Scheme 2.9 One pot Still-Gennari reaction towards a vinyl bromide **2.20**.*

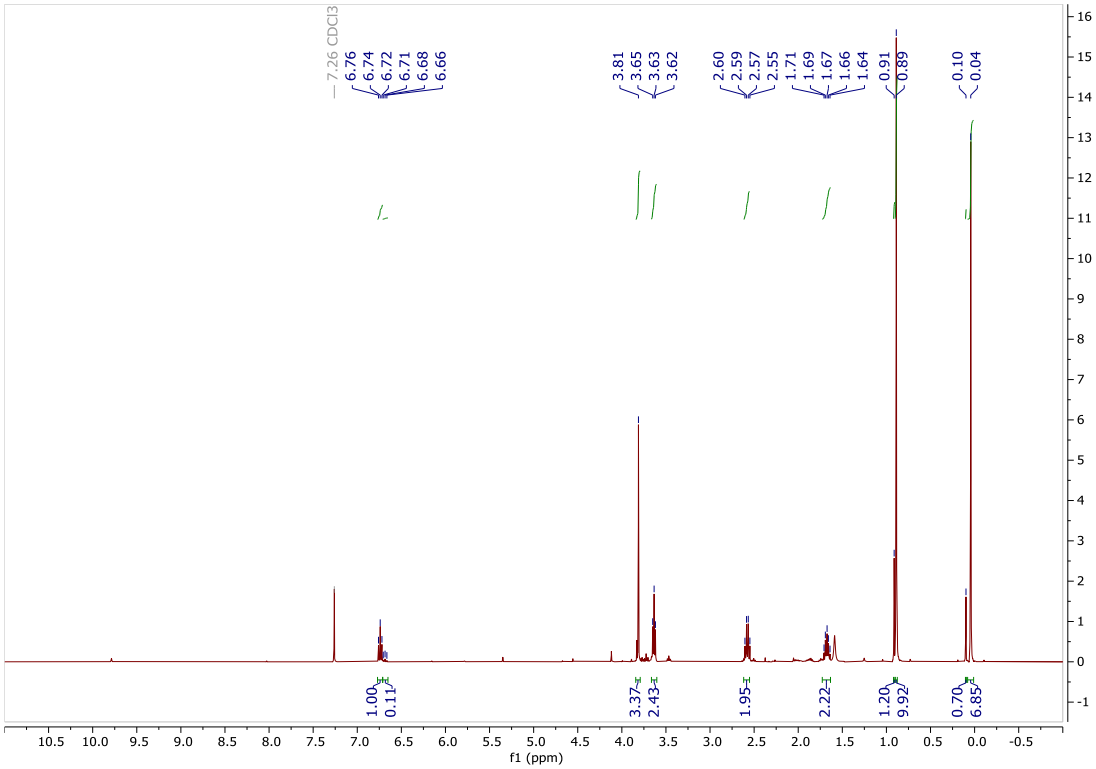

*Figure 2.1 ^{1}H NMR spectrum of **2.20** in $CDCl_3$.*

We questioned whether the low yield could have been caused by low compatibility of with the *tert*-butyldimethylsilyl protective group with the basic reaction conditions and so instead we decided to use an aldehyde **2.21** with a more stable triisopropylsilyl

protective group instead (Scheme 2.10). Using this aldehyde, the yield improved greatly to 70% and the stereochemical control was much higher with the *E*:Z ratio measured to be 50:1 (Figure 2.2). This result was promising so we proceeded to the next step, which was a removal of TIPS protecting group. Unfortunately, cleavage of the TIPS group proved to be more challenging, with the compound being unstable in the reaction with 3 equiv of 1 M TBAF over 1 h in THF. Conversion of **22.2** into an alcohol **2.23** was unsuccessful as the basic conditions lead to the decomposition of **2.23**.

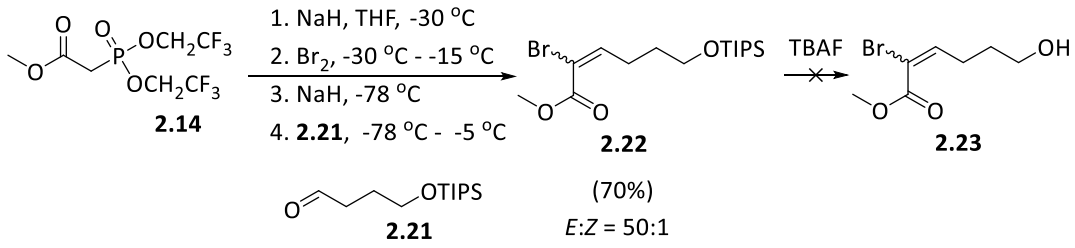

*Scheme 2.10 One pot Still-Gennari reaction towards a vinyl bromide **2.22**.*

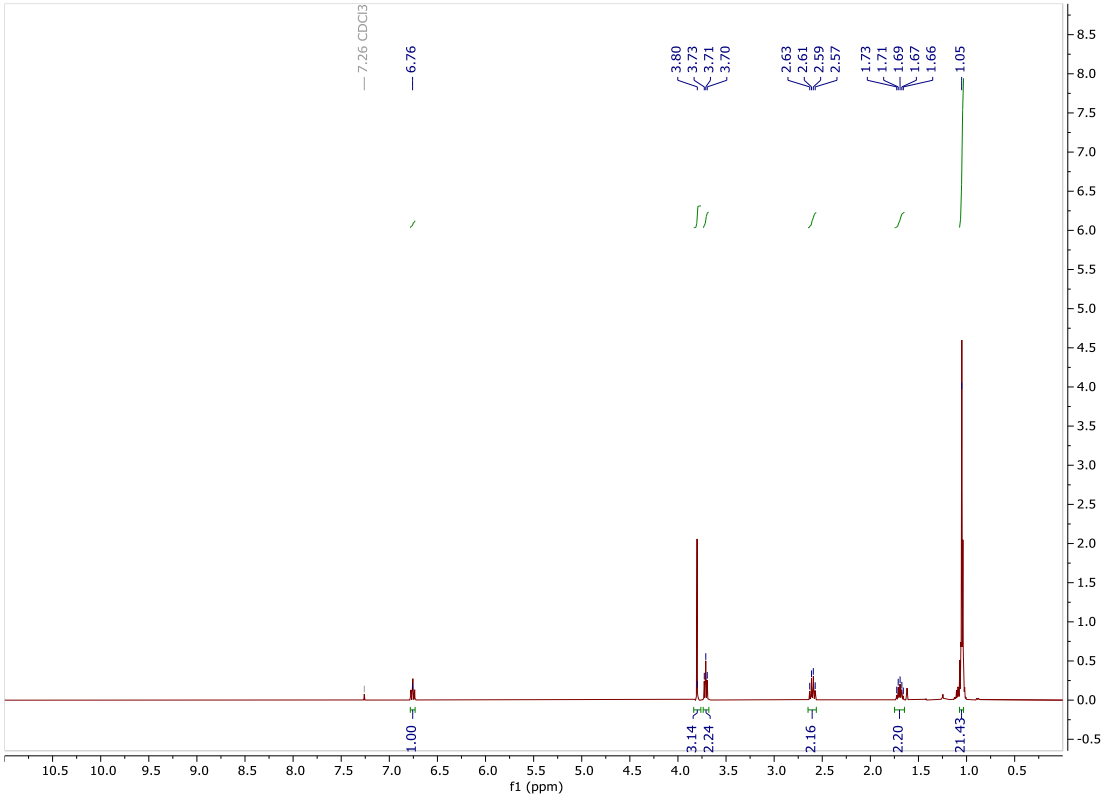

*Figure 2.2 ^{1}H NMR spectrum of **2.21** in $CDCl_3$.*

At this point, we questioned whether the alcohol revealed following the protecting group cleavage might be the reason for the instability of the product formed following TIPS cleavage. Therefore, we decided to attempt a Still-Gennari reaction with an aldehyde having terminal alkene **2.24** to form vinyl bromide **2.25** (Scheme 2.11)**.** The idea was that the terminal alkene **2.25** could then form an aldehyde **2.26** directly in an ozonolysis reaction and thus avoid an alcohol intermediate. Unfortunately, the one-pot Still-Gennari reaction between **2.14** and **2.24** did not work and unreacted Still-Gennari reagent **2.14** was recovered.

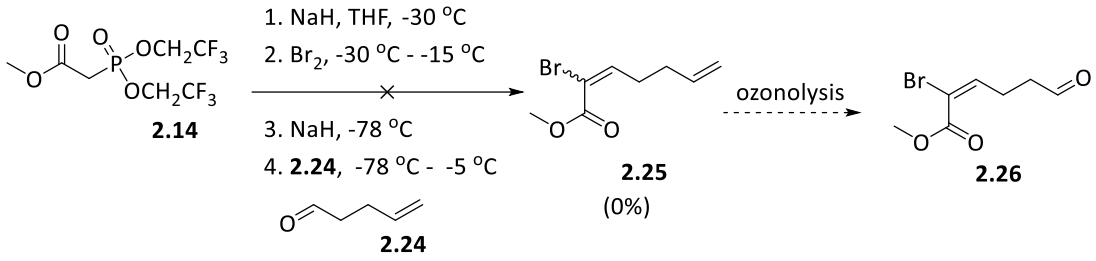

*Scheme 2.11 One pot Still-Gennari reaction towards a vinyl bromide **2.25**.*

Nevertheless, we wanted to continue with a protective group that would yield an aldehyde since we thought it would be beneficial for the stability of the intermediate. We therefore next chose an aldehyde with a tethered 1,3-dioxane ring **2.27** – i.e. an acetal protecting group**.** The acetal ring can be cleaved using TFA later, to reveal an aldehyde. We therefore repeated the Still-Gennari reaction using aldehyde **2.27** (Scheme 2.12). The reaction yielded the product **2.28** in a high yield (84%) with a high stereochemical control (*E*:*Z* of 16:1) (Figure 2.3). Next, we deprotected the acetal using TFA for 3 days, which resulted in the formation of aldehyde **2.29** in an excellent yield of 90%. This showed that the product could be deprotected easily. However, the addition of TFA caused isomerisation, altering the E:Z ratio to 1:0.3. As a result, we decided not to explore other aldehyde options which could improve the stereochemical control of the final product. Nonetheless, with this route we had successfully obtained the first brominated building block, giving hope that this approach might be viable.

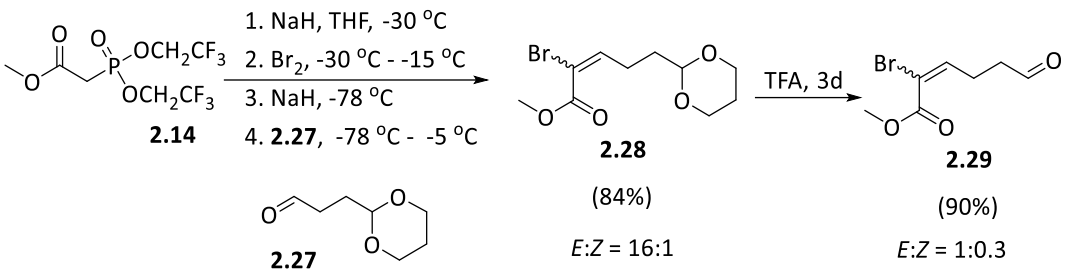

*Scheme 2.12 One pot Still-Gennari reaction towards a vinyl bromide **2.29**.*

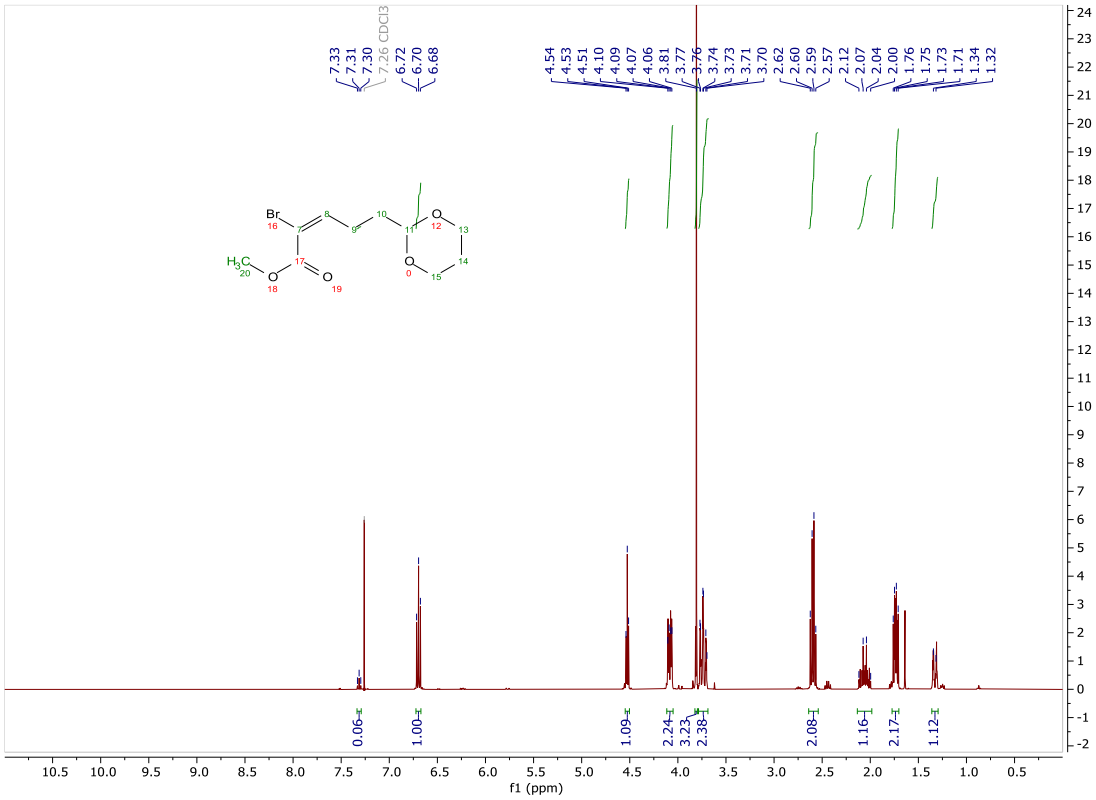

*Figure 2.3 ^{1}H NMR spectrum of **2.28** in $CDCl_3$.*

2.2.1.2 Suzuki cross-coupling

Geraniol **2.18** was oxidised in an excellent yield using manganese(IV) oxide to afford aldehyde geranial **2.17**. The carbon chain could then be extended via a Wittig reaction, with aldehyde **2.17** being converted into alkene 2.12 in an 84% yield (Scheme 2.13).

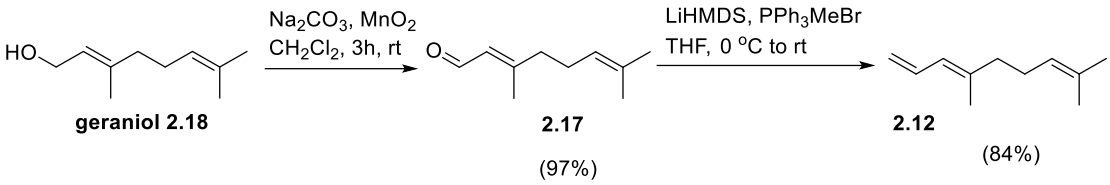

*Scheme 2.13 Synthetic route to alkene **2.12**.*

Having synthesised both alkene **2.12** and the vinyl bromide **2.28,** we proceeded with finding optimal conditions for Suzuki-Miyaura cross-couplings.. The coupling was investigated using both single brominated substrate **2.28** and the di brominated substrate **2.30**. The alkene **2.12** was firstly used to form **2.12b** *in situ* in a reaction with 0.5 M 9-BBN (Scheme 2.14). Next, freshly prepared **2.12b** would react with the vinyl bromide **2.28,** a palladium catalyst and a base.

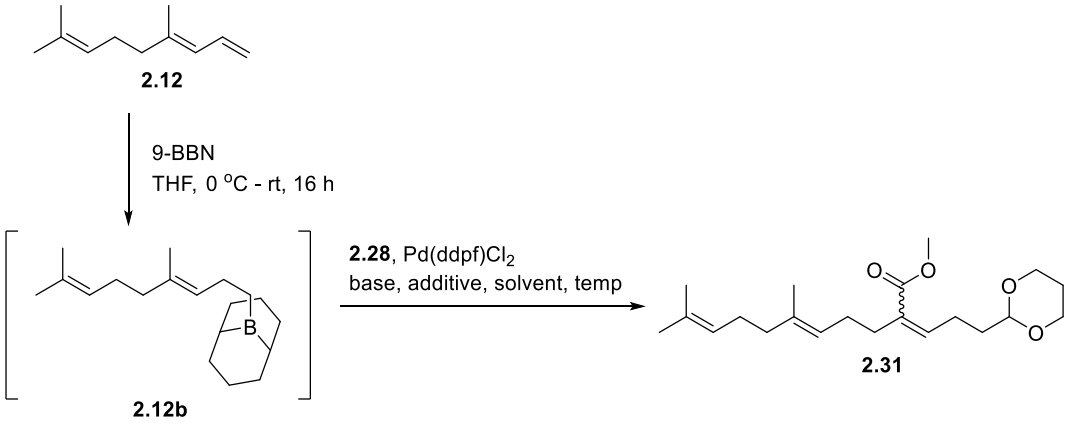

*Scheme 2.14 Suzuki cross-coupling to **2.31**.*

None of the attempted Suzuki-Miyaura cross-coupling reactions were successful. An overview of all attempted conditions is shown in Table 2.1.

Table 2.1 Comparison of Suzuki cross-coupling conditions.

Vinyl bromide	Palladium catalyst	Base	Additive	Solvent	Temp	Time	Yield
2.28	$Pd(dppf)Cl_2$	K_3PO_4	N/A	THF	reflux	12 h	0%
2.28	$Pd(dppf)Cl_2$	Cs_2CO_3	Ph_3As	DMF	reflux	12 h	0%
2.28	$Pd(dppf)Cl_2$	3M NaOH	N/A	THF	reflux	12 h	0%

Unfortunately, this approach was ultimately not successful for the synthesis of diol **1.97** or specifically the intermediate **2.31**. Although we varied the bases and solvents, we did not alter the catalyst or reaction times. Whilst it is possible that a target molecule could be synthesised using Suzuki cross-coupling with further optimisation, we considered an alternative approach due to the difficulties we encountered.

2.2.2 *Second attempt using consecutive alkylation*

A new synthetic route was conceived, involving consecutive LDA-mediated alkylation reactions (Scheme 2.15). It was proposed that diester **2.10** could be synthesised in an alkylation reaction between silyl ester **2.31** and an aldehyde **2.35**. The silyl ester **2.31** could in turn be synthesised from **2.31** and **2.32**. Alkyl iodide **1.87** could be obtained from geraniol **2.18**. Geraniol **2.18** was therefore identified as being a useful precursor, due to its pre-existing isoprene skeleton. The challenge lay in modifying geraniol **2.18** sufficiently so it can be extended. Finally, an aldehyde **2.13** could be formed in an alkylation reaction between silyl ester **2.31** and an aldehyde **2.16** with an appropriate protective group which can be deprotected to an aldehyde, similarly to the strategy we used previous in Scheme 2.12. This proposal follows closely the synthesis of dialdehyde **1.93** (Heathcock et al., 1992b) with the modification which would allow for the addition of an additional double bond as required for the squalene-like skeleton.

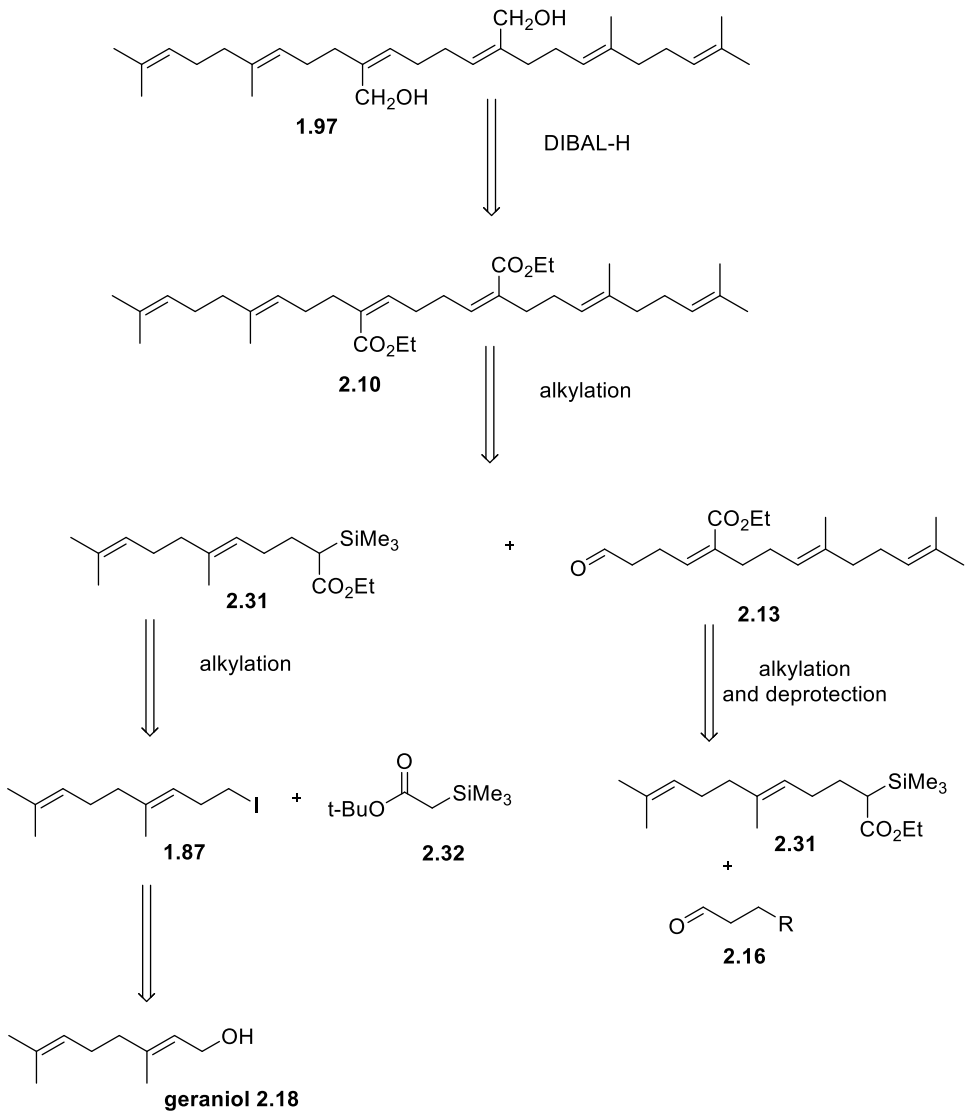

*Scheme 2.15 Retrosynthetic approach to diol **1.97** using LDA alkylation.*

2.2.2.1 Synthesis of homo-geranyl iodide 1.87.

Alkene **2.12** was synthesised as described previously (see section 2.2.1.2). To further functionalise alkene **2.12**, a leaving group needed to be introduced. We synthesised homo-geranyl iodide **1.87** following previously published method (Kocienski, Wadman and Cooper, 1989; Leopold, 1986). Firstly, the alkene **2.12** was hydroborated with 9-borabicyclo[3.3.1]nonane (9-BBN). The use of bulky 9-BBN allowed for the hydroboration to be performed with high regioselectivity, as boron preferentially adds to the least hindered carbon on the alkene. The subsequent oxidation of the formed borane **2.12b** with 30% hydrogen peroxide yields an anti-Markovnikov alcohol **2.35**. The

alcohol **2.35** was then converted into alkyl iodide **1.87** in an Appel reaction with iodine and triphenylphosphine in a high yield. This route (summarised in Scheme 2.16) afforded homo-geranyl iodide **1.87** in an overall yield of 25%.

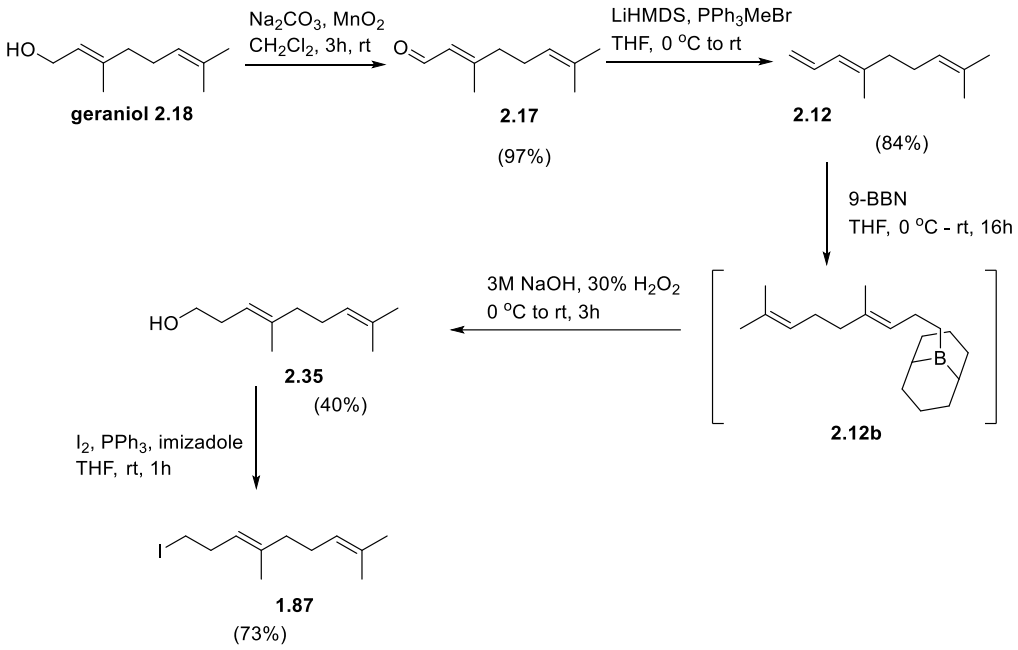

*Scheme 2.16 Synthetic route to homo-geranyl iodide **1.87**.*

2.2.2.2 Synthesis of the aldehyde 2.38

Having synthesised homo-geranyl iodide **1.87**, it reacted with trimethylsilyl acetate **2.24** to yield the product **2.31** in a good yield of 65% (Scheme 2.17), via an LDA mediated alkylation reaction. Then, the product **2.31** was used in another LDA mediated reaction, but this time the enolate formed following reaction with LDA was reacted with aldehyde **2.36**, in a Peterson type olefination (Peterson, 1968). The product **2.37** was formed in moderate yield of 44% as two stereoisomers and finally, the hydrolysis of **2.37** gave aldehyde **2.38** in an excellent yield as shown in Scheme 2.17.

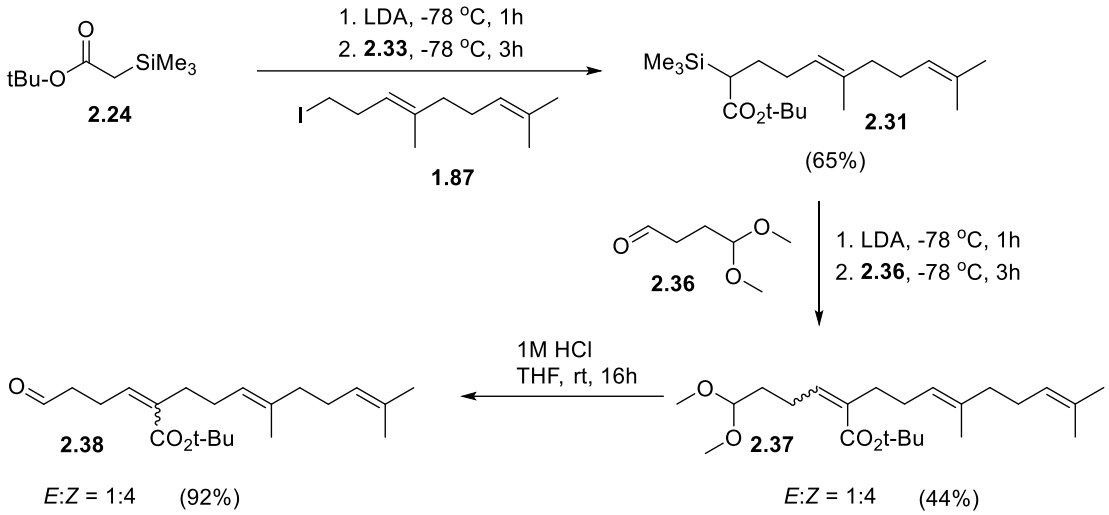

*Scheme 2.17 Synthetic route towards aldehyde **2.38**.*

In literature data for related ester compounds (Heathcock et al., 1992b) the alkene proton for the *E* stereoisomer is generally significantly more downfield than the *Z* isomer (ca. 6.6 ppm for *E* and ca 5.7 ppm for *Z*). Therefore, based on this, in the ^{1}H NMR spectrum of an aldehyde **2.38** (Figure 2.4), a triplet at 6.57 ppm was assigned to *E* stereoisomer and a triplet at 5.74 ppm to Z stereoisomer. The triplets were present 1:4 ratio (E:Z = 1:4).

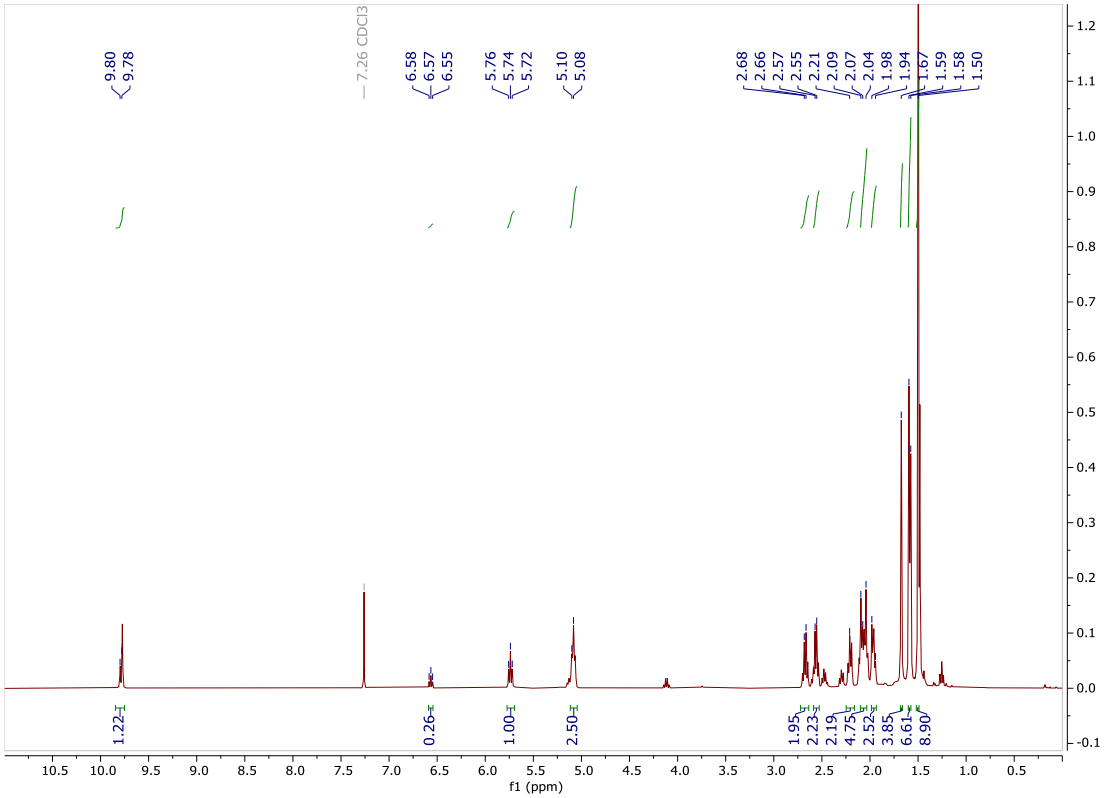

*Figure 2.4 ^{1}H NMR spectrum of **2.38** in $CDCl_3$.*

2.2.2.3 Final alkylation step

With the aldehyde **2.38** successfully synthesised, we wanted to use it in the final alkylation step with the silyl ester **2.31** (Scheme 2.18). Unfortunately, this reaction did not yield the expected product; a HREIMS mass peak for the desired product **2.10** was not observed when the crude reaction mixture was analysed, and the ^{1}H NMR spectrum of the crude mixture did not show presence of the new double bond at the expected ppm consistent with product formation. We were unable to identify the product of this reaction.

This result was surprising as a similar compound was synthesised successfully by Heathcock et al. starting from **2.24**. The main difference consisted of an additional double bond in **2.38**. Nevertheless, we did not explore the reasons why the reaction failed, nor did we attempt to vary any conditions.

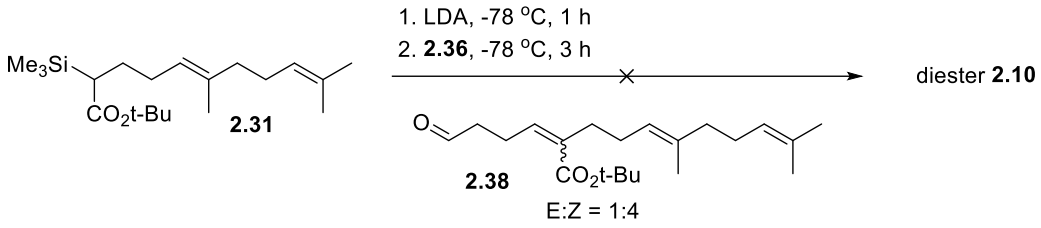

*Scheme 2.18 Synthetic route towards diester **2.10**.*

2.2.3 *Third generation retrosynthetic approach*

We decided to revise the synthesis once more to successfully synthesise diol **1.97**. Although the new synthetic scheme involved creating that double bond in an additional step, we hoped it would yield a targeted compound since it followed closely a similar route as described by (Heathcock et al., 1992b) and presented in Scheme 2.19. An aldehyde **2.34**, synthesised following the method described before, can be condensed with a lithium enolate of **2.39** to yield β-hydroxy ester **2.38**. The elimination of the hydroxy group would form the double bond leading to the formation of diester **2.10** which could be reduced to diol **1.97**.

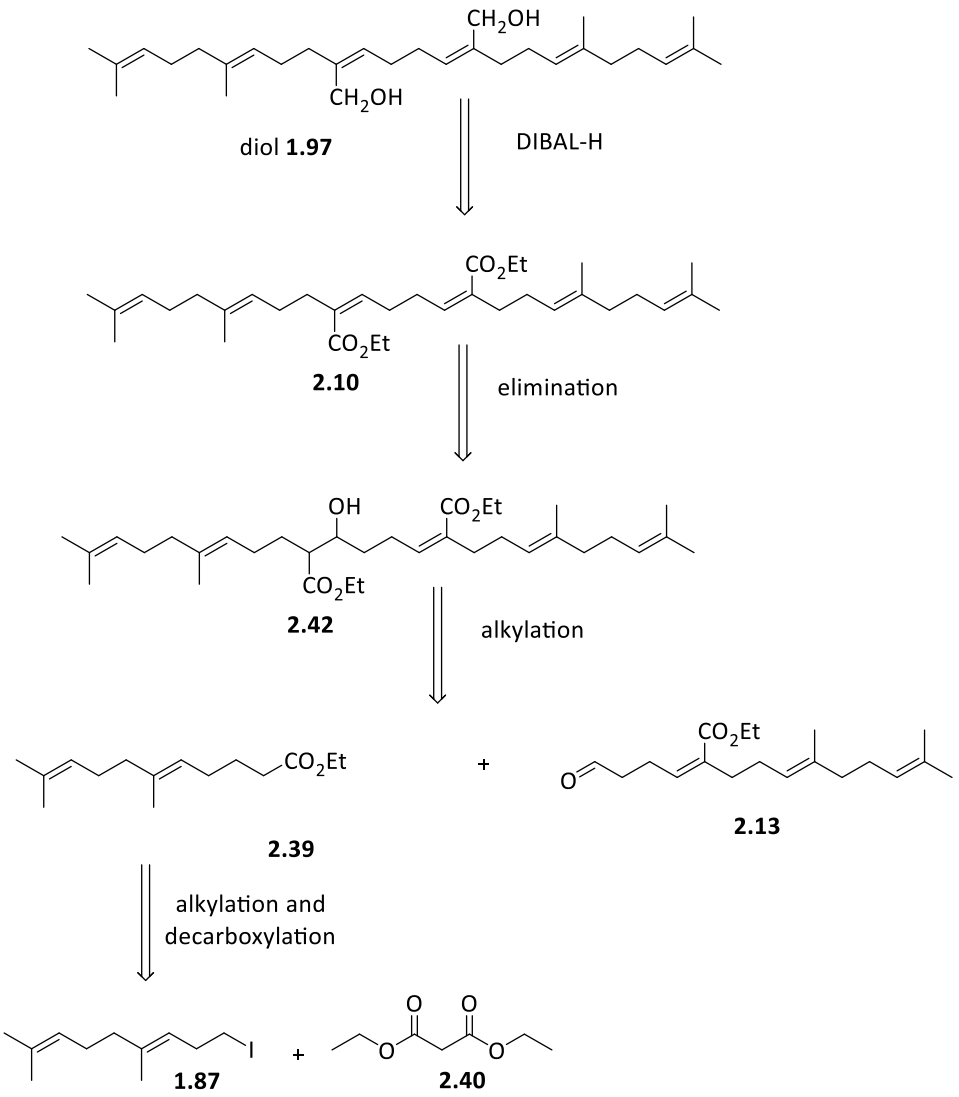

*Scheme 2.19 Retrosynthetic approach to diol **1.97** using LDA alkylation.*

2.2.3.1 Synthesis of the ester 2.39

Diethyl malonate **2.40** reacted with sodium ethoxide (itself prepared in situ by adding sodium metal to ethanol) to form an enolate. This in turn reacted with the previously synthesised homo-geranyl iodide **1.87** to give **2.41** in a 75% yield (Scheme 2.20). We followed a previously published method (Koohang et al., 2010).

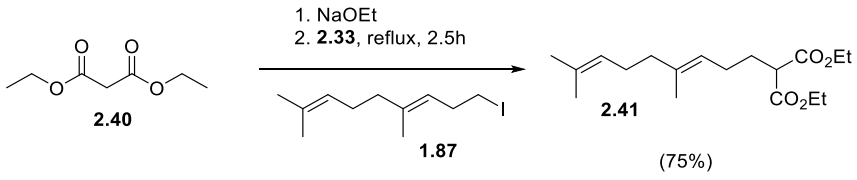

*Scheme 2.20 Synthesis of **2.41**.*

The malonic ester **2.41** was decarboxylated following Krapcho decarboxylation, using lithium chloride and water in DMSO at high temperature. This method allowed for the hydrolysis and decarboxylative cleavage of only one ester group to form **2.39** in a good yield (Scheme 2.21). **2.39** is a known compound, however we managed to formed it in a higher yield, compared to reported 28% (Eichelberger et al., 2002), showing that Krapcho decarboxylation is a more efficient way to obtain compound like **2.39**.

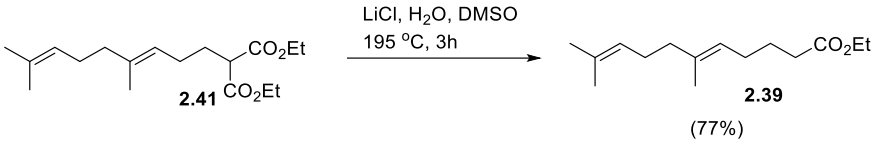

*Scheme 2.21 Synthesis of **2.39**.*

2.2.3.2 Synthesis of β-hydroxy ester 2.42

Previously synthesised aldehyde **2.38** was condensed with the lithium enolate of **2.39** which yielded β-hydroxy ester **2.42** (Scheme 2.22).

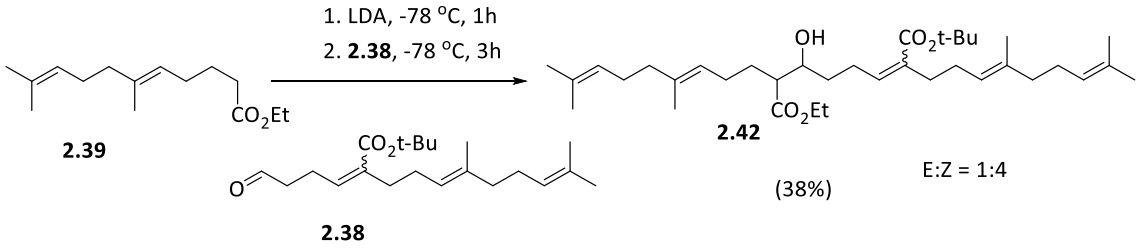

*Scheme 2.22 Synthesis of β-hydroxy ester **2.42**.*

The product **2.42** was formed successfully in moderate yield of 38% as a 1:4 mixture of geometrical isomers based on analysis of its ^{1}H NMR spectrum (**Error! Reference source not found.**). As described previously for compound **2.38**, we assigned a triplet at 6.62 ppm to *E* isomer and a triplet at 5.70 ppm to *Z* isomer. The triplets appeared in E:Z = 1:4 ratio.

Heathcock et al. reported the synthesis of a compound structurally similar to **2.42**, different only by the absence of a double bond adjacent to the ester moiety and achieved a significantly higher yield (70%). While our attempt at this reaction was limited

to a single trial without any optimisation, the difference in yield raises the question of how the presence of an additional double bond may influence the reaction outcome.

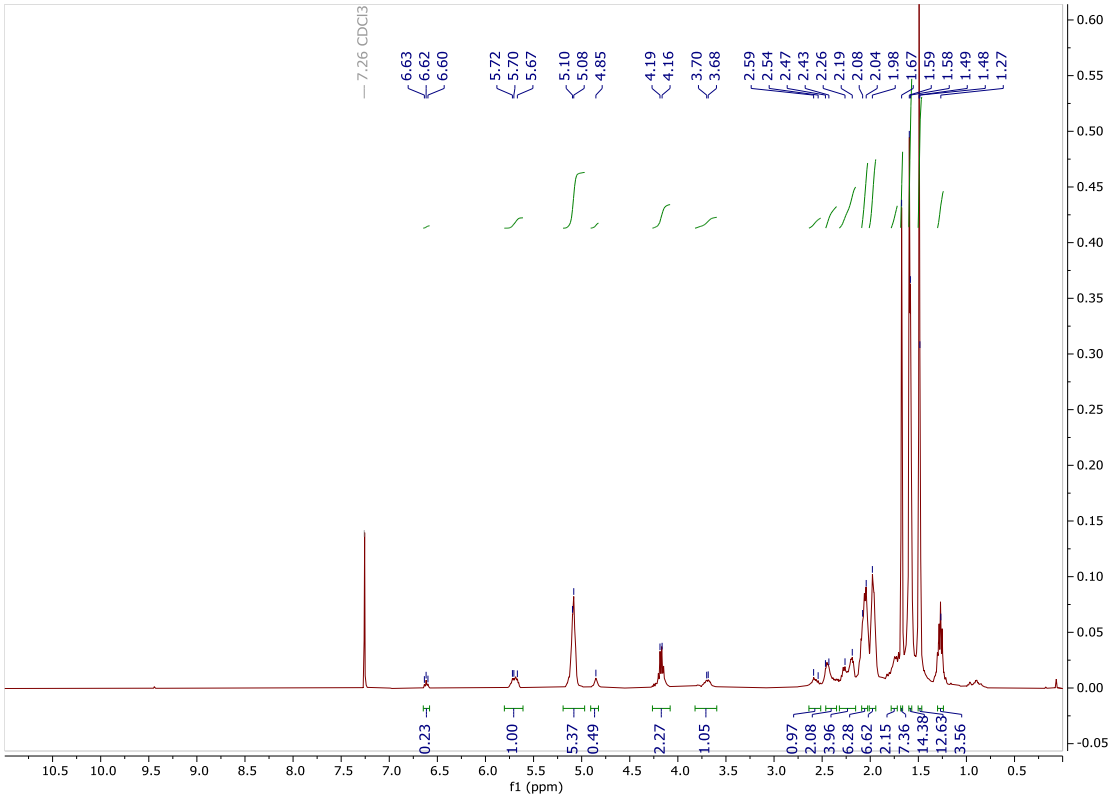

Figure 2.5 ^{1}H NMR spectrum of 2.42 in $CDCl_3$.2.2.3.3 Synthesis of diol 1.97.

2.2.3.3 Synthesis of diol 1.97.

Having successfully synthesised β-hydroxy ester **2.42**, we now had access to the squalene skeleton. To install the final double bond in the structure, we treated **2.42** with mesyl chloride to promote mesyl and elimination in situ, which resulted in the formation of alkene **2.43** in 70% yield. The procedure was adopted from Heathcock et al. in which they obtained their target diester in 87% yield (Heathcock et al., 1992b). The alkene was isolated as a mixture of diastereomers based on ^{1}H NMR spectrum. The main triplets at 6.74 ppm and 5.70 ppm were present in 3:1 ratio. We also observed a minor triplet at 6.62 ppm.

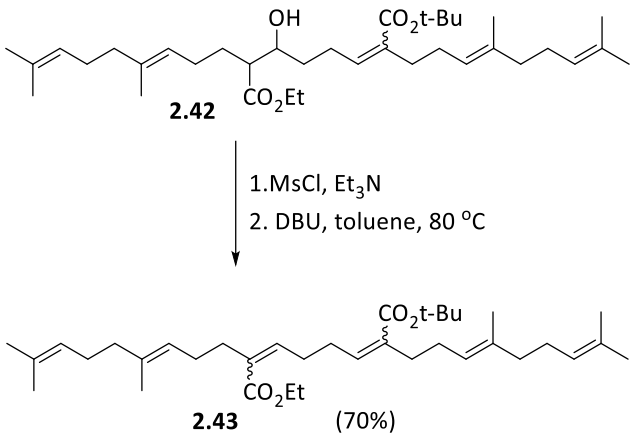

*Scheme 2.23 Synthesis of diester **2.43**.*

It is difficult to determine identity of the three stereoisomers in **2.43** due to the peak overlap in the ^{1}H NMR spectrum (Figure 2.6). The four possible isomers that could have formed are *E*:*Z*, *E*:*E, Z:E,* and *Z*:*Z*. As said previously, based on literature data for related compounds (Heathcock et al., 1992b) the alkene proton for the *E* isomer is generally significantly more downfield than the *Z* isomer. Therefore, a triplet at 5.72 ppm was assigned tentatively to the *Z* stereoisomer, while a triplet at 6.74 ppm to *E* stereoisomer. The main triplets at 6.74 ppm and 5.70 ppm were present in 3:2 ratio. We also observed a minor triplet at 6.62 ppm (in a 1:6 ratio with the triplet at 5.70 ppm). Due to ^{1}H signal overlap, the ratio of stereoisomers could not be assigned confidently.

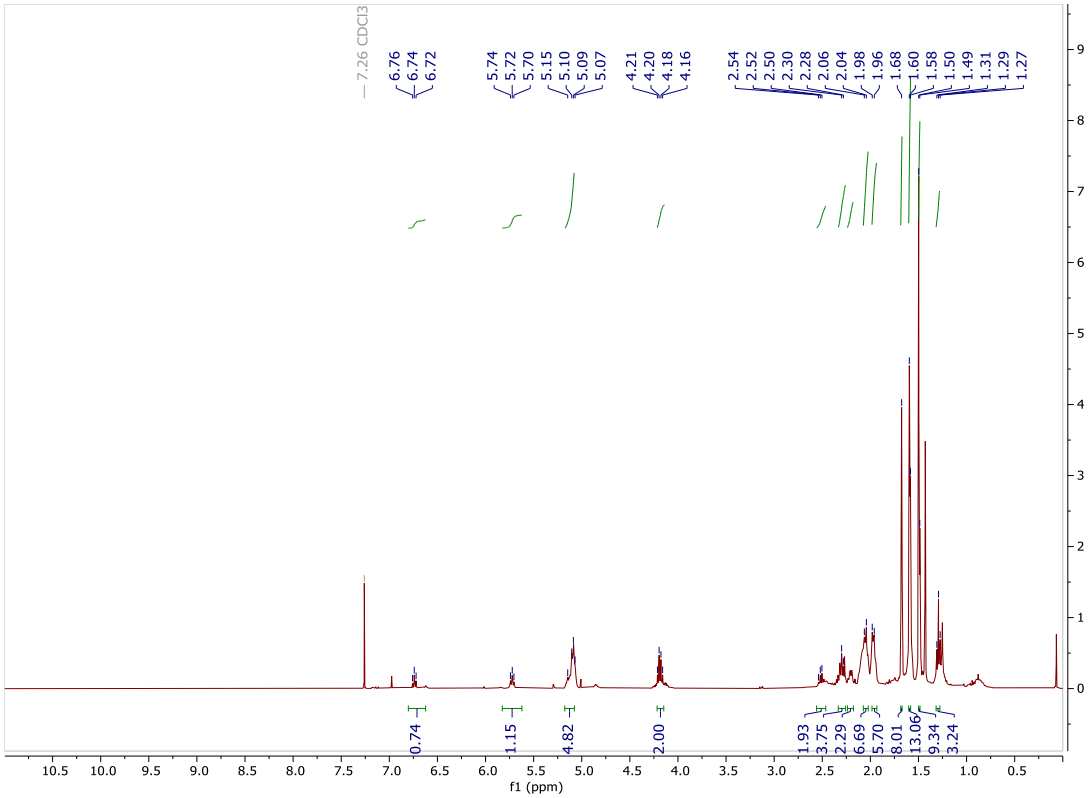

*Figure 2.6 ^{1}H NMR spectrum of **2.43** in $CDCl_3$.*

The final step performed was a DIBAL-H reduction of diester **2.43** (Scheme 2.24) which successfully produced the target molecule diol **1.97** in a yield of 34%. Therefore, we successfully completed the synthesis of diol **1.97**, completing the first major objective of the project.

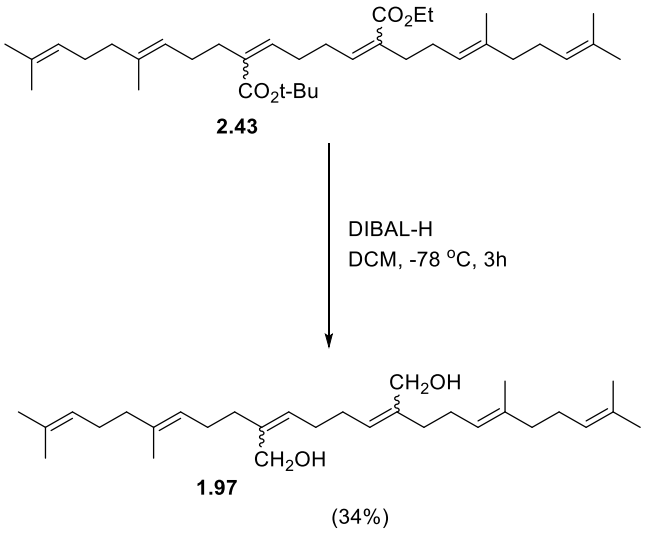

*Scheme 2.24 Synthesis of diol **1.97** showing possible stereoisomers of the product.*

Based on the ^{1}H NMR spectrum (Figure 2.7) it was difficult to establish the exact ratio of stereoisomers due to the overlap of the peaks in the ^{1}H NMR spectrum – a triplet at 5.42 ppm and two triplets overlapping at 5.31 ppm were observed. In literature data for related diol compounds (Heathcock et al., 1992b) the alkene proton for the *E* isomer is generally more downfield than the *Z* isomer (5.43 ppm for *E* and ca. 5.29 ppm for *Z*). Therefore, based on this, in the ^{1}H NMR spectrum of the precursor **1.97**, a triplet at 5.42 ppm was assigned tentatively to the *E* stereoisomer, while a triplet at 5.31 ppm to *Z* stereoisomer. The peaks at 5.42 and 5.31 ppm appeared in ≈1:1 ratio and likely represented the main *E*:*Z* isomer. Similarly, the doublets at 4.10 ppm and 4.04 ppm which appeared in 1:1 were tentatively as E and Z stereoisomers, respectively, based on the literate data (Heathcock et al., 1992b). However, due to the peak broadness overlap in ^{1}H NMR spectrum and a low signal intensity in ^{13}C NMR spectrum (see Appendix) we were not able to establish the ratio accurately or assign minor stereoisomers.

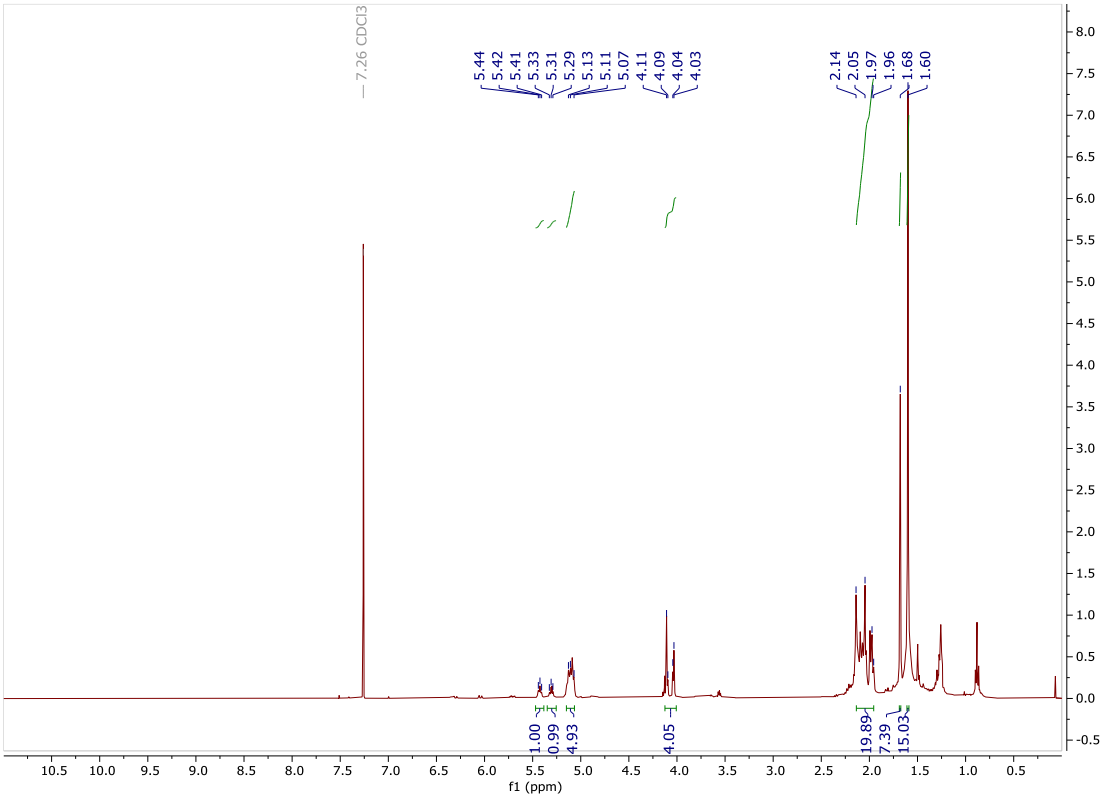

*Figure 2.7 ^{1}H NMR of **1.97** in $CDCl_3$.*

2.3 Conclusion

In summary, the hypothesised precursor to the *Daphniphyllum* alkaloid pathway – diol **1.97** was prepared as a mixture is isomers via an eight-step synthesis with an overall yield of 2%. While there is a potential to improve the yield and *E*:*Z* selectivity of the route through further optimisation of reaction conditions, the primary objective for this project was to produce sufficient material for biological assays, which was achieved.

In retrospect, the final synthesis closely followed Heathcock's original synthesis to pre-reduced diol **1.97** (Heathcock, Piettre, et al. 1992). Our efforts showed that for the synthesis of diol **1.97** formation of the final skeleton is more difficult that one would expect, i.e. the final alkylation between silyl ester **2.31** and aldehyde **2.34** was unsuccessful. Due to time constraints, detailed investigations into the failed reactions or identification of side products were not pursued. Despite these challenges, the successful synthesis of diol **1.97** fulfilled the primary goal of this project.

3 Isolation of *Daphniphyllum* alkaloids

3.1 Introduction

3.1.1 *Challenges in isolating and identifying Daphniphyllum alkaloids*

Daphniphyllum alkaloids, found in the plants from the genus *Daphniphyllum*, are typically found in small quantities and as part of complex mixtures. Although over 300 *Daphniphyllum* alkaloids have been already isolated and reported, obtaining those compounds as standards remains difficult. Their abundance is scarce in plants which makes them challenging to isolate. Those plants are not native to the United Kingdom and so we have limited access to them. Additionally, *D. macropodum* is a slow growing tree and a challenging plant to cultivate.

Many *Daphniphyllum* alkaloids are isobaric, meaning that high-resolution mass spectrometry is often insufficient to confidently identify the structure based solely on the molecular formula. Given our goal to investigate the biosynthetic pathway of these alkaloids, it was crucial to have access to standards for accurate structural annotation as well as substrates for the future enzymatic assays.

3.1.2 *Extraction and isolation techniques*

3.1.2.1 Plant tissue collections and preparation

The main difficulty was to obtain enough tissue material to obtain sufficient amount of pure alkaloid to collect good quality NMR data to fully characterise their chemical structures. We collected 100 g of fallen leaves of *D. macropodum* (plant B) from Castle Howard and 800 g of aerial tissue (leaves and stem) of a *D. macropodum* plant bought from the nursery (Architectural plants Ltd). Plant tissues were stored in -80 ^{o}C, then ground and repeatedly extracted with methanol. The extracts were filtered and concentrated to yield a residue which was resuspended in ethyl acetate. Then, the alkaloids were extracted with 0.01 M aqueous hydrochloric acid, followed by basification to pH 10 using saturated sodium carbonate. Finally, it was extracted with chloroform and concentrated to yield crude alkaloid extract (Li et al., 2007). For more detailed procedure see chapter 6, section 6.1.1.

3.1.2.2 Chromatographic separation of alkaloids

Purification of alkaloids was carried out using Interchim Puriflash 4250 prep HPLC system linked to an Advion Expression S Compact Mass Spec (CMS). The extracts were fractionated through C18 FlashPure 12 g column; flow rate: 30 mL/min into 5 fractions using a gradient of solvents (A) Ammonium bicarbonate buffer pH = 10.2 and (B) Methanol (0–5 min 98% A, 5.1–10 min 50% A, 10.1–16 min 40% A, 16.1–27 min 35% A, 27–38 min 35–5% A, 38.1–42 min 5%, 42–46 min 2%. The fractions were collected automatically in 20 mL vials. The semi-pure fractions were further purified using a semi-preparative column (Waters XBridge C18 5µm column of size 10 x 150 mm) and eluted with a gradient of solvents A) Ammonium bicarbonate buffer pH = 10.2 and (B) Methanol controlled manually to afford off-white powders. For more detailed procedure see chapter 6, section 6.1.1.

3.1.2.3 Mass spectrometry and NMR spectroscopy for structure elucidation

The fractions were then analysed using Waters Acquity I-Class ultra-performance liquid chromatography (UPLC) instrument interfaced to a Thermo Tribrid Fusion Orbitrap or Exploris 480 instrument using an atmospheric pressure chemical ionisation (APCI) ion source in positive ion mode. The mobile phases used were 10 mM ammonium bicarbonate (pH 10.2) and methanol. Full NMR data, ^{1}H, ^{13}C and 2D NMR spectra were collected to allow full assignment of the structure. For more detailed procedure see chapter 6, section 6.1.2.

3.1.3 *Aims*

The aim of this part of the project is to isolate and characterise *Daphniphyllum* alkaloids. We will use aerial tissues of *D. macropodum* to investigate plant extracts using liquid chromatography – mass spectrometry (LC-MS). We will develop an analytical method to determine the content of the extract as well as to determine the suitable method to separate and purify *Daphniphyllum* alkaloids in the extracts. The isolated alkaloids will be then characterised by high-resolution mass spectrometry and the structures will be identified using NMR. Characterisation of the isolated alkaloids will give us access to standards, allow us to compare MS^2 fragmentation patterns of different skeletons, give us substrates for feeding experiments as well as aid gene discovery.

3.2 Results

Purification of *Daphniphyllum* alkaloids was carried out in collaboration with Dr Swen Langer. Following alkaloids: daphnicalycine A **3.1** and 7-hydroxydaphnilongeranin D **3.4** were purified by Dr Swen Langer. Sample collection, extraction of alkaloids, purification of the remaining alkaloids and structure elucidation were carried by Barbara Radzikowska.

The purification of alkaloid extracts of *D. macropodum* yielded six *Daphniphyllum* alkaloids: We isolated four already known *Daphniphyllum* alkaloids and confirmed their structures via NMR: yuzurimine **1.10** (11 mg), deoxyyuzurimine **1.66** (4 mg), methyl homo-secodaphniphyllate **1.52** (11 mg) and daphnicalycine A **3.1** (4 mg). Additionally, we also isolated and characterised one *Daphniphyllum* alkaloid that was not reported – 7-hydroxydaphnilongeranin D **3.4** (3 mg). The structures of isolated *Daphniphyllum* alkaloids were presented in Figure 3.1.

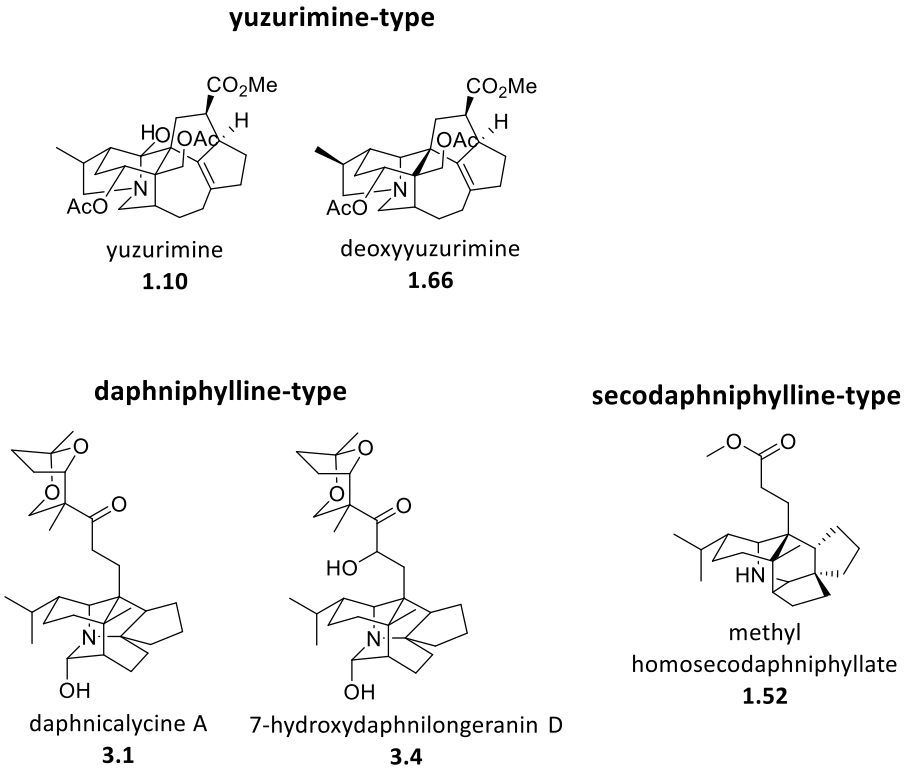

Figure 3.1 Structures of isolated Daphniphyllum *alkaloids.*

3.2.1 *C22A: Yuzurimine-type alkaloids*

3.3.1.1 M488.26T210 Yuzurimine 1.10

Based on the high-resolution mass m/z 488.2644 $[M+H]^+$ (calculated 488.2648), we calculated the molecular formula of the isolated compound as $C_{27}H_{37}NO_7$. Two distinct peaks were observed in the MS spectrum: $[M+H]^+$ = 488.2644 and usually more intensive $[M+H-H_2O]^+$ = 470.2539 which indicated presence of the hydroxyl group (Figure 3.2 and Figure 3.3).

There were several distinct peaks in the ^1H NMR spectrum, for example doublet of doublets at 5.36 ppm suggested a neighbouring acetyl group and so was assigned to CH(4). Similarly, two coupled doublets at 4.40 and 4.29 ppm were assigned to CH_2(C21) neighbouring acetyl groups. Meanwhile a singlet at 3.60 ppm was assigned to OCH_3(25) and the remaining two singlets at 2.01 and 1.99 to CH_3(23), CH_3(27), finally a doublet at 1.05 ppm was assigned to the methyl group CH_3(C20). Those peaks agreed with the characteristic peaks previously reported for yuzurimine **1.10** (Sakurai et al., 1967). It is worth noting that reported ^1H NMR spectrum is incomplete, therefore we also compared ^{13}C NMR spectra. As presented in Table 3.1, the literature values for ^{13}C spectrum are in a good agreement with the experimental values (Li et al., 2007; Sakurai et al., 1967). In order to fully assign peaks in ^1H NMR spectrum we collected and analysed data from 2D NMR experiments, i.e. HMQC, COSY, HMBC and DEPT.

The DEPT experiment distinguished CH and CH_3 groups from CH_2 carbons and identified quaternary carbons. Specifically, it confirmed the assignment of a quaternary C(1) at 97.2 ppm which was absent in the DEPT spectrum. Additionally, it helped to differentiate carbon peaks arising from impurities in the ^{13}C NMR spectrum.

COSY correlations determined assignment of CH(19) through its correlations with CH_3(20), while CH(6) showed COSY correlations with CH_2(7). Similar correlations were

observed between following pairs: CH_2(12) and CH_2(13), CH_2(3) and CH(4), CH_2(9) and CH(10).

HMBC correlations further supported the ^{13}C peak assignments, with C(26) and C(22) confirmed through their correlations with CH(4) and CH_2(21), respectively. HMBC correlations with C(24) also allowed to confident assignment of CH(10) and CH_2(9), while C(5) was identified based on its correlations with CH_2(21).

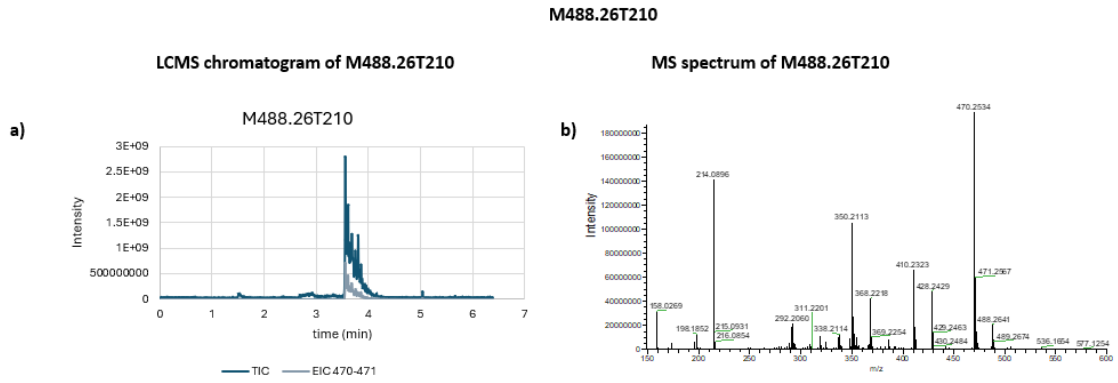

*Figure 3.2 LCMS chromatogram with TIC and extracted ion chromatogram of 470-471, $[M+H]^+$ representing molecular formula of $C_{27}H_{37}NO_7$; b) MS spectrum of yuzurimine **1.10** peak at 210 sec.*

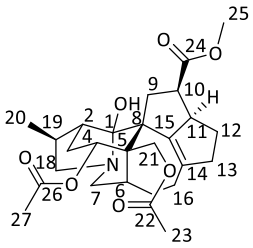

yuzurimine **1.10**
Chemical Formula: $C_{27}H_{37}NO_7$
Exact Mass: 487.2570

*Figure 3.3 Structure of yuzurimine **1.10**.*

*Table 3.1 Comparison between literature values ^{1}H and ^{13}C (100 MHz) and experimental ^{1}H (700MHz), ^{13}C (175 MHz) NMR data of yuzurimine **1.10** in $CDCl_3$* (Li et al., 2007; Sakurai et al., 1967).

C no.		1.10 (lit) δ_C	1.10 (exp) δ_C	1.10 (lit) δ_H *J* (Hz)	1.10 (exp) δ_H *J* (Hz)
1	C	96.9	97.2		
2	CH	42.1	42.3		2.49 – 2.23 m
3	CH_2	27.3	27.4		1.92 – 1.80 m 1.50 – 1.42 m
4	CH	72.9	72.9	5.36 q 12.0, 7.0	5.35 dd 12.0, 7.0
5	C	45.1	45.1		
6	CH	34.1	34.4		2.60 – 2.51 m
7	CH_2	58.6	58.7		3.36 – 3.29 m 3.27 – 3.15 m
8	C	52.1	52.2		
9	CH_2	37.5	37.6		3.10 – 2.97 m 2.49 – 2.23 m
10	CH	43.1	43.2		3.10 – 2.97 m
11	CH	57.5	57.6		3.55 – 3.47 m
12	CH_2	28.7	28.9		1.92 – 1.80 m 1.40 – 1.31 m
13	CH_2	43.2	43.3		2.71 – 2.63 m 2.49 – 2.23 m
14	C	136.7	136.9		
15	C	144.0	144.0		
16	CH_2	25.3	25.4		2.49 – 2.23 m 2.15 – 2.03 m
17	CH_2	27.1	27.2		2.49 – 2.23 m 2.15 – 2.03 m
18	CH_2	64.5	64.6		3.70 – 3.61 m 2.49 – 2.23 m
19	CH	34.4	34.5		2.85– 2.75 m
20	CH_3	14.7	14.8	1.11 d 7.0	1.03 d 7.5
21	CH_2	67.0	67.1	4.32 q 11.0	4.38 d 11.5 4.30 d 11.5
22/26	C	-	171.03		
23/27	CH_3	-	21.3	1.98 s	1.99s
24	C	175.3	175.4		
25	CH_3	-	51.23	3.53 s	3.60 s
22/26	C	-	170.3		
23/27	CH_3	-	21.2	1.98 s	2.01 s

3.3.1.2 M472.27T204 Deoxyyuzurimine 1.66

The molecular formula of M472.27T204 – $C_{27}H_{37}NO_6$ – was determined by the measured mass = 472.26931 $[M+H]^+$ (calculated 472.2699) (Figure 3.4). The only *Daphniphyllum* alkaloids of this exact mass already reported in the literature is deoxyyuzurimine **1.66** and it belongs to yuzurimine type (Li et al., 2007) In fact, comparison of both ^{1}H NMR spectra of yuzurimine **1.10** and M472.27T204 showed skeletal similarity between those two compounds. All distinct peaks such as methyl and acetyl groups were present in both spectra. The only difference between those two compounds was the lack of the hydroxy group at the position C(1), showed by the shift from 97.6 ppm in yuzurimine **1.10** to 66.1 ppm in the isolated compound which meant the structure matched deoxyyuzurimine **1.66** (Figure 3.5). The experimental ^{13}C NMR data closely matched reported literature values (Li et al., 2007) as presented in Table 3.2. Experimental ^{1}H NMR data of deoxyyuzurimine **1.66** were compared to the experimental data of yuzurimine **1.10** (described in section 3.3.1.1) due to the lack of reported literature data (see Table 3.2).

As previously, the assignment was confirmed with the analysis of additional NMR experiments. We observed COSY correlations between several pairs such as: CH_2(3) and CH(4), CH(10) and CH(11). We assigned CH(19) to a multiplet at 2.42 – 1.81 ppm due to a COSY correlation with CH(20). The difference in the shifts between deoxyyuzurimine **1.66** and yuzurimine **1.10** was likely caused by the lack of the hydroxy group. Meanwhile CH_2(21) only showed correlations between both protons in that CH_2 group supporting the assignment with no neighbouring hydrogens.

We assigned C(26) and C(22) peaks to 170.4 and 171.0 ppm due to HMBC correlations with CH(4) and CH2(21), respectively. C(24) showed HMBC correlations with CH_3(25). CH_2(21) showed strong HMBC correlations with following: CH(4), C5, CH(6) and C8, while CH(4) showed strong HMBC correlations with CH_2(3), C(5), CH(6) and CH(1). We also observed correlations between CH(3) and C(5), C(8) and CH(10), CH_2(16) and CH(6). The

peak assigned to C(14) was hidden in the baseline, however we observed it due to HMBC correlations.

Although we did not have a standard to compare ^{1}H NMR spectrum, comparison to yuzurimine **1.10** showed that they possess the same functional groups and the same skeleton. The structure was validated by the comparison of experimental and previosuly reported ^{13}C NMR spectra of dexyyuzurimine **1.66** (Z. Y. Li et al. 2007). It is important to note that our comparison was based on the experimental ^{1}H NMR spectrum of yuzurimine **1.10**, which we assigned ourselves, in the absence of reported literature data for direct reference.

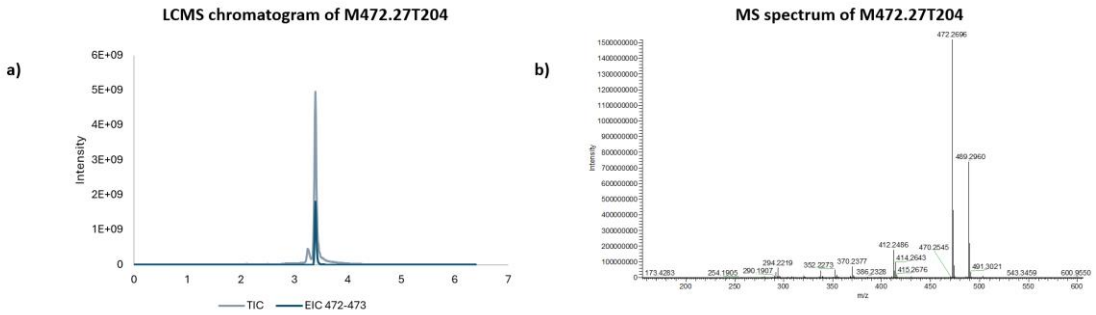

*Figure 3.4 a) LCMS chromatogram with TIC and extracted ion chromatogram of 472-473 $[M+H]^{+}$ representing molecular formula of $C_{27}H_{37}NO_6$ showing the deoxyyuzurimine **1.66**; b) spectrum of the deoxyyuzurimine **1.66** peak.*

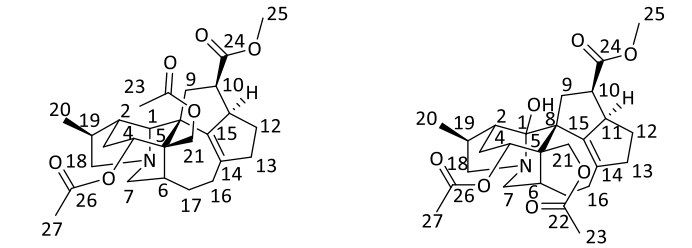

deoxyyuzurimine **1.66**
Chemical Formula: $C_{27}H_{37}NO_6$
Exact Mass: 471.2621

yuzurimine **1.10**
Chemical Formula: $C_{27}H_{37}NO_7$
Exact Mass: 487.2570

*Figure 3.5 Structure of deoxyyuzurimine **1.66** and yuzurimine **1.10**.*

*Table 3.2 Comparison between literature and experimental values for ^{13}C NMR data (100 and 175 MHz, respectively) for deoxyyuzurimine **1.66** and experimental ^{1}H NMR data between yuzurimine **1.10** and deoxyyuzurimine **1.66** (700 MHz) in $CDCl_3$* (Li et al., 2007; Sakurai et al., 1967).

c		**1.66 (lit) δ_C**	**1.66 (exp) δ_C**	**yuzurimine 1.10 (exp) δ_H *J* (Hz)**	**1.66 (exp) δ_H *J* (Hz)**
1	**CH/C**	67.1	67.1		3.43 – 3.37 m
2	CH	37.5	37.7	2.49 – 2.23 m	2.45 – 1.81 m
3	CH_2	27.2	27.2	1.92 – 1.80 m 1.50 – 1.42 m	2.45 – 1.81 m 1.66 – 1.27 m
4	CH	73.3	73.5	5.35 dd 12.0, 7.0	5.32 dd 12.0, 7.0
5	C	41.2	41.3		
6	CH	35.0	35.2	2.60 – 2.51 m	2.65 –2.58 m
7	CH_2	58.0	58.2	3.36 – 3.29 m 3.27 – 3.15 m	3.26 – 2.98 m
8	C	46.4	46.6		
9	CH_2	39.1	39.3	3.10 – 2.97 m 2.49 – 2.23 m	3.26 – 2.98 m 2.45 – 1.81 m
10	CH	42.7	43.0	3.10 – 2.97 m	2.90 dt 9.5, 3.5
11	CH	54.0	54.1	3.55 – 3.47 m	3.51 – 3.45 m
12	CH_2	28.2	28.3	1.92 – 1.80 m 1.40 – 1.31 m	2.45 – 1.81 m 1.66 – 1.27 m
13	CH_2	42.8	42.9	2.71 – 2.63 m 2.49 – 2.23 m	2.79 – 2.68 m 2.45 – 1.81 m
14	C	133.6	134.0		
15	C	144.4	144.6		
16	CH_2	25.3	25.5	2.49 – 2.23 m 2.15 – 2.03 m	2.45 – 1.81 m
17	CH_2	26.9	27.3	2.49 – 2.23 m 2.15 – 2.03 m	2.45 – 1.81 m
18	CH_2	64.8	64.9	3.70 – 3.61 m 2.49 – 2.23 m	3.71 – 3.61 m 2.45 – 1.81 m
19	CH	38.2	38.4	2.85– 2.75 m	2.45 – 1.81 m
20	CH_3	15.5	15.6	1.03 d 7.5	1.05 d 7.0
21	CH_2	67.0	67.1	4.38 d 11.5 4.30 d 11.5	4.40 d 11.5 4.31 d 11.5
22/26	C		171.0		
23/27	CH_3		21.4	1.99 s	2.00 s
24	C	175.0	175.2		
25	CH_3	51.1	51.3	3.60 s	3.61 s
22/26	C		170.4		
23/27	CH_3		21.2	2.01 s	2.00 s

3.2.2 *C30: Daphniphylline-type*

3.3.2.1 M486.35T240 Daphnicalycine A 3.1

Based on the high-resolution mass m/z 486.3580 $[M+H]^+$ (calculated 486.3583), we calculated the molecular formula of the isolated compound as $C_{30}H_{47}NO_4$ (Figure 3.6). All of the reported compounds of this molecular formula belong to the daphniphylline type (Shen et al., 2020; Yang et al., 2006; Di et al., 2008; Zhang et al., 2009a).

Based on the ^1H and ^{13}C NMR data the isolated compound matched the daphniphylline type skeleton, specifically, peaks at 65.1 and 72.8 ppm assigned to C(1) and C(11), respectively. The downfield peak at 80.9 ppm was assigned to CH(15) – a CH neighbouring a hydroxy group and a nitrogen. Based on the comparison with the literature data (Shen et al., 2020), the isolated compound was identified as daphnicalycine A **3.1** (Figure 3.7).

The observed experimental ^{13}C NMR data closely matched the literature reported data as presented in Table 3.3 with one inconsistency which was lack of the peak at 72.5 ppm (Shen et al., 2020), however that peak likely was hidden in the baseline. There were also some changes between reported and experimental ^1H NMR data, specifically there was a shift between a broad singlet at 5.17 ppm reported in the literature and the observed broad singlet at 5.54 ppm which were assigned to CH(15).

In fact, the downfield shift was also observed in CH(1) – a doublet at 2.97 ppm shifted to a broad peak at 3.39 – 3.31 ppm, and a triplet at 2.16 ppm assigned to CH(7) shifted to a triplet at 2.35 ppm. Similarly, a triplet assigned to CH(7) shifted downfield from the reported 2.16 ppm to 2.35 ppm. Also, we observed a broad peak at 2.73 – 2.61 ppm which we assigned to one of the protons of CH_2(9), while Shen at all reported it as a multiplet at 2.37 ppm. Those shifts could be caused by the difference in the sample concentration or the acidity of the used deuterated solvent.

The assignments were confirmed by the additional experiments. COSY correlations revealed proximity of CH_2(20) to CH_2(24) as well as CH_2(16) and CH_2(17). CH(27) was assigned based on COSY correlations with CH_3(28) and CH_3(29). We also observed that CH(21) showed HMBC correlations with CH(20), CH_2(24) and CH_3(26). CH_3(30) correlated with CH(15) and CH(1).

The analysis of the NMR data confirmed daphniphylline type skeleton based on the characteristic peaks as reported previously in literature (Shen et al., 2020).

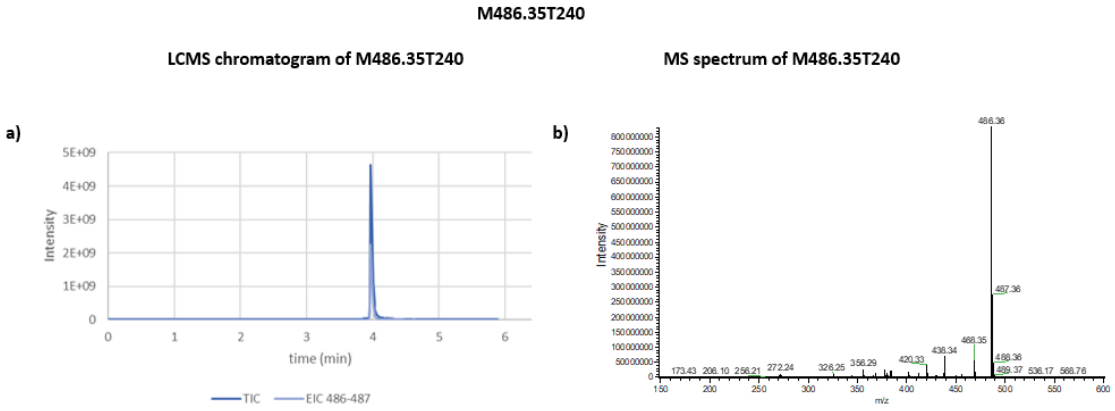

*Figure 3.6 a) LCMS chromatogram with TIC and extracted ion chromatogram of 486-487 $[M+H]^+$ representing molecular formula of $C_{30}H_{47}NO_4$ showing the daphnicalycine A **3.1**; b) spectrum of the daphnicalycine A **3.1** peak.*

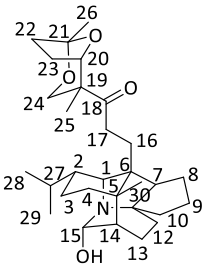

daphnicalycine A **3.1**

Chemical Formula: $C_{30}H_{47}NO_4$

Exact Mass: 485.3505

*Figure 3.7 Structure of daphnicalycine A **3.1**.*

*Table 3.3 Comparison between literature values ^{1}H (600MHz), ^{13}C (150 MHz) and experimental ^{1}H (700MHz), ^{13}C (150 MHz) NMR data od daphnicalycine A **3.1** in $CDCl_3$* (Shen et al., 2020).

C no.		3.1 (lit)δ_C	3.1 (exp) δ_C	3.1 (lit) δ_H *J* (Hz)	3.1 (exp) δ_H *J* (Hz)
1	CH	65.1	65.6	2.97 d 4.8	3.39 – 3.31 m
2	CH	37.7	37.9	1.44	1.57 – 1.42 m
3	CH_2	27.2	26.2	1.89 1.41	1.99 – 1.70 m 1.57 – 1.42 m
4	CH_2	36.4	36.1	1.88 1.44	1.99 – 1.70 m 1.57 – 1.42 m
5	C	38.4	38.5		
6	C	47.5	46.8		
7	CH	51.2	51.6	2.16 t 9.6	2.35 t 9.5
8	CH_2	28.8	29.1	1.71 1.43	1.99 – 1.70 m 1.57 – 1.42 m
9	CH_2	29.7	29.9	2.37 1.26	2.73 – 2.61 m 1.33 – 1.27 m
10	CH_2	41.6	40.4	1.80	2.14 – 2.05 m 1.99 – 1.70 m
11	C	72.5			
12	CH_2	25.1	25.2	1.69 1.30	1.99 – 1.70 m 1.57 – 1.42 m
13	CH_2	17.6	16.9	1.79 1.69	1.99 – 1.70 m
14	CH	47.1	45.9	1.63	1.99 – 1.70 m
15	CH	80.9	81.0	5.17 br s	5.54 br s
16	CH_2	23.2	23.1	1.87 1.42	1.99 – 1.70 m 1.57 – 1.42 m
17	CH_2	36.8	36.1	2.97 2.86	3.03 – 2.95 m 2.88 – 2.81 m
18	C	212.5	211.7		
19	C	49.9	49.9		
20	CH	81.0	81.4	4.70 d 6.6	4.67 d 7.0
21	C	105.4	105.5		
22	CH_2	34.0	33.9	2.08 1.87	2.14 – 2.05 m 1.99 – 1.70 m
23	CH_2	24.8	24.8	2.08 1.92	2.14 – 2.05 m 1.99 – 1.70 m
24	CH_2	65.6	65.9	4.29 d 12.0 3.52 d 12.0	4.27 d 12.0 3.54 d 12.0
25	CH_3	26.0	25.7	0.97 s	1.05 s
26	CH_3	23.8	23.8	1.42 s	1.42 s
27	CH	31.5	30.5	1.66	1.99 – 1.70 m

28	CH_3	21.5	22.0	1.03 d 6.0	1.09 d 6.5
29	CH_3	21.2	21.0	0.90 d 6.0	0.94 d 6.5
30	CH_3	17.9	17.8	0.78 s	0.79 s

3.3.2.3 M502.35T210 New Daphniphyllum alkaloid 3.5

Based on the high-resolution mass m/z 502.3530 $[M+H]^+$ (calculated 502.3532), we determined the molecular formula of the isolated compound as $C_{30}H_{47}NO_5$ (Figure 3.8). There was only one compound previously reported of this exact mass – daphnezomine V **3.2** (Figure 3.9). However, we realised that the experimental data were lacking the characteristic shifts due to the neighbouring N-oxide (C(1), C(11), and C(15) (δ_C 75.2, 90.6 and 61.8 ppm, respectively) that were expected in the spectrum of daphnezomine V **3.2**. Therefore, it suggested that the isolated alkaloid was not reported before.

Upon the close comparison with the literature data, M502.25T210 revealed close similarity between daphnicalycine A **3.1** and daphnilongeranin D **3.3** (Figure 3.9), both of which have daphniphylline type skeleton and the same molecular formula – $C_{30}H_{47}NO_4$. The main difference between daphnicalycine A **3.1** and M502.25T210 was the additional hydroxy group at CH(17) due to the difference in δ_C from 36.6 to 73.2 ppm and similar shift was observed in ^1H spectrum two doublets of doublets of doublets at 2.99 and 2.84 ppm shifted downfield to a doublet of doublets at 4.92 ppm due to the presence of a hydroxy group. The δ_C of CH(15) were similar for both compounds, 80.9 and 80.4 ppm for daphnicalycine A **3.1** and M502.25T210 **3.4**, respectively (Table 3.4).

The only difference between M502.25T210 **3.4** and daphnilongeranin D **3.3** was the additional hydroxy group at CH(15) which was observed by the change in δ_C from 48.3 to 81.7 ppm between daphnilongeranin D **3.3** and M502.25T210 **3.4**, respectively (Table 3.5). Similarly, we observed a shift in δ_H from a broad doublet at 3.27 ppm to a broad singlet at 5.55 ppm between daphnilongeranin D **3.3** and 502.25T210 **3.4**, respectively. Therefore, the structure of the new isolated alkaloid **3.4** was elucidated as shown in Figure 3.9.

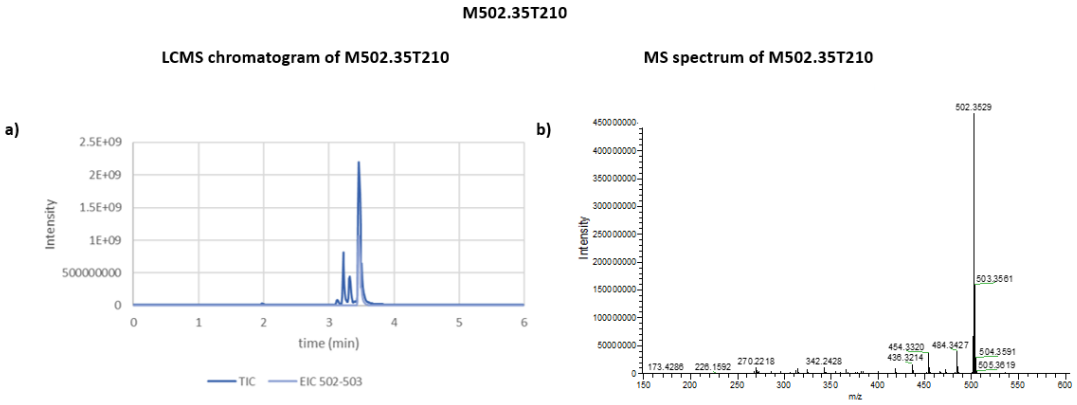

*Figure 3.8 a) LCMS chromatogram with TIC and extracted ion chromatogram of 502-503 $[M+H]^+$ representing molecular formula of $C_{30}H_{47}NO_5$ showing **3.4**; b) spectrum of **3.4** peak.*

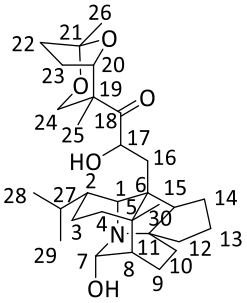

not reported **3.4**
7-hydroxydaphnilongeranin D

Chemical Formula: $C_{30}H_{47}NO_5$
Exact Mass: 501.3454

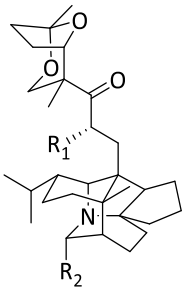

R_1 = H, R_2 = OH: daphnicalycine A **3.1**
R_1 = OH, R_2 = H: daphnilongeranin D **3.3**

Chemical Formula: $C_{30}H_{47}NO_4$
Exact Mass: 485.3505

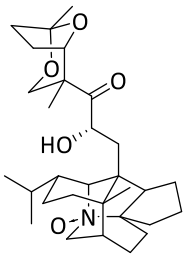

daphnezomine V **3.2**

Chemical Formula: $C_{30}H_{47}NO_5$
Exact Mass: 501.3454

Figure 3.9 (from the left) Structures of not previously reported Daphniphyllum *alkaloid **3.4**, daphnicalycine A **3.1**, daphnilongeranin D **3.3** and daphnezomine V **3.2**.*

*Table 3.4 Comparison between literature values ^{1}H (600MHz), ^{13}C (150 MHz) for daphnicalycine A **3.1** and experimental ^{1}H (600MHz), ^{13}C (150 MHz) NMR data of M502.25T210 **3.4** in $CDCl_3$* (Shen et al., 2020).

C no.		**3.1** (lit) δ_C	**3.4** (exp) δ_C	**3.1** (lit) δ_H *J* (Hz)	**3.4** (exp) δ_H *J* (Hz)
1	CH	65.1	65.3	2.97 d 4.8	3.16 br d 5.5
2	CH	37.7	37.8	1.44	2.16 – 1.46 m
3	CH_2	27.2	26.6	1.89 1.41	2.16 – 1.46 m
4	CH_2	36.4	36.2	1.88 1.44	2.16 – 1.46 m
5	C	38.4	38.7		
6	C	47.5	47.2		
7	CH	80.9	80.4	5.17 br s	**5.47 br s**
8	CH	47.1	46.7	1.63	2.16 – 1.46 m
9	CH_2	17.6	16.9	1.79 1.69	2.16 – 1.46 m
10	CH_2	25.1	25.1	1.69 1.30	2.16 – 1.46 m
11	C	72.5	71.6		
12	CH_2	41.6	41.0	1.80	2.16 – 1.46 m
13	CH_2	29.7	31.3	2.37 1.26	2.61 – 2.26 m 2.16 – 1.46 m
14	CH_2	28.8	29.2	1.71 1.43	2.16 – 1.46 m
15	CH	51.2	52.7	2.16 t 9.6	2.16 – 1.46 m
16	CH_2	23.2	**31.4**	1.87 1.42	**2.46 dd 15.5, 3.0** 1.36 – 1.32 m
17	CH_2/CH	36.8	**73.2**	2.97 2.86	**4.92 dd 8.0, 3.5**
18	C	212.5	**214.6**		
19	C	49.9	49.9		
20	CH	81.0	81.1	4.70 d 6.6	4.84 d 7.0
21	C	105.4	105.6		
22	CH_2	34.0	33.8	2.08 1.87	2.16 – 1.46 m
23	CH_2	24.8	24.5	2.08 1.92	2.16 – 1.46 m
24	CH_2	65.6	65.0	4.29 d 12.0 3.52 d 12.0	4.25 dd 13.0, 2.0 3.71 – 3.66 m
25	CH_3	17.9	**19.1**	0.78 s	**1.19 s**
26	CH_3	23.8	23.7	1.42 s	1.43 s
27	CH	31.5	30.4	1.66	2.16 – 1.46 m
28	CH_3	21.5	22.0	1.03 d 6.0	1.07 d 6.5
29	CH_3	21.2	21.1	0.90 d 6.0	0.92 d 6.5
30	CH_3	26.0	25.9	0.97 s	0.86 s

*Table 3.5 Comparison between literature values for daphnilongeranin D **3.3** and experimental ^{1}H (700MHz), ^{13}C (176 MHz) NMR data of the isolated alkaloid **3.4** in CD_3OD* (Yang et al., 2006).

C no.		3.3 (lit) δ_C	3.4 (exp) δ_C	3.3 (lit) δ_H *J* (Hz)	3.4 (exp) δ_H *J* (Hz)
1	CH	64.2	**68.9**	2.87 d 4.8	3.02 – 2.69 m
2	CH	39.4	38.4	1.54 m	2.24 – 1.47 m
3	CH_2	28.4	28.2	1.90 m 1.54 m	2.24 – 1.47 m
4	CH_2	43.3	**40.9**	1.72 m 1.35 m	2.24 – 1.47 m
5	C	38.4	39.7		
6	C	49.5	48.2		
7	CH	48.3	**81.7**	3.27 br d 14.2	**5.55 br s**
8	CH	43.2	**48.0**	1.33 m	2.24 – 1.47 m
9	CH_2	23.9	25.1	1.92 m 1.59 m	2.24 – 1.47 m 1.36 – 1.32 m
10	CH_2	30.3	29.6	1.80 m 1.50 m	2.24 – 1.47 m
11	C	74.1	**79.5**		
12	CH_2	37.7	36.4	2.01 m 1.39 dd 14.4, 8.4	2.24 – 1.47 m
13	CH_2	26.2	27.2	1.70 m 1.39 m	2.24 – 1.47 m
14	CH_2	32.0	30.1	2.04 m 1.40 m	2.54 – 2.45 m 2.24 – 1.47 m
15	CH	53.9	53.3	2.39 dd 10.3, 7.3	2.69 – 2.63 m
16	CH_2	34.6	33.1	2.71 br d 4.0 1.07 dd 15.8, 7.2	2.58 dd 16.0, 3.5 1.36 – 1.32 m
17	CH_2	73.6	72.5	4.85 dd 7.2, 3.7	4.92 dd 8.0, 3.5
18	C	215.1	214.7		
19	C	50.8	50.7		
20	CH	83.2	82.9	4.78 br d 5.9	4.80 d 6.5
21	C	106.7	106.6		
22	CH_2	35.1	34.8	2.10 m 1.83 m	2.24 – 1.47 m
23	CH_2	25.4	24.8	2.0 m	2.24 – 1.47 m
24	CH_2	66.6	66.3	4.53 dd 12.7, 1.8 3.70 d 12.7	4.51 dd 13.0, 2.0 3.74 d 13.0
25	CH_3	19.8	19.3	0.90 s	0.92 s
26	CH_3	24.3	24.1	1.35 s	1.38 s
27	CH	32.3	31.7	1.65 m	2.24 – 1.47 m
28/29	CH_3	21.7	21.0	0.98 d 6.4	1.01 d 6.5
28/29	CH_3	22.4	21.8	0.99 d 6.3	1.08 d 6.5
30	CH_3	26.2	25.2	0.93 s	0.86 s

3.2.3 C30: Secodaphniphylline-type

3.3.3.1 M360.29T312 Methyl homosecodaphniphyllate 1.52

The molecular formula, $C_{23}H_{37}NO_2$, was calculated based on measured m/z = 360.2898 (calculated 360.2902) (Figure 3.10). There were already two compounds reported that possessed this molecular formula: methyl homosecodaphniphyllate **1.52** and methyl homodaphniphyllate **1.56** which belong to daphniphylline and secodaphniphylline classes, respectively. Based on the ^{1}H and ^{13}C NMR chemical shifts, daphniphylline skeleton was not a match for the skeleton of the isolated alkaloid. Indeed, the experimental data closely matched the previously reported data for methyl homosecodaphniphyllate **1.52** (Figure 3.11) as presented in Table 3.6 (Ruggeri, Heathcock and Hansen, 1988; Zhang et al., 2012). Specifically, the characteristic carbons at the secodaphniphylline type skeleton such as δ_C at 59.4 and 48.9 ppm which were assigned to CH(1) and CH(15) due to the neighbouring nitrogen. A singlet at 3.67 ppm was assigned to a methyl group next to an oxygen atom.

We observed strong COSY correlations between CH(20) and CH_3(21)/CH_3(22). We also observed COSY correlations between CH_2(16) and CH_2(17) as well as between CH_2(8) and CH(7). We also analysed HMBC spectrum, in which the carbonyl C(18) showed strong correlations between CH_3(19). We also observed correlations between CH(1) and C(6) amongst others. While methyl homosecodaphniphyllate **1.52** belongs to a C30 group of *Daphniphyllum* alkaloid, it likely is a crucial intermediate in the pathway due to the fact that it lost the moiety characteristic for C30 type and can undergo skeletal rearrangements to form C22B and C22A compounds.

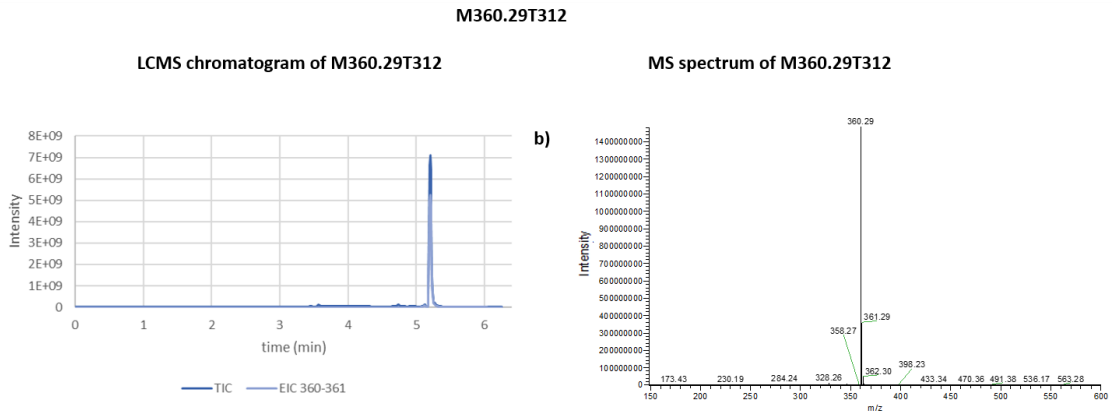

*Figure 3.10 a) LCMS chromatogram with TIC and extracted ion chromatogram of 360-361 $[M+H]^+$ representing molecular formula of $C_{23}H_{37}NO_2$ showing the methyl homosecodaphniphyllate **1.52**; b) spectrum of the methyl homosecodaphniphyllate **1.52** peak.*

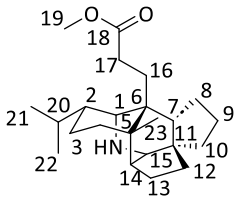

methyl homosecodaphniphyllate **1.52**

Chemical Formula: $C_{23}H_{37}NO_2$

Exact Mass: 359.2824

*Figure 3.11 Structure of methyl homosecodaphniphyllate **1.52**.*

*Table 3.6 Comparison between literature values ^{1}H (500MHz), ^{13}C (75 MHz) and experimental ^{1}H (700MHz), ^{13}C (175 MHz) NMR data for methyl homosecodaphniphyllate **1.52** in $CDCl_3$* (Ruggeri, Heathcock and Hansen, 1988; Heathcock et al., 1992a; Zhang et al., 2012).

C no.		**1.52 (lit)δ_C**	**1.52 (exp) δ_C**	**1.52 (lit) δ_H *J* (Hz)**	**1.52 (exp) δ_H *J* (Hz)**
1	CH	60.1	60.2	2.53 d 4.5	2.54 d 5.0
2	CH	53.2	53.4	1.90 –1.33 m	1.84 – 1.43 m
3	CH_2	22.8	23.0	1.90 – 1.33 m	1.84 – 1.43 m
4	CH_2	39.7	39.9	1.90 – 1.33 m	1.84 – 1.43 m
5	C	50.5	50.7		
6	C	36.8	37.0		
7	CH	48.5	48.6	1.90 – 1.33 m	1.90 t 5.0
8	CH_2	26.7	26.9	1.90 – 1.33 m	1.84 – 1.43 m
9	CH_2	20.7	20.8	1.90 – 1.33 m	1.84 – 1.43 m
10	CH_2	36.3	36.4	1.90 – 1.33 m	1.84 – 1.43 m
11	CH	39.0	39.1		
12	CH_2	36.3	36.4	1.90– 1.33 m	1.84 – 1.43 m
13	CH_2	27.8	28.0	1.90 – 1.33 m	1.84 – 1.43 m
14	CH	42.9	43.1	1.18 br d 13,3	1.18 d 13.0
15	CH	47.7	47.9	2.96 s	2.96 s
16	CH_2	29.6	29.7	2.39 ddd 15.5, 13.0, 4.5	2.40 ddd 17.0, 13.0, 5.0 1.84 – 1.43 m
17	CH_2	30.2	30.3	2.24 ddd 15.5, 12.5, 5.5 1.90 – 1.33 m	2.23 ddd 15.5, 12.0, 5.0 1.84 – 1.43 m
18	C	174.9	175.1		
19	CH_3	51.5	51.7	3.67 s	3.67 s
20	CH	28.7	28.9	1.90 – 1.33 m	1.84 – 1.43 m
21	CH_3	21.4	21.6	0.9 d 6.5	0.92 d 6.5
22	CH_3	21.0	21.2	0.9 d 6.5	0.96 d 6.5
23	CH_3	20.9	21.1	0.79 s	0.79 s

3.2.4 *Overview of results*

Table of all isolated alkaloids was collated (Table 3.7) showing their peak codes, chemical formulas and mass error between experimental and calculated mass. In summary, we successfully isolated four known *Daphniphyllum* alkaloids: yuzurimine **1.10**, deoxyyuzurimine **1.66**, daphnicalycine A **3.1** and methyl homo-secodaphniphyllate **1.52** and one *Daphniphyllum* alkaloid that was not previously reported – 7-hydroxydaphnilongeranin D **3.4**, structures shown in Figure 3.12.

The experimental data were compared to the literature data, specifically ^{13}C carbon spectra. When ^{1}H NMR spectra were not available or only reported as characteristic peaks (i.e. yuzurimine **1.10**), we validated our assignments by the analysis of 2D NMR experiments, as well as comparing NMR data to other *Daphniphyllum* alkaloids. Isolated alkaloids were used as standards in the following chapters. In the future they will be used as standards in further experiments as well as substrates in feeding experiments, specifically to aid gene discovery.

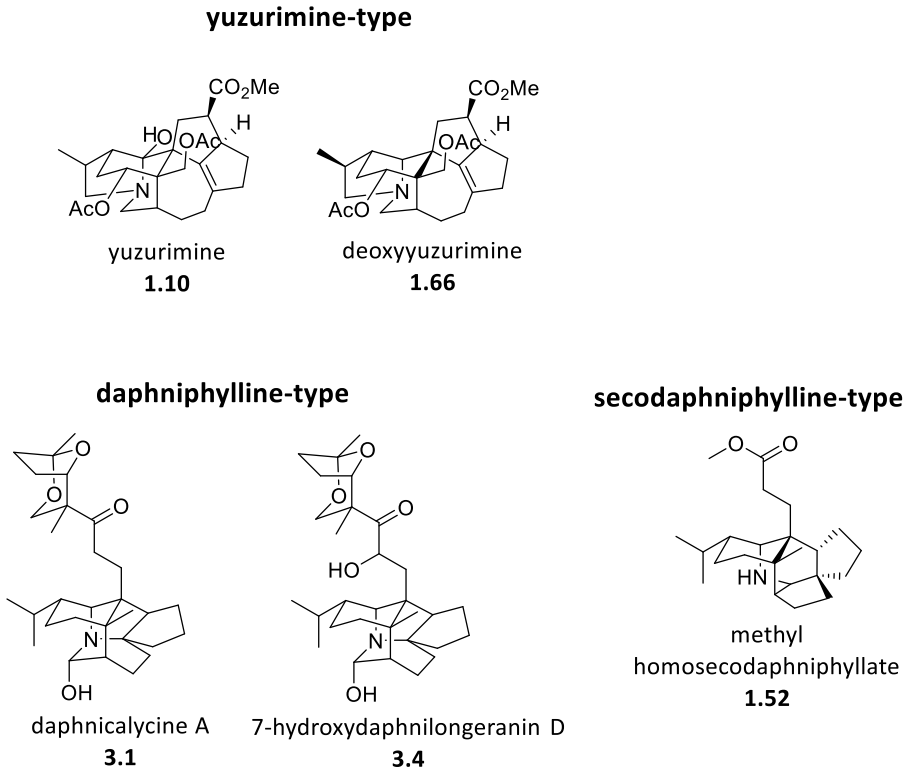

Figure 3.12 Structures of isolated Daphniphyllum *alkaloids.*

Table 3.7 Overview of isolated and characterised Daphniphyllum *alkaloids.*

Code name	Name	Chemical formula	Observed mass $[M+H]^+$	Calculated mass $[M+H]^+$	Error (ppm)
M488.26T210	yuzurimine **1.10**	$C_{27}H_{37}NO_7$	488.26443	488.264822	0.8
M472.27T204	deoxyyuzurimine **1.66**	$C_{27}H_{37}NO_6$	472.26931	472.269908	1.3
M486.35T240	daphnicalycine A **3.13**	$C_{30}H_{47}NO_4$	486.35803	486.35833	0.6
M502.35T210	7-hydroxydaphnilongeranin D **3.4**	$C_{30}H_{47}NO_5$	502.35297	502.353244	0.5
M360.29T312	methyl homo-secodaphniphyllate **1.52**	$C_{23}H_{37}NO_2$	360.28983	360.290252	1.2

4 What is a Precursor?

4.1 Introduction

4.1.1 *Hypothesis for the biosynthesis of Daphniphyllum alkaloids*

The hypothesis for the biosynthesis of *Daphniphyllum* alkaloids proposed that squalene was oxidised to diol **1.97** and dialdehyde **1.96**, followed by the introduction of a nitrogen atom as described in chapter 1. This leads to a scaffold forming step – likely creating a secodaphniphylline skeleton. This hypothesis was proposed based on the feeding experiments (Haruki, Yoshimasa and Suzuki, 1973; Suzuki et al., 1973) and biomimetic studies (Ruggeri and Heathcock, 1989; Pieitre and Heathcock, 1990; Heathcock et al., 1992b) which were described in detail in chapter 1.

4.1.2 *Simplified skeletons of Daphniphyllum alkaloids*

To simplify the metabolomic analysis of the plant extracts containing a number of possible of skeletal types, we divided the Daphniphyllum alkaloid class into simpler subtypes: C30, C22A and C22B°(Figure 4.1) as presented in detail in chapter 1 (Eljounaidi et al., 2024). The compounds not fitting those categories can be described as C22.

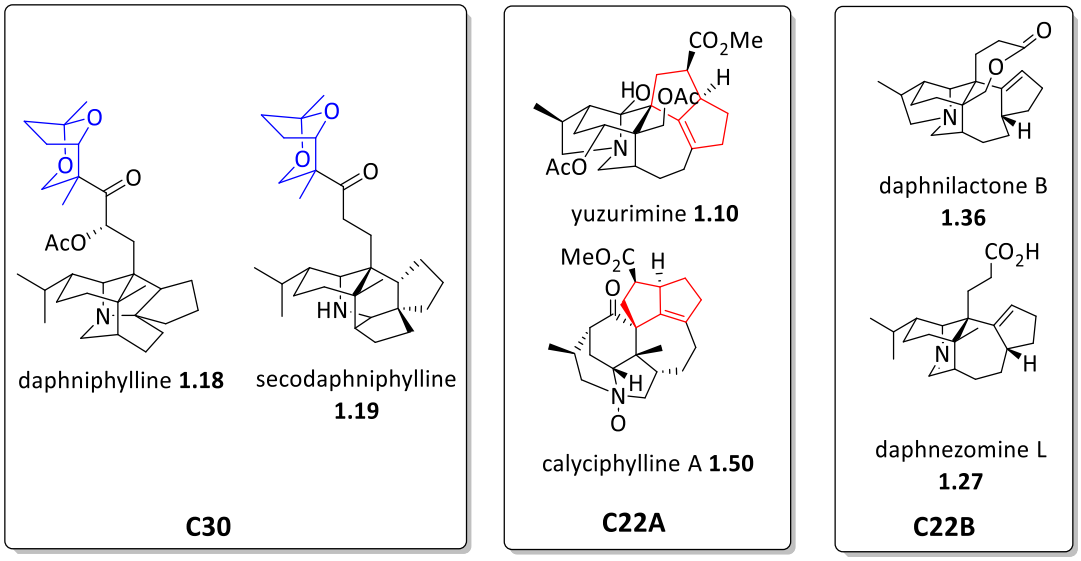

Figure 4.1 Representative Daphniphyllum *alkaloids, classified by carbon skeleton: C30 (blue highlighting C8 fragment lost in C22 compounds; C22A (presence of hexahydropentalene ring in red), C22B (absence of hexahydropentalene ring).*

C30 compounds include secodaphniphylline and daphniphylline type skeletons. The secodaphniphylline type is hypothesised to appear at the start of pathway as we can observe squalene molecule forming the secodaphniphylline skeleton (Scheme 4.1) and as was shown by DFT calculations and biomimetic studies (Heathcock, 1996; Tantillo, 2016).

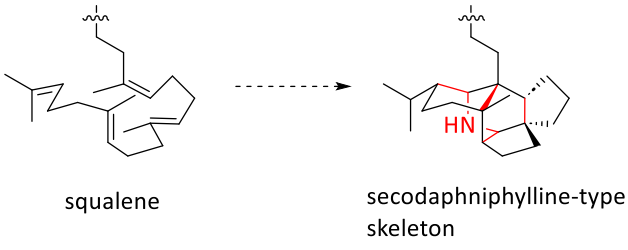

Scheme 4.1 Formation of secodaphniphylline skeleton from squalene.

4.1.3 *Untargeted mass spectrometry*

The goal was to determine the variation of *Daphniphyllum* alkaloids in tissue extracts and their dependence or lack of thereof based on the addition of precursors. Since we only have access to limited number of standards – which were described in chapter 3 – we used untargeted mass spectrometry. This also allowed for an unbiased detection of small molecules in complex set of samples. The data were collected on the high-resolution Thermo Tribid Orbitrap Fusion and Exploris 480 using an atmospheric pressure chemical ionisation (APCI) ion source in positive ion mode.

The data were analysed using various complimentary approaches. The molecular formulas were determined based on MS^1-based annotations and the possible structures were named using REAXYS and the curated *in silico* database of *Daphniphyllum* alkaloids consisting of 331 *Daphniphyllum* alkaloids which were categorised based on their carbon skeletons as introduced in chapter 1.

A limited number of peaks were annotated using chemical standards and MS^2 fragmentation data. Molecular networking, which clusters peaks based on their MS^2 fragmentation similarity, was done using the Global Natural Product Social Molecular Networking Platform (GNPS) using default settings (Wang et al., 2016). Molecular clusters with *Daphniphyllum* alkaloids were inspected manually. The chemical standards described in chapter 3 were also used in the clustering to determine the known skeletal types and structurally compounds.

The LC-MS data were processed using XCMS online to determine the peak area across all samples (Smith et al., 2006; Tautenhahn et al., 2012). The average of three technical replicates was used as a value of a biological replicate. For more detailed procedure see chapter 6, section 6.1.2.

4.1.4 *Feeding experiments*

Feeding assays are an experimental approach which can be used to study enzymatic activities and plant biosynthetic pathways. The substrates can be fed to plant crude protein extracts to investigate functions of unknown enzymes. Feeding of the substrates allows to observe and quantify the resulting products which helps to elucidate and characterise the biosynthetic pathways, identify the intermediates and products. Using protein extracts allows for the observation of multiple steps within a pathway, providing a broader, especially when a specific enzyme candidate for purification is not yet available. This approach can help in understanding the overall pathway dynamics before specific enzyme candidates are identified and characterised.

The substrates could include labelled or non-labelled compounds as well as a single purified protein or protein extracts. The protein extracts would contain a mixture of proteins from appropriate tissues as well as mixture of microsomal or soluble proteins.

The substrates can be labelled with stable isotopes, for example it was determined that squalene was a precursor to *Daphniphyllum* alkaloids when ^{14}C-labelled squalene was fed to the branches of *Daphniphyllum macropodum* which resulted in isolation of ^{14}C-labelled daphniphylline **1.18** and codaphniphylline **1.54** (Haruki, Yoshimasa and Suzuki, 1973). In the study of the biosynthesis of atisine-type diterpenoid alkaloids, L-[2-^{13}C,^{15}N]serine was fed to cell-free protein extracts (Zhao et al., 2009). This approach can be used if a step or steps in the biosynthetic are unknown, the proteins are unknown or access to other precursors is limited. That study showed that L-[2-^{13}C,^{15}N]serine was incorporated into spiramines A/B and C/D which meant that L-serine was one of the possible nitrogen sources in the biosynthetic pathway of atisine-type diterpenoid alkaloids.

The substrates do not need to be labelled for the feeding studies. In the study focused on solving the biosynthetic pathway of the alkaloid colchicine in *Gloriosa superba* species non-labelled substrates were fed to crude protein extracts (Nett and Sattely, 2021). For more detailed procedure see chapter 6, section 6.1.3.

4.2.4.1 Introduction to the experiment

The crude protein extracts were obtained following the previously published experimental approach (Nett and Sattely, 2021). In the experiments described in this chapter, squalene **1.11** and synthesised diol **1.97** were fed to the tissue extracts of root and leaf tissue which contain proteins, small molecules, such as *Daphniphyllum* alkaloids, and various other factors. The assays were then analysed using LC-MS to determine if and how the behaviour of *Daphniphyllum* alkaloids was affected by the addition of the proposed substrates.

4.1.5 *Aims*

In this study, we aim to investigate the role of squalene **1.11** and diol **1.97** in the leaf and roots tissue extracts to explore their role on the *Daphniphyllum* alkaloid biosynthesis. Specifically, we want to determine whether these substrates affect the metabolite profile and to gain insight into possible steps of the biosynthetic pathway. The tissue extracts will be analysed using high resolution LC-MS to allow for a confident determination of the molecular formulas of the detected metabolites.

Leaf and root tissue extracts containing a mixture of soluble and microsomal proteins will be incubated with the substrates to trace the biosynthetic origin of *Daphniphyllum* alkaloids. This study will be the first investigation of the role of hypothesised precursor diol **1.97** using protein extracts. Additionally, we will investigate whether the biosynthesis is tissue dependent.

4.2 Results

4.2.1 Overview of the experimental methodology

Overall, we conducted experiments using root and leaf tissue extracts. The assays contained soluble and microsomal protein extracts containing mixture of proteins and small molecules, buffer and substrates (squalene **1.11** or diol **1.97**). The controls included the tissue extracts, substrates and protease as well as a tissue extracts and buffer with no substrate added.

4.2.1.1 Plant selection

The plants that we used in the experiments described in this chapter were a 4-year-old plant F and 1-year-old offsprings of plant B which were grown from the seeds, all plants were *Daphniphyllum macropodum*. They were chosen for each experiment based on the availability. Initially, before successfully germinating seeds of *Daphniphyllum macropodum*, we were acquiring plants from various nurseries.

4.2.1.2 Protein extracts

The biosynthetic pathway of *Daphniphyllum* alkaloids is unknown with an unidentified number of steps required between production of squalene, formation of the scaffold and appearance of the first *Daphniphyllum* alkaloid. Therefore, we expected that multiple steps were required for the formation of the first *Daphniphyllum* alkaloid which would likely involve both soluble and membrane-bound proteins. So, in order to increase the chances of observing any changes, the mixture of crude soluble and membrane bound proteins was used. Since we initially hoped to observe the conversion of squalene **1.11** to diol **1.97** or a similar oxidised product, which would likely involve a P450 protein or a FAD-oxidase, the cofactors NADPH and FAD were used in the initial experiments to increase the chances of conversion of squalene to the hypothesised precursor – diol **1.97** – or another possible precursor. It is worth noting that plant P450s are membrane bound proteins (Bak et al., 2011).

4.2.1.3 Analytical process

There are many known but also unreported, but biosynthetically feasible *Daphniphyllum* alkaloids that often share the same high-resolution mass and molecular formula, classifying them as isobaric isomers. This similarity made it challenging to identify the specific compound of interest, yet it was crucial to differentiate between them. Since the number of known standards was limited, it was decided to code name the peaks. The created name of each peak consisted of two parts: firstly the high-resolution $[M+H]^+$ mass for example the name for characterised standard yuzurimine **1.10** would be created as follow: knowing that $[M+H]^+$ = M488.265 and the retention time of the peak was 3.50 min or 210 seconds, the code name of yuzurimine **1.10** was M488.265T210. A retention time shift was corrected to the standard yuzurimine **1.10** at 210 seconds. In some cases, the peak code reflected the biggest fragment that was used in the XCMS analysis – $[M+H-H_2O]^+$. For example, it was the case of M370.24T180 for which the molecular formula was in fact $C_{23}H_{33}NO_4$ and the fragment 370.24 m/z represented the loss of water. We decided to use the main ion used in the XCMS for the code naming the peak for simplicity as well as the possibility that we would not be able to determine the true $[M+H]^+$ in some cases.

Note that the peak codes represent $[M+H]^+$, indicating the exact mass of each alkaloid plus one proton. Consequently, the peak codes were 1 m/z unit larger than the exact mass of the corresponding neutral/free base alkaloid, represented as [M].

4.2.1.4 Global Natural Products Social Molecular Networking (GNPS) and MS analysis

GNPS is a tandem mass spectrometry (MS/MS) data curation and analysis approach. Molecular networking created by GNPS allows to visualise clusters of structurally similar compounds, based on the MS^2 fragmentation patterns (Wang et al., 2016). The colour of the node can represent samples from different tissue extracts or plants and cosine scores (edges) represent structural similarity of related compounds, with identical compounds getting score of 1. The molecular network was visualised using Cytoscape.

GNPS is a widely used tool in the field of natural products, specifically to dereplicate and prioritise discovery of novel natural products.

We used GNPS to help us determine the possible skeletons of the compounds of interest. We were looking for compounds similar to the isolated standards. The colours in the GNPS molecular network represent leaf tissue extract (teal), root tissue extract (coral) and the standards (gold). The colour is not quantitative and should only be treated as presence or absence. The gold fraction showed a number of compounds that were not characterised but were present in small quantity in the purified standards, too small to affect the NMR or characterisation but still detected by LC-MS. The MS1 annotation and the structural determination based on clustering in the GNPS molecular networking were validated using MS2 data.

4.2.2 Preliminary experiments

The first experiments involved separate soluble and microsomal protein extracts into which squalene and cofactors (NADPH and FAD) were added, we wanted to observe the first steps of the biosynthetic pathway: oxidation of squalene. However, diol **1.97** was not observed in any of the assays. Diol **1.97** was also not observed when root soluble and microsomal protein extracts were combined, and the substrates were added (Figure 4.2). The table 4.1 below shows a selection of C30 compounds in the root soluble and root microsomal protein extracts and lack of observed changes dependent on the addition of squalene. However, we observed changes in the alkaloid content in the root soluble protein extracts not dependent on the addition of squalene. This suggested that the alkaloids present in the extracts can behave as precursors in the pathway.

In this analysis, we assumed that substrate dependent changes were expected only for compounds that appear relatively early in the biosynthetic pathway. Biosynthesis follows a sequential transformation of metabolites, with each step depending on the availability of precursors from the preceding steps. We hypothesise that squalene **1.11** and diol **1.97** are precursors to *Daphniphyllum* alkaloid biosynthetic pathway. Thus, if certain *Daphniphyllum* alkaloids show changes only in response to the addition of these substrates, it suggests that their formation is directly reliant on the presence of those substrate. Therefore, these alkaloids can be placed near the beginning of the pathway i.e. within a few reactions from squalene **1.11** or diol **1.97**.

In contrast, *Daphniphyllum* alkaloids positioned further downstream in the pathway are likely derived from the intermediates which are already present within the tissue extracts, meaning that their formation is less likely to be dependent on the addition of those substrates. Instead, their levels could be influenced by the availability of other intermediates or enzymes present in the tissue extracts, regardless of substrate addition.

We categorised *Daphniphyllum* alkaloids based on their response to the substrate to determine their relative position in the pathway. If an alkaloid content increases only when the substrate is added, it is likely formed in the early steps. A significant decrease in the alkaloid content would suggest that those are likely to be intermediates in the pathway and their relative position is dependent on whether their depletion is influenced by the addition of the substrate. A decrease independent of the substrate addition would suggest that they can be placed later in the pathway. An increase would suggest that their formation is dependent on the addition of the substrate and so those compounds are placed relatively early in the pathway. Finally, alkaloids that exhibit changes independent of the substrate addition are likely positioned further downstream in the pathway.

To sum up, the observed changes were divided into several categories:

a) Substrate dependent – the observed changes were only observed in response to the addition of the substrate, suggesting that substrate was necessary to drive those changes. Thus, substrate dependent compounds can be placed early in the pathway. were only dependent on the addition of the substrate.
b) Is a precursor – a compound of interest showed a significant decrease suggesting that it was consumed during incubation, regardless of whether the substrate was added, therefore it likely acted as a precursor to other compounds.
c) Precursor available – a compound of interest showed significant increase, independent of the substrate addition. This behaviour suggested that precursors and enzymes were already present in the extracts.
d) Not consumed or made – this category included compounds that did now exhibit any statistically significant changes.

The observed changes were statistically significant. Some compounds could fit into multiple categories. For example, a compound could both use the added substrate as a precursor – be early in the pathway – and act as a precursor itself, showing consumption in the absence of the added substrate.

Interestingly, we noticed that when soluble and microsomal protein extracts were combined, the addition of squalene affected the *Daphniphyllum* alkaloid content. Therefore, we decided to repeat the experiments on the leaf tissue extracts, with soluble and microsomal extracts combined, and analyse the effect of squalene on the *Daphniphyllum* alkaloid content in detail.

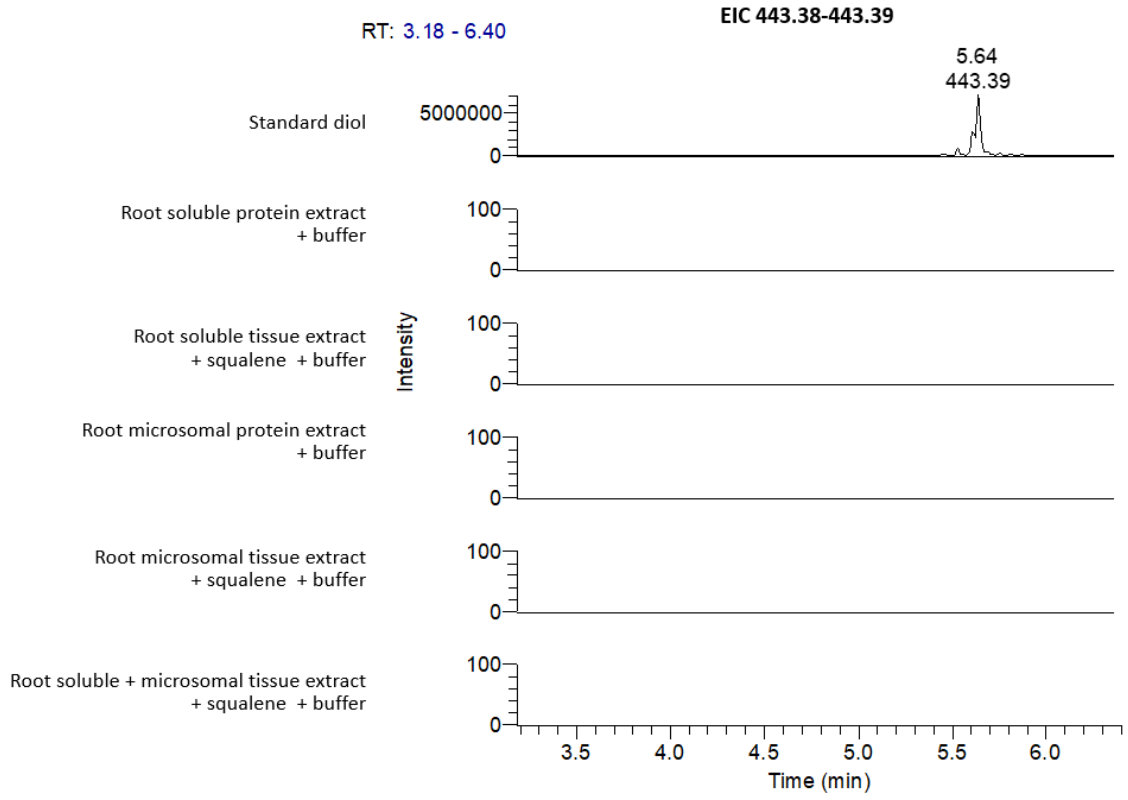

*Figure 4.2 LC-MS chromatogram with the extracted ion chromatogram of 443.38-443.39 representing molecular formula $C_{30}H_{51}O_2$ showing the synthesised standard diol **1.97** and root tissue extracts, all containing NADPH and FAD, (from the top) standard diol **1.97**, root tissue soluble protein soluble extracts + buffer, root tissue soluble protein extracts + buffer + squalene, root tissue microsomal protein extracts + squalene, root tissue combined soluble and microsomal extracts + squalene + buffer.*

Table 4.1 Summary of C30 compounds in preliminary experiments. RS represented root soluble protein extract, RM root microsomal protein extracts; 1: protein extracts treated with protease, buffer and squalene; 2: protein extracts and buffer, 3: protein extracts + squalene; fold change >1 represented an increase and <1 represented consumption. Statistical significance was represented by Y.

Exp	Peak name	Class	Peak area	fold change						Comments
				1 vs 2	sig	1 vs 3	sig	2 vs 3	sig	
RS	M470.363T280	C30	2E+06	1	N	1	N	1	N	Not consumed or made
RM	M486.358T240	C30	4E+05	1	N	1	N	1	N	Not consumed or made
RS	M486.358T240	C30	3E+06	1.05	N	1	N	0.95	N	Not consumed or made
RM	M488.374T270	C30	3E+05	1.05	N	1	N	1	N	Not consumed or made
RS	M488.374T270	C30	4E+05	1.25	Y	1.25	Y	1	N	Precursor available
RS	M512.374T220	C30	2E+05	1.75	Y	1.8	Y	1	N	Precursors available
RS	M512.374T240	C30	4E+05	1	N	1	N	1	N	Not consumed or made
RM	M512.374T314	C30	1E+06	1	N	1	N	1	N	Not consumed or made
RM	M528.369T320	C30	5E+06	1	N	1	N	1	N	Not consumed or made
RS	M528.369T320	C30	1E+07	0.7	Y	0.7	Y	1.05	N	is a precursor

4.2.3 Assays of the root and leaf tissue extracts treated with squalene

The first successful experiments showing changes in the *Daphniphyllum* alkaloids content dependent on the addition of squalene was conducted on the root and leaf tissue extracts from a 4-year-old plant F – *D. macropodum.* The changes in metabolites were analysed using LC-MS.

4.2.3.1 Overview of protocol

The first successful experiment involved obtaining the root and leaf tissue extracts containing mixture of proteins and small molecules to which squalene was added as a substrate. Since we wanted to observe the early steps of the biosynthetic pathway and verify whether squalene was in fact oxidised to a hypothesised precursor – diol **1.97** – the first assays included cofactors necessary for the oxidation step. We hypothesised that squalene could be oxidised to diol **1.97** by an enzyme such as P450 or FAD-oxidase, thus we added NADPH and FAD as cofactors needed for those enzymes. Since we did not know what other steps were necessary in the pathway, what types of enzymes or what cofactors, we hoped that we would be able to observe the intermediates such as diol **1.97**.

4.2.3.2 GNPS plot

A GNPS molecular network (Figure 4.3) was produced by uploading assays from experiments described in this chapter into the GNPS server. Additionally, nine standards described in chapter 3 were also added to the network in order to detect those compounds in the assays as well as identify alkaloids from the same class. The colours represented different tissue of assays: root tissue extracts were coral and leaf tissue extracts were teal. The gold notes represented the standards. Note that number of gold notes exceeded nine standards, it was because the standards were not completely pure and contained small quantities of other alkaloids which were picked up by the MS.

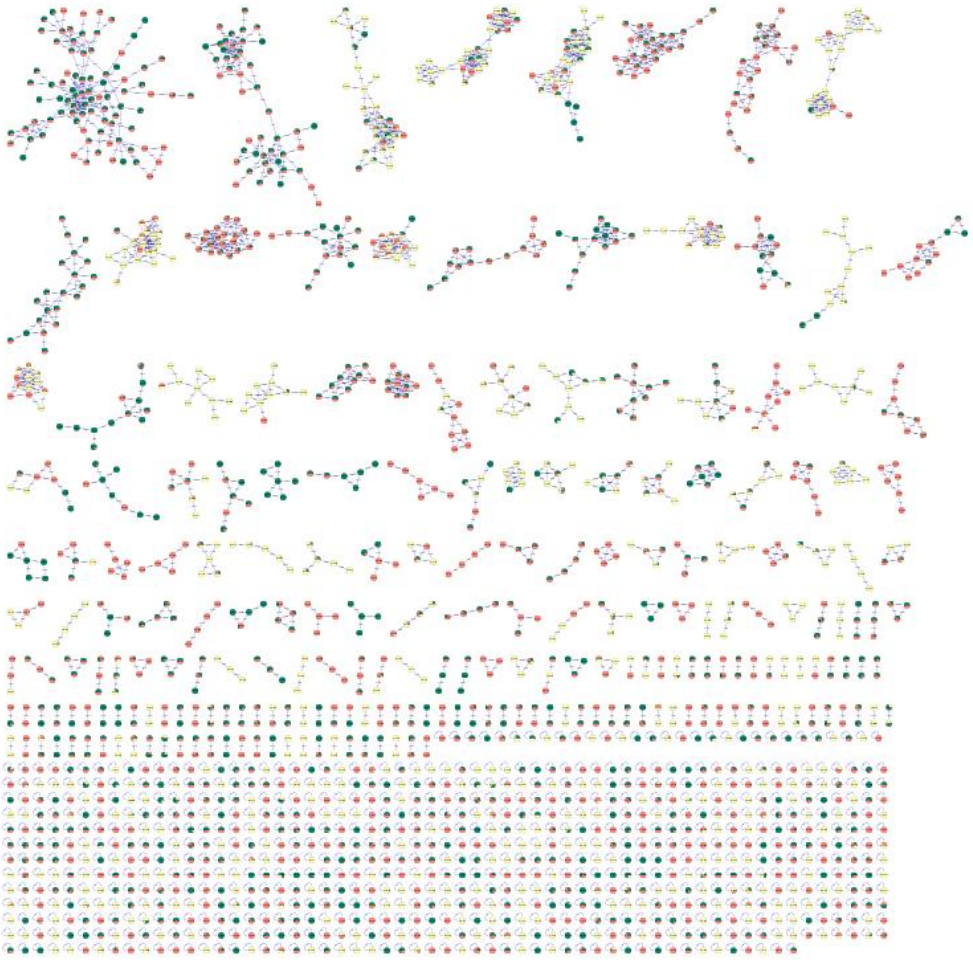

Figure 4.3 GNPS molecular network for root (coral nodes), leaf (teal) tissue extracts from D. macropodum (plant F) and 9 standards (gold), note that gold represented all the compounds present in not fully purified standards.

4.2.3.2.1 Examples of molecular clusters for known standards

Below we present examples of different clusters.

4.2.3.2.1.1 Daphnicalycine A cluster (daphniphylline type)

The presence of standards allowed us to determine the skeletal structures of analysed compounds of interest. For example, the known peak daphnicalycine A **3.1** (daphniphylline type alkaloid) clustered with many C30 compounds that were analysed in this chapter which allowed us to predict that they have daphniphylline-type skeleton. It is worth noting that the colours of the nodes represented presence or absence of the compounds in each extract. Interestingly, daphniphylline type compounds in this cluster were either present exclusively in the root tissue extracts or in both types of tissues. This

could suggest that the root and leaf biosynthetic pathway towards *Daphniphyllum* alkaloids diverged in C30 compounds leading to accumulation of different alkaloids.

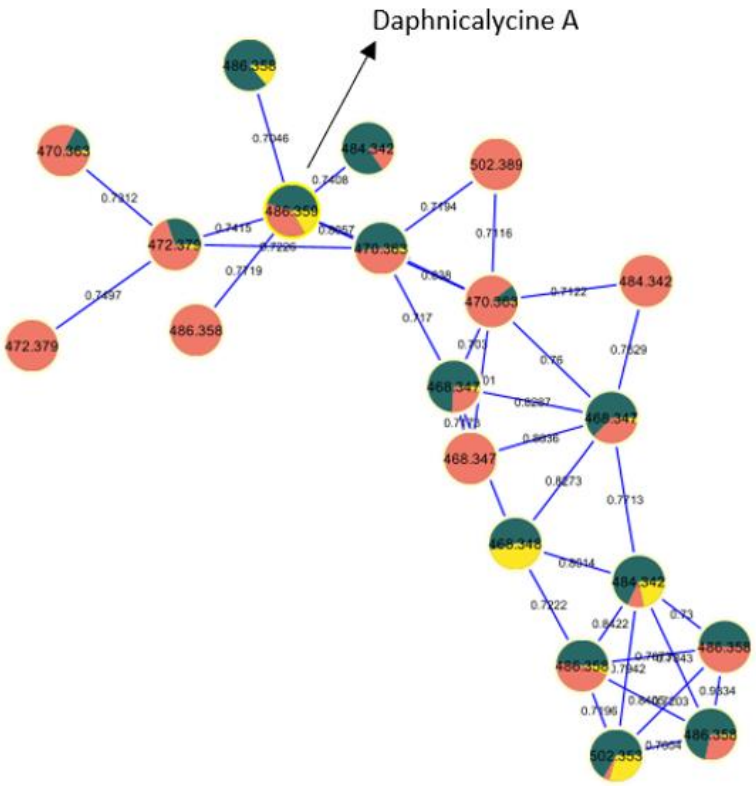

Figure 4.4 GNPS molecular network showing clustering around M470.36 with the molecular formula of $C_{30}H_{47}NO_3$ (teal: leaf extracts, coral: root extracts, gold: present in the standards)

4.2.3.2.1.2 Methyl homosecodaphniphyllate (C22 secodaphniphylline type)

Methyl homosecodaphniphyllate **1.52** has secodaphniphylline-type skeleton but it lost C8 moiety which is why it was classified as C22 compound. Interestingly, this type of skeleton was predominantly present in the root extracts (Figure 4.5).

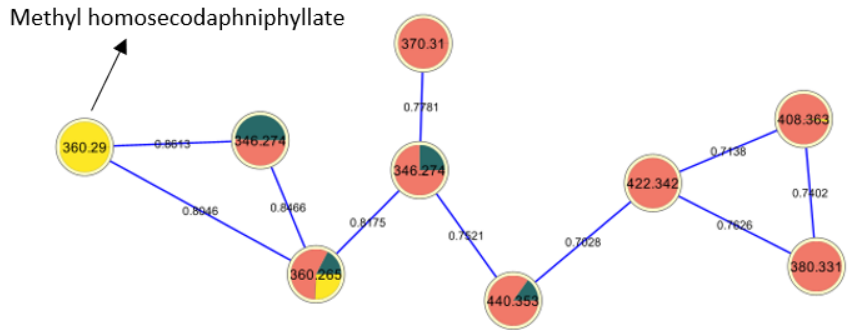

Figure 4.5 GNPS network containing M360.290T310 (methyl homosecodaphniphyllate ***1.52****) with the molecular formula of* $C_{23}H_{37}NO_2$.

4.2.3.2.1.3 Speculated C30 secodaphniphylline type cluster

None of the available standards were part of this cluster suggesting that it might be a secodaphniphylline type cluster. It also seemed like a cluster of high interest due to the high number of compounds annotated to be as C30 *Daphniphyllum* alkaloids.

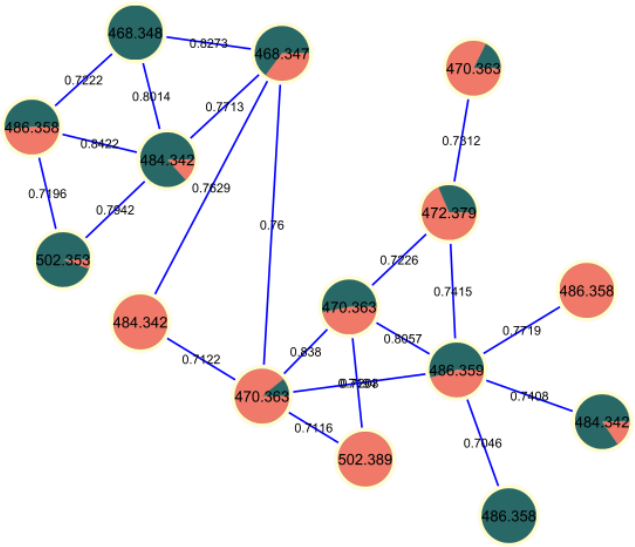

Figure 4.6 GNPS molecular network of C30 Daphniphyllum *alkaloids speculated to be secodaphniphylline type.*

4.2.3.3 Examples of changes in the Daphniphyllum alkaloid content

We observed a number of changes dependent and independent on the addition of squalene in the *Daphniphyllum* alkaloid content. The table showing an overview of the collected data in each section was collated. It included the peak code and the possible skeletal classes based on MS^1 annotation, GNPS clustering or MS^2 fragmentation

compared to the characterised standards. The results were summarised in the Table 4.2 showing the peak code and the fold change between each assay. The fold change was calculated and the fold change above 1 meant an increase while the fold change below 1 meant consumption of an alkaloid. The significant fold change was represented by "*". The statistical significance was calculated by a t-test and was obtained if $p < 0.05$. A possible assignment of the compound of interest was speculated based on the reported compounds and similarity to the standards was assessed using GNPS and manual comparison of MS^2 spectra.

Table 4.2 Summary of compounds in the root (R1) and leaf (L1) tissue extracts, their peak area, the fold changes between the assays (1: tissue extracts treated with protease, squalene and buffer, 2: tissue extracts + buffer, 3: tissue extracts treated with squalene and buffer; fold change >1 represented an increase, <1 represented consumption, significant change was represented by "".*

	Peak name	Class	Subtype	Peak area	Fold change			Comment	Behaviour
					1 vs 2	1 vs 3	2 vs 3		
R1	M528.369T325	C30	daphniphylline	7E+06	0.7*	1	1.5*	Assigned from GNPS	Squalene dependent, M528.369T325 is a precursor
L1	M528.369T320	C30	daphniphylline	2E+07	1	1.1*	1.1*	Assigned from GNPS	Squalene dependent, none available
R1	M528.369T320	C30	daphniphylline	2E+06	0.8*	1	1.2*	Assigned from GNPS	Squalene dependent, M528.369T320 is a precursor
R1	M528.369T314	C30	daphniphylline	3E+06	1.1*	1.1*	1	Assigned from GNPS	Precursors available
L1	M528.369T314	C30	daphniphylline	2E+07	1	1.1*	1.1	Assigned from GNPS	Squalene dependent, none available
L1	M528.369T260	C30		1E+07	1.2*	1.2*	1	unclear	Precursors available
R1	M528.369T260	C30		3E+06	1	1	1	unclear	Not consumed or made
L1	M512.374T324	C30		6E+06	1.1*	1.2*	1	unclear	Precursors available
R1	M512.374T314	C30	daphniphylline	6E+06	1.1*	1.2*	1	Assigned from GNPS	Precursors available
L1	M512.374T314	C30	daphniphylline	3E+06	1	1.1*	1.1*	Assigned from GNPS	Precursors available
L1	M512.374T240	C30		4E+05	1.2*	1.2*	1	unclear	Precursors available
R1	M512.374T240	C30		3E+05	1.1*	1.1*	1	Unclear	Precursors available
R1	M512.373T220	C30		80000	1.8*	2.1*	1.2*	acetylation from 470	Squalene dependent, precursors available
R1	M488.374T270	C30	daphniphylline	2E+06	1	1	1	calyciphylline P? based on MS[1]	Not consumed or made
L1	M488.265T210	C22 A	yuzurimine	1E+08	1	1	1	standard: yuzurimine	Not consumed or made
L1	M486.358T310	C30	daphniphylline	1E+06m	1	1.3*	1.2*	Assigned from GNPS	Squalene dependent, none available
R1	M486.358T240	C30	daphniphylline	2E+06	1	1.1*	1.1*	standard: daphnicalycine A	Squalene dependent, none available
R1	M472.379T315	C30	secodaphniphylline	5E+06	1.8*	1.8*	1	unclear	Precursors available

R1	M470.363T314	C30	daphniphylline	4E+07	1	1.3*	1.2*	Assigned from GNPS	Squalene dependent, none available
L1	M470.363T314	C30	daphniphylline	8E+06	1.1*	1.1*	1		Precursors available
R1	M470.363T310	C30	daphniphylline	5E+06	1	1.3*	1.2*	Assigned from GNPS	Squalene dependent, none available
L1	M470.363T310	C30	daphniphylline	1E+07	0.85*	1	1.1*	Assigned from GNPS	Squalene dependent, M470.363T310 is a precursor
R1	M470.254T210	C22 A	yuzurimine	1E+06	1	1.1*	1.1*	standard: yuzurimine	Squalene dependent, none available
L1	M390.264T250	C22	daphnezomine L?	60000	0.65*	0.65*	1	daphnezomine W?	is a precursor
L1	M388.249T180	C22 A		2E+07	1	1	1		Not consumed or made
L1	M386.233T175	C22 A	yuzurimine	1E+06	1.3*	1.3*	1		Precursors available
R1	M386.233T150	C22 A	yuzurimine	4E+06	1	1.1*	1.1*		Squalene dependent, none available
L1	M384.217T80	C22		1E+06	1	1	1		Not consumed or made
R1	M382.202T145	C22		60000	2.1*	2.2*	1		Precursors available
L1	M376.249T130	C22 B		70000	1	1.5*	1.6*		Squalene dependent, none available
R1	M370.238T175	C22	not yuzurimine	3E+06	1.1*	1.2*	1.1*		Squalene dependent, precursors available
R1	M368.222T150	C22		3E+06	1.1*	1.2*	1.2*		Squalene dependent, precursors available
L1	M360.254T90	C22		1E+06	1.4*	1.4*	1		Precursors available
R1	M360.217T170	C22 A		1E+05	1	1.2*	1.2*	daphhimalenine D?	Squalene dependent, none available
R1	M359.270T286	C22	daphnilactone B	2E+05	0.05*	0.3*	4.8*		Squalene dependent, M359.270T286 is a precursor
L1	M356.222T90	C22		1E+06	0.9*	0.9*	1		M356.222T90 is a precursor
L1	M356.222T210	C22		3E+05	1	1	1		Not consumed or made
L1	M356.222T180	C22		1E+06	1.2*	1.2*	1		Precursors available

R1	M346.27T150	C22	secodaphniphylline	1E+07	1	1.2*	1.15*	intermediate of C30 and C22, Assigned from GNPS	Squalene dependent, none available
R1	M346.27T140	C22		2E+07	1.15*	1.2*	1		Precursors available
R1	M342.24T160	C22	daphnilactone B	1E+07	0.2*	0.2*	1		is a precursor
L1	M342.24T160	C22	daphnilactone B	2E+07	0.12*	0.1*	1		is a precursor
R1	M332.259T325	C30	daphniphylline	67000	0.3*	1.2*	4*	daphnezomine O?	Squalene dependent, M332.259T325 is a precursor
R1	M316.264T290	C22		90000	1.4*	1.3*	1	caldaphnidine G?	Precursors available

4.2.3.3.1 Significant increase dependent on the addition of squalene

We observed that the addition of squalene significantly increased the levels of certain *Daphniphyllum* alkaloids, suggesting that those alkaloids were likely positioned early in the biosynthetic pathway. Without the addition of squalene, no changes in those alkaloid levels were detected which likely indicated the absence of necessary precursors in the tissue extracts. The addition of squalene allowed the enzymes access to the precursor needed for the formation of some *Daphniphyllum* alkaloids.

The examples of compounds that showed significant increase dependent on the addition of squalene were M470.363T310 and M486.358T260 (Figure 4.7).

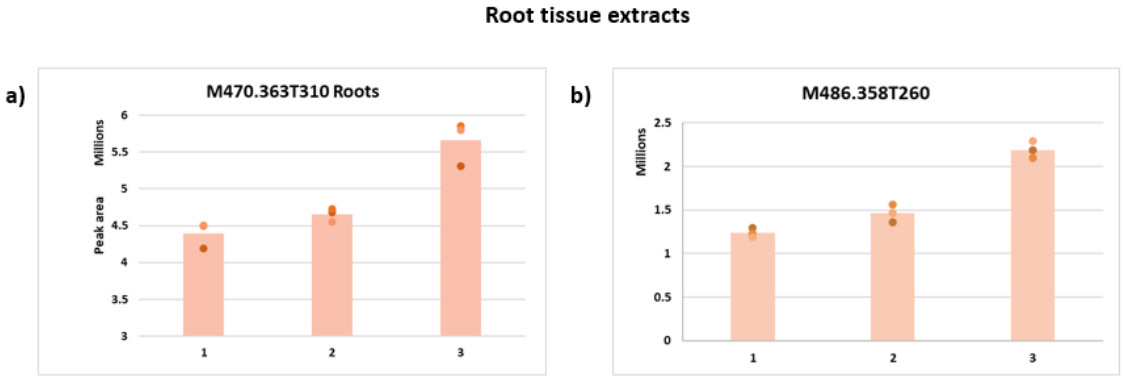

Figure 4.7 Peak areas of selected peaks in the root tissue extracts with a) $[M+H]^+$ = 470.363 at 310 seconds matching molecular formula of $C_{30}H_{47}NO_3$ and b) $[M+H]^+$ = 486.358 at 260 seconds matching molecular formula of $C_{30}H_{47}NO_4$; 1) Root tissue extract + protease + squalene + buffer, 2) Root tissue extract + buffer, 3) Root tissue extract + squalene + buffer. Each point represents a single compound from a single sample taken as an average of three biological repeats; bar represents an average peak area of a single compound across all samples.

Based on the GNPS molecular network, which clustered closely with daphnicalycine A **3.1** – which was the isolated and characterised by NMR standard described in chapter 3 – those compounds belong to daphniphylline type. The M486.358 are closely related to M470.363, in fact there are reported pairs of those two compounds (Irikawa et al., 1968; Yang et al., 2006; Di et al., 2008; Mu et al., 2008; Shen et al., 2020) in which M486.358 were hydroxylated M470.363 showing that those two were likely separated by one step in the biosynthetic pathway (Scheme 4.2). Additionally, hydroxylation of codaphniphylline **1.54** could lead to at least two different alkaloids: daphnilongeranin D **3.3** and daphnicalycine A **3.1**. We do not know which would be a preferred pathway or would we observe both pathways happening in parallel. On top of that, it is not an only

example of multiple possible pathway that we could observe. This could depend on the specific plant, time of the year, tissue or environmental response. The numerous possibilities of metabolomic changes that happen in *Daphniphyllum* alkaloid biosynthetic pathway adds to the complexity of this data.

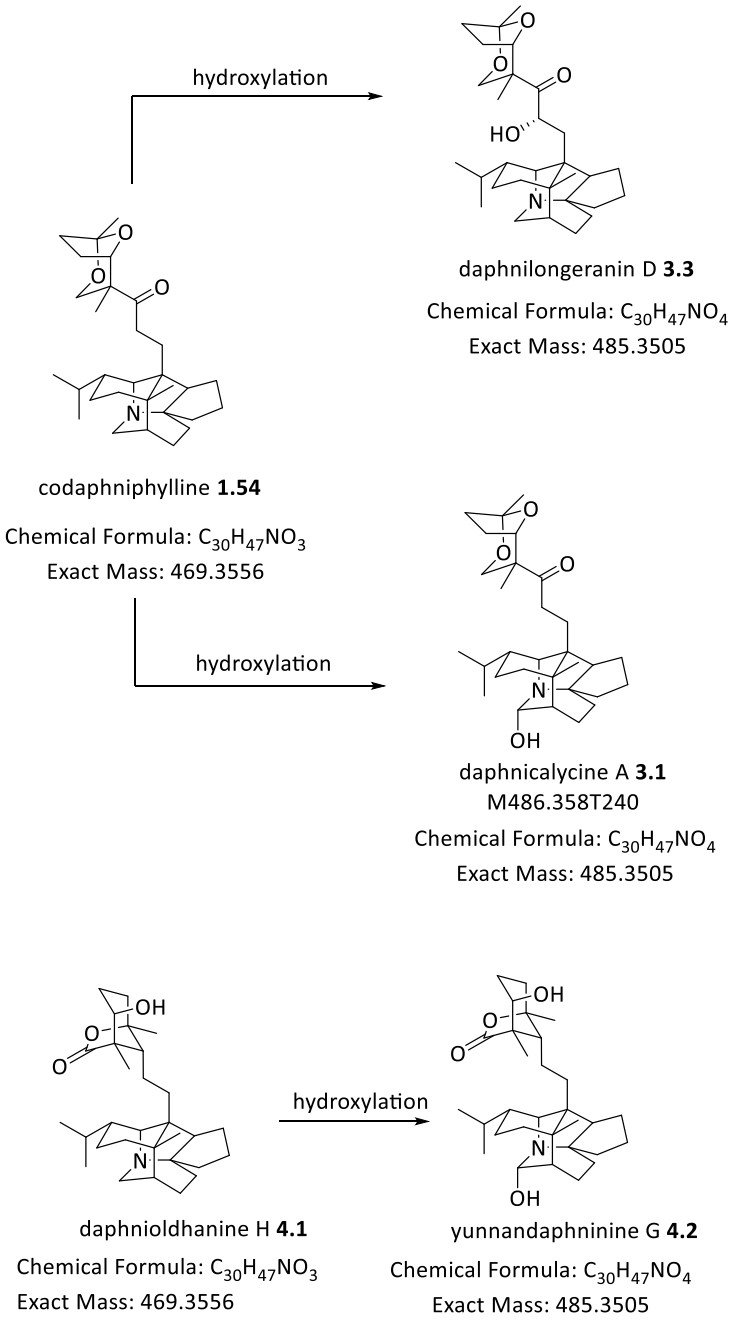

Scheme 4.2 Scheme showing a proposed biosynthetic pathway between M470.363 ($C_{30}H_{47}NO_3$) and 486.358 ($C_{30}H_{47}NO_4$).

4.2.3.3.2 Significant increase independent of the addition of squalene

We observed significant enzymatic changes independent of the addition of squalene which indicated the presence of intermediates in the mixture. This suggested that those alkaloids were positioned later in the biosynthetic pathway as they were not affected by the addition of squalene.

An example of such behaviour was exhibited by M386.233T175 with molecular formula of $C_{23}H_{33}NO_4$ (Figure 4.8). The known compounds of this molecular formula belong to C22A subtypes such as yuzurimine and calyciphylline A types.

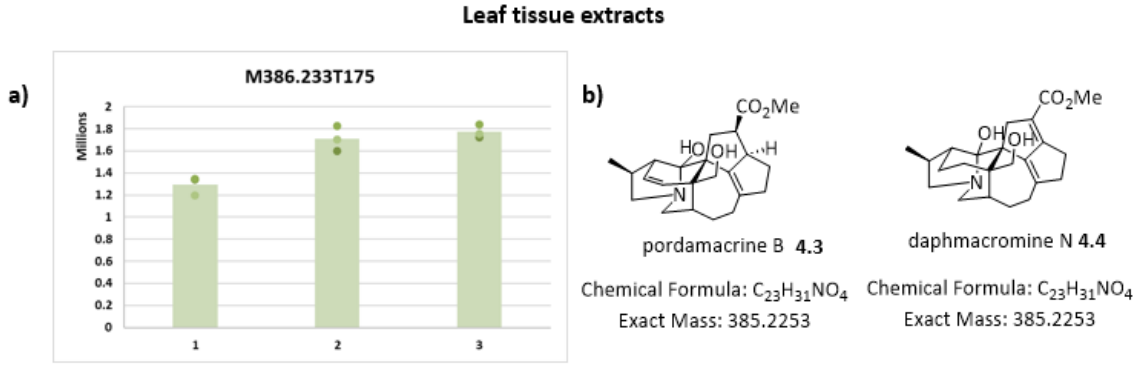

Figure 4.8 a) Peak areas of selected peaks with $[M+H]^+$ = 386.233 at 175 seconds matching molecular formula of $C_{23}H_{31}NO_4$; 1) Root tissue extract + protease + squalene + buffer, 2) Root tissue extract + buffer, 3) Root tissue extract + squalene + buffer. Each point represents a single compound from a single sample taken as an average of three biological repeats; bar represents an average peak area of a single compound across all samples. b) structure of pordamacrine B with the molecular formula of $C_{23}H_{31}NO_4$ matching the exact mass of $[M+H]^+$ = 386.233.

In the GNPS network, M386.233T175 did not appear in the same cluster as yuzurimine **1.10** or other yuzurimine-type standards mentioned in chapter 3. Initially, it suggested that M386.233T175 could belong to yuzurimine or yuzurine type. However, it could also be pordamacrine B **3.4** or daphmacromine N **4.4** which although belong to yuzurimine type, possess an additional double bond in the caged skeleton which would explain different MS/MS fragmentation pattern to yuzurimine **1.10**. However, there are many possible types of *Daphniphyllum* alkaloids that could possess this exact molecular formula which include calyciphylline A, calyciphylline C, yuzurimine, yuzurine (see Appendix table A.1), and without a standard, we cannot confidently determine the structure.

4.2.3.3.3 Consumption of an alkaloid independent of the addition of squalene

Another observed behaviour was consumption of *Daphniphyllum* alkaloids that was not recovered by the addition of squalene (Figure 4.9). This behaviour could indicate that the compounds that were consumed behaved as vital intermediates placed later in the pathway. An example of such compound would be M342.24T160 – with the known compounds fitting it into C22B category. It is worth noting that this compound showed the same behaviour in both root and leaf extracts (Figure 4.9).

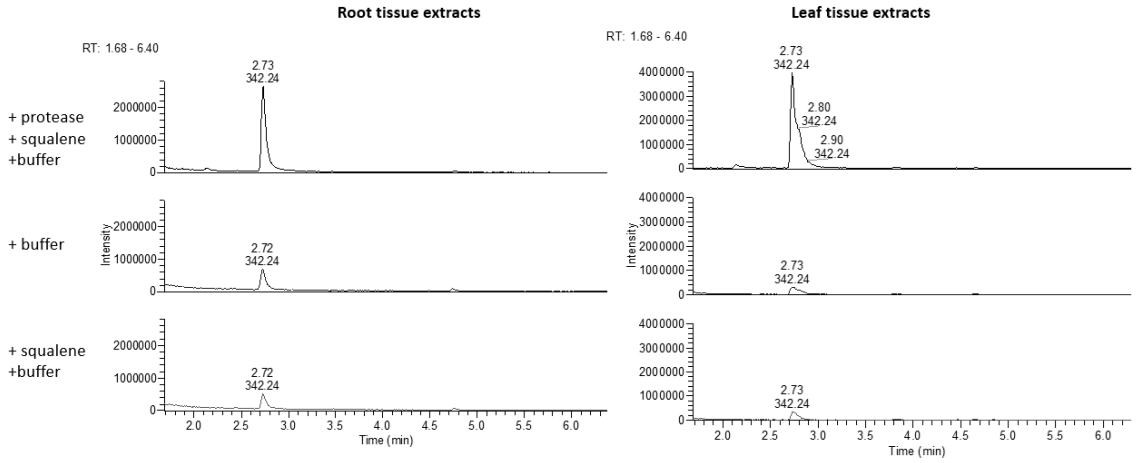

Figure 4.9 LC-MS chromatograms of root and leaf with extracted ion chromatogram of 342.24 – 342.25; (from the top) tissue extract + protease + squalene + buffer, tissue extract + buffer and tissue extract + squalene + buffer; (from the left) root tissue extract and leaf tissue extract.

Additionally, the same behaviour – although somewhat recovered by the addition of squalene – was observed by M359.270T286 with the molecular mass $C_{22}H_{34}N_2O_2$. The only *Daphniphyllum* alkaloid of this molecular formula, reported so far, was macropodumine H **4.6** (daphnilactone B type) (Figure 4.10). It could be then assumed that two compounds that showed the same behaviour were structurally related thus the structure of M342.24T160 could be predicted as daphnilactone B **1.36** or isodaphnilactone B **4.5**.

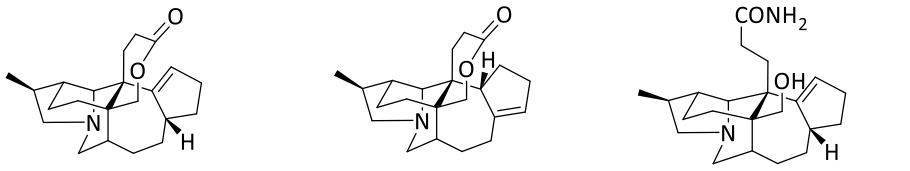

daphnilactone B **1.36**

Chemical Formula: $C_{22}H_{31}NO_2$
Exact Mass: 341.2355

isodaphnilactone B **4.5**

Chemical Formula: $C_{22}H_{31}NO_2$
Exact Mass: 341.2355

macropodumine H **4.6**

Chemical Formula: $C_{22}H_{34}N_2O_2$
Exact Mass: 358.2620

Figure 4.10 The structures of daphnilactone B type alkaloids.

4.2.3.3.4 Consumption and recovery of an alkaloid dependent on the addition of squalene

The final observed type of behaviour was consumption of a *Daphniphyllum* alkaloid that was recovered with the addition of the substrate, squalene (Figure 4.11). This behaviour could suggest that while these compounds would act as intermediates in the pathway, they were positioned at an early stage in the process. Consequently, their depletion was compensated by the addition of squalene.

An example of the compound that exhibited such behaviour in the leaf tissue extracts was M470.363T310. Based on the GNPS networking, the skeletal structure was assigned as a daphniphylline type.

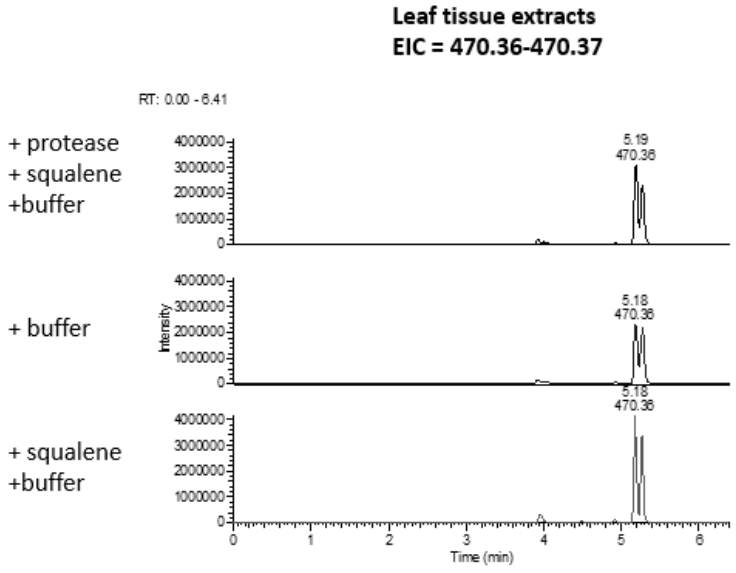

Figure 4.11 LC-MS chromatograms of extracted ion chromatogram of 470.36-470.37 (from the top) leaf tissue extract + protease + squalene + buffer, leaf tissue extract + buffer and tissue extract + squalene + buffer.

4.2.3.4 Overview of the results

We observed variation in changes between root and leaf tissue extracts, specifically in which specific compounds showed those changes. Nevertheless, we observed similar changes in the same type of compounds across those tissues, suggesting that *Daphniphyllum* alkaloids are produced in those tissues separately. For example, C30 compounds showed significant increases dependent on the addition of squalene in both tissue extracts. Specifically, M470.363T310, M470.363T314 and M486.358T240, all assigned as daphniphylline type based on the GNPS cluster. M486.358T240 was assigned as daphnicalycine A **3.1** which compared to the characterised standard described in chapter 3. Compounds that matched the exact mass of M486.358 were hydroxylated M470.363, and several pairs of M470.263 and M486.358 have been reported already showing proximity in the pathway as shown in Scheme 4.2.

In the leaf tissue extract, the sole effect of the addition of squalene was observed in M486.358T310 as well as M528.369T314 and M528.369T320, also daphniphylline-types. In the roots the same change was observed in M470.363T310 and M486.358T260, also C30 compounds. While we did not know the exact structure of those compounds, we were able to propose the part of the leaf pathway which could be placed early on in the overall biosynthetic pathway with already reported compounds (Scheme 4.3). Based on the GNPS, there was a similarity between the characterised standard – daphnicalycine A **3.1** – and the observed C30 compounds identifying them as likely belonging to the daphniphylline type. The structural difference would probably be in the position of the affected hydroxy group.

The pairs of *Daphniphyllum* alkaloids M486 and M528 shown in Scheme 4.3 are not only possible pairs, however those are only reported pairs in the literature so far, for example M528 that would be an acetylated equivalent of daphnicalycine A **3.1** is not known.

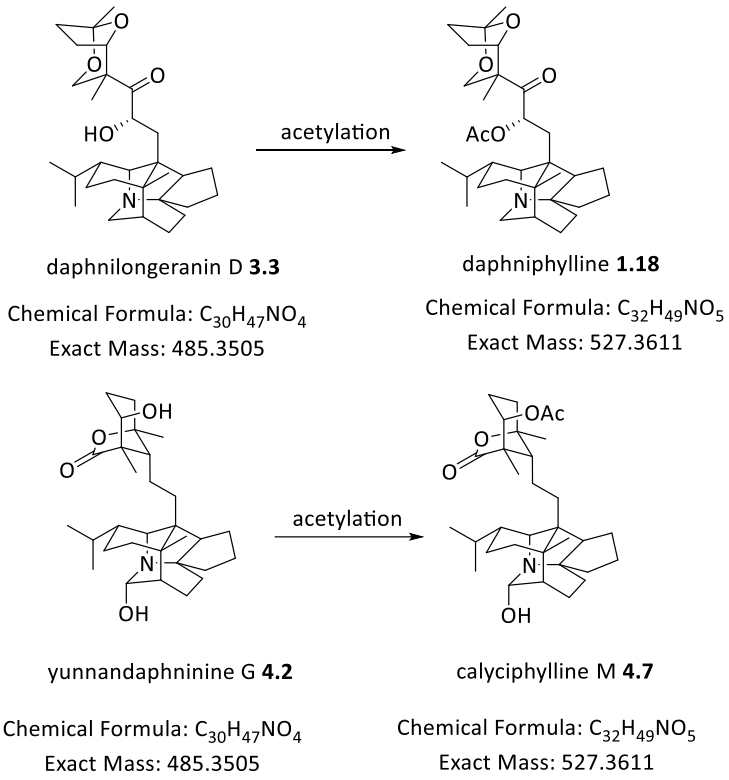

daphnilongeranin D **3.3**

Chemical Formula: $C_{30}H_{47}NO_4$
Exact Mass: 485.3505

daphniphylline **1.18**

Chemical Formula: $C_{32}H_{49}NO_5$
Exact Mass: 527.3611

yunnandaphninine G **4.2**

Chemical Formula: $C_{30}H_{47}NO_4$
Exact Mass: 485.3505

calyciphylline M **4.7**

Chemical Formula: $C_{32}H_{49}NO_5$
Exact Mass: 527.3611

Scheme 4.3 Possible route from M486.358 to M528.369 through acetylation.

The C30 compounds were assigned to belong to daphniphylline type based on the GNPS cluster with the characterised standard daphnicalycine A **3.1** (daphniphylline type). However, we have not isolated the standard which would have secodaphniphylline-type skeleton and as such we cannot exclude that those two skeletons could cluster together. While there were other C30 clusters that could be formed of secodaphniphylline type compounds, the lack of standards can make the skeletal determination somewhat uncertain. Nevertheless, the MS^2 spectra of compounds of interest were compared to daphnicalycine A **3.1** (daphniphylline type) and methyl homo-secodaphniphyllate **1.52** (secodaphniphylline type) as an attempt to establish the skeleton type.

The only compound showing significant changes that we confidently assigned as secodaphniphylline type (albeit C22 subtype) was M346.27T150 in the root extract. The GNPS molecular network placed M346.27T150 in the same cluster as the characterised standard methyl homosecodaphniphyllate **1.52** (M360.290T310) which would suggest that M346.27T150 could be assigned as daphnezomine M **1.53** (Figure 4.12). The difference between daphnezomine M **1.53** and methyl homosecodaphniphyllate **1.52**

lies in functional groups: a methyl ester in the standard and the carboxylic group in the daphnezomine M **1.53**. Methyl homosecodaphniphyllate **1.52** was not observed in the root or leaf extracts of this plant.

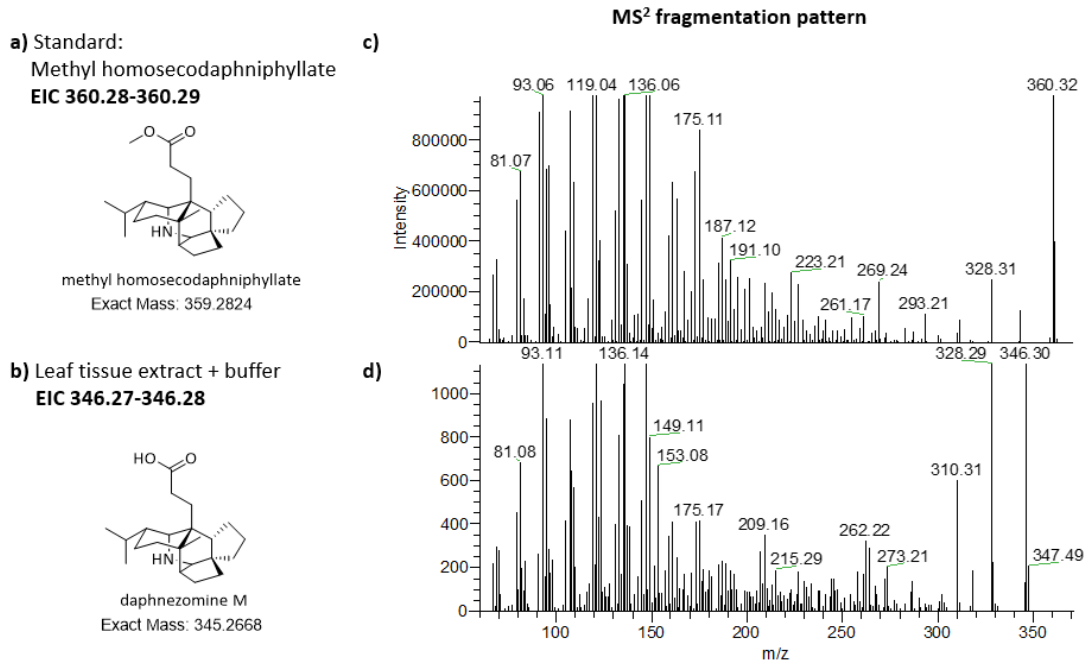

*Figure 4.12 Structures of a) methyl homosecodaphniphyllate **1.52** ($C_{23}H_{37}NO_2$) and b) daphnezomine M **1.53** ($C_{22}H_{35}NO_2$), MS^2 fragmentation patterns of c) methyl homosecodaphniphyllate **1.52** and d) M346.274T150.*

The alkaloid that showed the highest fold change, albeit not dependent on the addition of the substrate, was M472.379T315 in the root extracts. There were four *Daphniphyllum* alkaloids of the molecular formula $C_{30}H_{49}NO_3$ belonging to daphniphylline and secodaphniphylline-type (Figure 4.13).

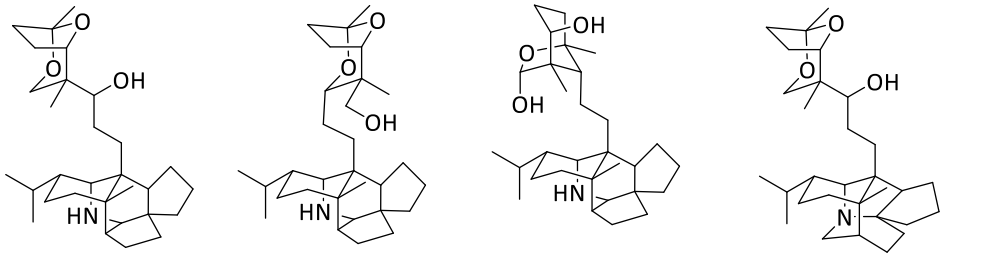

caldaphnidine E | daphniteijsmanine | daphnioldhanin F | yunnandaphninine H

Chemical Formula: $C_{30}H_{49}NO_3$
Molecular Weight: 471.7260

Figure 4.13 (from the left) Structures of known M472.370 matching the molecular formula $C_{30}H_{49}NO_3$: caldaphnidine E, daphniteijsmine, daphnioldhanin F and yunnandaphninines H.

M472.379T315 was part of a GNPS cluster, likely containing secodaphniphylline-type compounds. Although we do not have a C30 standard with a secodaphniphylline-type skeleton, standard daphnicalycine A **3.1** (daphniphylline-type) was not part of this cluster. This suggests that the compounds in this cluster, including M472.379T315, could belong to secodaphniphylline-type alkaloids.

Even though the increase was not dependent on the addition of squalene, the content of M472.379T315 almost doubled which was the highest fold change independent of the addition of squalene observed in C30 compound (Figure 4.14). The other C30 alkaloid that showed such high fold change was M512.373T220 which also showed a significant increase dependent on the addition of squalene. This behaviour suggested that not only squalene was a precursor for this alkaloid but also a precursor which was converted to M512.373T220 was already present in the root extracts.

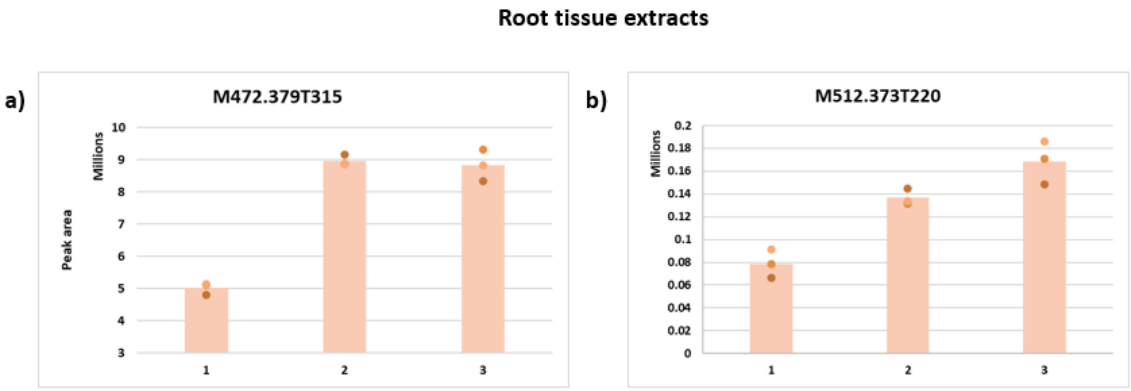

Figure 4.14 Peak areas of selected peaks in the root tissue extracts a) with $[M+H]^+$ = 472.379 at 315 seconds matching molecular formula of $C_{30}H_{49}NO_3$ and b) $[M+H]^+$ = 512.373 at 220 seconds matching molecular formula of $C_{32}H_{49}NO_4$; 1) Root tissue extract + protease + squalene + buffer, 2) Root tissue extract + buffer, 3) Root tissue extract + squalene + buffer. Each point represents a single compound from a single sample taken as an average of three biological repeats; bar represents an average peak area of a single compound across all samples.

Two reported compounds of the molecular formula $C_{32}H_{49}NO_4$ which could be M512.373T220 were similar with the exception of the skeleton type (Figure 4.15).

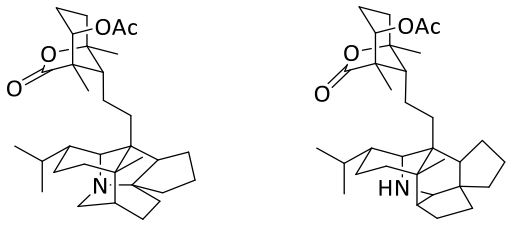

daphmacrine daphnioldhanin E

Chemical Formula: $C_{32}H_{49}NO_4$
Molecular Weight: 511.7470

Figure 4.15 Structures of known M512.373 (C30 type) with the molecular formula $C_{32}H_{49}NO_4$.

The M512.373 and M470.363 were closely related, in fact M512.373 could be obtained by acetylation of an equivalent M470.363 (Scheme 4.4). It is worth noting that many *Daphniphyllum* alkaloids, especially those early in the pathway, still need to be isolated and reported. This can be observed with many compounds that appeared in the GNPS clusters that were not reported yet as well as with the presumed gaps in the pathway as presented below – the M470.363 equivalent of daphnioldhanin E was not reported yet.

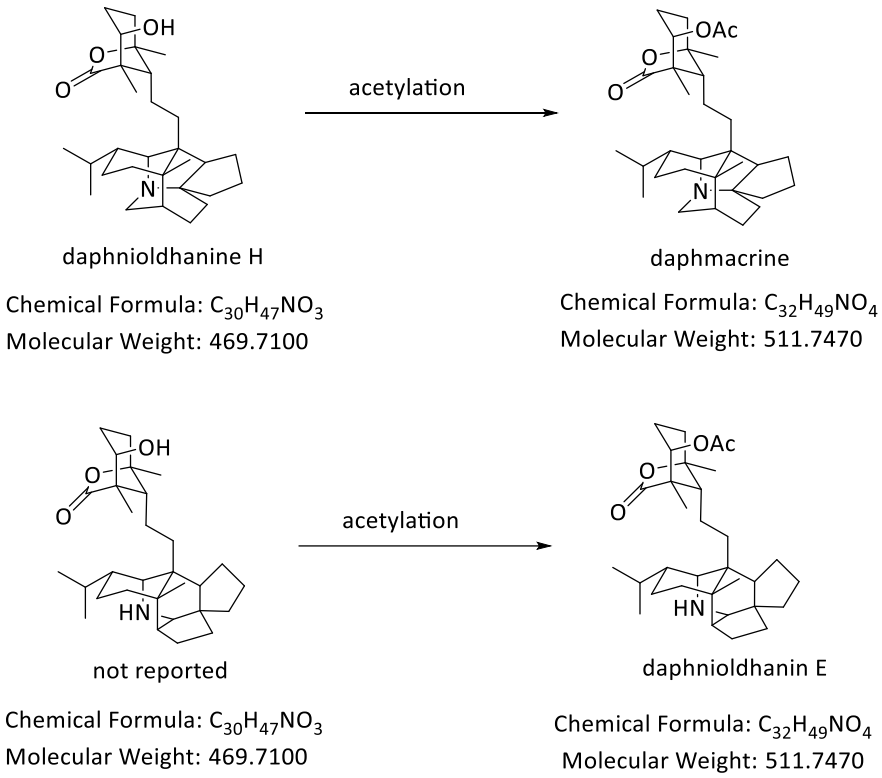

Scheme 4.4 Possible biosynthetic route to M512.373.

4.2.3.5 Discussion

We named C30 compounds as daphniphylline-type based on them forming a GNPS cluster with the characterised standard daphnicalycine A **3.1** (daphniphylline type). We have not isolated a C30 compound belonging to seco-daphniphylline type and so we cannot be certain whether GNPS would consider them structurally related to form one cluster. Thus, MS^2 spectra of daphnicalycine A **3.1**, methyl homosecodaphniphyllate **1.52** (C22 compound of secodaphniphylline skeleton) and compounds of interest were compared manually.

The difference in behaviour between different tissues might suggest the possibility of distinct pathways in roots and leaves. It would not be unusual for there to be separate pathways in roots and leaves sharing a common precursor. In fact, there are precedents for it, for example biosynthetic pathway in *Catharanthus roseus* involved tabersonine **1.15** which in the root specific pathway is modified to lochnericine **1.17** and in the leaf

specific pathway to vindoline **1.16** as shown in Scheme 4.5 (Amor Stander et al., 2020; Li et al., 2023) .

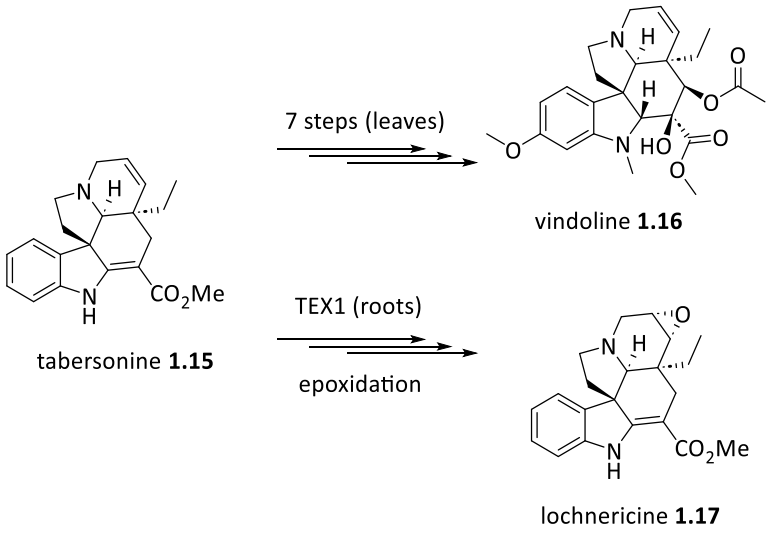

Scheme 4.5 Leaf and root specific pathway in Catharanthus roseus (Amor Stander et al., 2020; Li et al., 2023).

However, some compounds showed consistent behaviour across both tissue extracts. For example, M342.24T160 was consistently consumed, and M512.374T240 consistently increased independently of squalene addition. Additionally, we observed pairs of C30 compounds which showed squalene dependency in both roots and leaves. In the roots we proposed pairs of M470 and M486 which are linked by a hydroxylation (Scheme 4.2) and in the leaves pairs of M486 and M528 by acetylation (Scheme 4.3).For example a pathway could start from codaphniphylline **1.54** which would undergo a hydroxylation to produce daphnilongeranin D **3.3** which then would be acetylated in the same position to yield daphniphylline **1.18**. This suggests the pathway could be the same in both tissues. The observed variations could be due to other reasons, such as the high accumulation of alkaloids – precursors – in the leaves.

It was already indicated that precursors were available for subsequent reactions, and we observed different behaviour dependent on from which type of tissues the extracts were obtained. The inconsistency of the changes across the tissues might be caused by the difference in the metabolomic profile of each extract and the availability of the precursors as well as the available ratio of proteins.

Curiously, only in the root tissue extracts, the effect of squalene was observed in yuzurimine type alkaloids (C22A). Specifically, an increase of yuzurimine (M470.254T210) and M386.233T150. This was surprising, we expected that yuzurimine **1.10** would be the "end-point" of the pathway based on the fact that yuzurimine **1.10** accumulated highly in the leaves of *D. macropodum* (plant B). However, yuzurimine **1.10** was present in both tissue extracts and as expected it did not show any changes in the leaf assays. This would suggest that observed changes that were independent of the addition of squalene were highly dependent on the precursor content in each extract. Those were different which could account for the observed changes.

We also observed alkaloids that likely were precursors in the pathway while still showing an increase when squalene was added. In the leaf tissue extracts it was M470.363T310 (daphniphylline type) – the same alkaloid only showed an increase dependent on the addition of squalene in the root extracts. While in the root extracts the same behaviour was observed in daphniphylline types (M528.369T310, M528.369T320, M528.369T325), as described previously, those compounds were expected to be positioned relatively early in the pathway.

The results showed that squalene was a precursor in both root and leaf pathways. It was the first time that squalene was observed to affect the alkaloid content *in vitro* since the previous experiments included feeding "live" branches (Haruki, Yoshimasa and Suzuki, 1973; Suzuki et al., 1973) or studies on the hydroponics seedling (Eljounaidi et al., 2024).

Since diol **1.97** was never detected, it was debated about the necessity of using cofactors. It was considered that all needed cofactors and small molecules might already be present in the tissue extracts due to the many changes that did not show dependence on the addition of the substrate. Thus, the following experiments were modified as it was decided not to add any additional cofactors to minimise the potential changes that would not be dependent on the addition of the substrate.

Similarly, to verify whether diol **1.97** was a precursor to *Daphniphyllum* alkaloids, the tissue extracts assays were repeated with squalene **1.11** and diol **1.97** as substrates.

4.2.4 Assays on root and leaf tissues of 1-year old plants treated with squalene 1.11 and diol 1.97

The leaves and roots of several small 1-year old plants were used to obtain tissue extracts as previously described. The plants were chosen based on their availability, but they were all *D. macropodum.*

4.2.4.1 Introduction

As before, the results were compiled in the Table 4.3. Interestingly, the alkaloids present in the older plants differed from those in the younger plants. Additionally, the alkaloids showing significant changes varied between the two experiments. There were likely two explanations for this variation. First, we did not use any cofactors, which could limit the number of enzymatic changes independent of substrate addition. Second, older plants might produce a greater variety of metabolites that could act as intermediates in the pathways. The differences in observed compounds between older and younger plants likely contributed to the variation between the extracts.

*Table 4.3 Summary of compounds in the root (R2) and leaf (L2) tissue extracts, their peak area, the fold changes between the assays (1: tissue extracts treated with protease, squalene **1.11**, diol **1.97** and buffer, 2: tissue extracts + buffer, 3: tissue extracts treated with squalene **1.11** and buffer, 4: tissue extracts treated with diol **1.97** and buffer; fold change >1 represented an increase, <1 represented consumption, significant change was represented by "*".*

Exp	Peak name	Class	Peak area	Fold change					Comment	Comments
				1 vs 2	1 vs 3	2 vs 3	1 vs 4	2 v 4		
R2	M512.374T140	C30	1E+07	1	1.5*	1.3*	1	1		Squalene dependent, none available
L2	M510.358T285	C30	2E+06	0.4*	0.4*	1	0.9*	2.5*		Diol **1.97** dependent, M510.358T265 is a precursor
R2	M488.374T180	C30	2E+07	1	1.4*	1.6*	1	1		Squalene dependent, none available
L2	M486.358T240	C30	2E+07	0.9*	1.2*	1.3*	1.2*	1.3*	standard: daphnicalycine A **3.1**	Squalene **1.11** and diol **1.97** dependent, M486.358T240 is a precursor
L2	M470.363T250	C30	8E+07	0.5*	0.5*	1	1	1.7*		Diol **1.97** dependent, M470.363T250 is a precursor
L2	M470.363T200	C30	7E+05	1	1.15*	1.2*	1	1		Squalene dependent, none available
L2	M458.254T140	C22A	1E+06	1	1.2*	1.3*	1	1		Squalene dependent, none available
L2	M430.259T260	C22A	2E+07	1	1	1	1	1		Not consumed or made
L2	M428.244T230	C22A	5E+08	1.5*	1.3*	0.8*	1.4*	1		Precursors available
L2	M426.226T230	C22	8E+06	1.3*	1.6*	1.2*	1.3*	1		Squalene dependent, precursors available
L2	M414.228T135	C22	1E+08	0.06*	0.06*	1.1*	0.06*	1		Squalene dependent, M414.228T135 is a precursor
R2	M402.264T150	C22	5E+06	1	1.7*	1.7*	1	1		Squalene dependent, none available

L2	M402.228T215	C22A	6E+07	1.2*	1.2*	1	1.2*	1		Precursors available
R2	M388.249T210	C22	1E+07	1	1	1	1	1		Not consumed or made
L2	M388.249T165	C22	3E+06	1	1.2*	1.1*	1.1*	1		Squalene dependent, precursors available
L2	M386.27T210	C22	3E+06	1.6*	1.5*	1	1.5*	1		Precursors available
L2	M386.233T210	C22A	5E+08	1.4*	1.4*	1	1.4*	1		Precursors available
R2	M384.217T220	C22A	4E+07	0.5*	0.5*	1.12*	0.8*	1.7*		Diol **1.97** dependent, M384.217T220 is a precursor
L2	M376.285T240	C22	2E+07	1.1*	1.1*	1	1.1*	1		Precursors available
L2	M374.27T255	C22	1E+07	1.4*	1.3*	1	1.3*	1		Precursors available
L2	M374.233T205	C22A	2E+07	1.2*	1.2*	1	1.2*	1		Precursors available
L2	M374.197T155	C22	5E+05	1	1	1	1.4*	1.4*	assigned from MS1: macropodumine A?	Diol **1.97** is a precursor
L2	M372.217T120	C22	2E+08	0.2*	0.2*	1	0.2*	1		M372.217T120 is a precursor
L2	M360.290T310	C22	2E+09	1.2*	1.2*	1	1.2*	1	standard: methyl homosecodaphniphyllate	Precursors available
L2	M360.29T245	C22	4E+07	1	1	1	1.15*	1.15*		Diol **1.97** dependent, none available
L2	M360.254T90	C22	3E+08	1	1	1	1	1		Not consumed or made
L2	M359.270T286	C22B	1E+07	1.4*	1.4*	1	1.4*	1	assigned from MS1: macropodumine I_1?	Precursors available
L2	M356.223T265	C22	2E+06	1	1	1	1	1		Not consumed or made

L2	M356.223T125	C22	6E+07	0.7*	0.7*	1	0.7*	1		M356.223T125 is a precursor
L2	M346.275T175	C22	1E+08g	0.5*	0.5*	1	0.5*	1		M346.275T175 is a precursor
L2	M344.259T170	C22	2E+07	0.5*	0.5*	1	0.5*	1		M344.259T170 is a precursor
L2	M344.223T200	C22A	5E+05	0.95	0.95	1	1.05	1.05		Not consumed or made
L2	M340.191T115	C22	1E+06	9*	9*	0.95	9*	1		Precursors available
L2	M324.296T215	C22	8E+06	1	1	1	1	1	daphnezomine O	Not consumed or made
L2	M324.19T215	C22	8E+06	1	1	1	1	1		Not consumed or made

4.2.4.2 Overview of the experiment

The previously described experiment was repeated with small adjustments: soluble and microsomal protein extracts were combined with an addition of the substrates – squalene and synthesised diol **1.97**. We did not add any cofactors. We wanted to observe whether there were any changes dependent on the addition of diol **1.97** which would indicate that it was a precursor in the *Daphniphyllum* alkaloid pathway. As before, the controls included tissue extracts treated with protease and substrates as well as a tissue extracts with buffer and no substrates added.

4.2.4.2.1 Significant increase dependent on the addition of squalene and diol 1.97

Across all root and leaf assays, there was a compound that showed a significant increase based on the addition of both squalene and diol **1.97** (Figure 4.16). It was a C30 compound – M486.358T240 with a molecular formula $C_{30}H_{47}NO_4$ – known as daphnicalycine A **3.1** (Figure 4.17). The significant increase of M486.358T240 (daphnicalycine A) dependent on the addition of diol **1.97** was only observed in the leaf tissue extracts.

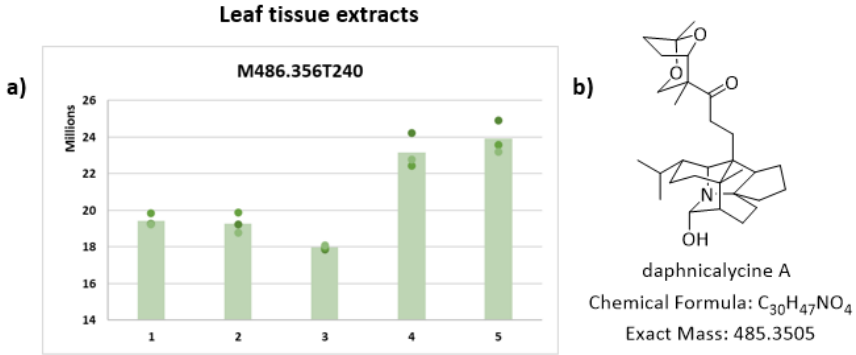

*Figure 4.16 Peak areas of selected peaks in the leaf tissue extracts with a) $[M+H]^+$ = 486.358 at 240 seconds matching molecular formula of $C_{30}H_{47}NO_4$; 1) Leaf tissue extract + protease + squalene + buffer, 2) Leaf tissue extract + protease + diol **1.97** + buffer 3) Leaf tissue extract + buffer, 4) Leaf tissue extract + squalene + buffer, 5) Leaf tissue extract + diol **1.97** + buffer; Each point represents a single compound from a single sample taken as an average of three biological repeats; bar represents an average peak area of a single compound across all samples. b) chemical structure of daphnicalycine A **3.1** (M486.358T240).*

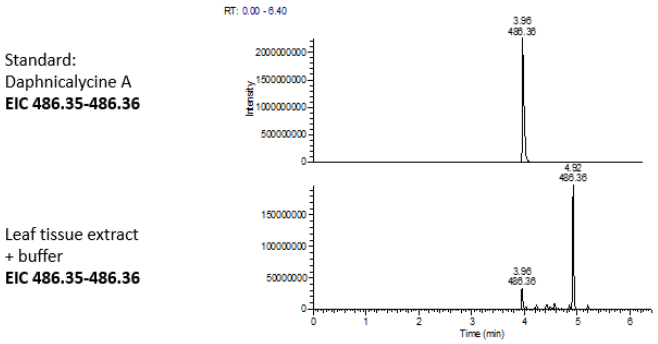

*Figure 4.17 from the top) LC-MS chromatogram of leaf extract + buffer and the chemical standard daphnicalycine A **3.1**, extracted ion chromatogram 486.3-486.4.*

As in the previous experiment, we observed a variation between root and leaves tissue extracts. For example, we observed significant increase dependent on the addition of the substrate – squalene **1.11** – M488.374T180 in the roots and M470.363T200 in the leaves, both C30 compounds. Daphnicalycine A **3.1**, which showed dependency on both substrates, was only observed in the leaf extract. As presented in the Table 4.2 and Table 4.3, most of the observed *Daphniphyllum* alkaloids only appeared in either roots or leaves suggesting that the root and leaf pathways are different and diverged at some point. Significant increase independent of the addition of squalene and diol **1.97**.

Another observed standard was methyl homosecodaphniphyllate **1.52** (M360.290T310) which showed a significant increase with the precursors already available in the extracts (Figure 4.18). It was a secodaphniphylline type alkaloid which was present in the leaf tissue extracts in a high quantity. This showed that even though it appeared that most of the C30 compounds observed in the leaf tissue were daphniphylline type, the secodaphniphylline type alkaloids can also accumulate in the leaves.

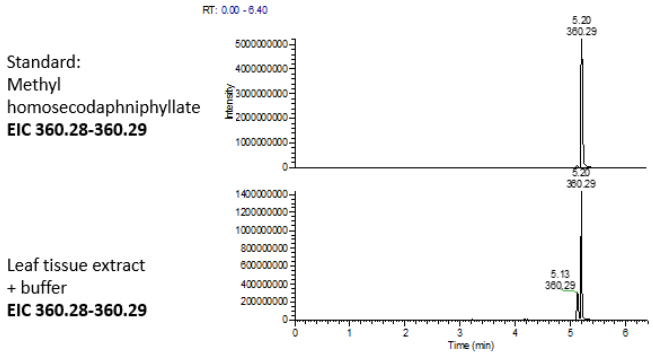

*Figure 4.18 from the top) LC-MS chromatogram of the chemical standard methyl homosecodaphniphyllate **1.52** and leaf extract + buffer with the extracted ion chromatograms of 360.28-360.29.*

However, the compound that showed the highest – almost 10-fold increase – was M340.191T115 in the leaf tissue extracts (Figure 4.20). The observed change was not dependent on the addition of the substrate, suggesting that the precursor to M340.191T115 must have been abundant in the leaf tissue extracts. The only known compound of this molecular formula – $C_{21}H_{25}NO_3$ – was daphnicyclidin G (daphnicyclidin type). However, the none of the compounds that were consumed were reported as daphnicyclidin type. This could mean that either M340.191T115 belongs to different skeletal family, such as daphnilactone B or the daphnicyclidin-type precursor was yet unknown. This behaviour was not observed in the root tissue extracts of 1-year old *D. macropodum* plants in this study.

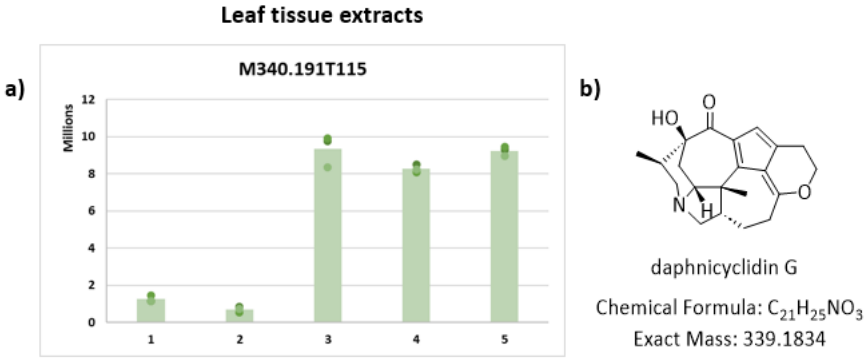

*Figure 4.19 Peak areas of selected peaks in the leaf tissue extracts with a) $[M+H]^+$ = 340.191 at 115 seconds matching molecular formula of $C_{21}H_{25}NO_3$; 1) Leaf tissue extract + protease + squalene + buffer, 2) Leaf tissue extract + protease + diol **1.97** + buffer 3) Leaf tissue extract + buffer, 4) Leaf tissue extract + squalene + buffer, 5) Leaf tissue extract + diol **1.97**+ buffer; Each point represents a single compound from a single sample taken as an average of three biological repeats; bar represents an average peak area of a single compound across all samples. b) structure of daphnicyclidin G.*

4.2.4.2.2 Consumption of an alkaloid and recovery dependent on the addition of diol 1.97

There also were changes dependent on the addition of diol **1.97** in the root extracts. Both M510.358T285 (C30 type) and M384.217T220 were consumed compared to the root tissue extracts treated with protease (Figure 4.20). However, in the root tissue extract with buffer and added diol **1.97**, the alkaloid content was significantly higher than compared to the assay in which no substrate was added or in which squalene was added. The known M384.217 belong to C22A types or daphnicyclidin types. To determine whether M384.217T220 could belong to yuzurimine type, we consulted GNPS. M384.217T220 formed a cluster with other alkaloids there were present in both root and leaf extracts, however it did not cluster with any of the standards which suggested it likely was not a yuzurimine type. Also, the MS2 did not show similarities between yuzurimine type compounds suggesting that it might be daphnicyclidin or calyciphylline A type alkaloid.

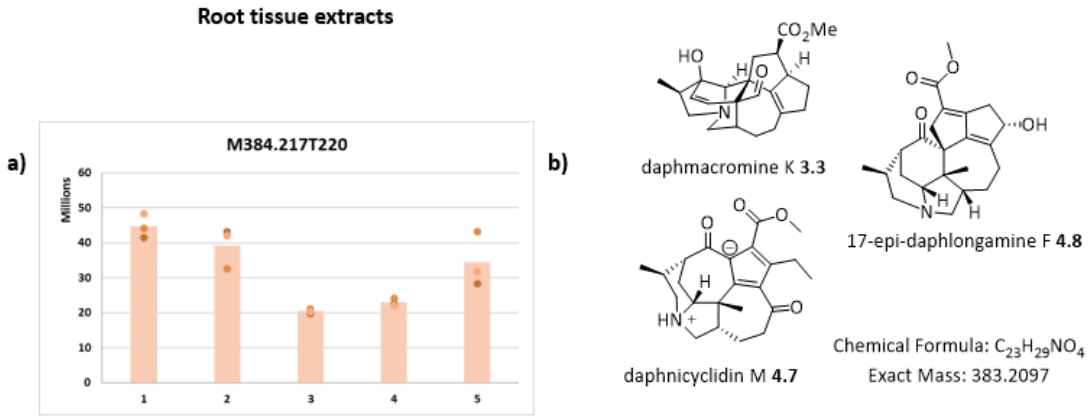

*Figure 4.20 a) Peak areas of selected peaks in the leaf tissue extracts with $[M+H]^+$ = 384.217 at 220 seconds matching molecular formula of $C_{23}H_{29}NO_4$; 1) Root tissue extract + protease + squalene + buffer, 2) Root tissue extract + protease + diol **1.97** + buffer 3) Root tissue extract + buffer, 4) Root tissue extract + squalene + buffer, 5) Root tissue extract + diol **1.97** + buffer; Each point represents a single compound from a single sample taken as an average of three biological repeats; bar represents an average peak area of a single compound across all samples. b) known structures of* Daphniphyllum *alkaloid matching molecular formula of $C_{23}H_{29}NO_4$,, examples from each class that could be possible M394.217T220: daphmacromine K **3.2** (yuzurimine type), daphnicyclidin M **4.7** (daphnicyclidin type) and 17-epi-daphlongamine F **4.8** (calyciphylline A type).*

In the leaves, however, this change was observed in a C30 compound – M510.358T285 (Figure 4.21). Interestingly, the only known compound of the exact mass matching M510.358T285 and so the molecular formula of $C_{32}H_{47}NO_4$, was daphnioldhanin I (secodaphniphylline type).

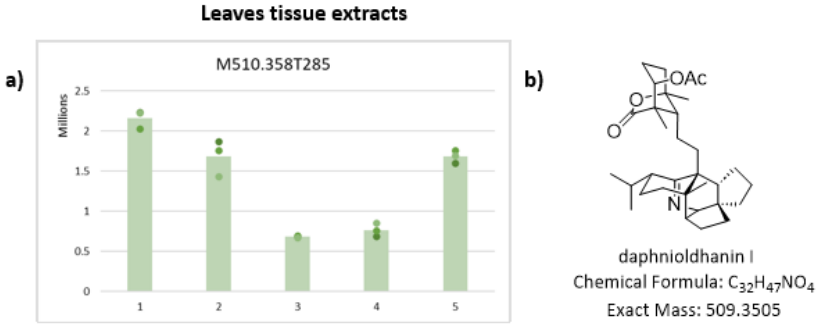

*Figure 4.21 a) Peak areas of selected peaks in the leaf tissue extracts with $[M+H]^+$ = 510.358 at 285 seconds matching molecular formula of $C_{32}H_{48}NO_4$; 1) Leaves tissue extract + protease + squalene + buffer, 2) Leaves tissue extract + protease + diol **1.97** + buffer 3) Leaves tissue extract + buffer, 4) Leaves tissue extract + squalene + buffer, 5) Leaves tissue extract + diol **1.97** + buffer; Each point represents a single compound from a single sample taken as an average of three biological repeats; bar represents an average peak area of a single compound across all samples. b) known structure of* Daphniphyllum *alkaloid matching molecular formula of $C_{32}H_{47}NO_4$, daphnioldhanin I (secodaphniphylline type), a possible M510.358T285.*

4.2.4.3 Discussion

As in the previous experiment the addition of squalene led to the increase in C30 alkaloids content. However, the effect of the addition of diol **1.97** was more complex. There was only one alkaloid that showed a consistent behaviour of a significant increase with the addition of both squalene and diol **1.97** – daphnicalycine A **3.1** – in the leaf tissue extracts. There were other C30 compounds that showed a significant increase just when squalene was added in both root and leaf tissue extracts. This led to the question: is the diol **1.97** a precursor in the pathway? Or is the variation caused by different number of steps required from the substrate to the alkaloid? It could be the latter since in the leaf extracts, we observed an increase of C30 intermediates (M470.363T250 and M510.358T285) only when diol **1.97** was added, and no effect caused by the addition of squalene. A significant increase only dependent on diol **1.97** in the leaf extracts was also

observed in M374.197T155 with only one compound reported of this molecular formula ($C_{21}H_{27}NO_5$) – macropodumine A.

The increase caused by the addition of diol **1.97** was also observed in the compounds that behaved as precursors to other alkaloids but increased when diol **1.97** was added. In the leaf tissue extracts, this behaviour showed C30 compounds: M470.363T250 and M510.358T285. In the root tissue extracts a consistent increase caused by the addition of squalene and diol **1.97** was observed in C22A or daphnicyclidin type compound – M384.217T220.

In this set of data, we have not observed the same alkaloids being present in the root and leaf extracts. This revealed another complexity in analysing *Daphniphyllum* alkaloid biosynthesis. Not only we are analysing a complex set of alkaloids but also the metabolomic profile is dependent on the specific plants used. This likely is caused by different needs of those plants to produce different alkaloids.

4.3 Overall discussion and conclusion

The tissue extracts were complex mixtures containing proteins, *Daphniphyllum* alkaloids, amino acids, and potentially necessary cofactors. Because of this complexity, the changes observed might not be solely attributed to the addition of the substrate, but also to the simultaneous reactions of various present alkaloids. Consequently, this experiment did not provide enough information to determine the steps or reactions in the biosynthetic pathway. However, it confirmed that squalene was as a substrate in the *Daphniphyllum* alkaloid pathway, as initially hypothesized, with evidence supported across different tissues and plants of varying ages. The variation in the alkaloid behaviour based on tissue type was observed. For example, M528.369T320, a daphniphylline-type compound, used squalene as a precursor in the leaf extract, showing that it might be accumulating in the leaves of *D. macropodum*. In contrast, in the root extract, it showed both dependence on the addition of squalene and it acted as a precursor being consumed.

Since it was shown that *Daphniphyllum* alkaloids originate from squalene and are likely to start at one entry-point, it was therefore possible that C22 compounds were preceded in the pathway by one or more C30 *Daphniphyllum* alkaloids. The biomimetic synthetic studies place secodaphniphylline skeleton as the precursor to other subtypes. (Pieitre and Heathcock, 1990). It is also thought that daphniphylline skeleton is not an intermediate skeleton but an end-product (Heathcock and Joe, 1995). This was consistent with the changes we observed in the content of daphnicalycine A **3.1**. It was a compound that accumulated in one of the *D. macropodum* plants which allowed us to isolate 4 mg of purified alkaloids. Additionally, it was an alkaloid that showed changes dependent on the addition of the substrate.

The feeding study done on the root and leaf tissue showed that squalene was a precursor in the *Daphniphyllum* alkaloid pathway, and its addition led to several changes in behaviour of the alkaloids. This likely meant that *Daphniphyllum* alkaloids were

produced in both tissues with no need for transport which supported the labelling studies done previously (Eljounaidi et al., 2024). While the changes were not consistent amongst the same compounds in root and leaf tissue extract, it was likely caused by different metabolomic profile of those tissue extracts and not different pathways.

The variation in observed changes between the addition of squalene and diol **1.97** meant that it was unclear whether diol **1.97** was a substrate in the biosynthetic pathway. The validation of the hypothesis of *Daphniphyllum* alkaloid biosynthetic pathway in which squalene is oxidised to diol **1.97** needs further study. However, the fact that the *Daphniphyllum* alkaloids showed changes dependent on the addition of diol **1.97** indicated that diol **1.97** might be a precursor in the pathway. Further study is needed to determine the intermediates in the pathway with confidence.

5 Where does nitrogen come from?

5.1 Introduction

5.1.1 Introduction to isotope labelling

Isotope labelling in studies of plant metabolites is a technique used to obtain information about precursors based on their incorporation of a heavy isotope precursor (Simpson and Chapple, 2022). Untargeted mass spectrometry can show unbiased range of metabolites present in plants extracts. However, it may be challenging to identify compounds related to the fed precursors amongst thousands of features detected in a LCMS run. Isotope labelling allows to detect features related to the fed precursor and to the specific pathway. The reactant is labelled by replacing one atom with the heavy isotope, contributing to the change in mass which in case of stable isotope labelling can be detected by high-resolution mass spectrometry or NMR.

5.1.2.1 Isotope labelling studies in Daphniphyllum macropodum

Isotope labelling has been used previously to study the biosynthetic pathway of *Daphniphyllum* alkaloids. Radioactive labelling showed that the alkaloids originate from terpenoids (Suzuki et al., 1973; Haruki, Yoshimasa and Suzuki, 1973) by feeding ^{14}C and ^{3}H-labelled DL-mevalonic acid to isolate labelled daphniphylline **1.18** and codaphniphylline **1.54** (see chapter 1, section 1.2.4 and scheme 1.9). Recently, stable isotope labelling of $^{13}C_6$-glucose and mevalonolactone-2-^{13}C supported that evidence and led to proposing the biosynthetic pathway in which C30 alkaloids are made first, followed by C22B and ending with C22A type (Eljounaidi et al., 2024).

5.1.3 The origin of the nitrogen atom

5.1.3.1 Examples of introduction of nitrogen in pseudoalkaloids

There are several ways in which nitrogen can be introduced into a skeleton of pseudoalkaloids. For example, the proposed biosynthetic pathway of cyclopamine produced from *Veratrum californicum* starts from cholesterol which undergoes series of oxidation and then transamination (Scheme 5.1), transferring an amino group from γ-aminobutyric acid to an aldehyde (Augustin et al., 2015).

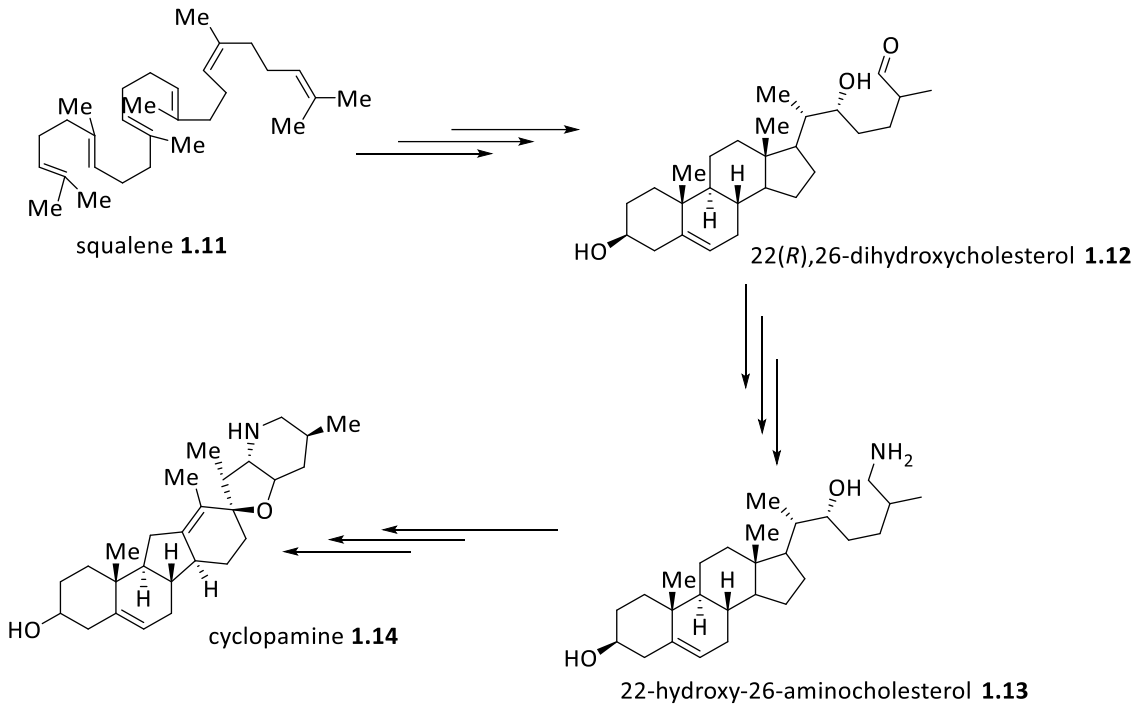

*Scheme 5.1 Biosynthesis of steroid alkaloid cyclopamine **1.14** as proposed by Augustin et al.*

Similarly, transamination step occurs in the biosynthesis of solanidine **5.4**, and other alkaloids from *Solanum* sp. (Scheme 5.2) (Grzech et al., 2024).

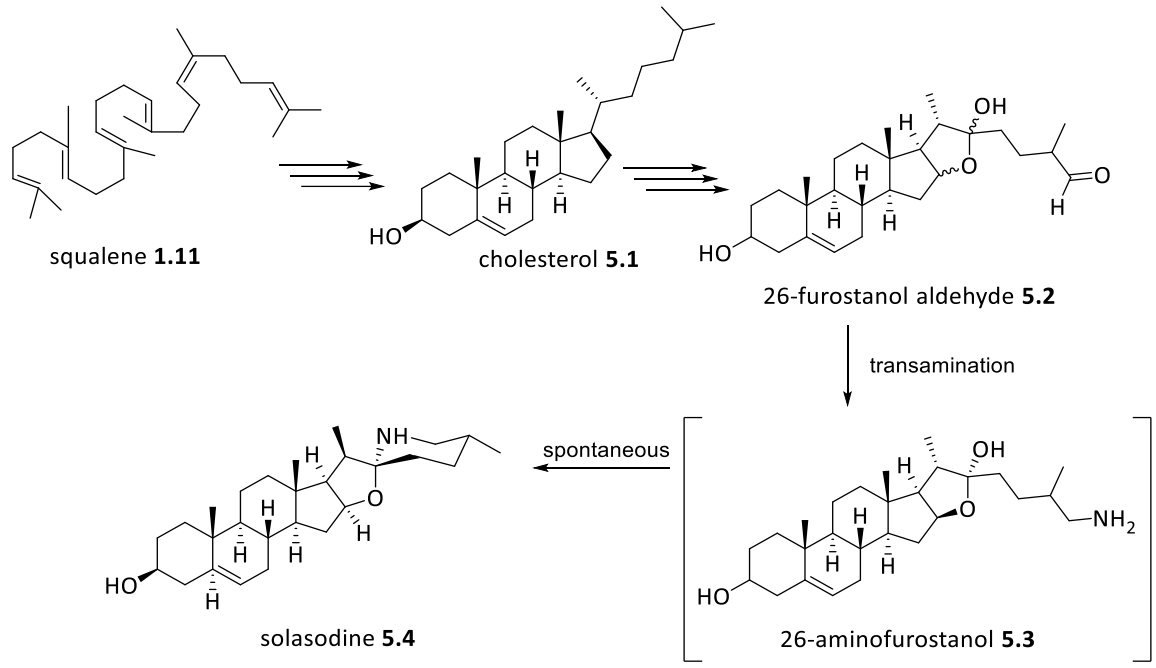

*Scheme 5.2 Biosynthesis of an alkaloid solasodine **5.4** as proposed by Grzech et al.*

An example of a pseudoalkaloid in which nitrogen is introduced non-enzymatically, through a condensation of an amino acid with an aldehyde, is the atisine-type diterpenoid alkaloids (Scheme 5.3). According to previous studies, pyrophosphoric ethanolamine or L-serine were used to test the origin of nitrogen in alkaloids (Rontein et al., 2001). Consequently, in the study of the biosynthetic pathway of atisine-type diterpenoid alkaloids, labelled L-[2-^{13}C,^{15}N]serine was used as a precursor. ^{15}N incorporation into spiramine C/D **5.6** it was detected which showed that L-serine can be a nitrogen source for spiramine C/D **5.6** (Zhao et al., 2009).

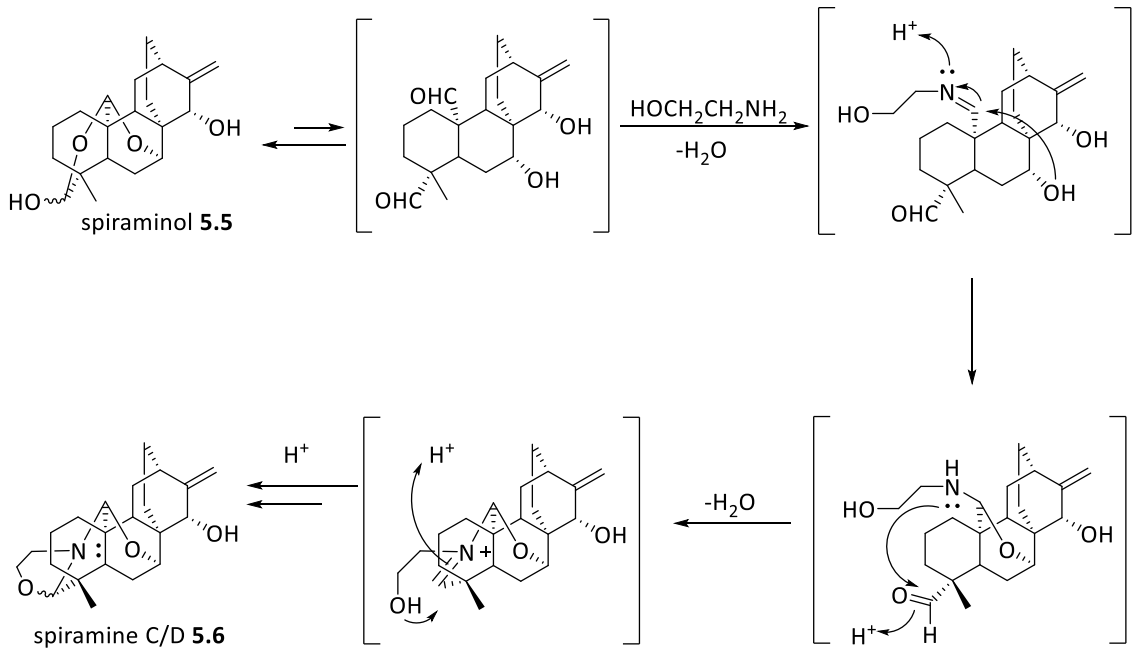

*Scheme 5.3 Proposed pathway to atisine type diterpenoid alkaloid spiramine C/D **5.6** adopted from* (Zhao et al., 2009).

5.1.3.2 Introduction of nitrogen into Daphniphyllum alkaloid skeleton

The origin of nitrogen in *Daphniphyllum* alkaloids skeleton is unknown. The hypothetical biosynthetic pathway towards *Daphniphyllum* alkaloids proposed by Heathcock et al. was based on the reaction between dialdehyde **1.93** and ammonia, and methyl amine as presented in Scheme 5.4. This was explored in detail in chapter 1, section 1.2.7. It was therefore hypothesised that the scaffold forming steps would involve firstly a reduction of dialdehyde **1.96**, followed by introduction of a nitrogen possibly from an amino acid, or by reductive transamination. However, the exact mechanism of the incorporation of nitrogen into *Daphniphyllum* alkaloid scaffold was never identified.

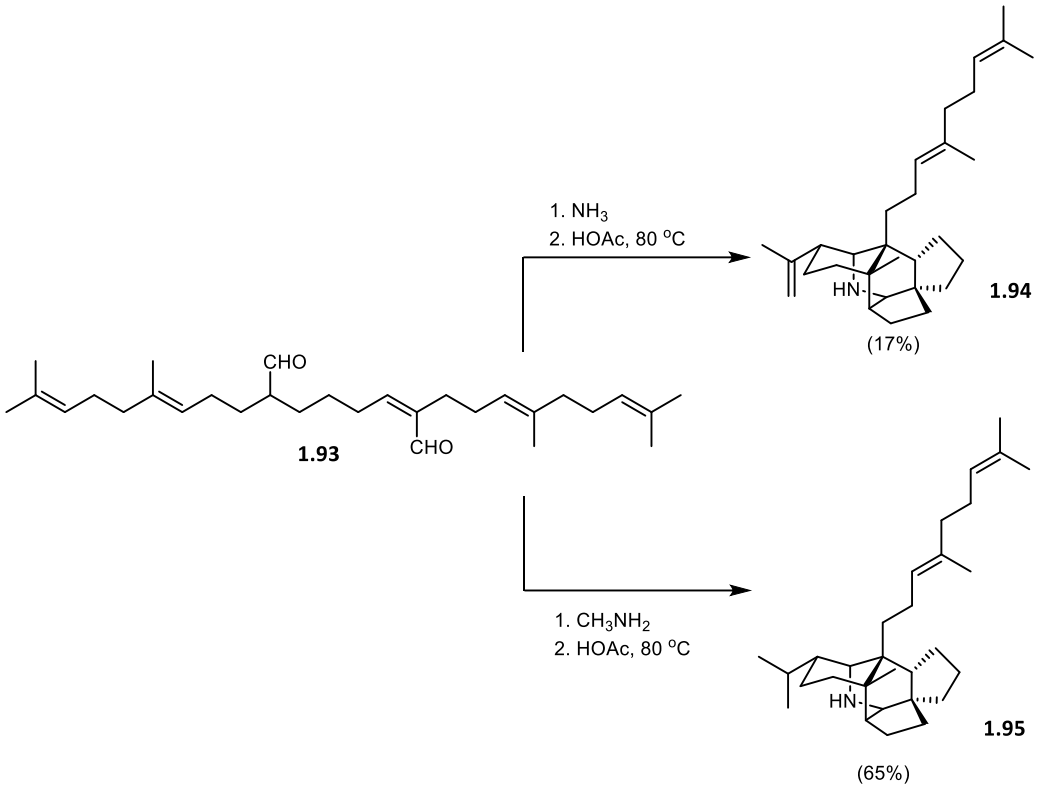

*Scheme 5.4 Synthesis of "proto-daphniphylline **1.94** and **1.95**" using ammonia and methyl amine* (Heathcock, 1996).

5.1.4 Aims

In this study, we investigate the origin of nitrogen in the *Daphniphyllum* alkaloid biosynthetic pathway. Additionally, ^{15}N labelling was not previously observed in *Daphniphyllum* alkaloids. We will test ^{15}N incorporation with different labelled precursors to determine whether incorporation is amino acid or tissue specific. To test this, we will use two different experiments. We will adopt tissue extract feeding experiments from the chapter 4 to test different ^{15}N labelled amino acids, together with the proposed squalene **1.11** and diol **1.97** precursors. We will also use a selection of hydroponically grown *D. macropodum* seedlings of the same age, size and maternal origin to which we will feed labelled and unlabelled amino acids as putative precursors. We hypothesise that feeding these precursors will lead to ^{15}N labelling in the alkaloid skeleton. Variation between ^{15}N incorporation in the alkaloids between amino acids and tissues would indicate origin of *Daphniphyllum* alkaloids. Then, the tissue extracts, roots, stem and leaves will be analysed using LC-MS to detect ^{15}N incorporation into *Daphniphyllum* alkaloids.

5.2 Feeding experiment using tissue extracts

The tissue extract feeding experiments followed the procedure described in chapter 4.

5.2.2 Introduction to the experiment

The feeding experiments described in chapter 4 showed that the addition of squalene **1.11** or diol **1.97** to the *D. macropodum* tissue extracts influences the amount of *Daphniphyllum* alkaloids present in the extracts, suggesting that squalene **1.11** or diol **1.97** are precursors. We adopted the same procedure as described in chapter 4 but with each precursor we also added labelled or unlabelled source of nitrogen: L-alanine, L-alanine-^{15}N, L-glutamic acid, L-glutamic acid-^{15}N, ammonium chloride or ammonium chloride-^{15}N. The results were analysed using LC-MS adapting previously described analytical method (Eljounaidi et al., 2024) (for more details see chapter 6, section 6.1.2).

Leaf tissue extracts containing soluble and microsomal protein extracts containing mixture of proteins and small molecules and buffer were treated with putative precursors either with squalene **1.11** or diol **1.97**, as well as ^{15}N-labelled amino acids and incubated for 16 h. The controls included the tissue extracts with buffer and unlabelled substrates. We were looking for *Daphniphyllum* alkaloids that would show incorporation of ^{15}N to test whether it was amino acid specific as well as observe differences between feeding squalene **1.11** or diol **1.97**.

5.3 Results

5.3.1 Analytical method

The tissue extracts assays were run on the LCMS following the same method used in chapter 4, however we used LCMS Orbitrap with the resolution allowing to differentiate between ^{13}C and ^{15}N isotopologs. We searched for compounds that would show a peak equivalent to $[M(^{15}N)+H]^+$ compared to $[M(^{14}N)+H]^+$ of known *Daphniphyllum* alkaloids.

5.3.2 Assays on leaf tissue extracts

We did not observe any significant ^{15}N labelling in *Daphniphyllum* alkaloids in any of the conditions. This was unexpected as our previous experiment (see chapter 4) showed that the addition of squalene **1.11** and diol **1.97** affects the amount of *Daphniphyllum* alkaloids present, therefore we anticipated that ^{15}N labelled would be incorporated into the scaffold.

Below are examples of the extracted ion chromatograms of a C30 compound of the molecular formula of $C_{30}H_{47}NO_4$ that showed changes dependent on the addition of squalene **1.11** in the previous experiment (Figure 5.1 and Figure 5.2). The extracted ion chromatograms corresponding to the ^{15}N isotopolog of the *Daphniphyllum* alkaloids did not show incorporation above the natural abundance of ^{15}N isotope or above the level present in the controls.

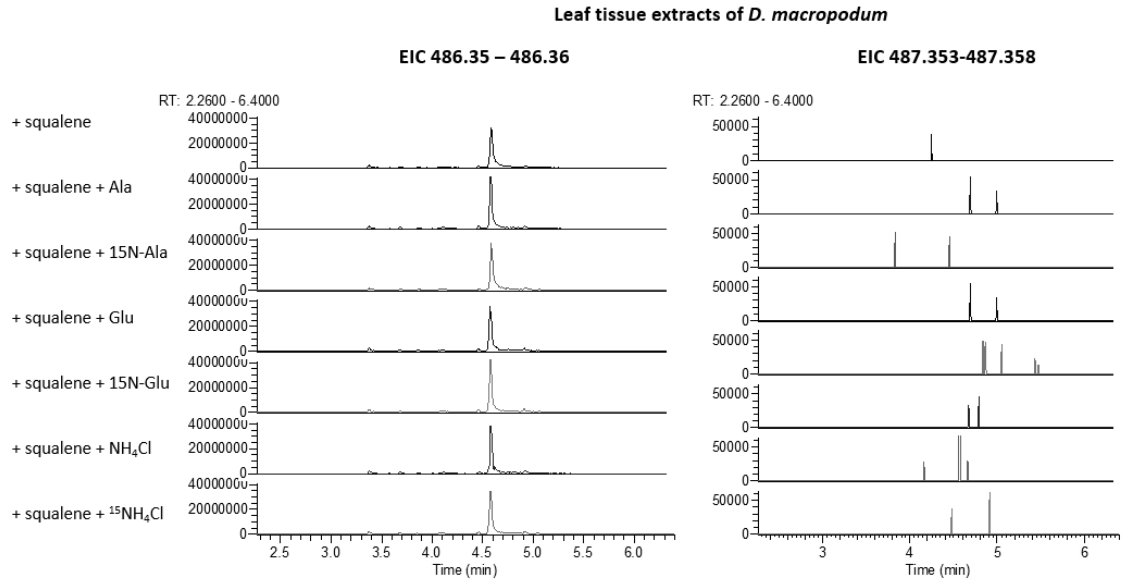

*Figure 5.1 LCMS chromatograms of leaf tissue extract assays with extracted ion chromatogram of 486.35 – 486.36 (left) and 487.355 – 487.356; (from the top): leaf tissue extract + squalene **1.11**, leaf tissue extract + squalene **1.11** + L-alanine, leaf tissue extract + squalene **1.11** + L-alanine-^{15}N, leaf tissue extract + squalene **1.11** + L-glutamic acid, leaf tissue extract + squalene **1.11** + L-glutamic acid-^{15}N, leaf tissue extract + squalene **1.11** + ammonium chloride, leaf tissue extract + squalene + ammonium chloride-^{15}N.*

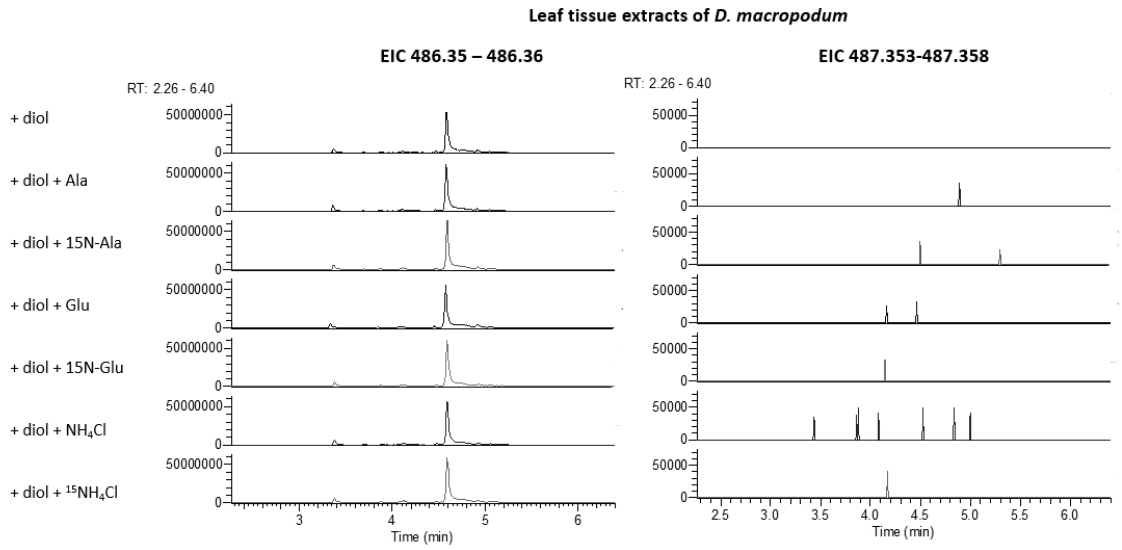

*Figure 5.2 LCMS chromatograms of leaf tissue extract assays with extracted ion chromatogram of 486.35 – 486.36 (left) and 487.355 – 487.356; (from the top): leaf tissue extract + diol **1.97**, leaf tissue extract + diol **1.97** + L-alanine, leaf tissue extract + diol **1.97** + L-alanine-^{15}N, leaf tissue extract + diol **1.97** + L-glutamic acid, leaf tissue extract + diol + L-glutamic acid-^{15}N, leaf tissue extract + diol **1.97** + ammonium chloride, leaf tissue extract + diol **1.97** + ammonium chloride-^{15}N.*

Lack of ^{15}N incorporation from any of the labelled precursor was observed across all *Daphniphyllum* alkaloids in all the samples no matter which source of nitrogen was fed, or which potential precursor was fed, squalene **1.11** or diol **1.97**.

5.4 Discussion

None of the *Daphniphyllum* alkaloids showed ^{15}N labelling due to the addition of L-alanine-^{15}N, L-glutamic acid-^{15}N or $^{15}NH_4Cl$. The tissue extracts feeding experiments did not result in any significant labelling of *Daphniphyllum* alkaloids for a number of possible reasons. For example, introduction of nitrogen could require a specific precursor which was not tested in this experiment or the precursor needed to be appropriately modified before it could enter the pathway. We expected that one of the contributing factors could be cell-specific biosynthesis which is the issue we could overcome by altering our approach as described in the following section.

5.5 Stable isotope labelling studies in hydroponic seedlings

5.5.1 Introduction to the experiment

We attempted to observe nitrogen incorporation into alkaloids using a new approach: whole plant feeding assay. This involved using hydroponic seedlings and feeding them with labelled precursors by adding these into the liquid media. We had limited number of seedlings and so we were not able to test different conditions such as length of feeding or concentration of amino acids. We had previous success feeding hydroponics seedlings in the ^{13}C labelling experiments in which ^{13}C MVA was fed to hydroponic plants. We detected incorporation of six labelled carbons into *Daphniphyllum* alkaloids via LCMS, verifying the squalene **1.11** origin of those compounds (Eljounaidi et al., 2024). We adapted this method by adding ^{15}N labelled amino acids to observe ^{15}N labelling following the experimental method which was already used in *D. macropodum* (Suzuki et al., 1973; Haruki, Yoshimasa and Suzuki, 1973; Eljounaidi et al., 2024).

5.6 Results

5.6.1 Overview of the experimental methodology

We used stable isotope precursor feeding of hydroponic seedlings followed by metabolomics analysis to observe the origin of nitrogen in *Daphniphyllum* alkaloids. We were curious whether the nitrogen was introduced non-enzymatically by a spontaneous condensation of an amino acid with dialdehyde as hypothesised and if so whether it was amino acid dependent. We chose 18 hydroponic seedlings of similar age, height and seed origin. Each seedling was fed one of the ^{15}N labelled amino acids: L-alanine, L-glutamic acid or L-serine; the control seedlings were fed equivalent unlabelled amino acids. After 16 days of continuous feeding, root, stem and leaf tissues were analysed separately using LC-MS to determine ^{15}N incorporation in *Daphniphyllum* alkaloids. ^{15}N-labelled amino acids were added into the liquid media and so they were uptaken by the roots. The stem and leaves were not fed separately but removed from the same plant. Therefore, in order to observe ^{15}N incorporation in stem and leaves either ^{15}N-labelled amino acids need to travel into tissues or the biosynthesised alkaloid would have to be transported into those tissues. For each condition, we had three different seedlings (biological replicates) and upon LC-MS performed three separate injections for each sample (technical replicates). When presenting data, we show it as an average of three biological samples and their technical replicates. The LC-MS samples were run using high-resolution Orbitrap Exploris 480 at 180000 resolution which was sufficient to differentiate between ^{15}N and ^{13}C isotopes. Samples were ionised using an atmospheric pressure chemical ionisation (APCI) ion source in positive ion mode.

The data were analysed using various complimentary approaches. The molecular formulas were determined based on MS^1-based annotations and the possible structures were named using REAXYS and the curated *in silico* database of *Daphniphyllum* alkaloids consisting of 331 *Daphniphyllum* alkaloids which were categorised based on their carbon skeletons as introduced in chapter 1.

The potentially labelled features were identified as containing one ^{15}N isotope compared to an existing feature, same retention time and were present in at least ten times higher abundance compared to an unlabelled sample. Isotopolog percentage was calculated as a proportion of peak area of the isotopolog divided by the total peak area of isotopolog and major (unlabelled) peak area. Corrected isotopolog percentages were calculated by subtracting an average background isotopolog percentages (from samples fed with unlabelled precursors). Peak areas were also normalised by concentration of the fed substrate. Peaks were grouped by alkaloid type.

The final concentration of each labelled amino acid in the media of the hydroponic seedlings varied: L-alanine/L-alanine-^{15}N (5 mM), L-glutamic acid/L-glutamic acid-^{15}N (2.5 mM) and L-serine/L-serine-^{15}N (0.5 mM). This variation was due to different amount of labelled amino acids available and insufficient plants to test the appropriate concentration of the amino acids. The lowest concentration used was for serine, and the concentration of other amino acids was increased to make sure we were able to detect incorporation of an isotope.

5.6.2 Analytical method

The features were picked as described in section 6.1.2.3. *Daphniphyllum* alkaloids appear in various tissues with different abundance. Since we were comparing an incorporation of the stable isotope in roots, leaves and stem, we normalised the results by calculating a percentage incorporation of ^{15}N isotope. Percentage ^{15}N incorporation of *Daphniphyllum* alkaloids in each sample was calculated as peak area of the $[M(^{15}N)+H]^+$ as a proportion of total peaks area of $[M(^{15}N)+H]^+$ and $[M(^{14}N)+H]^+$ within a single sample. Peaks were grouped by the subtypes and number of carbons in the skeleton.

$$\%\ ^{15}N = \frac{[M(^{15}N) + H]^+}{[M(^{14}N) + H]^+ + [M(^{15}N) + H]^+} \times 100\%$$

5.6.2.1 Example of the analysis

An example of the analysis was presented below on the M342.243T95 peak with the molecular formula $C_{21}H_{31}NO_2$ (Figure 5.3). Three hydroponic seedlings were being fed L-alanine and three hydroponic seedlings were being fed L-alanine-^{15}N. The metabolites were extracted from roots, stem and leaves with 80% methanol and the tissue extracts were analysed using LCMS Orbitrap with the resolution allowing to differentiate between ^{13}C and ^{15}N isotopologs.

The extracted ion chromatograms showed no peaks equivalent to ^{15}N labelled isotopolog when unlabelled alanine was fed, and a peak assigned to $C_{21}H_{31}{}^{15}NO_2$ when L-alanine-15N was fed. Although we did not analyse the effects of feeding non-labelled amino acids to the hydroponic plants in detail, we observed a reduction in the peak area (Figure 5.3) of extracted ion chromatogram of 342.24-342.35 in the hydroponic seedlings fed with L-alanine-^{15}N compared to the control seedlings fed with L-alanine (a significant difference based on t-test p = 0.002).

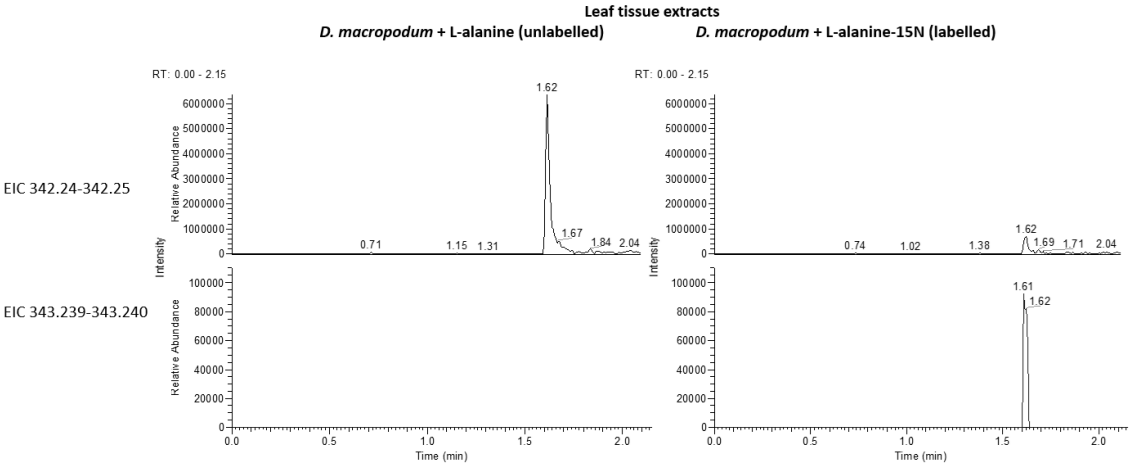

Figure 5.3 LCMS spectra of a chosen peak with the extracted ion chromatogram of 342.24-342.25 and 343.239-342.240 of leaf extracts of D. macropodum hydroponic seedlings fed with L-alanine and L-alanine-^{15}N.

To make sure that we observed true isotopologs, we calculated the theoretical m/z value for each isotopolog and calculated the mass error between the theoretical and experimental values. As shown in Figure 5.4 observed m/z values for $C_{20}{}^{13}CH_{31}NO_2$ were 343.2461 and for $C_{21}H_{31}{}^{15}NO_2$ 343.2397. The calculated m/z values were 343.2461 and 343.2398, respectively, which corresponded in the mass errors of 0 ppm and 0.29 ppm. This showed that the peaks we observed, were indeed the ^{15}N isotopologs.

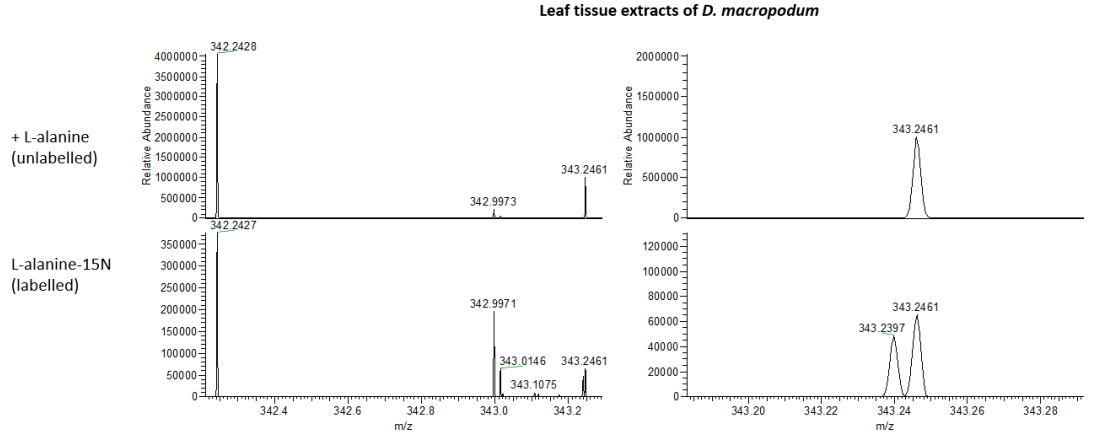

Figure 5.4 Mass spectra of M342.243T95 of the leaf extracts of D. macropodum fed with L-alanine (top) and L-alanine-^{15}N (bottom) showing peaks of ^{13}C (343.2461) and ^{15}N (343.2397) isotopologs.

The data were collected for each of the three biological replicates and the mean was calculated for each peak. Following M342.343T95 example, the mean value of the peak area was calculated as a mean of peak areas of three biological replicates (Figure 5.5).

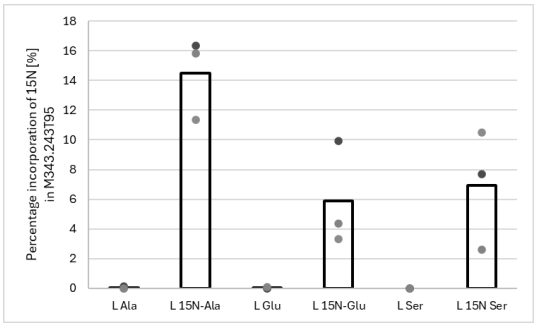

Figure 5.5 Percentage of ^{15}N isotopolog of a chosen peak – M342.243T95 in unlabelled and labelled sample Each point represents an average ^{15}N incorporation across three biological replicates for a single alkaloid. The bars are the averages across all data points.

There was some variation observed between ^{15}N incorporation in the seedlings which could be explained by various reasons. The plants of similar age and size were chosen but they were at various developmental stages. The *D. macropodum* seedlings were sowed at the same time but there was variation between their germination rates. The seeds of *D. macropodum* have epicotyl morphophysiological dormancy which affects seed germination (Chien et al., 2010). Variation development of tissues could affect the uptake and transport of amino acids within the plants (Weih, Hamnér and Pourazari, 2018; Fang, Fernie and Luo, 2019). Additionally, we observed differences in alkaloid accumulation between plants even those of the same maternal origin as described in the previous chapter. The plants grown from seeds are likely hybrids between plant B – mother originating from Japan – and plant A – male of unknown geographic origin – or plant D – male from Fanjin Shan, Guizhou in China. Although all those plants are classified as *D. macropodum*, they have different morphologies and their metabolomic profiles are different (Eljounaidi et al., 2024), suggesting that, at least some of the offsprings used in the study, might be hybrids. This would explain variations between individuals. Taking an average value of biological replicates meant to counter the variations between individuals.

5.6.3 *Alkaloids that showed incorporation of ^{15}N isotope*

Following this process, the average peak area of three biological replicates was calculated and the percentage incorporation of ^{15}N was determined across all *Daphniphyllum* alkaloids. It resulted in 39 *Daphniphyllum* alkaloids that showed higher abundance of ^{15}N isotopolog when labelled amino acids were fed compared to the control. The percentage of ^{15}N isotopologs in labelled and unlabelled samples was plotted (Figure 5.6). It is worth noting that we observed ^{15}N incorporation into *Daphniphyllum* alkaloids with all three ^{15}N-labelled amino acids in all tissues.

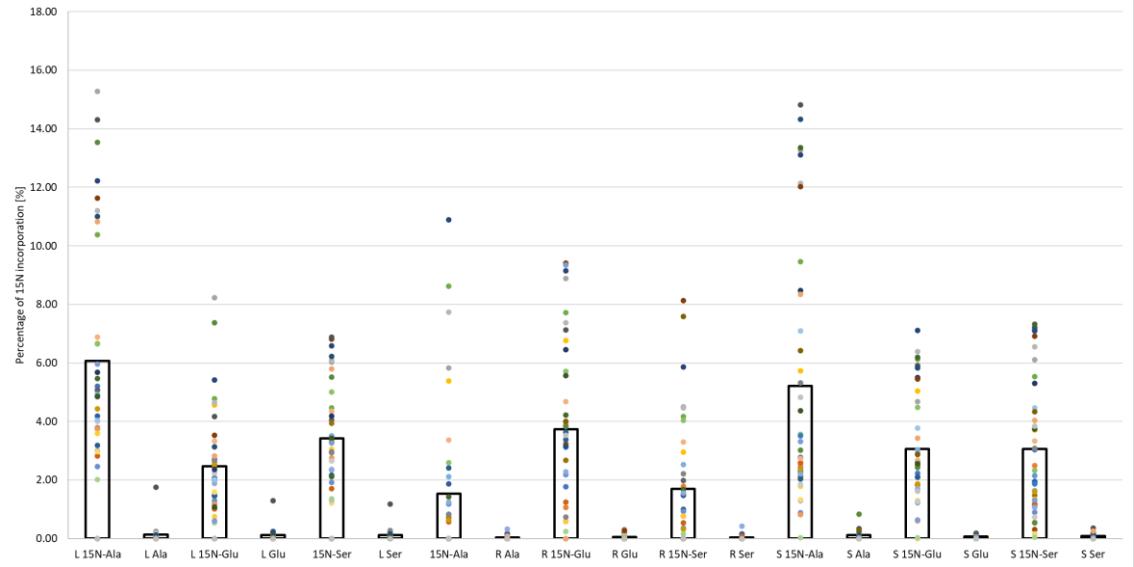

Figure 5.6 Stable isotope labelling experiment in Daphniphyllum *macropodum comparing labelled and unlabelled samples. Each point represents an average of three biological replicates. Letters represent tissue type: leaves (L), stem (S), roots (R) and amino acids: alanine (Ala), glutamic acid (Glu), serine (Ser). Each point represents an average ^{15}N incorporation across three biological replicates for a single alkaloid. The bars are the averages across all data points.*

Typical percentage ^{15}N incorporation is a proportion of $[M(^{15}N)+H]^+$ and $[M(^{14}N)+H]^+$ peak areas (see section 5.6.2). We detected background ^{15}N isotopolog abundance. Therefore, the isotope enrichment was corrected by subtracting the average background isotopolog abundance from samples fed with unlabelled precursors. This resulted in 39 *Daphniphyllum* alkaloids that showed ^{15}N incorporation. An overview of the results normalised this way was presented in the Table 5.1 below. The chosen alkaloids were discussed in detail in this chapter.

Table 5.1 Overview of the results of the stable isotope feeding experiment using hydroponic seedlings showing corrected percentage incorporation of ^{15}N (mean percentage in the labelled sample – mean percentage in unlabelled sample) in leaf, root and stem tissues of the hydroponics plant, using L-alanine-^{15}N (^{15}N Ala), L-glutamic acid-^{15}N (^{15}N Glu), L-serine-^{15}N (^{15}N Ser). C22/C30 type represents C22 compounds of secodaphniphylline or daphniphylline skeleton lacking C8 moiety. C22A represents yuzurimine or calyciphylline type and C30 seco- or daphniphylline type.

Type	Skeleton family	Peak code	Percentage of ^{15}N incorporation (%)								
			Leaves			Roots			Stem		
			^{15}N Ala	^{15}N Glu	^{15}N Ser	^{15}N Ala	^{15}N Glu	^{15}N Ser	^{15}N Ala	^{15}N Glu	^{15}N Ser
C22	Daphnicyclidin/Calyciphylline A	M324.196T165	5.2	2.7	3.3	0.0	1.8	0.0	2.2	2.2	3.0
C22		M324.196T90	3.8	2.5	3.5	0.0	1.1	1.8	2.5	2.4	2.5
C30/C22	buttingine, calyciphylline B, daphnilactone B	M342.243T95	15.2	8.2	6.0	5.8	8.9	4.5	13.1	4.7	5.9
C30/C22		M342.243T170	6.6	4.4	2.5	5.4	6.8	3.0	5.6	5.0	3.5
C30/C22	daphnezomile L, daphnilactone B, secodaphniphylline	M344.258T105	3.7	1.3	2.3	1.2	3.1	0.4	2.2	2.5	2.0
C30/C22	secodaphniphylline	M346.274T150	10.2	4.6	4.3	8.5	7.7	4.1	9.3	5.9	5.4
C30/C22	daphnezomile L, daphniphylline, secodaphniphylline	M346.274T175	12.1	5.2	6.4	10.7	9.0	5.7	12.9	6.9	7.0
C30/C22		M346.274T225	4.9	1.4	3.3	0.0	3.2	0.8	2.1	1.8	0.3
C30/C22		M346.274T230	4.9	1.0	3.9	0.0	3.9	2.0	2.3	2.1	1.2
C30/C22		M346.274T260	4.7	0.9	3.8	0.7	2.6	1.5	1.9	2.4	1.4
C22A	daphhimalenine A	M354.206T100	3.1	1.5	2.2	2.4	3.4	1.0	1.8	2.0	1.9
C22/C30	buttingine, daphnezomine L, daphnilactone A, daphniphylline, yuzurine	M358.274T220	5.5	2.0	2.1	1.4	4.2	1.7	13.3	6.1	7.3
C22/C30		M358.274T260	2.4	1.2	1.8	0.8	2.0	0.9	0.7	1.0	0.7
C22/C30		M358.274T290	3.7	1.1	2.8	0.0	0.6	0.0	0.8	0.6	0.6
C22/C30	secodaphniphylline, daphniphylline, daphnezomile L	M360.290T170	11.0	4.5	5.9	7.6	7.4	4.5	12.0	6.3	6.5
C22/C30		M360.290T260	3.5	0.7	2.9	0.0	0.6	0.8	1.8	1.3	1.3
C22/C30	methyl homosecodaphniphyllate	M360.290T310	4.9	2.1	3.4	2.0	3.7	2.4	2.1	3.0	1.5
C22/C30	Seco-, daphniphylline, daphnezomile L	M360.290T315	6.6	2.0	5.0	2.4	5.6	3.9	3.5	4.4	2.2
C22/C30	Daphnezomine AB, daphniphylline	M362.269T100	4.1	1.9	2.8	1.7	3.4	1.3	2.7	2.5	1.8

C22/C30	Daphnezomine AB, daphniphylline	M362.269T95	2.7	0.8	1.6	0.5	1.0	0.5	2.5	1.7	1.1
C22A	Calyciphylline A	M368.222T200	4.6	2.5	2.7	0.8	0.7	2.2	5.2	2.9	3.0
C22A	calyciphylline A, calyciphylline C, Daphmanidin A, yuzurimine	M370.238T215	4.3	2.3	3.2	0.6	4.0	0.3	2.3	1.8	1.5
C22/C22A	calyciphylline A, yuzurimine, daphlongeramine AB, daphniglaucin C	M372.217T80	0.0	0.0	0.0	0.0	0.0	0.0	3.5	2.6	1.9
C22/C30	buttingine, calyciphylline B, daphnilactone B, daphnezomine L	M374.269T135	13.4	7.3	5.4	0.0	3.8	0.0	2.2	2.4	0.5
C22/C30	secodaphniphylline, daphniphylline, daphnezomile L	M376.285T260	2.9	1.8	2.2	0.9	2.0	1.1	1.2	1.6	0.9
C22/C30	Daphnicyclidin/Calyciphylline A	M382.201T160	6.8	3.3	4.3	3.3	4.5	3.3	2.7	2.5	3.3
C22/C22A	Yuzurimine, yuzurine	M386.233T180	3.8	2.1	2.5	0.0	0.0	0.0	1.7	1.1	0.6
C22/C22A	Yuzurimine, yuzurine, paxdaphnine A	M388.248T180	2.9	1.5	1.1	0.0	0.0	0.0	1.3	0.0	0.2
C22/C22A	yuzurimine, calyciphylline A	M402.228T135	4.0	2.0	1.3	0.0	0.0	0.0	7.1	3.8	4.3
C22/C22A	Daphmanidin A, Calyciphylline A	M428.243T200	2.0	0.5	1.3	0.0	0.2	0.2	0.0	0.0	0.0
C30	daphniphylline	M470.363T305	5.7	2.3	4.2	0.0	6.4	0.0	8.4	5.4	5.3
C30		M470.363T310	11.6	3.4	6.8	0.0	9.1	8.1	11.9	5.4	6.9
C30	daphniphylline or secodaphniphylline	M472.378T315	12.6	2.9	5.7	0.0	7.1	0.0	14.5	5.7	6.8
C30		M472.378T270	0.0	0.0	0.0	0.0	4.0	7.6	6.1	2.8	4.1
C30		M472.378T300	10.9	2.9	6.1	0.0	3.2	0.0	14.2	5.8	7.0
C30		M472.378T305	4.8	1.0	3.4	0.0	5.6	0.0	4.3	2.5	3.7
C30		M486.358T280	6.0	0.6	3.3	0.0	9.3	0.0	3.3	0.6	1.3
C30	daphniphylline	M488.373T260	10.8	2.8	5.8	0.0	0.0	0.0	8.3	3.4	3.8
C30	daphniphylline or secodaphniphylline	M514.389T165	0.0	0.0	0.0	0.0	3.5	0.0	4.8	1.6	3.8

5.6.3.1 Normalisation by concentration

Due to lack of available plants, we were not able to test appropriate concentrations of amino acids prior to the experiment and so we added amino acids at different concentrations. The concentration of L-serine-^{15}N was determined by the maximum amount of available labelled amino acid. However, we were concerned that the concentration of 0.5 mM would be too low to allow detection of labelled *Daphniphyllum* alkaloids and so we increased the concentration of L-glutamic acid and L-alanine (Bindschedler, Palmblad and Cramer, 2008). The unlabelled substrates were fed to the control plants at the same concentrations as their labelled equivalents. Although higher concentration might increase the uptake of an amino acid and labelling, too high concentration could lead to saturation of the system or even be toxic to the plant, altering plants metabolism. On top of that, ^{15}N labelling had never previously been observed in *Daphniphyllum* alkaloids.

The results were already normalised in each sample by calculating the percentage of incorporation. However, since the concentration of the precursor can affect the uptake and incorporation, the results can also be normalised by the concentration to account for the variation. To do this, the percentage of ^{15}N incorporation was divided by the original concentration of the fed amino acid and the overview of the results was plotted in Figure 5.7.

The normalisation showed that generally L-serine was a preferred amino acid in all tissues (based on a t test comparing average normalised incorporation across all tissues with L-serine-^{15}N compared to combined L-alanine-^{15}N and L-glutamic acid-^{15}N – p value = 0.0003). Even though, the concentration of L-alanine was twice the concentration of L-glutamic acid, there was no significant difference between the average incorporations with L-alanine-^{15}N or L-glutamic acid-^{15}N as substrates.

We observed differences in the incorporation levels when the results were not normalised by the concentration. Therefore, the similarity in the labelling levels were unlikely to be a result of seedling saturation from an excessively high concentration of L-alanine-^{15}N. Instead, this may indicate that neither amino acid was preferentially used in the plant system, and the high

incorporation levels were simply a consequence of the higher concentration of the fed precursors.

The results indicated that across all tissues and ^{15}N-labelled *Daphniphyllum* alkaloids, L-serine was a preferred amino acid towards incorporation into the skeleton of *Daphniphyllum* alkaloids.

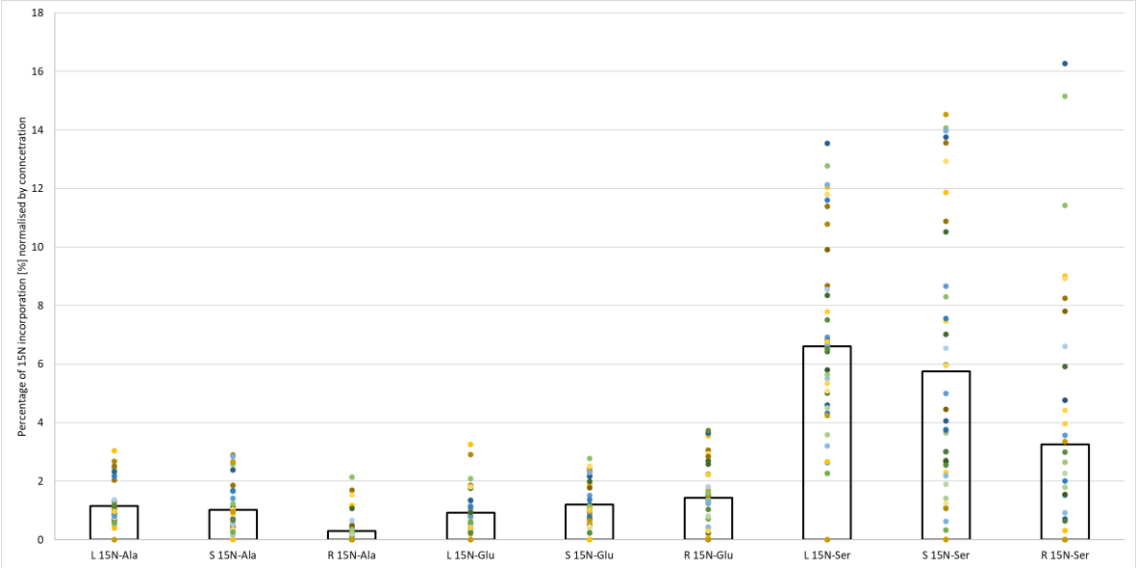

Figure 5.7 Stable isotope labelling experiment in Daphniphyllum *macropodum showing percentage of ^{15}N incorporation normalised by the concentration of fed precursor across all* Daphniphyllum *alkaloids showing labelling. Each point represents an average of three biological replicates. Letters represent tissue type: leaves (L), stem (S), roots (R) and amino acids: L-alanine-^{15}N (15N-Ala), L-glutamic acid-^{15}N (15N-Glu), L-serine-^{15}N (15N-Ser). Each point represents an average ^{15}N incorporation across three biological replicates for a single alkaloid. The bars are the averages across all data points.*

5.6.3.2 C30 alkaloids

There were nine *Daphniphyllum* alkaloids that showed labelling across all samples. When the ^{15}N incorporation was normalised by the concentration of the fed amino acids, it showed the highest incorporation in the leaf and stem tissues when L-serine-^{15}N was added (Figure 5.8). Interestingly, the incorporation was in C30 alkaloids was tissue dependent. There was no incorporation of ^{15}N in the roots when L-alanine-^{15}N was fed, and only in two alkaloids – M470.363T310 and M472.378T270 – when L-serine-^{15}N was fed. However, the ^{15}N incorporation was generally the highest in the roots when L-glutamic acid-^{15}N was fed to the seedlings.

This could mean two things: firstly, there might be a preference for one of the amino acids in the roots – L-glutamic acid – especially, that the only *Daphniphyllum* alkaloids that did not show labelling in the roots with any of the amino acids were M514.389T165 and M488.373T260.

Meanwhile, the high incorporation of ^{15}N in the two alkaloids (M470.363T310 and M472.378T270) in the roots when L-serine-^{15}N was added, could suggest that the lower concentration of amino acids could have led to more targeted incorporation in C30 alkaloids which would appear at the earlier steps of the biosynthetic pathway and therefore could be less universally labelled. The differences between the incorporation from different amino acids could also be caused by their different roles in primary metabolism (Pott, Osorio and Vallarino, 2019; Batista-Silva et al., 2019; Yang, Zhao and Liu, 2020). Lower concentration of L-serine-^{15}N could have led to smaller number of universally labelled *Daphniphyllum* alkaloids.

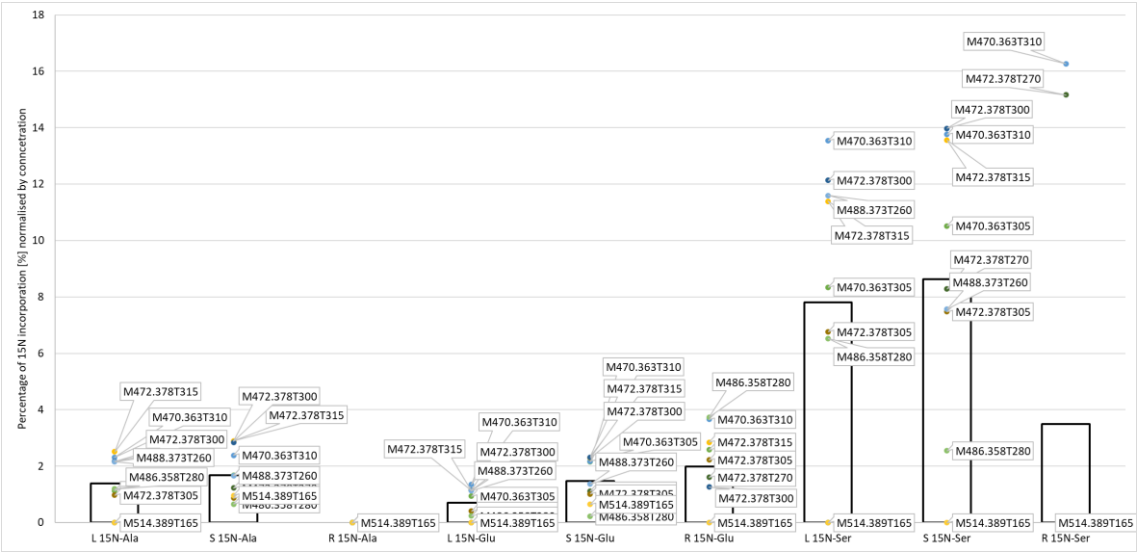

Figure 5.8 Stable isotope labelling experiment in Daphniphyllum *macropodum showing percentage of ^{15}N incorporation normalised by the concentration of fed precursor across C30* Daphniphyllum *alkaloids showing labelling. Each point represents an average of three biological replicates. Letters represent tissue type: leaves (L), stem (S), roots (R) and amino acids: L-alanine-^{15}N (15N-Ala), L-glutamic acid-^{15}N (15N-Glu), L-serine-^{15}N (15N-Ser). Each point represents an average ^{15}N incorporation across three biological replicates for a single alkaloid. The bars are the averages across all data points.*

5.6.3.3 C22/C30 alkaloids

The alkaloids that have daphniphylline or secodaphniphylline skeleton but do not have 30 or 32 carbons because they miss C8 moiety, could act as intermediates in the pathway. Similarly to C30 alkaloids, the highest ^{15}N incorporation was observed across all tissues when L-serine-^{15}N was fed (Figure 5.9). In fact, there was no statistically significant difference between incorporations in those tissues. The difference, however, was statistically significant between feeding L-serine-^{15}N compared to feeding with L-alanine-^{15}N and L-glutamic acid-^{15}N, p = 2.9E-13, p = 1.1E-11, respectively. Additionally, the incorporation in C22B alkaloids was the lowest when L-alanine-^{15}N was fed even though it was added at the highest concentration. The combined ^{15}N incorporation from L-alanine-^{15}N was significantly lower compared to the one from L-glutamic acid-^{15}N (p = 0.009).

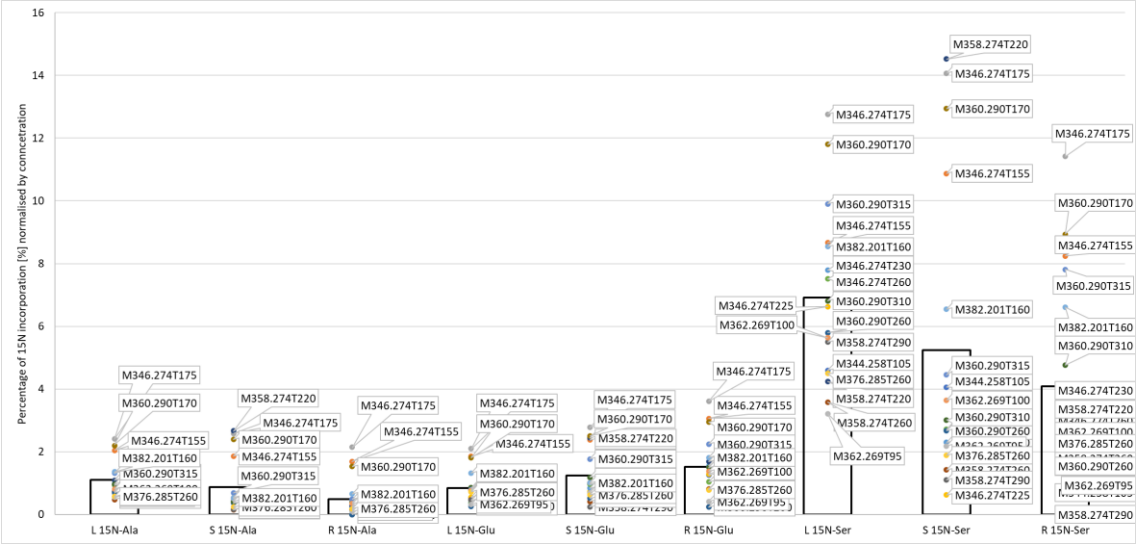

Figure 5.9 Stable isotope labelling experiment in Daphniphyllum *macropodum showing percentage of ^{15}N incorporation normalised by the concentration of fed precursor across C22/C30* Daphniphyllum *alkaloids showing labelling. Each point represents an average of three biological replicates. Letters represent tissue type: leaves (L), stem (S), roots (R) and amino acids: L-alanine-^{15}N (15N-Ala), L-glutamic acid-^{15}N (15N-Glu), L-serine-^{15}N (15N-Ser). Each point represents an average ^{15}N incorporation across three biological replicates for a single alkaloid. The bars are the averages across all data points.*

5.6.3.4 C22B alkaloids

C22B alkaloids fit the category of intermediates before C22A compounds that have daphnezomine L or daphnilactone B types. Indeed, both types of intermediates, C22B and C22/C30, showed the same behaviour (Figure 5.10). The highest ^{15}N incorporation was observed in the leaves, stem and root of seedlings treated with L-serine-^{15}N. Indeed, there

was no significant difference between them. There was also no significant difference between leaves of seedlings treated with L-alanine-^{15}N and L-glutamic acid-^{15}N. There was, however, a significant difference between the incorporation of ^{15}N in the leaves and roots of the seedlings treated with L-alanine-^{15}N (p = 0.039). However, combining all samples there was no significant difference between seedlings treated with those two amino acids.

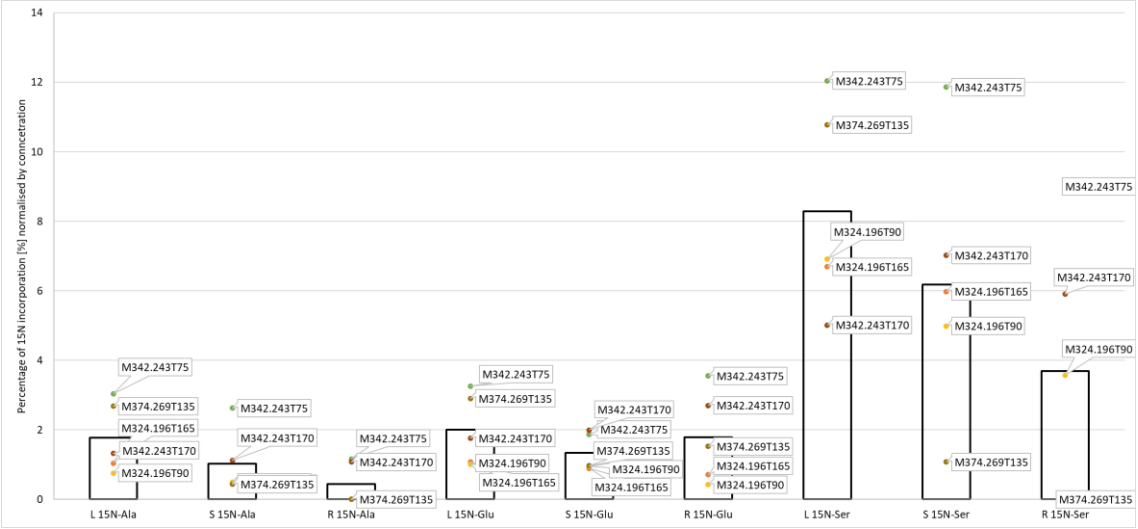

Figure 5.10 Stable isotope labelling experiment in D. macropodum showing percentage of ^{15}N incorporation normalised by the concentration of fed precursor across C22B Daphniphyllum *alkaloids showing labelling. Each point represents an average of three biological replicates. Letters represent tissue type: leaves (L), stem (S), roots (R) and amino acids: L-alanine-^{15}N (15N-Ala), L-glutamic acid-^{15}N (15N-Glu), L-serine-^{15}N (15N-Ser).*

5.6.3.5 C22A alkaloids

The final subtype of *Daphniphyllum* alkaloids that we were interested in was C22A (Figure 5.11). Again, the ^{15}N incorporation in the leaves and stems of the seedlings treated with L-serine-^{15}N was significantly higher than in other samples. Similarly, there was no significant difference in the incorporation between the leaves and stem (p = 0.85). There was no significant difference between the incorporation in the roots of the seedlings treated with L-serine-^{15}N and combined samples of other seedlings treated with L-alanine-^{15}N or L-glutamic acid-^{15}N. There was also no significant difference between incorporation in the tissues of the seedlings treated with L-glutamic acid-^{15}N. Whilst, in the case of the seedlings treated with L-alanine-^{15}N, there was no significant difference between leaves and stem and significantly lower incorporation in the roots.

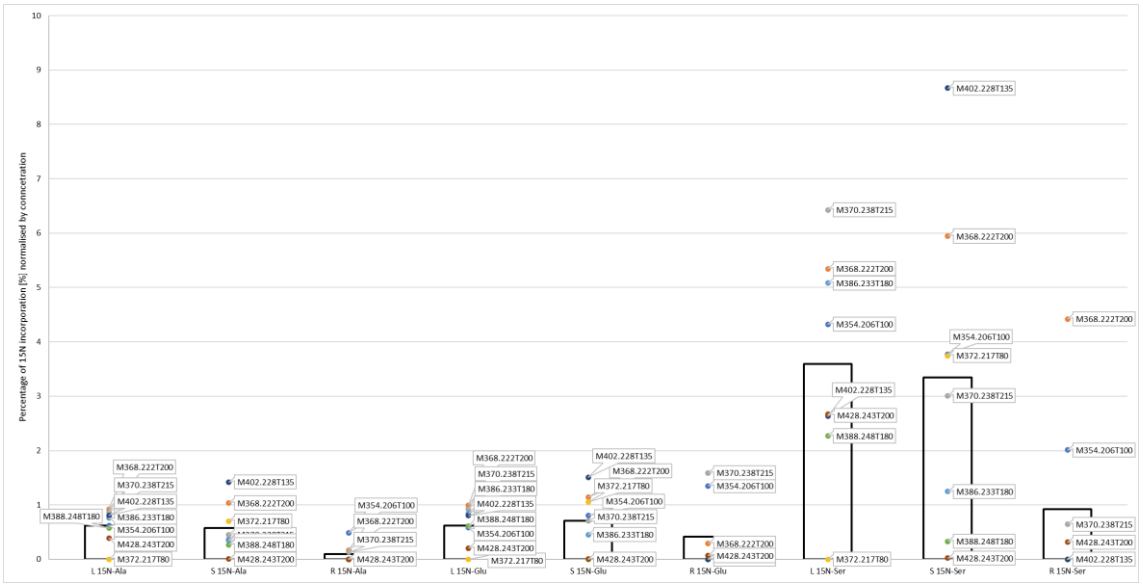

Figure 5.11 Stable isotope labelling experiment in Daphniphyllum *macropodum showing percentage of ^{15}N incorporation normalised by the concentration of fed precursor across C22A* Daphniphyllum *alkaloids showing labelling. Each point represents an average of three biological replicates. Letters represent tissue type: leaves (L), stem (S), roots (R) and amino acids: L-alanine-^{15}N (15N-Ala), L-glutamic acid-^{15}N (15N-Glu), L-serine-^{15}N (15N-Ser).*

5.7 Overall discussion and conclusion

In summary this stable isotope labelling experiment in hydroponic seedlings allowed to observe ^{15}N labelling in *Daphniphyllum* alkaloids for the first time. The labelling was observed in all tissues in the seedlings treated with the three labelled amino acids. The highest incorporation was observed in the leaves and stem treated with L-serine-^{15}N.

^{15}N was incorporated with all three amino acids, possibly due to metabolism of those amino acids into primary metabolic pathways. Interestingly, even though L-serine-^{15}N was added to the liquid media at the lowest concentration, the percentage of ^{15}N incorporation was the highest. It suggested that introduction of nitrogen might be an amino acid specific in the young hydroponic seedlings of *D. macropodum.* Additionally, the ^{15}N-labelled amino acids were fed to the roots, so L-serine-^{15}N likely needed to be transported into the aerial tissues first before being incorporated into the *Daphniphyllum* alkaloid skeleton.

Interestingly, there was no incorporation observed in the roots of the seedlings treated with L-alanine-^{15}N in C30 alkaloids even though the labelling was observed in other subtypes of alkaloids in the same tissues. Since the *Daphniphyllum* alkaloids start with C30 compounds, it was puzzling to observe labelling in other subtypes even though it was low, below 1.5%. The highest incorporation was observed in C22/C30 types, the suspected intermediates in the pathway. This may suggest that we observed different stages of the biosynthetic pathway after C30 alkaloids lost C8 moiety and before the new C30 alkaloids were labelled.

The compounds that showed the highest labelling, likely should be placed early in the pathway and those included C30 alkaloids such as M472.3783T315, M472.3783T310 and M470.3627T310 as well as C22 compounds that likely were intermediates: M346.2740T175. This result was consistent with the hypothesis and the results described in the previous chapter in which C30 compounds precede C22A compounds. While C22A compounds still showed ^{15}N incorporation it was not as high as in C30 compounds.

The ^{15}N labelled amino acids needed to be uptaken by the roots which meant that the biosynthesised alkaloids needed to travel to different tissues in order to observe labelling across all plants. Alternatively, the amino acids were transported first, and we observed de novo biosynthesis in those tissues. In chapter 4 and in the previous study (Eljounaidi et al., 2024), the results indicated de novo biosynthesis of alkaloids in various tissues. This could explain preferential incorporation for different amino acids in roots and aerial tissues.

Although the results suggested that L-serine was a preferred amino acid in the biosynthesis of *Daphniphyllum* alkaloids, the differences between different amino acids could be caused by different metabolomic pathways in different tissues. Plants can synthesise all proteinaceous amino acids which means that not only the fed labelled amino acid could be diluted but also the fed labelled amino acid can be metabolised into other amino acids before the observed incorporation, or can be a part of further metabolomic pathways (Ishihara et al., 2015). For example, glutamic acid and serine are used in photorespiration (Ros, Muñoz-Bertomeu and Krueger, 2014) which could explain the lower incorporation of ^{15}N isotope in the leaves when the seedlings were treated with those two amino acids.

Nevertheless, it showed that in those conditions a high concentration of an amino acid is not necessary to observe ^{15}N labelling. Also, L-serine is a preferred amino acid over L-alanine and L-glutamic acid and the incorporation was observed in all tissues. This experiment did not however, answer the question how nitrogen is introduced into the *Daphniphyllum* alkaloid skeleton.

The seedlings were fed labelled amino acids for two and half weeks, following the previous feeding experiments conducted on *Daphniphyllum macropodum* (two weeks (Haruki, Yoshimasa and Suzuki, 1973) and three weeks (Eljounaidi et al., 2024) and we observed labelling under all conditions. In retrospective, this approach could have been adjusted for the pulse chase method.

The pulse-chase method is a technique which can be used to study dynamic processes like biosynthetic pathways within the plant system or degradation of molecules. The method starts with the pulse phase, during which an organism is exposed to a labelled compound such

as a stable isotope labelled amino acid for a short period of time. The labelled compound is then incorporated into a molecule of interest. The isotope label can then be used as a marker to track the biosynthetic pathway using analytical techniques such as mass spectrometry. Then, in the chase phase, the labelled precursors are removed, and the plant is exposed to the unlabelled precursor. In the chase phase, no more compounds get labelled which guarantees only tracking the molecules biosynthesised during the pulse phase.

However, pulse chase experiments need to be optimised and can vary for each plant. For example, in one of the study the optimal pulse time for *Arabidopsis thaliana* was 45 min with 7 h chase while for *Juncus prismatocarpus* the optimal time was found to be 2 h and 13.5 h, respectively (Yin and Tsukaya, 2016). The method needs optimisation because too short pulse and chase periods would lead to low signals while too long pulse and chase would cause too many unsynchronised signals. At the time we did not have seedlings available to repeat this experiment or to optimise the conditions of the pulse chase method.

6 Methodologies

6.1 General methods

6.1.1 Isolation of alkaloids

6.1.1.1 General method for alkaloid extraction

Plant leaf tissue of *Daphniphyllum macropodum* (100 g) was ground to a fine powder under liquid nitrogen with a pestle and mortar or an automatic mill. The powder was extracted, at room temperature whilst stirring, with methanol (350 mL for 2 h, then 150 mL for 16 h). The methanolic extract was filtered and dried in vacuo. The residue was resuspended in ethyl acetate (200 mL) which was extracted with aq. HCl (0.01 M, pH 2, 3 x 200 mL). The aqueous layers were combined and washed with ethyl acetate (200 mL). The aqueous layer was basified to pH 10 with sat. Na_2CO_3 and then extracted with chloroform (4 x 100 mL). The organic fractions were combined and dried in vacuo to yield crude alkaloid extract. The solvent volumes were adjusted for extraction from 800 g of *D. macropodum* aerial tissue.

6.1.1.2 Purification of alkaloids

Purification of alkaloids was carried out using Interchim Puriflash 4250 prep HPLC system linked to an Advion Expression S Compact Mass Spec (CMS). The extract was fractionated through C18 FlashPure 12 g column; flow rate: 30 mL/min into 5 fractions using a gradient of solvents (A) Ammonium bicarbonate buffer pH = 10.2 and (B) Methanol (0–5 min 98% A, 5.1–10 min 50% A, 10.1–16 min 40% A, 16.1–27 min 35% A, 27–38 min 35–5% A, 38.1–42 min 5%, 42–46 min 2%. The fractions were collected automatically in 20 mL vials. The semi-pure fractions were further purified using a semi-preparative column (Waters XBridge C18 5µm column of size 10 x 150 mm) and eluted with a gradient of ammonium bicarbonate buffer pH = 10.2 and methanol controlled manually with 6.6 mL/min flow rate. The structures were elucidated using ^{1}H, ^{13}C and 2D NMR.

6.1.2 UPLC-MS/MS with Orbitrap

6.1.2.1 Sample preparation

For the extraction of metabolites 50 mg of powdered plant tissue sample was dispensed into an Eppendorf tube, alongside blanks and standards. 500 µl of 80% methanol was added to each sample. The samples were then vortexed, followed by centrifugation at 10,000 g for 15 minutes. Subsequently, 450 µl of 80% methanol was placed into each LC-MS vial and 50 µl of the supernatant was carefully transferred into these vials, avoiding disturbance of the pellet. Samples prepared for LC-MS analysis were stored at 4 °C.

6.1.2.2 LC-MS/MS

LC-MS/MS runs were performed using a Waters Acquity I-Class UPLC instrument interfaced to a Thermo Tribrid Fusion Orbitrap or Exploris 480 instrument using an APCI ion source in positive ion mode. To enable resolution between ^{13}C and ^{15}N isotopes, data were collected on an Orbtrap Exploris 480 mass spectrometer with MS^1 data mass resolution FWHM = 180000 (at m/z 200). UPLC runs were controlled by Waters Empower software. 2 µL injections were made onto an Acquity BEH C18 column (100 x 2.1 mm, 1.7 µm particle size), held at 60 °C. The column was run at 0.5 mL/min with mobile phase A = 10 mM ammonium bicarbonate (pH 10.2) and B = MeOH, under the following gradient program: initial isocratic 2% B; 0.2–0.5 min linear to 40% B; 0.5–5.3 min linear to 95% B; 5.3–5.8 min isocratic 95% B; 5.8–5.9 min return to initial conditions and hold until 6.4 min (total run time). MS parameters were controlled by Thermo Xcalibur 4.1 software. Eluent flow was diverted into the APCI source between 0.66 and 4.5 min (6 min for plant F analysis). The source was maintained at 350 °C and a spray current setting of 4 µA. Nitrogen was used as sheath, aux, and sweep gas, set to 35, 5, and 0.5 arbitrary units, respectively. The ion transfer tube was held at 275 °C. Data were collected in data-dependent MS^2 mode. MS^1 data were collected in profile mode using a cycle time of 0.4 s and a desired minimum point across the peak setting of 6, over a m/z range of 200-2000 with orbitrap resolution set to 60 000 (FWHM @ 200 m/z). Easy-IC internal calibration was used to reduce MS^1 mass errors to ~< 1 ppm. Low resolution data-dependent

MS^2 data were collected as centroided data in rapid scan mode in the ion trap, using alternating collision induced dissociation (CID) and higher energy collisional dissociation (HCD) fragmentation modes and precursor quadrupole isolation windows set to 1 m/z. HCD data were collected at stepped normalised collision energies of 34, 40, and 45%, and CID data were collected using a fixed normalised collision energy of 40%. Dynamic exclusion was set to collect one CID and HCD MS2 scan from each precursor ion and to exclude further fragment scans from the same precursor for 2 s.

6.1.2.3 Data analysis and processing

The LCMS data were processed using XCMS online (Smith et al., 2006; Tautenhahn et al., 2012) to determine the peak area across all samples and determine the features. Files were converted from .raw to .mzML or .mzXML format using the Proteowizard msConvert tool. Peak areas obtained from XCMS online were then analysed across samples as described in section 4.2.1.3. This analysis led to features (i.e. peaks) described across samples named "MXXX.XXXTZZ" where X represents the m/z of the feature and T represents the retention time (RT) corrected to the retention time of yuzurimine **1.10** at 210 seconds.

The data containing samples potentially labelled with ^{15}N isotope were initially processed by Dr Tony Larson. Data were collected on an Orbtrap Exploris 480 mass spectrometer with MS1 data mass resolution FWHM = 180000 (at m/z 200), to enable resolution between 13C and 15N isotopes. .mzML files were processed using R (4.2.3) scripts run in a linux environment, using XCMS (3.20.0). LC-MS data were processed with XMCS (3.12.0) and CAMERA (1.33.3) (Kuhl et al., 2012) to identify features. Files were converted from .raw to .mzML format using the Proteowizard msConvert tool, and subsequently processed using bespoke scripts in R 4.0.3 in a linux environment. . For feature detection, xcmsSet() with the following parameters were used: method = 'centWaveWithPredictedIsotopeROIs', ppm = 2, snthresh = 3, peakwidth = c(2, 10), prefilter = c(3, 1000), integrate = 2, mzdiff = -0.0001, snthreshIsoROIs = 3. The do_define_isotopes function used by the 'centWaveWithPredictedIsotopeROIs' method was modified to enable detection of 13C, and 15N isotope regions of interest with the following allowed combinations: C = 0:32; N = 0, 1. Subsequent feature list filtering was performed as

follows: 1) potentially unlabelled and labelled feature pairs had to coelute within 2s of each other; 2) a hard limit of +/- 0.002 m/z units was imposed for matching any light and heavy isotope pairs; 3) feature areas of putative heavy isotopes were required to be at least 3 x more abundant in labelled vs unlabelled samples.

6.1.2.4 Molecular networking

Molecular Networking was created using Molecular Networking workflow on GNPS (https://gnps.ucsd.edu, (Wang et al., 2016) using default settings. A molecular network was then created where edges were filtered to have a cosine score above 0.7 and more than 6 matched peaks. The molecular network was visualized using Cytoscape software (Shannon et al., 2003).

6.1.3 Total tissue protein extracts

Unless otherwise stated, all the steps were carried out on ice.

6.1.3.1 General method for total tissue protein extracts

Adapted from (Nett and Sattely, 2021). Mature leaves and roots of *D. macropodum* (plant G F, and B offsprings) were collected and snapped frozen in liquid nitrogen and stored at −80 °C for future use. To isolate crude protein lysates, frozen tissue of roots (10 g) and mature leaves (15 g) were ground in liquid nitrogen using automatic mill until the tissue was fully homogenised. Afterwards, the tissues were transfer into pre-chilled tubes and 20 mL of ice-cold tricine buffer (100 mM tricine, pH 7.5, 20 mM 2-mercaptoethanol) with polyvinylpolypyrrolidone (PVPP) (5% of dried weight). Samples were centrifuged at 15 000 g and 4 °C for 15 min to pellet plant debris. The supernatant was decanted into new, prechilled tubes, and a portion of the supernatant (5 mL) was kept as soluble protein fractions and used immediately. To prepare a microsomal protein fraction, the remaining protein lysate (15 mL) was ultracentrifuged at 50 000g and 4 °C for 1 h. The supernatants from these samples were discarded, and the pellets which represented the microsomal protein fraction were resuspended in ice-cold tricine buffer (4 mL) and aliquoted into prechilled Eppendorf tubes and used immediately. Protein abundance was measured using Bradford assay. The soluble and microsomal tissue extracts were not purified to remove small molecules and so contained native *Daphniphyllum* alkaloids.

6.1.3.2 Tissue extract assays

The reactions were prepared to contain 40 µg of microsomal protein, the undiluted soluble protein extracts were making bulk of the reaction. Unless mentioned otherwise all assays contained combined microsomal and soluble crude protein extracts. Tissue enzyme assays described in chapter 4 section 4.2.3 contained squalene **1.11** (0.5 mM) or cofactors: NADPH (1 mM) and FAD (0.1 mM), HEPES buffer (50 mM) and NaCl (100 mM). Tissue enzyme assays described in chapter 4 section 4.2.4 contained squalene **1.11** (0.5 mM) or diol **1.97** (0.5 mM),

HEPES buffer (50 mM) and NaCl (100 mM). The controls included tissue extracts treated with proteinase K for 1 h at 37 ^{o}C before substrates were added and tissue extracts treated with buffer with no substrates added.

Tissue assays described in chapter 5, section 5.2 contained squalene **1.11** (0.5 mM) or diol **1.97** (0.5 mM) with either L-glutamic acid-^{15}N (0.5mM), L-alanine-^{15}N (0.5mM), ^{15}N-ammonium chloride (0.5 mM), L-glutamic acid (0.5mM), L-alanine (0.5mM), ammonium chloride (0.5 mM), HEPES buffer (50 mM) and NaCl (100 mM). The controls also included tissue assays with only one substrate, each mentioned above. The assays were run on the same day, as extraction of tissue extracts, for 16h at 30 ^{o}C and were open to O_2. After 16h they were quenched with MeOH. Samples were then prepared for LC-MS analysis. The assays were run in triplicated and LC-MS samples in technical repeats.

6.1.3.3 Preparation of lipid suspension

The lipids, L-A-phosphatidylcholine (Sigma Type II-S, from Soybean) were used for vesicle preparation following previously published procedure (Fraser, Shimada and Misawa, 1998). 10 mg of lipid was resuspended in acetone (1 mL), 100 µL of the solution was transferred in the Eppendorf tube, the lipid was dried onto the surface of the tubes under nitrogen by dispersing the lipid on the bottom of the tube. 0.4 mM Tris/HCl pH 8.0 buffer (100 µL) was placed onto the residue. Sonication (3 x 2 s bursts, full power) yielded suitable lipid suspension. Lipid vesicles were stored in -20 °C and will be sonicated prior to incubation. The squalene **1.11** and diol **1.97** were be added directly to the suspension.

6.1.4 Daphniphyllum plant growing conditions

6.1.4.1 Seed propagation

Previously published procedure was used (Eljounaidi et al., 2024). *Daphniphyllum macropodum Miq.* seeds were harvested when the fruit was ripe (dark purple/blue). The fleshy tissue (epicarp and mesocarp) was removed, and the seed rinsed with water and air-dried. The seed was sterilised with chlorine vapor for 5 h and then transferred to Petri dishes containing seed germination media (gelrite (0.5% w/v), Lloyd and McCown's woody plant medium with vitamins (50% strength), Plant Preservative Mixture (1 ml L^{-1}), streptomycin (50 µg mL^{-1}), cefotaxime (250 µg mL^{-1}), gibberellic acid 4 + 7 (200 µg mL^{-1}), pH 5.8). The seeds were incubated (14 h: 10 h, 20°C:10°C; dark) until radicle emergence, when they were placed in stratification conditions (4°C). After 14 d, incubation conditions were modified and light introduced (1 h, 10°C, light; 13 h, 20°C, light; 1 h 20°C, dark; 9 h, 10°C, dark; light = 40 µmol m^{-2} s^{-1}). After hypocotyl emergence the temperature was increased (1 h, 15°C, light; 13 h, 25 °C, light; 1 h 25°C, dark; 9 h, 15 °C, dark; light = 40 µmol m^{-2} s^{-1}). When hypocotyl > 2.5 cm the seed coat was removed and seedling transferred to hydroponics system. Seedlings were grown under axenic conditions at 25 °C under light intensity of 40 µmol m^{-2} s^{-1} and a photoperiod of 14 h: 10 h, light: dark.

6.1.4.2 Hydroponic labelling experiment

Seedlings of approximately the same age and developmental stage were transferred to woody plant medium containing L-alanine/L-alanine-^{15}N (5 mM), L-glutamic acid/L-glutamic acid-^{15}N (2.5 mM) and L-serine/L-serine-15N (0.5 mM) Three biological replicates were used for each experimental condition. After 16 days of incubation, leaf, stem and root tissues of the plants were rinsed with water, frozen in liquid nitrogen and prepared for LC-MS analysis as described in section 6.1.2.1.

6.2 Experimental procedures for Chapter 2 and 3

6.2.1 General information

Except where stated, all reagents were purchased from commercial sources and used without further purification. Detailed procedures were presented below. Anhydrous THF, DCM and toluene were obtained from an Innovative Technology Inc. PureSolv® solvent purification system. ^{1}H and ^{13}C NMR spectra were recorded on either a JEOL ECS400 spectrometer, operating at 400 MHz and 100 MHz, a Bruker AVIIIHD 600 Widebore operating at 600 MHz, 151 MHz and 253 MHz or a Bruker 700MHz NEO with a TCI Prodigy Cryoprobe, operating at 700 MHz and 176 MHz. All spectral data were acquired at 295 K. Chemical shifts (δ) are quoted in parts per million (ppm). The residual solvent peak, δ_H 7.26 ppm and δ_C 77.16 ppm for $CDCl_3$ or δ_H 4.87 ppm and δ_C 49.2 for CD_3OD were used as a reference. Coupling constants (*J*) are reported in Hertz (Hz) to the nearest 0.5 Hz. The multiplicity abbreviations used are: s singlet, d doublet, t triplet, q quartet, quin. quintet, sex. sextet, m multiplet. Signal assignment was achieved by analysis of DEPT, COSY, HMBC and HMQC experiments where required. Infrared (IR) spectra were recorded on a PerkinElmer UATR 2 spectrometer as a thin film dispersed from either CH_2Cl_2 or $CDCl_3$. Mass-spectra (low and high-resolution) were obtained by the University of York Mass Spectrometry Service, using electrospray ionisation (ESI) on a Bruker Daltonics, Micro-tof spectrometer. Thin layer chromatography was carried out on Merck silica gel 60F254 pre-coated aluminium foil sheets and were visualised using UV light (254 nm) and stained with a basic potassium permanganate solution, vanillin or ninhydrin solution. Flash column chromatography was carried out using slurry packed Fluka silica gel (SiO2), 35– 70 µm, 60 Å, under a light positive pressure, eluting with the specified solvent system.

6.2.2 Experimental procedures

Compound 2.17 (3,7-dimethyl-2,6-octadienal).

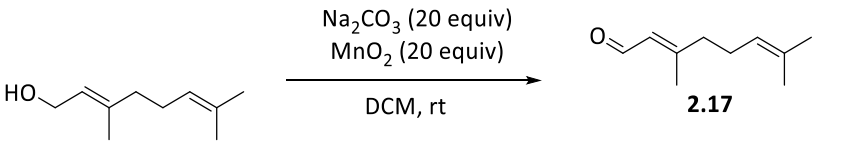

geraniol **2.18**
1.0 equiv

(97%)
Chemical Formula: $C_{10}H_{16}O$
Molecular Weight: 152.2370

Geraniol **2.18** (6.60 mL, 30.0 mmol) was dissolved in DCM (30 mL) in dry conditions under argon. Na_2CO_3 (63.6 g, 600 mmol) and MnO_2 (52.3 g, 600 mmol) were then added, and the resulting mixture was stirred overnight at room temperature. The reaction mixture was then filtered to remove insoluble MnO_2 and the filtrate was concentrated under reduced pressure to afford compound **2.17** as a transparent, yellow oil (4.43 g, 97%).

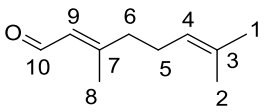

R_f (hexane/ether = 9/1, UV + $KMnO_4$: 0.49). ^1H NMR (400 MHz, ($CDCl_3$): δ 9.99 (d, *J* = 8.0 Hz, 1H, H-10), 5.88 (d, *J* = 8.0, 1H, H-9), 5.10 – 5.04 (m, 1H, H-4), 2.23 – 2.19 (m, 4H, H-6 and H-5), 2.16 (s, 3H, H-8), 1.68 (s, 3H, H-1 or H-2), 1.60 (s, 3H, H-1 or H-2). The NMR spectroscopic data of the compound **2.17** matched the previously reported data (Kon et al., 2021).

Compound 2.12 ((*E*)-4,8-dimethylnona-1,3,7-triene).

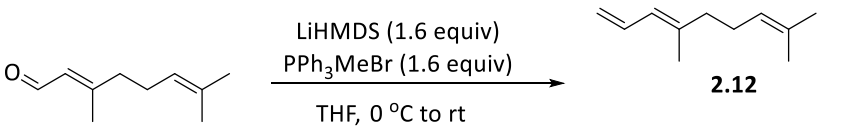

2.17
1 equiv

(84%)
Chemical Formula: $C_{11}H_{18}$
Molecular Weight: 150.2650

A solution of LHMDS (1.0 M in THF, 30 mL, 30 mmol) and PPh_3MeBr (15.50 g, 43.39 mmol) in anhydrous THF (15 mL) was stirred at 0 °C for 1 h. A solution of aldehyde **2.17** (2.20 g, 14.46

mmol) in dry THF (10 mL) was added dropwise. The mixture was stirred at 0 °C for 1 h, warmed to room temperature and quenched by adding NH_4Cl (1.0 M aq., 100 mL). The phase was extracted with Et_2O (4 × 70 mL). The organic layers were combined and washed with brine (50 mL), dried with $MgSO_4$ and concentrated. The residue was purified by column chromatography on silica gel (100% hexane) to yield the title compound as a transparent, yellow oil (1.82 g, 84%).

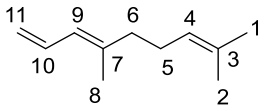

R_f (hexane/ether = 1/1, UV + $KMnO_4$: 0.8). ^1H NMR (400 MHz, $CDCl_3$): δ 6.58 (dt, *J* = 16.5, 10.0 Hz, 1H, H-10), 5.86 (d, J = 10.0 Hz, 1H, H-9), 5.19 – 5.05 (m, 2H, H-11), 4.99 (d, *J* = 10.0 Hz, 1H, H-4), 2.15 – 2.04 (m, 4H, H-5 and H-6), 1.76 (s, 3H, H-8), 1.67 (s, 3H, H-1 or H-2), 1.61 (s, 3H, H-1 or H-2). The NMR spectroscopic data of the compound **2.12** matched the previously reported data (Schwartz et al., 2009).

Compound 2.35 ((*E*)-4,8-dimethylnona-3,7-dien-1-ol).

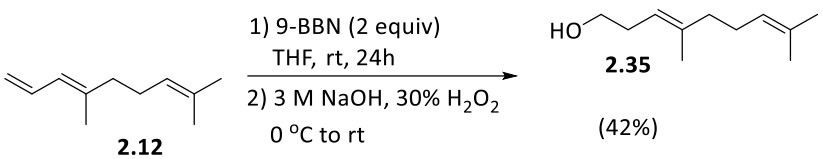

2.12
1 equiv

2.35

(42%)

Chemical Formula: $C_{11}H_{20}O$
Molecular Weight: 168.2800

A dry round bottomed flask under argon was charged with triene **2.12** (3.95 g, 26.3 mmol, 1 equiv) in THF (15 mL). The solution was cooled down to 0 °C and 9–BBN (0.5 M in THF, 53.0 mL, 26.5 mmol, 2 equiv) was added dropwise over 1 h. The reaction mixture was stirred at 0 °C for 5 h, gradually allowed to warm up to the room temperature and stirred overnight. The reaction mixture was cooled down to –10 °C, and a solution of NaOH (3 M aq., 10 mL) was added in one portion, followed by a dropwise addition of H_2O_2 (30%, 10 mL) over 5 min. The reaction mixture was stirred at 0 °C for 2 h and then for 1 h at room temperature. A solution of saturated aq. sodium sulphite was added slowly (30 mL). The organic and aqueous layers were separated, the aqueous layer was extracted with Et_2O (3 × 50 mL), and the combined organic extracts were washed with brine (40 mL), dried with $MgSO_4$ and concentrated to yield a residue which was purified on silica gel (hexane/EA = 4/1) to yield transparent oil (1.89 g, 11.2 mmol, 42%).

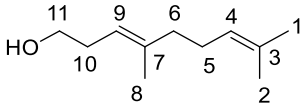

R_f (hexane/EA = 3/1, UV + $KMnO_4$: 0.30). ^{1}H NMR (400 MHz, ($CDCl_3$): δ 5.17 – 5.05 (m, 2H, H-4 and H-9), 3.61 (t, *J* = 6.5 Hz, 2H, H-11), 2.27 (q, *J* = 7.0, 2H, H-10), 2.10 – 2.03 (m, 4H, H-5 and H-6), 1.68 (s, 3H, H-8), 1.64 (s, 3H, H-1 or H-2), 1.60 (s, 3H, H-1 or H-2). The NMR spectroscopic data of the compound **2.35** matched the previously reported data (Blanc and Toste, 2006).

Compound 1.87 ((*E*)-9-iodo-2,6-dimethylnona-2,6-diene).

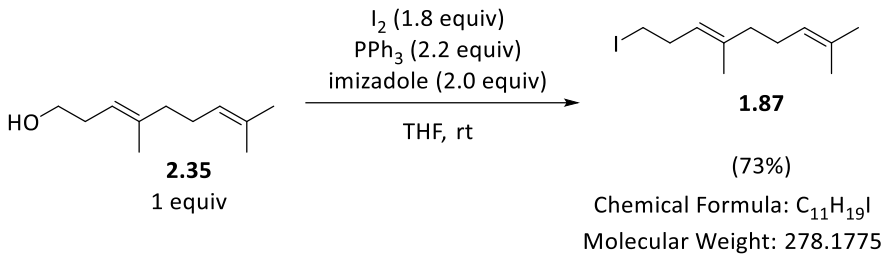

A solution of iodine (1.60 g, 6.30 mmol), PPh_3 (2.01 g, 7.68 mmol) and imidazole (0.475 g, 6.98 mmol) in dry THF (10 mL) was stirred at room temperature for 15, followed by the addition of **2.35** (0.588 g, 3.49 mmol) in THF (5 mL). The reaction mixture was stirred overnight and quenched with saturated aq. sodium bicarbonate. The reaction mixture was extracted with hexane (3 × 20 mL), concentrated and the residue was purified by column chromatography on silica gel (100% hexane) to yield the title compound as a pale-yellow oil (708.9 mg, 73%).

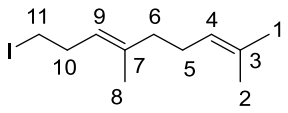

R_f (hexane = 100%, UV + $KMnO_4$: 0.63). ^1H NMR (400 MHz, $CDCl_3$): δ 5.14 – 5.03 (m, 2H, H-4 and H-9), 3.11 (t, J = 7.5 Hz, 2H, H-11), 2.58 (q, *J* = 7.5 Hz, 2H, H-10), 2.13 – 1.97 (m, 4H, H-5 and H-6), 1.68 (s, 3H, H-8), 1.61 (s, 6H, H-1 and H-2). The NMR spectroscopic data of the compound **1.87** matched the previously reported data (Blanc and Toste, 2006).

Compound 2.20 (methyl (*E*)-2-bromo-6-((*tert*-butyldimethylsilyl)oxy)hex-2-enoate).

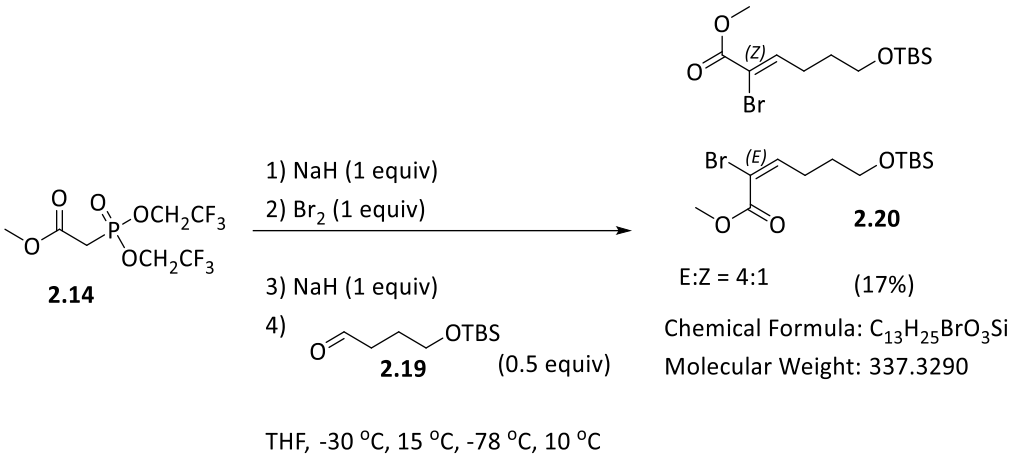

Following a previously published procedure (Qing and Zhang, 2001)**.** Ethyl bis(trifluoroethyl)phosphonoacetate **2.14** (0.578 g, 1.82 mmol, 1 equiv) in an anhydrous THF (1.80 ml) under argon was added dropwise at −30 °C to a slurry of sodium hydride (60% w/w in mineral oil, 77 mg, 2.0 mmol) in anhydrous THF (3.6 mL). After stirring for 30 min at −30 °C, bromine (0.1 mL, 2.0 mmol, 1.1 equiv) in THF (3.6 mL) was added dropwise at −30 °C. The reaction mixture was briefly warmed to 10–15 °C, then cooled to −78 °C and sodium hydride (60% w/w in mineral oil, 70 mg, 1.8 mmol, 1 equiv) was added in a single portion. The reaction mixture was stirred for 30 min at −78 °C, followed by an addition of **2.19** (146 mg, 0.5 equiv, 0.9 mmol, 0.5 equiv) in THF (3.6 ml) was added dropwise to the mixture to maintain the temperature at −78 °C. Stirring continued for 4 h at −78 °C, then overnight at 5 – 10 °C. The reaction was quenched with saturated aqueous NH_4Cl and extracted with ethyl acetate (3 x 10 mL). The combined organic layer was washed with water and brine, dried and concentrated. The residue was purified by column chromatography on silica gel (hexane:ethyl acetate = 4:1) to give the title compound as an oil (52 mg, 0.2 mmol, 17% yield). *E*:*Z* ratio = 8/1.

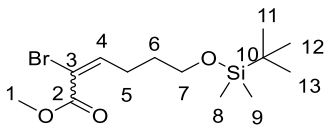

R_f (hexane/EA = 4/1, UV+$KMnO_4$: 0.64). ^{1}H NMR (400 MHz, $CDCl_3$) δ 6.74 (t, *J* = 8.0 Hz, 1H, H-4 (*E*)), 6.68 (t, J = 8.0 Hz, 1H, H-4 (*Z*)), 3.81 (s, 3H, H-1, both), 3.71 (t, *J* = 6.0 Hz, 1H, H-7), 2.58 (m, 2H, H-5, both), 1.67 (m, 2H, H-6, both), 0.91 (s, 9H, H-11, H-12 and H-13 (*Z*)), 0.89 (s, 9H, H-11, H-12 and H-13 (*E*)), 0.10 (s, 6H, H-8 and H-9 (*Z*)), 0.05 (s, 6H, H-8 and H-9 (*E*)); ^{13}C NMR (100 MHz, $CDCl_3$) signals for the major *E* isomer only. δ 163.3 (C2), 149.3 (C4), 110.6 (C3), 62.6 (C7), 52.8 (C1), 31.9 (C5), 28.4 (C6), 26.0 (C10), 25.9 (C11, C12 and C13), –3.4 (C8 or C9), –5.2 (C8 or C9).

HRMS (ESI$^+$): m/z $[M+H]^+$ Calcd. for $C_{13}H_{26}O_3Si$: 337.0829. Found: 337.0828.

Compound 2.22 (methyl (*E*)-2-bromo-6-((triisopropylsilyl)oxy)hex-2-enoate).

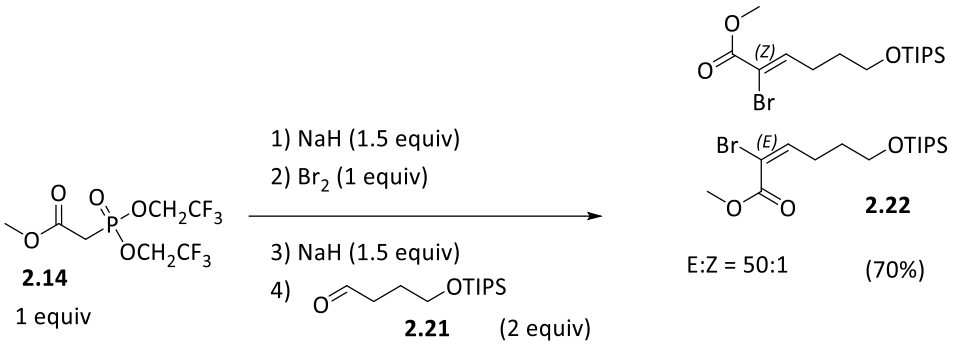

Chemical Formula: $C_{16}H_{31}BrO_3Si$
Molecular Weight: 379.4100

Following a previously published procedure (Qing and Zhang, 2001)**.** To a slurry of sodium hydride (60% w/w in mineral oil, 52 mg, 1.4 mmol, 1.5 equiv) in an anhydrous THF (2.4 mL) was added **2.14** (0.17 mL, 0.8 mmol, 1 equiv) in THF (0.8 ml) dropwise at −30 °C. The solution was stirred for 30 min at −30 °C, followed by a dropwise addition of 1.6 mL of freshly prepared 0.5 M solution of bromine in THF at −30 °C. The reaction mixture became cloudy and dark. The reaction mixture was warmed to 10 – 15 °C for 10 min, then cooled to −78 °C and sodium hydride (60% w/w in mineral oil, 51 mg, 1.3 mmol, 1.5 equiv) was added all at once and stirred for 30 min at −78 °C. Then **2.21** (387 mg, 0.9 mmol, 0.5 equiv) in anhydrous THF (3.6 ml) was added dropwise to maintain the temperature at −78 °C, stirred for 4h at −78 °C and overnight at 5 – 10 °C. After quenching with saturated aq. NH_4Cl solution (15 mL), the organics were extracted with ethyl acetate (3 x 15 mL), washed with brine, dried with $MgSO_4$ and concentrated. The residue was purified by silica gel column chromatography (hexane:ethyl acetate = 20:1) to give the title compound, with a majority of *E* stereoisomer in *E:Z* ratio = 50/1 as an oil (209 mg, 0.6 mmol, 70% yield).

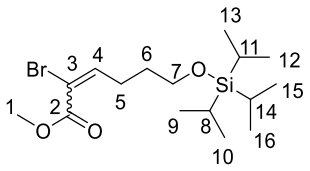

R_f (hexane/EA = 10/1, UV+$KMnO_4$: 0.32).^{1}H NMR (400 MHz, $CDCl_3$) δ 6.76 (t, *J* = 8.0 Hz, 1H, H-4 (*E*)), 3.80 (s, 3H, H-1), 3.71 (t, *J* = 6.0 Hz, 2H, H-7), 2.60 (q, *J* = 8.0Hz, 2H, H-5), 1.74 – 1.64 (m,

2H, H-6), 1.07 – 1.03 (m, 21H, H-8, H-9, H-10, H-11, H-12, H-13, H-14, H-15, H-16); ^{13}C NMR (100 MHz, $CDCl_3$) δ 163.5 (C2), 149.4 (C4), 110.7 (C3), 62.8 (C7), 52.9 (C1), 32.1 (C6), 28.6 (C5), 18.1 (C9, C10, C12, C13, C15 and C16), 12.1 (C8, C11 and C14).

HRMS (ESI^+): m/z $[M+H]^+$ Calcd. for $C_{16}H_{32}{}^{79}BrO_3Si$: 339.1299. Found: 339.1298.

Compound 2.45 (4-(*tert*-butyldimethylsiloxy)-1-butanol).

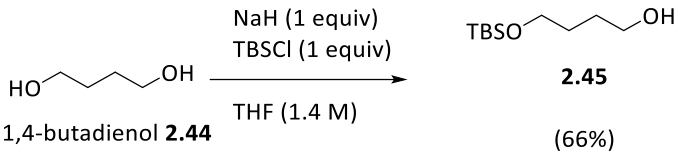

1,4-butadienol **2.44**

2.45

(66%)

Chemical Formula: $C_{10}H_{24}O_2Si$

Molecular Weight: 204.3850

1,4-butadienol **2.44** (1.0 mL, 11.5 mmol, 1.4 equiv) in anhydrous THF (8.0 mL) was treated with NaH (60% w/w in mineral oil, 0.924 g, 8.2 mmol, 1 equiv) and stirred at 0 °C for 30 min. TBSCl (1.24 g, 8.21 mmol, 1 equiv) was added to the suspension and the mixture was stirred for 2h. The reaction was then quenched with saturated aq. NH_4Cl (25 mL), extracted with diethyl ether (3 x 50 mL), washed with brine, dried and concentrated to yield **2.45** as a transparent oil (1.11 g, 5.43 mmol, 66%).

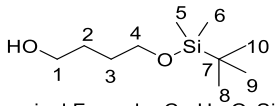

Chemical Formula: $C_{10}H_{24}O_2Si$

Molecular Weight: 204.39

^{1}H NMR (400 MHz, $CDCl_3$) δ 3.69 – 3.64 (m, 4H, H-1 and H-4), 1.73 – 1.62 (m, 4H, H-2 and H-3), 0.89 (s, 9H, H-8, H-9, H-10), 0.06 (s, 6H, H-5 and H-6). The NMR spectroscopic data of the compound **2.45** matched the previously reported data (Throup, Patterson and Sheldrake, 2016).

Compound 2.19 (4-(*tert*-butyldimethylsilanyloxy)butanal).

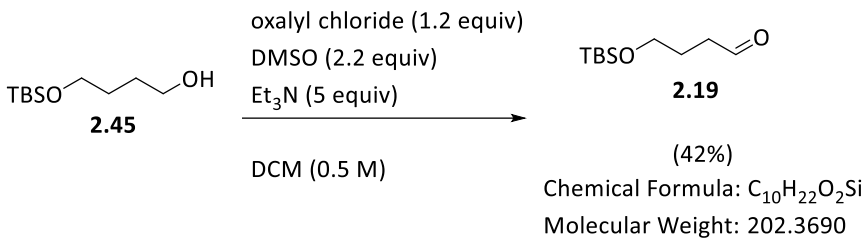

To a solution of oxalyl chloride (0.40 mL, 4.7 mmol, 1.2 equiv) in dry DCM (9 mL), was added DMSO (0.60 mL, 8.6 mmol, 2.2 equiv) at −78 °C and stirred for 30 min. A solution of **2.45** (0.796 g, 3.9 mmol, 1 equiv) in dry DCM (19.5 mL) was added dropwise and stirred for 1 h. Triethylamine was added (2.7 mL, 19.5 mmol, 5 equiv) and stirred for 10 min, quenched with water, extracted with DCM. The product was dried with $MgSO_4$, and concentrated to yield a cloudy, pale, yellow oil that was purified by column chromatography on silica gel (hexane/ethyl acetate = 4/1) to yield the title compound as an oil (332 mg, 1.6 mmol, 42%).

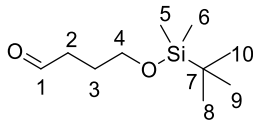

R_f (hexane/EA = 4/1, UV+$KMnO_4$: 0.51). ^{1}H NMR (400 MHz, $CDCl_3$) δ 9.78 (t *J* = 1.5 Hz, 1H, H-1), 3.64 (t, *J* = 6.0 Hz, 2H, H-4), 2.49 (td, *J* = 7.0, 1.5 Hz, 2H, H-2), 1.85 (p, *J* = 7.5 Hz, 2H, H-3), 0.87 (s, 9H, H-8, H-9 and H-10), 0.03 (s, 6H, H-5 and H-6). The NMR spectroscopic data of the compound **2.19** matched the previously reported data (Throup, Patterson and Sheldrake, 2016).

Compound 2.46 (4-[[tris(propan-2-yl)silyl]oxy]butan-1-ol).

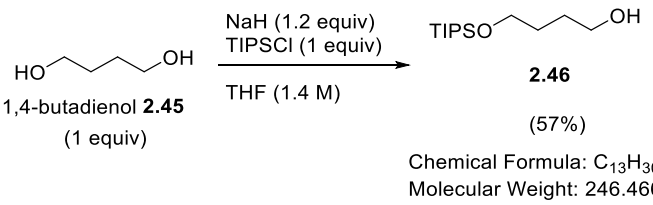

1,4-butadienol **2.45**
(1 equiv)

2.46

(57%)

Chemical Formula: $C_{13}H_{30}O_2Si$
Molecular Weight: 246.4660

At 0 °C, NaH (60% w/w in mineral oil, 0.74 g, 19.3 mmol, 1.2 equiv) was slowly added to a solution of 1,4-butanediol **2.14** (1.3 mL, 15 mmol, 1 equiv) in dry THF (15 mL) under argon. The reaction mixture was allowed to warm up to the room temperature and stirred for 45 min before triisopropyl chloride (1.7 mL, 7.7 mmol) was added. The reaction was stirred overnight and quenched with saturated solution of $NaHCO_3$, extracted with diethyl ether (3 x 30 mL). Organics were combined, dried with $MgSO_4$ and concentrated to afford a thick, transparent oil (2.56 g) which was purified by column chromatography on silica gel (hexane/ethyl acetate = 2/1) to yield the title compound as **2.45** (2.11 g, 8.5 mmol, 57%).

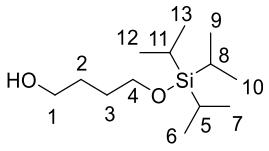

Chemical Formula: $C_{13}H_{30}O_2Si$
Molecular Weight: 246.4660

R_f (hexane/EA = 2/1, UV+$KMnO_4$: 0.38). ^1H NMR (400 MHz, $CDCl_3$) δ 3.74 (t, *J* = 5.5, 2H, H-1), 3.65 (t, *J* = 5.5, 2H, H-4), 1.71 – 1.60 (m, 4H, H-2 and H-3), 1.14 – 1.01 (m, 21H, H-5, H-6, H-7, H-8, H-9, H-10, H-11, H-12 and H-13). The NMR spectroscopic data of the compound **2.46** matched the previously reported data (Dias et al., 2005).

Compound 2.21 (4-triisopropylsilyloxybutanal).

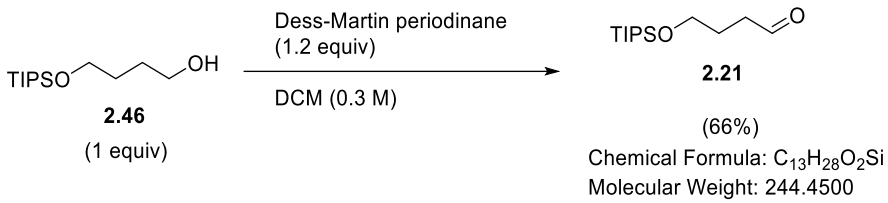

To a solution of alcohol **2.46** (0.697 g, 3.0 mmol, 1 equiv) in dry DCM (10 mL) was added Dess-Martin periodinane (1.550 g, 3.72 mmol, 1.2 equiv) in one portion at 0 °C. The solution was allowed to warm up to the room temperature and stirred overnight. The reaction was quenched with saturated aq. solution of $NaHCO_3$ (5 mL), extracted with DCM (2 x 20 mL), dried and concentrated to yield 0.590 g of oil that was purified by column chromatography on silica gel (hexane/ethyl acetate = 2/1) to yield the title compound as **2.46** (395 mg, 1.62 mmol, 66%).

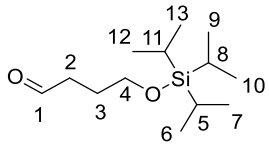

R_f (hexane/EA = 2/1, UV+$KMnO_4$: 0.64). ^{1}H NMR (400 MHz, $CDCl_3$) δ 9.80 (t, *J* = 2.0 Hz, 1H, H-1), 3.73 (t, *J* = 6.0 Hz, 2H, H-4), 2.54 (td, *J* = 7.0, 2.0 Hz, 2H, H-2), 1.94 – 1.84 (m, , 2H, H-3), 1.07 – 1.03 (m, 21H). The NMR spectroscopic data of the compound **2.21** matched the previously reported data (Duchemin et al., 2020).

Compound 2.27 2-(2'-Formylethyl)-1,3-dioxane.

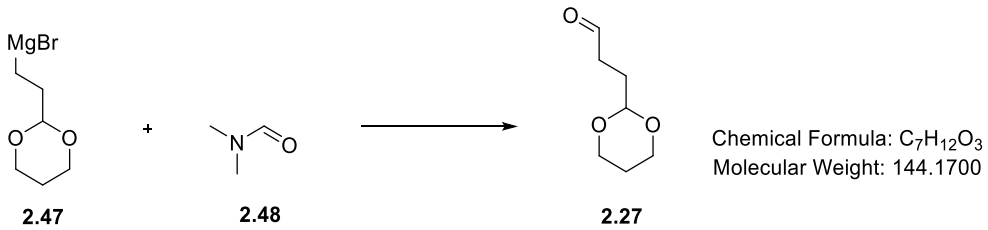

2.47 **2.48** **2.27**

(76%)

To a solution of Grignard reagent **2.47** (10 mL, 0.5 M in THF, 1 equiv) in anhydrous THF (5.5 mL) was added anhydrous DMF **2.48** (0.42 mL, 5.5 mmol, 1.1 equiv) at –78 °C and stirred for 10 min. The reaction mixture was allowed to warm up to the room temperature and stirred for 1.5 h, followed by quenching with 1 M aq. citric acid, extracted with diethyl ether (4 x 10 mL), washed with water (3 x 10 mL) and concentrated which resulted in transparent oil **2.27** (549 mg, 3.81 mmol, 76%) which was used in the following reaction without purification.

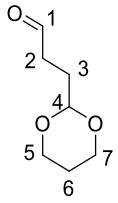

^{1}H NMR (400 MHz, $CDCl_3$) δ_H 9.75 (1H, *J* = 1.5 Hz, H-1), 4.59 (1H, t, *J* = 5.0 Hz, H-4), 4.07 (2H, ddd, *J* = 10.5, 5.0, 1.5 Hz, H-5 or H-7), 3.80 – 3.63 (2H, m, H-5 or H-7), 2.54 (2H, td, *J* = 7.0, 1.5 Hz, H-2), 2.15 – 1.96 (1H, m, H-6a), 1.99 – 1.88 (2H, m, H-3), 1.36 – 1.29 (1H, m, H-6b). The NMR spectroscopic data of the compound **2.27** matched the previously reported data (Fuchs and Paquette, 1994).

Compound 2.28 Methyl (*E*)-2-bromo-5-(1,3-dioxan-2-yl)pent-2-enoate.

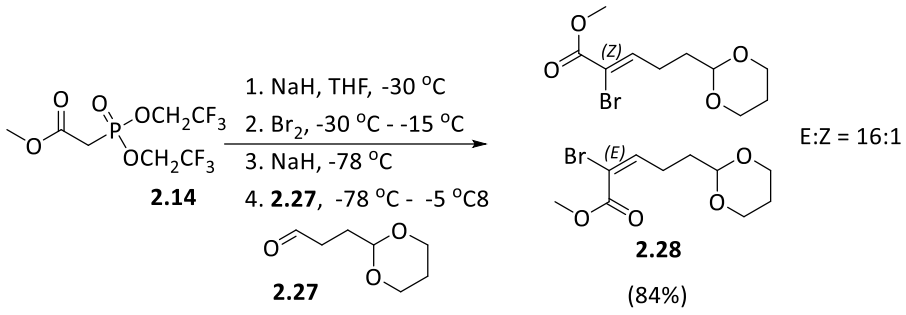

Chemical Formula: $C_{10}H_{15}BrO_4$
Molecular Weight: 279.1300

Following a previously published procedure (Qing and Zhang, 2001)**.** To a slurry of sodium hydride (60% w/w in mineral oil, 152 mg, 3.96 mmol, 1.5 equiv) in anhydrous THF (7.6 mL) was added Still-Gennari reagent **2.14** (0.540 mL, 2.53 mmol, 1 equiv) in THF (2.5 mL) dropwise at −30 °C. The solution was stirred for 30 min at −30 °C, followed by dropwise addition of bromine (0.140 mL, 2.71 mmol, 1.1 equiv) in THF (5.4 mL) at −30 °C. The reaction mixture was warmed briefly at 10 – 15 °C, then cooled to −78 °C and sodium hydride (60% w/w in mineral oil, 175 mg, 4.55 mmol, 1.8 equiv) was added in one portion and stirred for 30 min at −78 °C. A solution of aldehyde **2.27** (548 mg, 3.8 mmol, 1.5 equiv) in anhydrous THF (15.2 mL) was added dropwise to the mixture at −78 °C and stirred for 4 h at −78 °C, followed by stirring overnight at 5 – 10 °C. The reaction mixture was quenched with saturated aq. NH_4Cl solution (20 mL) and organics were extracted with ethyl acetate (3 x 30 mL). The combined organic layer was washed with brine, dried with $MgSO_4$ and concentrated. The residue was purified by column chromatography on silica gel (hexane:ethyl acetate = 4:1) to give the title compound **2.28** as a mixture of *E*:*Z* isomers in 16:1 ratio as a viscous pale yellow oil (589 mg, 2.1 mmol, 84% yield).

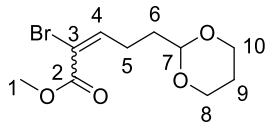

Note ^{13}C NMR data reported only for the major *E* isomer.

R_f (hexane/EA = 4/1, UV+$KMnO_4$: 0.35). ^{1}H NMR (300 MHz, $CDCl_3$) δ_H 7.31 (1H, d, *J* = 7.0 Hz, H-4 (*Z*)), 6.70 (1H, t, *J* = 8.0 Hz, H-4 (*E*)), 4.53 (1H, t, *J* = 5.5 Hz, H-7, both), 4.13 – 4.03 (2H, m, H-8 or H-10, both), 3.82 (3H, s, H-1, (*Z*)), 3.81 (3H, s, H-1, (*E*)), 3.80 – 3.67 (2H, m, H-8 or H-10, both), 2.59 (2H, q, *J* = 7.5, H-5 or H-6, both), 2.13 – 1.97 (1H, m, H-9a, both), 1.74 (2H, td, *J* = 7.5, 5.5 Hz, H-5 or H-6), 1.39 – 1.27 (1H, m, H-9b); ^{13}C NMR (100 MHz, $CDCl_3$) δ_C 163.4 (C2), 148.4 (C4), 111.0 (C3), 101.3 (C7), 66.9 (C8 and C9), 52.9 (C1), 33.9 (C5 or C6), 26.2 (C5 or C6), 25.8 (C9).

HRMS (ESI$^+$): m/z $[M+H]^+$ Calcd. for $C_{16}H_{32}{}^{79}BrO_3Si$: 301.0046. Found: 301.0048 (error –0.5 ppm).

IR (thin film) ν_{max} 3050, 2928, 1709, 1451, 1367, 1250, 1125, 1152, 1125, 1063, 849.6 cm^{-1};

Compound 2.29 Methyl (*E*)-2-bromo-6-oxohex-2-enoate.

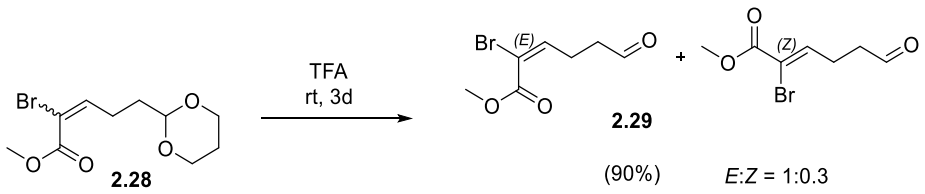

Chemical Formula: $C_7H_9BrO_3$
Molecular Weight: 221.0500

To the vinyl bromide **2.28** (30 mg, 0.100 mmol) was added TFA (1.0 mL) and the reaction mixture was stirred at room temperature for 72 h. Afterwards, the reaction mixture was concentrated *in vacuo* to yield reddish/brown oil and the crude product was purified by column chromatography on silica gel (hexane:acetone = 10/1) to yield pale yellow viscous oil as a title compound **2.29** (18 mg, 0.08 mmol, 80%) as two stereoisomers in 1:0.3 *E*:*Z* ratio.

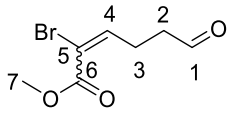

^{1}H NMR (300 MHz, $CDCl_3$) δ_H 9.80 (1H, s, H-1, (*Z*)), 9.77 (1H, s, H-1, (*E*)), 7.29 (t, *J* = 7.0 Hz, H-4, (*Z*)), 6.70 (t, *J* = 8.0 Hz, H-4, (*E*)), 3.80 (3H, s, H-7, (*Z*) and(*E*)), 2.83 – 2.74 (2H, m, H-2 or H-3, (*Z*) and (*E*)), 2.73 – 2.56 (2H, m, H-2 or H-3, (*Z*) and (*E*)); ^{13}C NMR (100 MHz, $CDCl_3$) δ_C 200.5 (C1, (*E*)), 200.2 (C1, (*Z*)), 163.2 (C6, (*E*)), 162.8 (C6, (*Z*)), 146.6 (C4, (*E*)), 144.0 (C4, (*Z*)), 117.3 (C5, (*Z*)), 112.2 (C5, (*E*)), 53.4 (C7, (*Z*)), 53.1 (C7, (*E*)), 42.4 (C2, (*E*)), 41.4 (C2, (*Z*)), 24.7 (C3, (*Z*)), 24.1 (C3, (*E*)).

HRMS (ESI): m/z $[M+Na]^+$ Calcd. $C_7H_9{}^{79}BrNaO_3$: 242.9627. Found: 242.9612 (4.5 ppm error).

Compound 2.50 (diethyl (*E*)-2-(4,8-dimethylnona-3,7-dien-1-yl)malonate).

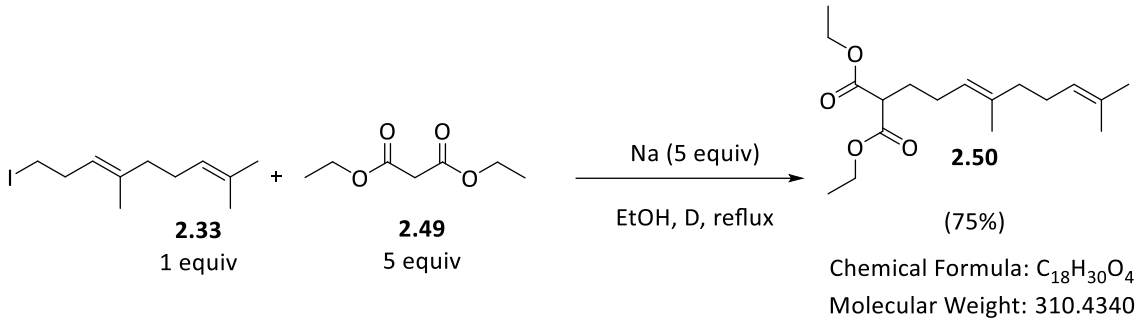

A dry round bottom flask was charged with dry EtOH (20 mL) and sodium metal (0.54 g, 23.7 mmol) was added carefully, and then stirred for 2 h. Diethyl malonate **2.49** (6.1 mL, 40.2 mmol) was then added dropwise to the sodium ethoxide solution, and the reaction mixture was stirred as 50 °C for 30 min. A solution of **1.87** (2.24 g, 8.04 mmol) in dry EtOH (5 mL) was then added dropwise and stirred under reflux for 2.5 h. The solvent was then evaporated, and water (5 mL) was added, followed by acidifying the reaction mixture with 1 M aq. HCl. The organics were extracted with ethyl acetate (3 x 50 mL), dried with $MgSO_4$ and concentrated to a brown oil. Purified on silica gel (hexane/EA = 9/1) to yield a pale-yellow oil **2.50** (1.882 g, 75%).

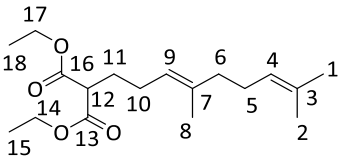

R_f (hexane/EA = 9/1, $KMnO_4$: 0.47). ^1H NMR (400 MHz, $CDCl_3$) δ_H 5.13 – 5.04 (m, 2H, H-4 and H-9), 4.20 – 4.11 (m, 4H, H-14 and H-17), 3.34 (t, *J* = 7.0 Hz, 1H, H-12), 2.12 – 1.90 (m, 8H, H-5, H-6, H-10 and H-11), 1.68 (s, 3H, H-8), 1.60 (s, 3H, H-1 or H-2), 1.57 (s, 3H, H-1 or H-2), 1.27 (t, *J* = 7.0 Hz, 6H, H-15 and H-18)); ^{13}C NMR (100 MHz, $CDCl_3$) δ_C 169.7 (C13 and C16), 136.9 (C3), 131.5 (C7), 124.3 (C4 or C9), 122.7 (C4 or C9), 61.4 (C14 and C17), 51.4 (C12), 39.8 (C11), 28.9 (C10), 26.6 (C6), 25.8 (C8), 25.6 (C5), 17.8 (C1 or C2), 16.0 (C1 or C2), 14.2 (C15 and C18).

HRMS (ESI$^+$): m/z $[M+Na]^+$ Calcd. for $C_{18}H_{30}NaO_4$: 333.2036. Found: 333.2034.

IR (thin film) ν_{max} 2980, 2929, 1749, 1731, 1446, 1369, 1301, 1226, 1249, 1176, 1145, 1095, 1028, 861, 589 cm^{-1}.

Compound 2.39 (Ethyl (*E*)-6,10-dimethylundeca-5,9-dienoate).

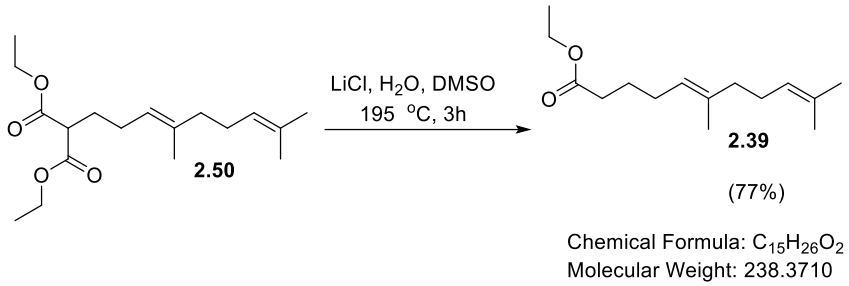

A mixture of the malonate **2.50** (1024 mg, 3.3 mmol, 1 equiv), LiCl (422 mg, 9.9 mmol, 3 equiv), H_2O (60 µL, 3 equiv) and DMSO (6.6 mL) was stirred at reflux for 3 h, followed by quenching with sat. solution of NH_4Cl (20 mL). The organics were extracted with diethyl ether (3 x 15 mL), washed with brine (10 mL), dried with $MgSO_4$, filtered, and concentrated to yield pale yellow oil **2.39** (605 mg, 2.54 mmol, 74%) which was used in the next reaction without additional purification.

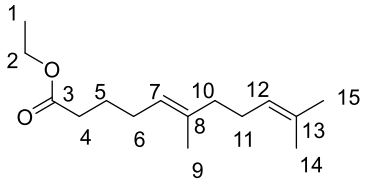

R_f (hexane/ethyl acetate = 1/1, UV + $KMnO_4$: 0.75). ^{1}H NMR (400 MHz, $CDCl_3$) δ_H 5.14 – 5.04 (m, 2H, H-7 and H-12), 4.12 (q, *J* = 7.0 Hz, 2H, H-2), 2.28 (t, *J* = 7.5 Hz, 2H, H-4), 2.14 – 1.90 (m, 6H, H-6, H-10, H-11), 1.72 – 1.64 (m, 2H, H-5, overlap), 1.68 (s, 3H, H-9), 1.59 (s, 3H, H-14 or H-15), 1.57 (s, 3H, H-14 or H-15), 1.25 (t, *J* = 7.0 Hz, 3H, H-1); ^{13}C NMR (100 MHz, $CDCl_3$): δ_C 174.1 (C3), 136.2 (C8 or C23), 131.5 (C8 or C13), 124.4 (C7 or C12), 123.6 (C7 or C12), 60.3 (C2), 40.0 (C6), 33.9 (C4), 27.3 (C10 or C11), 26.8 (C10 or C11), 25.8 (C9), 25.2 (C4), 17.8 (C14), 16.1 (C15), 14.4 (C1).

HRMS (ESI$^+$): m/z $[M+Na]^+$ Calcd. for $C_{15}H_{26}NaO_2$: 261.1825. Found: 261.1828 (mean error 1.7 ppm)

Compound 2.51 (ethyl (*E*)-2-(3-(1,3-dioxan-2-yl)-1-hydroxypropyl)-6,10-dimethylundeca-5,9-dienoate).

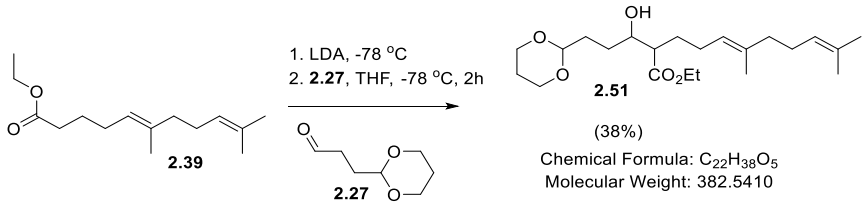

To a solution of diisopropylamine (0.14 mL, 1.0 mmol, 1.1 equiv) in 1 mL of THF at 0 °C was added 2.5 M n-butyllithium solution (0.40 mL, 1.01 mmol, 1.1 equiv). After 20 min, the solution was cooled to –78 °C, a solution of ester **2.39** (220 mg, 0.92 mmol, 1 equiv) in THF (1.5 mL) was added dropwise. The solution was stirred at –78 °C for 50 min, followed by treatment with a solution of aldehyde **2.27** (200 mg, 1.38 mmol, 1.5 equiv) in THF (1 mL) at –78 °C and stirred for further 2h at –78 °C. The reaction mixture was quenched with sat. aq. solution of NH_4Cl (20 mL), organics were extracted with diethyl ether (3 x 15 mL), washed with brine, dried with $MgSO_4$, filtered, and concentrated to yield pale yellow oil (309 mg) which was purified by column chromatography on silica gel (gradient elution with 10:1, 2:1, 1:1 hexane:ethyl acetate) to provide recovered ester **2.39** (136 mg), followed by the desired hydroxy ester **2.51** (133 mg, 0.35 mmol, 38%).

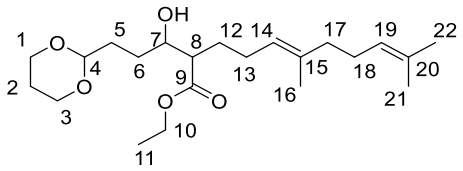

R_f (hexane/ethyl acetate = 1/1, UV + $KMnO_4$: 0.31). ^1H NMR (400 MHz, $CDCl_3$) δ 5.12 – 5.02 (m, 2H, H-14 and H-19), 4.55 (t, *J* = 5.0 Hz, 1H, H-4) 4.21 – 4.11 (m, 2H, H-10), 4.08 (dd, *J* = 12.0, 5.0, 2H, H-1a and 3a), 3.80 – 3.68 (m, 3H, H-1b, H-3b and H-8), 2.46 – 2.36 (m, 1H, H-7), 2.07 – 1.92 (m, 6H, H-12, H-13, H-17 and H-18), 1.84 – 1.66 (m, 2H, H-6), 1.65 (s, 3H, H-16), 1.58 (s, 3H, H-21), 1.56 (s, 3H, H-22), 1.34 – 1.29 (m, 1H, H-2b), 1.28 – 1.22 (m, 2H, H-11); ^{13}C NMR (100 MHz, ($CDCl_3$): δ 175.3 (C9), 136.3 (C15 or C20), 131.5 (C15 or C20), 124.4 (C14 or C19), 123.4 (C14 or C19), 102.1 (C4), 72.3 (C8), 67.0 (C1 and C3), 60.5 (C10), 51.1 (C7), 39.8

(C12), 31.8 (C5 or C6), 31.6 (C5 or C6), 26.8 (C17), 26.1 (C13), 25.9 (C18), 25.8 (C16), 25.7 (C2), 17.8 (C21), 16.1 (C22), 14.4 (C11).

HRMS (ESI$^+$): m/z [M+Na]$^+$ Calcd. for $C_{36}H_{58}NaO_4$: 577.4227. Found: 577.4224 (mean error 2.3 ppm)

IR (thin film) ν_{max} 3667 (broad), 2929, 2855, 1729, 1449, 1377, 1145, 1095, 1001 cm^{-1};

Compound 2.52 (ethyl (5E)-2-(3-(1,3-dioxan-2-yl)propylidene)-6,10-dimethylundeca-5,9-dienoate).

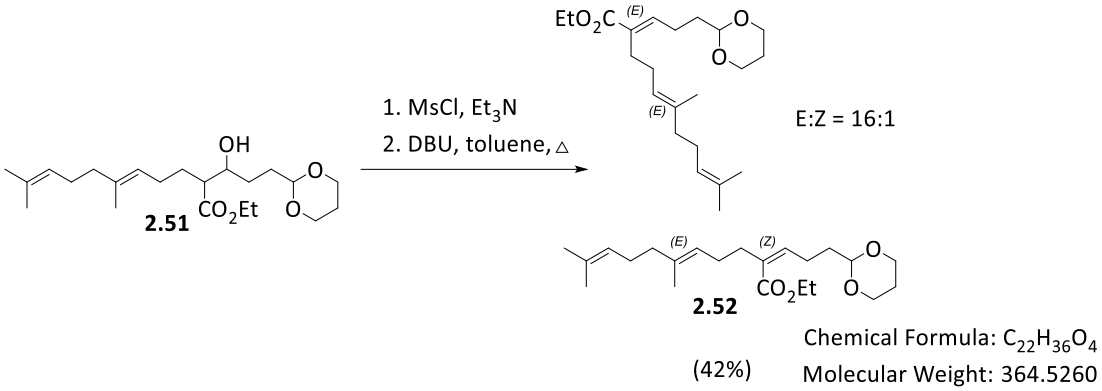

To a 0 °C solution of hydroxy ester **2.51** (100 mg, 0.26 mmol, 1 equiv) and triethylamine (0.15 mL, 1.09 mmol, 4 equiv) in CH_2Cl_2 (1 mL) was added methanesulfonyl chloride (40 µL, 0.52 mmol, 2 equiv). The ice bath was removed, and the solution was allowed to stir at room temperature for 3 h. After dilution with 20 mL of CH_2Cl_2, the solution was washed with aqueous $NaHCO_3$ (2 x 10 mL), 0.1 M HCl (10 mL), and brine (10 mL). The aqueous phases were extracted once with CH_2Cl_2 (15 mL) and the combined organic phases were dried over $MgSO_4$, filtered and concentrated to provide a pale brown oil, which was taken up in 8 mL of toluene, treated with 1,8-Diazabicyclo[5.4.0]undec-7-ene (DBU) (0.2 mL, 0.8 mmol, 3 equiv). The reaction mixture was stirred at 80 °C overnight after which it was cooled to room temperature, the solution was diluted with ether (20 mL), washed with 0.1 M aq. HCl (2 x 10 mL), sat. aq. $NaHCO_3$ (10 mL), and brine (10 mL), and dried over $MgSO_4$, filtered and concentrated to yield pale brown oil (117 mg) which was purified by silica gel chromatography (hexane:ethyl acetate = 30:1) to yield colourless oil **2.52** (40 mg, 0.11 mmol, 42%) in *E*:*Z* = 16:1 ratio.

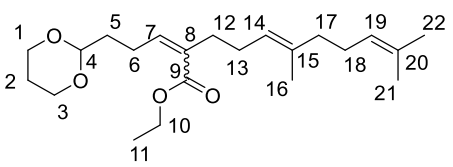

R_f (hexane/ethyl acetate = 5/1, UV + $KMnO_4$: 0.32). ^{1}H NMR (400 MHz, $CDCl_3$) δ 6.72 (t, *J* = 7.5 Hz, 1H, H-7, (*E*)), 5.84 (t, *J* = 7.5 Hz, 1H, H-7, (*Z*)), 5.20 – 5.02 (m, 2H, H-14 and H-19), 4.51 (t, *J*

= 5.0 Hz, 1H, H-4), 4.18 (q, *J* = 7.0 Hz, 2H, H-10), 4.14 – 4.05 (m, 2H, H-1a and 3a), 3.81 – 3.69 (m, 2H, H-1b and H-3b), 2.39 – 2.21 (m, 4H, H-5 and H-6), 2.12 – 2.00 (m, 4H, H-17 and H-18), 2.00 – 1.88 (m, 2H, H-12), 1.76 – 1.69 (m, 2H, H-13), 1.68 (s, 3H, H-16), 1.60 (s, 3H, H-21), 1.59 (s, 3H, H-22), 1.37 – 1.33 (m, 1H, H-2a), 1.29 (t, *J* = 7.0 Hz, 3H, H-11), 1.26 – 1.23 (m, 1H, H-2b); ^{13}C NMR (100 MHz, $CDCl_3$): δ 168.1 (C9), 141.7 (C8), 135.9 (C20 or C15), 132.8 (C20 or C15), 131.5 (C7), 124.5 (C14 or C19), 123.6 (C14 or C19), 101.4 (C4), 67.0 (C1 and C3), 60.5 (C10), 39.8 (C12), 34.2 (C13), 27.8 (C17 or C18), 27.0 (C17 or C18), 26.8 (C5), 25.9 (C2), 25.8 (C16), 23.2 (C6), 17.8 (C21), 16.1 (C22), 14.4 (C11).

HRMS (ESI$^+$): m/z $[M+Na]^+$ Calcd. for $C_{22}H_{36}NaO_4$: 387.2506. Found: 387.2512. (error -1.8 ppm)

IR (thin film) ν_{max} 2933, 2860, 1710, 1453, 1375, 1271, 1140 cm^{-1};

Compound 2.54 (*tert*-butyl (*E*)-2-(*tert*-butyl)-6,10-dimethylundeca-5,9-dienoate).

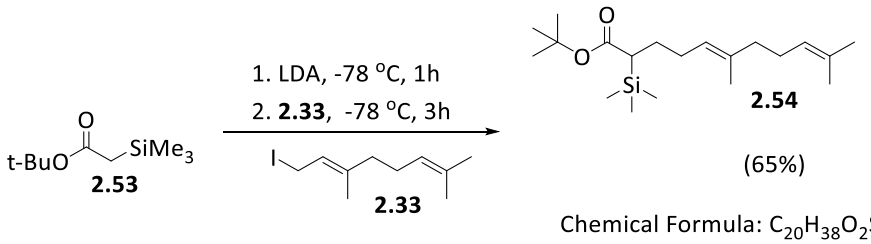

Chemical Formula: $C_{20}H_{38}O_2Si$
Molecular Weight: 338.6070

To a solution of diisopropylamine (1.70 mL, 11.9 mmol, 1.2 equiv) in THF (20 mL) at 0 °C was added 2.5 M n-butyllithium solution (4.8 mL, 11.9 mmol, 1.2 equiv). After 20 min, the solution was cooled to –78 °C, and *tert*-butyl(trimethylsilyl)acetate **2.53** (1.87 g, 9.93 mmol, 1 equiv) in THF (10 mL) was added dropwise and the reaction mixture was stirred at –78 °C for 1 h. Then, a solution of homo geranyl iodide **1.87** (2.76 g, 9.93 mmol, 1 equiv) in THF (15 mL) was added dropwise and the resulting mixture was stirred for 3 h. The mixture was then warmed to room temperature and stirring continued for 16 h. The crude solution was poured into 100 mL of brine, extracted with CH_2Cl_2 (3 x 50 mL), dried with $MgSO_4$, filtered and concentrated to yield pale brown oil (3.85 g) which was purified by column chromatography on silica gel (hexane:ethyl acetate = 100:1), unreacted homo geranyl iodide **1.87** was recovered (950 mg), and the desired product **2.54** (2.200 g, 6.50 mmol, 65%) as pale yellow oil.

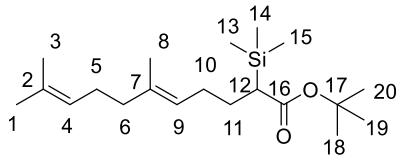

^{1}H NMR (400 MHz, ($CDCl_3$): δ 5.13 – 5.05 (m, 2H, H-4 and H-9), 2.12 – 1.74 (m, 7H, H-5, H-6, H-10, H-12), 1.68 (s, 3H, H-8), 1.60 (s, 3H, H-1 or H-2), 1.59 (s, 3H, H-1 or H-2), 1.44 (s, 9H, H-18, H-19, H-20), 1.38 – 1.22 (m, 2H, H-11), 0.06 (s, 9H, H-13, H-14, H-15). The NMR spectroscopic data of the compound **2.54** matched the previously reported data (Heathcock et al., 1992b).

Compound 2.37 (*tert*-butyl (5*E*)-2-(4,4-dimethoxybutylidene)-6,10-dimethylundeca-5,9-dienoate).

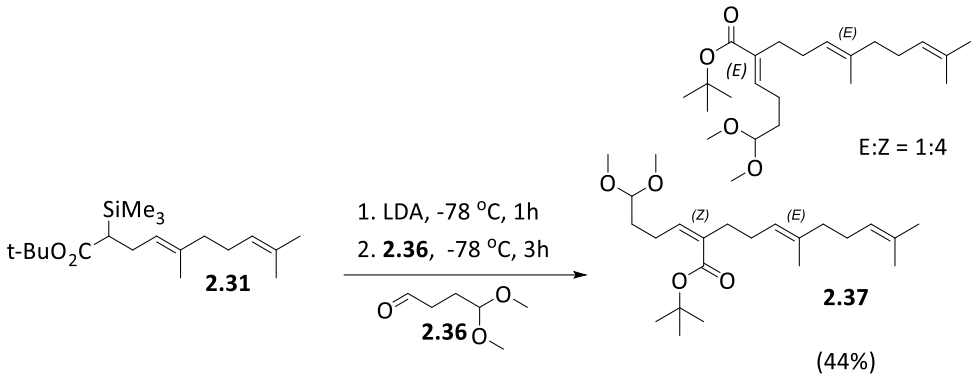

Chemical Formula: $C_{23}H_{40}O_4$
Molecular Weight: 380.5690

To a solution of diisopropylamine (0.37 mL, 2.62 mmol, 1.2 equiv) in THF (3 mL) at 0 °C was added 2.5 M n-butyllithium solution (1.1 mL, 2.75 mmol, 1.2 equiv). After 20 min, the solution was cooled to -78 °C, and a solution of **2.31** (740 mg, 2.18 mmol, 1 equiv) in THF (4 mL) was added dropwise, followed by stirring for 1 h -78 °C. The aldehyde **2.36** (350 mg, 2.65 mmol, 1.2 equiv) in THF (6 mL) was added dropwise and stirred at -78 °C for 30 min and at 0 °C for additional 30 min. The reaction mixture was quenched with sat. solution of NH_4Cl (30 mL), extracted with CH_2Cl_2 (3 x 20 mL), dried with $MgSO_4$, filtered and concentrated to afford yellow oil (1.14 g) which was purified by column chromatography on silica gel (hexane:ethyl acetate = 100:1), unreacted **31** was recovered (240 mg), and the desired product **2.37** (370 mg, 0.97 mmol, 44%) as pale yellow oil in *E*:*Z* = 1:4 ratio.

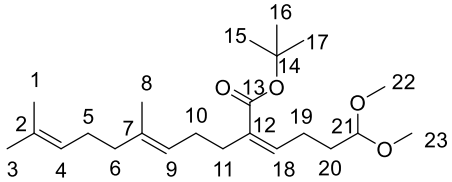

R_f (hexane/ethyl acetate = 4/1, UV + $KMnO_4$: 0.64). ^1H NMR (400 MHz, ($CDCl_3$): δ 6.63 (t, *J* = 7.5 Hz, 1H, H-18, (*E*)), 5.72 (t, *J* = 7.5 Hz, 1H, H-18 (*Z*)), 5.15 – 5.05 (m, 2H, H-4 and H-9), 4.36 (t, *J* = 6.0 Hz, 1H, H-21), 3.32 (6H, s, H-22 and H-23, (*E*)), 3.31 (6H, s, H-22 and H-23, (*Z*)), 2.46 – 2.36 (m, 2H, H-19), 2.26 – 1.89 (m, 8H, H-5, H-6, H-10, H-11) 1.76 – 1.70 (m, 2H, H-20), 1.68

(s, 3H, H-8), 1.60 (s, 6H, H-22 and H-23, (*Z*)), 1.58 (s, 6H, H-22 and H-23, (*E*)), 1.50 (s, 9H, H-15, H-16 and H-17, (*Z*)), 1.49 (s, 9H, H-15, H-16 and H-17, (*E*)); ^{13}C NMR (100 MHz, ($CDCl_3$): δ 167.7 (C13), 138.4 (C18), 135.8 (C12), 134.1 (C7), 131.5 (C2), 124.5 (C9 or C4), 123.6 (C9 or C4), 104.3 (C21), 80.6 (14), 52.9 (C22 and C23), 39.9 (C11), 35.1 (C6), 32.5 (C20), 28.4 (C15, C16 and C17), 27.7 (C10), 26.9 (C5), 25.8 (C8), 25.0 (C19), 17.8 (C1 or C3), 16.1 (C1 or C3).

HRMS (ESI^+): m/z $[M+Na]^+$ Calcd. for $C_{23}H_{40}NaO_4$: 403.2819. Found: 403.2824. (error –1.4 ppm)

IR (thin film) ν_{max} 2967, 2929, 2859, 2833, 1710, 1451, 1367, 1251, 1153, 1126, 1065, 849 cm^{-1};

Compound 2.38 (*tert*-butyl (2*Z*,5*E*)-6,10-dimethyl-2-(4-oxobutylidene)undeca-5,9-dienoate).

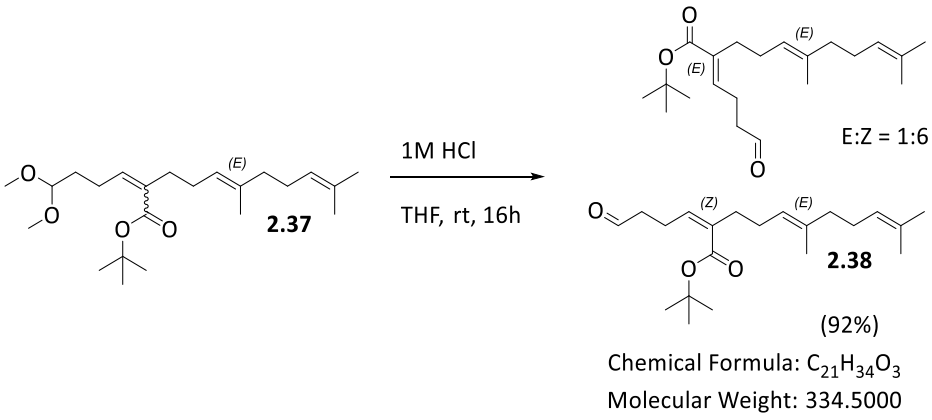

A solution of **2.37** (360 mg, 0.94 mmol, 1 equiv), THF (4.70 mL) and 1 M HCl (4.70 mL, 5 equiv) was stirred together at room temperature for 16 h. The was then poured into brine (20 mL) and extracted with CH_2Cl_2 (3 x 20 mL), dried with $MgSO_4$, filtered and concentrated to yield **2.38** as pale yellow oil (290 mg, 0.87 mmol, 92%) *E*:*Z* = 1:4 ratio and used in the next reaction without further purification.

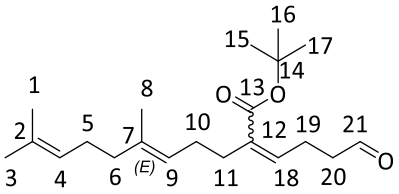

Note, NMR data for the major stereoisomer only is reported.

R_f (hexane/ethyl acetate = 10/1, UV + $KMnO_4$: 0.34). ^{1}H NMR (400 MHz, ($CDCl_3$): δ 9.78 (d, *J* = 9.0 Hz, 1H, H-21), 6.57 (t, *J* = 7.5 Hz, 1H, (*E*)), 5.74 (t, *J* = 7.5 Hz, 1H, (*Z*)), 5.12 – 5.04 (m, 2H, H-4, H-9), 2.72 – 2.63 (m, 2H, H-19 or H-20), 2.60 – 2.52 (m, 2H, H-19 or H-20), 2.24 – 2.17 (m, 2H, H-11 or H-6), 2.12 – 2.01 (m, 4H, H-5 and H-10), 2.00 – 1.93 (m, 2H, H-11 or H-6), 1.67 (s, 3H, H-8), 1.59 (s, 3H, H-1 or H-3), 1.58 (s, 3H, H-1 or H-3), 1.50 (s, 9H, H-15, H-16 and H-17); ^{13}C NMR (100 MHz, ($CDCl_3$): δ 202.0 (C21), 167.4 (C13), 136.9 (C18), 135.9 (C12), 135.1 (C7), 131.5 (C2), 124.4 (C4 or C9), 123.4 (C4 or C9), 80.9 (C14), 43.7 (C20), 39.8 (C6), 35.0 (C10),

28.4 (C15, C16 and C17), 27.6 (C5), 26.9 (C10), 25.8 (C8), 22.4 (C19), 17.9 (C1 or C3), 16.2 (C1 or C3).

HRMS (ESI^+): m/z $[M+Na]^+$ Calcd. for $C_{21}H_{34}NaO_3$: 357.2400. Found: 357.2401. (mean error – 1.9 ppm)

Compound 2.42 (1-(*tert*-butyl) 8-ethyl 2,7-bis((*E*)-4,8-dimethylnona-3,7-dien-1-yl)-6-hydroxyoct-2-enedioate).

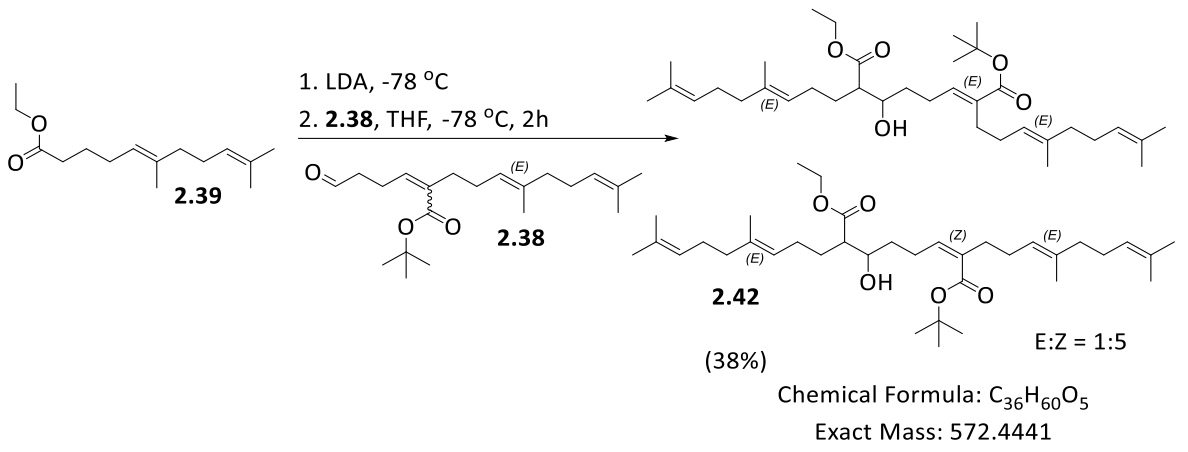

To a solution of diisopropylamine (0.13 mL, 0.87 mmol, 1.2 equiv) in THF (1 mL) at 0 °C was added 2.5 M n-butyllithium solution (0.35 mL, 0.87 mmol, 1.2 equiv). After 20 min, the solution was cooled to –78 °C, and a solution of **2.39** (175 mg, 0.72 mmol, 1 equiv) in THF (1 mL) was added dropwise and the reaction mixture was stirred at –78 °C for 1 h. The aldehyde **2.38** (290 mg, 0.87 mmol, 1.2 equiv) in THF (1 mL) was added dropwise and stirred at –78 °C for 30 min, followed by stirring at 0 °C for additional 30 min. The reaction mixture was quenched with sat. solution of NH_4Cl (15 mL), extracted with CH_2Cl_2 (3 x 15 mL), dried with $MgSO_4$, filtered and concentrated to give yellow oil which was purified by column chromatography on silica gel (hexane:ethyl acetate = 100:1), to yield product **2.42** (160 mg, 0.27 mmol, 38%) as pale yellow oil in *E*:*Z* = 1:5 ratio.

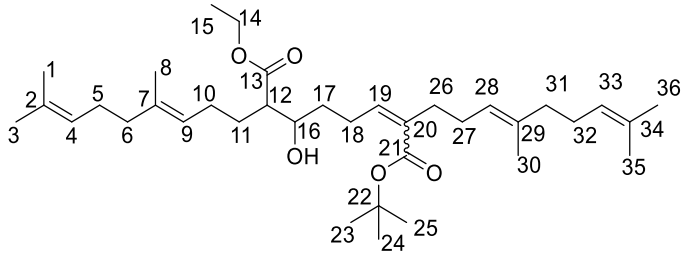

R_f (hexane/ethyl acetate = 6/1, UV + $KMnO_4$: 0.33). ^1H NMR (400 MHz, ($CDCl_3$): δ 6.62 (t, *J* = 7.5 Hz, 1H, H-19 (*E*)), 5.72 (t, *J* = 7.5 1H, H-19 (*Z*)), 5.15 – 5.04 (m, 4H, H-4, H-9, H-28 and H-33 (*Z*), 4.91 – 4.81 (m, 4H, H-4, H-9, H-28 and H-33 (*E*), 4.27 – 4.22 (m, 2H, H-14 (*E*), 4.18 (q, *J* =

7.0 Hz, 2H, H-14 (*Z*), 3.85 – 3.60 (m, 1H, H-12 (*Z*)), 2.64 – 2.51 (m, 1H, H-16 (*Z*)), 2.48 – 1.72 (m, 12H, H-5, H-6, H-10, H-11, H-17, H-18), 1.67 (s, 6H, H-8 and H-30), 1.59 (s, 9H, H-23, H-24 and H-25), 1.49 (s, 12H, H-1, H-3, H-35 and H-36), 1.27 (t, *J* = 6.5 Hz, 3H, H-15); ^{13}C NMR (100 MHz, ($CDCl_3$): δ 175.8 (C21), 167.2 (C13), 138.4 (C19), 134.7 (C20), 131.5 (C2 and C34), 124.4 (C7 and C29), 123.5 (C4 and C33), 80.1 (C22), 71.4 (C12), 60.5 (C14), 51.1 (C16), 39.8 (C11), 35.2 (C17 and C18), 28.4 (C23, C24, C25), 28.3 (C5, C26, C27 and C32), 27.7 (C10), 27.9 (C31), 27.8 (C6), 25.8 (C8 and C30), 17.8 (C1 and C35), 16.1 (C3 and C36), 14.5 (C15).

HRMS (ESI$^+$): m/z $[M+Na]^+$ Calcd. for $C_{36}H_{60}NaO_5$: 595.4333. Found: 595.4340 (mean error –1.3 ppm)

IR (thin film) ν_{max} cm^{-1}; 3380 (br), 2968, 2951, 2926, 1709.

Compound 2.43 (1-(*tert*-butyl) 8-ethyl 2,7-bis((*E*)-4,8-dimethylnona-3,7-dien-1-yl)octa-2,6-dienedioate).

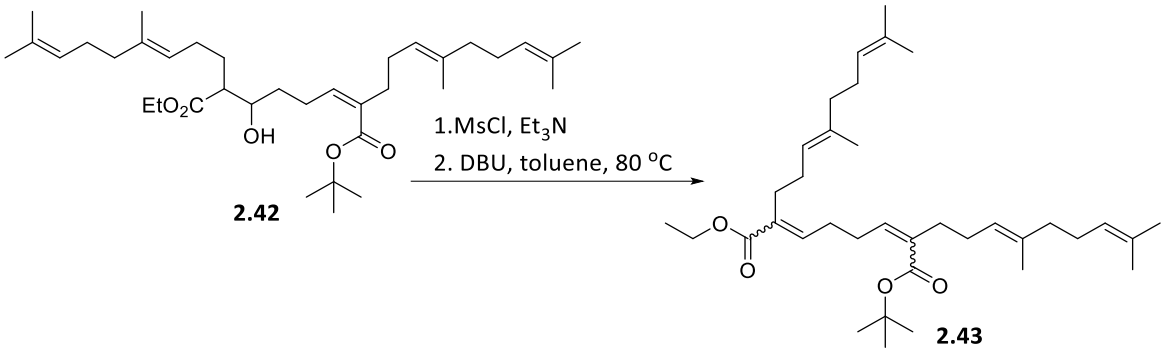

(70%)
Chemical Formula: $C_{36}H_{58}O_4$
Molecular Weight: 554.8560

Prepared following a previously reported procedure (Heathcock et al., 1992b). To a 0 °C solution of **2.42** (160 mg, 0.28 mmol, 1 equiv) and triethylamine (0.15 mL, 1.1 mmol, 4 equiv) in 1 mL of CH_2Cl_2 was added methanesulfonyl chloride (45 µL, 0.56 mmol, 2 equiv). The solution was allowed to warm up to the room temperature and stirred for 3 h. Then, the reaction mixture was diluted with 10 mL of CH_2Cl_2 and washed with aqueous $NaHCO_3$, 0.1 M HCl and brine. The combined organic phases were dried with $MgSO_4$, filtered and concentrated to yield a brown oil which was taken up in 1 mL of toluene. Then, DBU (125 µL, 0.84 mmol, 3 equiv) was added, and the reaction mixture was heated to 80 °C for 12 h. The reaction mixture was allowed to cool down to the room temperature, was diluted with 10 mL of diethyl ether, washed with sat. aq. $NaHCO_3$, 0.1 M aq. HCl and brine, dried over $MgSO_4$, filtered and concentrated to give yellow oil which was purified by column chromatography on silica gel (hexane:ethyl acetate = 40:1), to yield product **2.43** (110 mg, 0.19 mmol, 70%) as pale yellow oil as a mixture of diastereoisomers, we were not able to confidently determine the ratio of stereoisomers.

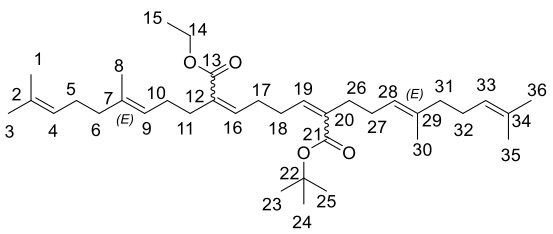

Note, NMR data for the major stereoisomer only is reported.

R_f (hexane/ethyl acetate = 4/1, UV + $KMnO_4$: 0.53). ^1H NMR (400 MHz, ($CDCl_3$): δ 6.74 (t, *J* = 7.0 Hz, 1H, H-16), 5.72 (t, *J* = 7.0 Hz, 1H, H-19), 5.13 – 5.06 (m, 4H, H-4, H-9, H-28 and H-33), 4.19 (q, *J* = 7.0 Hz, 2H, H-14), 2.56 – 1.92 (m, 16H, H-5, H-6, H-10, H-11, H-17, H-18, H-26, H-27, H-31 and H-32), 1.68 (s, 6H, H-8 and H-30), 1.59 (s, 9H, H-23, H-24 and H-25), 1.49 (s, 12H, H-1, H-3, H35 and H-36), 1.29 ((t, *J* = 7.0 Hz, 3H, H-15); ^{13}C NMR (100 MHz, ($CDCl_3$): δ 168.0 (C12 or C21), 167.5 (C12 or C21), 141.6 (C16 or C19), 138.1 (C16 or C19), 136.0 (C13 or C20), 135.8 (C13 or C20), 134.6 (C9 or C28), 132.9 (C9 or C28), 131.5 (C2 and C34), 124.5 (C7 and C29), 123.6 (C4 and C33), 80.7 (C22), 60.5 (C14), 39.9 (C11 and C26), 35.1 (C17 or C18), 34.4 (C17 or C18), 28.7 (C23, C24, C25), 28.4 (C5 and C32), 27.8 (C10 or C27), 27.2 (C10 or C27), 26.9 (C6 or C31), 26.8 (C6 or C31), 25.8 (C8 and C30), 17.8 (C1 and C35), 16.1 (C3 and 36), 14.4 (C15).

HRMS (ESI^+): m/z $[M+Na]^+$ Calcd. for $C_{36}H_{58}NaO_4$: 577.4227. Found: 577.4224. (mean error 2.3 ppm)

IR (thin film) ν_{max} cm^{-1} 2968, 2927, 2858, 1709;

Compound 1.97 (1-(*tert*-butyl) 8-ethyl 2,7-bis((*E*)-4,8-dimethylnona-3,7-dien-1-yl)octa-2,6-dienedioate).

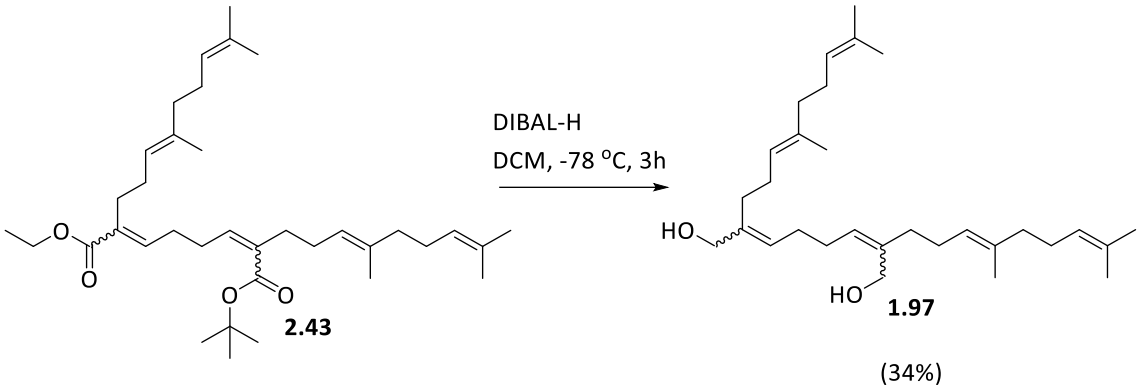

(34%)

Chemical Formula: $C_{30}H_{50}O_2$

Molecular Weight: 442.7280

To a solution of **2.43** (110 mg, 0.19 mmol,1 equiv) in 1 mL of CH_2Cl_2 at – 78 °C was added 1 M solution of DIBAL-H in CH_2Cl_2 (2 mL, 20 mmol, 10 equiv). The reaction mixture was stirred at – 78 °C for 3 h, after which it was quenched by slow addition of 0.2 mL of methanol. The reaction mixture was allowed to warm up to room temperature after which 10 mL of diethyl ether and 10 mL of Rochelle salt (sat. solution of sodium potassium tartrate) were added and the solution was stirred until two phases separated. The layers were separated, and the aqueous phase was extracted with diethyl ether (3 x 20 mL). The combined organic phases were washed with brine, dried over $MgSO_4$, filtered and concentrated to yield an oil which purified by column chromatography on silica gel (hexane:ethyl acetate = 4:1), to yield product **2.43** (30 mg, 0.06 mmol, 34%) as pale yellow oil as a mixture of diastereoisomers, we were not able to confidently determine the ratio of stereoisomers.

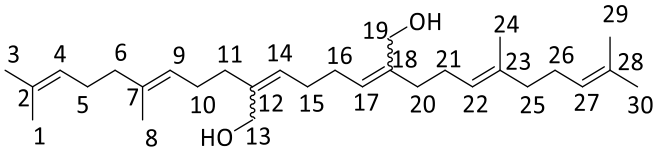

Note, NMR data for the major stereoisomer only is reported.

R_f (hexane/ethyl acetate = 4/1, UV + $KMnO_4$: 0.27). ^1H NMR (400 MHz, ($CDCl_3$): δ 5.42 (t, *J* = 7.0, 1H, H-14 or H-17), 5.31 (t, *J* = 7.0, 1H, H-14 or H-17), 5.17 – 5.05 (m, 4H, H-4, H-9, H-22

and H-27), 4.14 – 4.01 (m, 4H, H-13 and H-19), 2.16 – 1.94 (m, 20H, H-5, H-6, H-10, H-11, H-15, H-16, H-20, H-21, H25 and H26), 1.68 (s, 6H, H-8 and H-24), 1.60 (s, 12H, H-1, H-3, H-29 and H-30); ^{13}C NMR (100 MHz, ($CDCl_3$):

δ 139.8 (C12 or C18), 139.27 (C12 or C18), 135.96 (C2, C7, C23 or C23), 131.5 (C2, C7, C23 or C28), 127.7 (C14 or C17), 126.4 (C14 or C17), 124.4 (C9 and C22 or C4 and C27), 124.0 (C9 and C22 or C4 and C27), 67.2 (C13 or C19), 60.2 (C13 or C19), 39.9 (C5 and C26), 35.2 (C15 and C16), 28.4 (C11 and C20), 27.5 (C6 and C25), 26.8 (C10 and C21), 25.8 (C8 and C24), 17.8 (C3 and C30), 16.2 (C1 and C29).

HRMS (ESI^+): m/z $[M+Na]^+$ Calcd. for $C_{30}H_{50}NaO_2$: 465.3703. Found: 465.3724. (mean error –3.0 ppm)

IR (thin film) v_{max} cm^{-1} 3370 (br), 2969, 2926, 2862, 1449, 1377, 1016;

7 References

Aleku, G. A. et al. (2017). A reductive aminase from Aspergillus oryzae. *Nature chemistry*, 9 (10), pp.961–969. [Online]. Available at: doi:10.1038/nchem.2782.

Amatore, C., Jutand, A. and Le Duc, G. (2011). Kinetic data for the transmetalation/reductive elimination in palladium-catalyzed Suzuki-Miyaura reactions: unexpected triple role of hydroxide ions used as base. *Chemistry (Weinheim an der Bergstrasse, Germany)*, 17 (8), pp.2492–2503. [Online]. Available at: doi:10.1002/chem.201001911.

Amor Stander, E. et al. (2020). Identifying Genes Involved in Alkaloid Biosynthesis in Vinca minor through Transcriptomics and Gene Co-Expression Analysis. *Biomolecules*, 10 (12), p.1595. [Online]. Available at: doi:10.3390/biom10121595.

Augustin, M. M. et al. (2015). Elucidating steroid alkaloid biosynthesis in Veratrum californicum: production of verazine in Sf9 cells. *The Plant Journal*, 82, pp.991–1003. [Online]. Available at: doi:10.1111/tpj.12871.

Bak, S. et al. (2011). Cytochromes p450. *The Arabidopsis book / American Society of Plant Biologists*, 9, p.e0144. [Online]. Available at: doi:10.1199/tab.0144.

Barchenger, D. W. and Bosland, P. W. (2016). Exogenous applications of capsaicin inhibits seed germination of Capsicum annuum. *Scientia horticulturae*, 203, pp.29–31. [Online]. Available at: doi:10.1016/j.scienta.2016.03.009.

Batista-Silva, W. et al. (2019). The role of amino acid metabolism during abiotic stress release: Amino acid metabolism in abiotic stress release. *Plant, cell & environment*, 42 (5), pp.1630–1644. [Online]. Available at: doi:10.1111/pce.13518 [Accessed 26 September 2024].

Bhambhani, S., Kondhare, K. R. and Giri, A. P. (2021). Diversity in Chemical Structures and Biological Properties of Plant Alkaloids. *Molecules* , 26 (11), pp.3374–3403. [Online]. Available at: doi:10.3390/molecules26113374.

Bindschedler, L. V., Palmblad, M. and Cramer, R. (2008). Hydroponic isotope labelling of entire plants (HILEP) for quantitative plant proteomics; an oxidative stress case study. *Phytochemistry*, 69 (10), pp.1962–1972. [Online]. Available at: doi:10.1016/j.phytochem.2008.04.007.

Bird, D. A., Franceschi, V. R. and Facchini, P. J. (2003). A Tale of Three Cell Types: Alkaloid Biosynthesis Is Localized to Sieve Elements in Opium Poppy. *The Plant cell*, 15 (11), pp.2626–2635. [Online]. Available at: doi:10.1105/tpc.015396.

Blanc, A. and Toste, F. D. (2006). Enantioselective Synthesis of Cyclic Ethers through a Vanadium-Catalyzed Resolution/ Oxidative Cyclization. *Angewandte Chemie, International Edition*, 45 (13), pp.2096–2099. [Online]. Available at: doi:10.1002/anie.200503852.

Cao, M. et al. (2012). Daphmacromines A-J, alkaloids from Daphniphyllum macropodum. *Journal of natural products*, 75 (6), pp.1076–1082. [Online]. Available at: doi:10.1021/np200960z.

Chattopadhyay, A. K. and Hanessian, S. (2017). Recent Progress in the Chemistry of Daphniphyllum Alkaloids †. *Chemical Reievs*, 117 (5), pp.4104–4146. [Online]. Available at: doi:10.1021/acs.chemrev.6b00412.

Chen, D. et al. (2018). Polyamine function in plants: Metabolism, regulation on development, and roles in abiotic stress responses. *Frontiers in plant science*, 9, p.1945. [Online]. Available at: doi:10.3389/fpls.2018.01945.

Cherney, E. C. and Baran, P. S. (2011). Terpenoid-Alkaloids: Their Biosynthetic Twist of Fate and Total Synthesis. *Israel journal of chemistry*, 51 (3–4), pp.391–405. [Online]. Available at: doi:10.1002/ijch.201100005.

Chien, C.-T. et al. (2010). Germination and storage behaviour of seeds of the subtropical evergreen tree Daphniphyllum glaucescens (Daphniphyllaceae). *Australian journal of botany*, 58 (4), p.294. [Online]. Available at: doi:10.1071/bt09232.

Christiansen, J. L. et al. (1997). Effect of drought stress on content and composition of seed alkaloids in narrow-leafed lupin, Lupinus angustifolius L. *European journal of agronomy: the journal of the European Society for Agronomy*, 7 (4), pp.307–314. [Online]. Available at: doi:10.1016/s1161-0301(97)00017-8.

Dewick, P. M. (2011). *Medicinal Natural Products*. 3rd ed. Hoboken, NJ: Wiley-Blackwell. [Online]. Available at: doi:10.1002/9780470742761.

Di, Y.-T. et al. (2008). Yunnandaphninines F and G, new C_{30} alkaloids from *Daphniphyllum yunnanense*. *Helvetica chimica acta*, 91 (5), pp.838–843. [Online]. Available at: doi:10.1002/hlca.200890086.

Dias, L. C. et al. (2005). Total synthesis of (+)-crocacin D. *The Journal of organic chemistry*, 70 (6), pp.2225–2234. [Online]. Available at: doi:10.1021/jo047732k.

Duchemin, N. et al. (2020). Direct Access to Highly Enantioenriched α-Branched Acrylonitriles through a One-Pot Sequential Asymmetric Michael Addition/Retro-Dieckmann/Retro-Michael Fragmentation Cascade. *Organic letters*, 22 (15), pp.5995–6000. [Online]. Available at: doi:10.1021/acs.orglett.0c02079.

Eichelberger, U. et al. (2002). Synthesis of analogues of the 2-O-alkyl glycerate part of the moenomycins. *Tetrahedron*, 58 (3), pp.545–559. [Online]. Available at: doi:10.1016/s0040-4020(01)01167-x.

Eljounaidi, K. et al. (2024). Variation of terpene alkaloids in Daphniphyllum macropodum across plants and tissues. *The New phytologist*, 243 (1), pp.299–313. [Online]. Available at: doi:10.1111/nph.19814.

Fang, C., Fernie, A. R. and Luo, J. (2019). Exploring the diversity of plant metabolism. *Trends in plant science*, 24 (1), pp.83–98. [Online]. Available at: doi:10.1016/j.tplants.2018.09.006.

Fraser, P. D., Shimada, H. and Misawa, N. (1998). Enzymic confirmation of reactions involved in routes to astaxanthin formation, elucidated using a direct substrate in vitro assay. *European journal of biochemistry / FEBS*, 252, pp.229–236.

Fuchs, K. and Paquette, L. A. (1994). Access to Protected 2-Alkylidene 1,3-Diones by Modified Knoevenagel Reaction in the Presence of Thiophenol. A New Approach to Spirocyclopentanol Construction. *The Journal of organic chemistry*, 59 (9), pp.528–532.

Grzech, D. et al. (2024). Incorporation of nitrogen in antinutritional Solanum alkaloid biosynthesis. *Nature chemical biology*. [Online]. Available at: doi:10.1038/s41589-024-01735-w.

Haruki, N., Yoshimasa, H. and Suzuki, K. (1973). Biosynthesis of daphnilactone-B. *Tetrahedron Lettersdron*, 24 (23), pp.2129–2132.

Heathcock, C. H. et al. (1986). Total synthesis of (.+-.)-methyl homodaphniphyllate. *Journal of the American Chemical Society*, 108 (18), pp.5651–5652.

Heathcock, C. H. et al. (1992a). Daphniphyllum alkaloids. 11. Biomimetic total synthesis of methyl homosecodaphniphyllate. Development of the tetracyclization reaction. *The Journal of organic chemistry*, 57 (9), pp.2544–2553. [Online]. Available at: doi:10.1021/jo00035a008.

Heathcock, C. H. et al. (1992b). Daphniphyllum Alkaloids. 12. A Proposed Biosynthesis of the Pentacyclic Skeleton, proto-Daphniphylline. *The Journal of organic chemistry*, 57 (9), pp.2554–2566. [Online]. Available at: https://pubs.acs.org/sharingguidelines.

Heathcock, C. H. (1992). The Enchanting Alkaloids of Yuzuriha. *Angewandte Chemie International Edition In English*, 31 (6), pp.665–804. [Online]. Available at: http://onlinelibrary.wiley.com/doi/10.1002/anie.198201553/abstract.

Heathcock, C. H. (1996). Nature knows best: An amazing reaction cascade is uncovered bydesign and discovery. *Proceedings of the National Academy of Sciences of the United States of America*, 93 (25), pp.14323–14327.

Heathcock, C. H. and Joe, D. (1995). Daphniphyllum Alkaloids. 17. A Possibly Biomimetic Transformation of the Secodaphnane to the Daphnane Skeleton. *The Journal of organic chemistry*, 60 (5), pp.1131–1142. [Online]. Available at: doi:10.1021/jo00110a014.

Heathcock, C. H., Ruggeri, R. B. and McClure, K. F. (1992). Daphniphyllum alkaloids. 15. Total syntheses of (.+-.)-methyl homodaphniphyllate and (.+-.)-daphnilactone A. *The Journal of organic chemistry*, 57 (9), pp.2585–2594. [Online]. Available at: doi:10.1021/jo00035a012.

Horodysky, A. G., Waller, G. R. and Eisenbraun, E. J. (1969). Biosynthesis of methylcyclopentane monoterpenoids. IV. Verbenalin. *The Journal of biological chemistry*, 244 (12), pp.3110–3116. [Online]. Available at: doi:10.1016/S0021-9258(18)95791-1.

Huang, W. et al. (2022). Biosynthesis investigations of terpenoid, alkaloid, and flavonoid antimicrobial agents derived from medicinal plants. *Antibiotics (Basel, Switzerland)*, 11 (10), p.1380. [Online]. Available at: doi:10.3390/antibiotics11101380.

Irikawa, H. et al. (1968). The structures of daphniphylline and codaphniphylline. *Tetrahedron*, 24 (16), pp.5691–5700. [Online]. Available at: doi:10.1016/0040-4020(68)88167-0.

Ishiai, S. et al. (2016). Hordenine is responsible for plant defense response through jasmonate-dependent defense pathway. *Physiological and molecular plant pathology*, 96, pp.94–100. [Online]. Available at: doi:10.1016/j.pmpp.2016.10.003.

Ishihara, H. et al. (2015). Quantifying protein synthesis and degradation in arabidopsis by dynamic 13 CO2 labeling and analysis of enrichment in individual amino acids in their free pools and in protein. *Plant physiology*, 168 (1), pp.74–93. [Online]. Available at: doi:10.1104/pp.15.00209.

Kocienski, P., Wadman, S. and Cooper, K. (1989). A highly stereoselective and iterative approach to isoprenoid chains: synthesis of homogeraniol, homofarnesol, and homogeranylgeraniol. *The Journal of organic chemistry*, 54 (5), pp.1215–1217. [Online]. Available at: doi:10.1021/jo00266a047.

Kohnen-Johannsen, K. L. and Kayser, O. (2019). Tropane alkaloids: Chemistry, pharmacology, biosynthesis and production. *Molecules (Basel, Switzerland)*, 24 (4), p.796. [Online]. Available at: doi:10.3390/molecules24040796.

Kon, Y. et al. (2021). Pt-Catalyzed selective oxidation of alcohols to aldehydes with hydrogen peroxide using continuous flow reactors. *Organic & biomolecular chemistry*, 19 (5), pp.1115–1121. [Online]. Available at: doi:10.1039/d0ob02213f.

Koohang, A. et al. (2010). Enantioselective inhibition of squalene synthase by aziridine analogues of presqualene diphosphate. *The Journal of organic chemistry*, 75 (14), pp.4769–4777. [Online]. Available at: doi:10.1021/jo100718z.

Leopold, E. J. (1986). Selective hydroboration of a 1,3,7-triene: homogeraniol. *Organic syntheses; an annual publication of satisfactory methods for the preparation of organic chemicals*, 64, p.164. [Online]. Available at: doi:10.15227/orgsyn.064.0164.

Li, C. et al. (2023). Single-cell multi-omics in the medicinal plant Catharanthus roseus. *Nature chemical biology*. [Online]. Available at: doi:10.1038/s41589-023-01327-0.

Li, Z. Y. et al. (2007). Further Daphniphyllum alkaloids from the bark of Daphniphyllum macropodum Miq. *Helvetica chimica acta*, 90 (7), pp.1353–1359. [Online]. Available at: doi:10.1002/cjoc.200890067.

Lichman, B. R. (2021). The scaffold-forming steps of plant alkaloid biosynthesis. *Natural product reports*, 38 (1), pp.103–129. [Online]. Available at: doi:10.1039/d0np00031k.

Maeda, H. A. (2019). Evolutionary diversification of primary metabolism and its contribution to plant chemical diversity. *Frontiers in plant science*, 10, p.881. [Online]. Available at: doi:10.3389/fpls.2019.00881.

Mancinotti, D., Frick, K. M. and Geu-Flores, F. (2022). Biosynthesis of quinolizidine alkaloids in lupins: mechanistic considerations and prospects for pathway elucidation. *Natural product reports*, 39 (7), pp.1423–1437. [Online]. Available at: doi:10.1039/d1np00069a.

Matos, K. and Soderquist, J. A. (1998). Alkylboranes in the Suzuki-Miyaura coupling: Stereochemical and mechanistic studies. *The Journal of organic chemistry*, 63 (3), pp.461–470. [Online]. Available at: doi:10.1021/jo971681s.

McKenna, C. E. and Khawli, L. A. (1986). Synthesis of halogenated phosphonoacetate esters. *The Journal of organic chemistry*, 51 (26), pp.5467–5471. [Online]. Available at: doi:10.1021/jo00376a092.

Miyaura, N. and Suzuki, A. (1995). Palladium-catalyzed cross-coupling reactions of organoboron compounds. *Chemical reviews*, 95 (7), pp.2457–2483. [Online]. Available at: doi:10.1021/cr00039a007.

Morita, H. and Kobayashi, J. (2003). Calyciphyllines A and B, two novel hexacyclic alkaloids from Daphniphyllum calycinum. *Organic letters*, 5 (16), pp.2895–2898. [Online]. Available at: doi:10.1021/ol034969e.

Morita, H. and Kobayashi, J. (2007). Daphniphyllum alkaloids: Structures, Biogenesis, and Activities. In: *Modern Alkaloids*. Weinheim, Germany: Wiley-VCH Verlag GmbH & Co. KGaA. pp.541–589. [Online]. Available at: doi:10.1002/9783527621071.ch18.

Morita, H., Yoshida, N. and Kobayashi, J. (1999). Daphnezomines A and B, novel alkaloids with an Aza-adamantane core from Daphniphyllum humile. *The Journal of organic chemistry*, 64 (19), pp.7208–7212. [Online]. Available at: doi:10.1021/jo990882o.

Morita, H., Yoshida, N. and Kobayashi, J. (2000). Daphnezomines H, I, J, and K, new daphnilactone-type and yuzurimine-type alkaloids from Daphniphyllum humile. *Tetrahedron*, 56 (17), pp.2641–2646. [Online]. Available at: doi:10.1016/S0040-4020(00)00197-6.

Mu, S.-Z. et al. (2008). Alkaloids from Daphniphyllum oldhami. *Journal of natural products*, 71 (4), pp.564–569. [Online]. Available at: doi:10.1021/np070512s.

Nett, R. S. and Sattely, E. S. (2021). Total Biosynthesis of the Tubulin-Binding Alkaloid Colchicine. *Cite This: J. Am. Chem. Soc*, 143, p.19454−19465. [Online]. Available at: doi:10.1021/jacs.1c08659.

Niwa, H. et al. (1972). Daphnilactone-B, a major alkaloid, from the fruits of daphniphyllaceae. *Tetrahedron letters*, 13 (26), pp.2697–2700. [Online]. Available at: doi:10.1016/s0040-4039(01)84910-8.

Nützmann, H.-W. and Osbourn, A. (2014). Gene clustering in plant specialized metabolism. *Current opinion in biotechnology*, 26, pp.91–99. [Online]. Available at: doi:10.1016/j.copbio.2013.10.009.

Parthasarathy, A. et al. (2021). Amino acid-derived defense metabolites from plants: A potential source to facilitate novel antimicrobial development. *The journal of biological chemistry*, 296 (100438), p.100438. [Online]. Available at: doi:10.1016/j.jbc.2021.100438.

Peterson, D. J. (1968). Carbonyl olefination reaction using silyl-substituted organometallic compounds. *The Journal of organic chemistry*, 33 (2), pp.780–784. [Online]. Available at: doi:10.1021/jo01266a061.

Pieitre, S. and Heathcock, C. H. (1990). Biomimetic Total Synthesis of Proto-Daphniphylline. *Science*, 248 (4962), pp.1532–1534.

Pott, D. M., Osorio, S. and Vallarino, J. G. (2019). From Central to Specialized Metabolism: An Overview of Some Secondary Compounds Derived From the Primary Metabolism for Their Role in Conferring Nutritional and Organoleptic Characteristics to Fruit. *Frontiers in Plant Science*, 10. [Online]. Available at: doi:10.3389/fpls.2019.00835 [Accessed 26 September 2024].

Qi, X. et al. (2004). A gene cluster for secondary metabolism in oat: implications for the evolution of metabolic diversity in plants. *Proceedings of the National Academy of Sciences of the United States of America*, 101 (21), pp.8233–8238. [Online]. Available at: doi:10.1073/pnas.0401301101.

Qing, F. L. and Zhang, X. (2001). A one-pot synthesis of (E)-α-bromo-α,β-unsaturated esters and their trifluoromethylation: A general and stereoselective route to (E)-α-trifluoromethyl-α,β-unsaturated esters. *Tetrahedron letters*, 42 (34), pp.5929–5931. [Online]. Available at: doi:10.1016/S0040-4039(01)01153-4.

Ripperger, H. (1998). Solanum Steroid Alkaloids - an Update. In: *Alkaloids: Chemical and Biological Perspectives*. Alkaloids: chemical and biological perspectives. Elsevier. pp.103–185. [Online]. Available at: doi:10.1016/s0735-8210(98)80004-6.

Rontein, D. et al. (2001). Plants synthesize ethanolamine by direct decarboxylation of serine using a pyridoxal phosphate enzyme. *The Journal of biological chemistry*, 276 (38), pp.35523–35529. [Online]. Available at: doi:10.1074/jbc.M106038200.

Ros, R., Muñoz-Bertomeu, J. and Krueger, S. (2014). Serine in plants: biosynthesis, metabolism, and functions. *Trends in plant science*, 19 (9), pp.564–569. [Online]. Available at: doi:10.1016/j.tplants.2014.06.003.

Ruggeri, R. B. and Heathcock, C. H. (1989). A proposal for biosynthesis of the Daphniphyllum alkaloids. *Journal of Macromolecular Science, Part A:Pure and Applied Chemistry*, 61 (3), pp.289–292. [Online]. Available at: doi:10.1351/pac198961030289.

Ruggeri, R. B., Heathcock, C. H. and Hansen, M. M. (1988). Total synthesis of (+-)-methyl homosecodaphniphyllate. A remarkable new tetracyclization reaction. *Journal of the American Chemical Society*, 110 (26), pp.8734–8736.

Ruggeri, R. B., McClure, K. F. and Heathcock, C. H. (1989). Daphniphyllum alkaloids. Part 5. Total synthesis of (.+-.)-daphnilactone A: a novel fragmentation reaction. *Journal of the American Chemical Society*, 111 (4), pp.1530–1531. [Online]. Available at: doi:10.1021/ja00186a075.

Sakurai, H. et al. (1967). Isolation of yuzurimines A and B from Daphniphyllum macropodum miquel. *Tetrahedron letters*, 8 (30), pp.2883–2888. [Online]. Available at: doi:10.1016/S0040-4039(00)90880-3.

Sasaki, K. and Hirata, Y. (1972). Structure of a new Daphniphyllum alkaloid, Daphnilactone A. *Tetrahedron letters*, 13 (13), pp.1275–1278. [Online]. Available at: doi:10.1016/s0040-4039(01)84566-4.

Scheller, P. N. et al. (2015). Imine reductase-catalyzed intermolecular reductive amination of aldehydes and ketones. *ChemCatChem*, 7 (20), pp.3239–3242. [Online]. Available at: doi:10.1002/cctc.201500764.

Schwartz, B. D. et al. (2009). Asymmetric [4 + 3] Cycloadditions between Vinylcarbenoids and Dienes: Application to the Total Synthesis of the Natural Product (-)-5-epi-Vibsanin E. *Chem. Soc., Perkin Trans. II*, 131 (23), pp.8329–8332. [Online]. Available at: doi:10.1021/ja9019484.

Shen, S. M. et al. (2020). Further new complex daphniphyllum alkaloids from the stems and leaves of Daphniphyllum calycinum: Structure and stereochemistry. *Tetrahedron*, 76 (49), p.131616. [Online]. Available at: doi:10.1016/j.tet.2020.131616.

Shittu, H. et al. (2010). Glucose uptake stimulatory effect of akuammicine from Picralima nitida (Apocynaceae). *Phytochemistry letters*, 3 (1), pp.53–55. [Online]. Available at: doi:10.1016/j.phytol.2009.11.003.

Simpson, J. and Chapple, C. (2022). Tag you're it : Application of stable isotope labeling and LC-MS to identify the precursors of specialized metabolites in plants. *Methods in enzymology*, 676, pp.303–279. [Online]. Available at: doi:10.1016/bs.mie.2022.07.039.

Smit, S. J. and Lichman, B. R. (2022). Plant biosynthetic gene clusters in the context of metabolic evolution. *Natural product reports*, 39 (7), pp.1465–1482. [Online]. Available at: doi:10.1039/d2np00005a.

Smith, C. A. et al. (2006). XCMS: processing mass spectrometry data for metabolite profiling using nonlinear peak alignment, matching, and identification. *Analytical chemistry*, 78 (3), pp.779–787. [Online]. Available at: doi:10.1021/AC051437Y.

Smith, G. B. et al. (1994). Mechanistic studies of the Suzuki cross-coupling reaction. *The Journal of organic chemistry*, 59 (26), pp.8151–8156. [Online]. Available at: doi:10.1021/jo00105a036.

Still, W. C. and Gennari, C. (1983). Direct synthesis of Z-unsaturated esters. A useful modification of the horner-emmons olefination. *Tetrahedron letters*, 24 (41), pp.4405–4408. [Online]. Available at: doi:10.1016/s0040-4039(00)85909-2.

Suzuki, K. T. et al. (1973). Biosynthesis of daphniphyllum alkaloids. *Tetrahedron letters*, 14 (11), pp.799–802. [Online]. Available at: doi:10.1016/S0040-4039(01)95717-X.

Tago, K. and Kogen, H. (2000a). A highly stereoselective synthesis of (E)-α-bromoacrylates. *Tetrahedron*, 56 (45), pp.8825–8831. [Online]. Available at: doi:10.1016/S0040-4020(00)00811-5.

Tago, K. and Kogen, H. (2000b). Bis(2,2,2-trifluoroethyl)bromophosphono-acetate, a Novel HWE Reagent for the Preparation of (E)-r-Bromoacrylates: A General and Stereoselective Method for the Synthesis of Trisubstituted Alkenes. *Organic letters*, 2 (13), pp.1975–1978. [Online]. Available at: doi:10.1021/ol006074x.

Tang, M.-S. et al. (2012). The Diversity Pistillate Flowers Its Taxonomic Value Classification Daphniphyllum (Daphniphyllaceae). *Botanical Studies*, 53, pp.509–524.

Tantillo, D. J. (2016). Does Nature Know Best? Pericyclic Reactions in the Daphniphyllum Alkaloid-Forming Cation Cascade. *Organic letters*, 18 (18), pp.4482–4484. [Online]. Available at: doi:10.1021/acs.orglett.6b01919.

Tautenhahn, R. et al. (2012). XCMS online: A web-based platform to process untargeted metabolomic data. *Analytical chemistry*, 84 (11), pp.5035–5039. [Online]. Available at: doi:10.1021/AC300698C/ASSET/IMAGES/LARGE/AC-2012-00698C_0003.JPEG.

Throup, A., Patterson, L. H. and Sheldrake, H. M. (2016). Intramolecular thermal stepwise [2 + 2] cycloadditions: investigation of a stereoselective synthesis of [n.2.0]-bicyclolactones. *Organic & biomolecular chemistry*, (40), pp.9554–9559.

Toda, M. et al. (1974). The alkaloids from the fruits of the plant Daphniphyllaceae. *Tetrahedron*, 30 (16), pp.2683–2688. [Online]. Available at: doi:10.1016/s0040-4020(01)97429-0.

Toda, M., Hirata, Y. and Yamamura, S. (1972). Daphniphyllum alkaloids-II. Secodaphniphylline and methyl homosecodaphniphyllate. *Tetrahedron*, 28 (6), pp.1477–1484. [Online]. Available at: doi:10.1016/0040-4020(72)88030-X.

Trenti, F. et al. (2021). Early and late steps of quinine biosynthesis. *Organic letters*, 23 (5), pp.1793–1797. [Online]. Available at: doi:10.1021/acs.orglett.1c00206.

Turner, M. W. et al. (2019). Steroidal alkaloid variation in Veratrum californicum as determined by modern methods of analytical analysis. *Fitoterapia*, 137 (104281), p.104281. [Online]. Available at: doi:10.1016/j.fitote.2019.104281.

Wadsworth, W. S. and Emmons, W. D. (1961). The utility of phosphonate carbanions in olefin synthesis. *Journal of the American Chemical Society*, 83 (7), pp.1733–1738. [Online]. Available at: doi:10.1021/ja01468a042.

Wang, M. et al. (2016). Sharing and community curation of mass spectrometry data with Global Natural Products Social Molecular Networking. *Nature biotechnology*, 34 (828–837). [Online]. Available at: doi:10.1038/nbt.3597.

War, A. R. et al. (2019). Plant defense and insect adaptation with reference to secondary metabolites. In: *Reference Series in Phytochemistry*. Cham: Springer International Publishing. pp.1–28. [Online]. Available at: doi:10.1007/978-3-319-76887-8_60-1.

Weih, M., Hamnér, K. and Pourazari, F. (2018). Analyzing plant nutrient uptake and utilization efficiencies: comparison between crops and approaches. *Plant and soil*, 430 (1–2), pp.7–21. [Online]. Available at: doi:10.1007/s11104-018-3738-y.

Wilderman, P. R. et al. (2004). Identification of syn-pimara-7,15-diene synthase reveals functional clustering of terpene synthases involved in rice phytoalexin/allelochemical biosynthesis. *Plant physiology*, 135 (4), pp.2098–2105. [Online]. Available at: doi:10.1104/pp.104.045971.

Winzer, T. et al. (2012). A Papaver somniferum 10-gene cluster for synthesis of the anticancer alkaloid noscapine. *Science (New York, N.Y.)*, 336 (6089), pp.1704–1708. [Online]. Available at: doi:10.1126/science.1220757.

Witte, L., Ehmke, A. and Hartmann, T. (1990). Interspecific flow of pyrrolizidine alkaloids. *Die Naturwissenschaften*, 77 (11), pp.540–543. [Online]. Available at: doi:10.1007/bf01139268.

Wu, H. et al. (2013). Daphniphyllum alkaloids: Recent findings on chemistry and pharmacology. *Planta medica*, 79 (17), pp.1589–1598. [Online]. Available at: doi:10.1055/s-0033-1351024.

Yang, Q., Zhao, D. and Liu, Q. (2020). Connections between amino acid metabolisms in plants: Lysine as an example. *Frontiers in plant science*, 11, p.928. [Online]. Available at: doi:10.3389/fpls.2020.00928.

Yang, S. P. et al. (2006). Alkaloids from Daphniphyllum longeracemosum. *Journal of natural products*, 69 (1), pp.79–82. [Online]. Available at: doi:10.1021/NP0503449.

Yin, X. and Tsukaya, H. (2016). Methods A pulse-chase strategy for EdU labelling assay is able to rapidly quantify cell division orientation. *The New phytologist*, 211, pp.1462–1469. [Online]. Available at: doi:10.1111/nph.13980.

Yoichi, W. et al. (2023). Genetic differentiation and evolution of broad-leaved evergreen shrub and tree varieties of Daphniphyllum macropodum (Daphniphyllaceae). *Heredity*, 131 (3), pp.211–220. [Online]. Available at: doi:10.1038/s41437-023-00637-2.

Zhang, C.-R. et al. (2009a). Alkaloids from the Leaves of Daphniphyllum subverticillatum. *Journal of natural products*, 72 (9), pp.1669–1672. [Online]. Available at: doi:10.1021/np9003799.

Zhang, Q. et al. (2009b). Daphenylline, a new alkaloid with an unusual skeleton, from Daphniphyllum longeracemosum. *Organic letters*, 11 (11), pp.2357–2359. [Online]. Available at: doi:10.1021/ol9007958.

Zhang, X. et al. (2012). Deoxycalyciphylline B, a hepatotoxic alkaloid from Daphniphyllum calycinum. *Molecules* , 17 (8), pp.9641–9651. [Online]. Available at: doi:10.3390/molecules17089641.

Zhao, P. J. et al. (2009). Approach to the biosynthesis of atisine-type diterpenoid alkaloids. *Journal of natural products*, 72 (4), pp.645–649. [Online]. Available at: doi:10.1021/np800657j.

8 Appendix

8.1 Chapter 2. Synthesis of diol

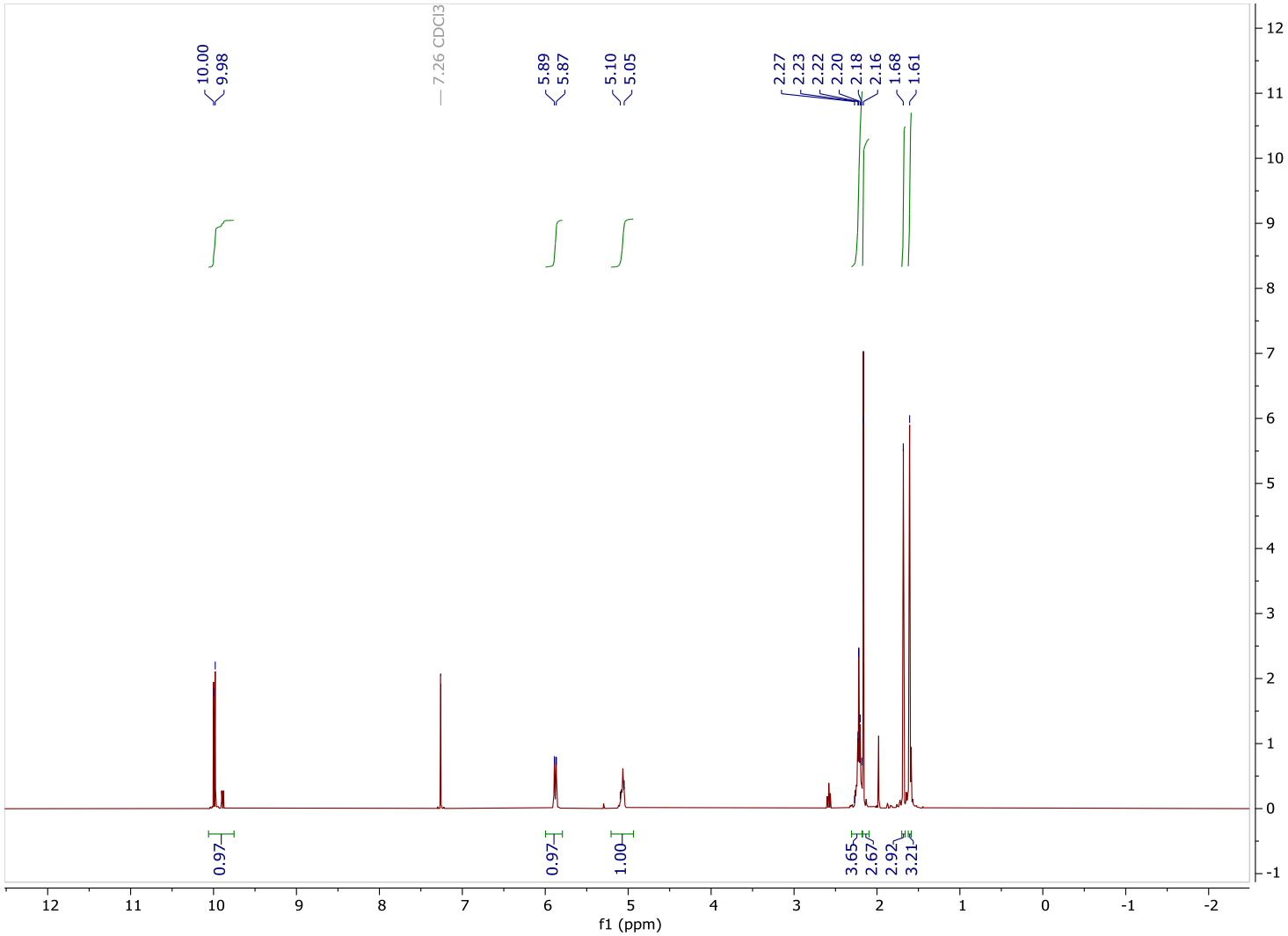

*Figure A.2.1 ^{1}H NMR spectrum of **2.17** in $CDCl_3$.*

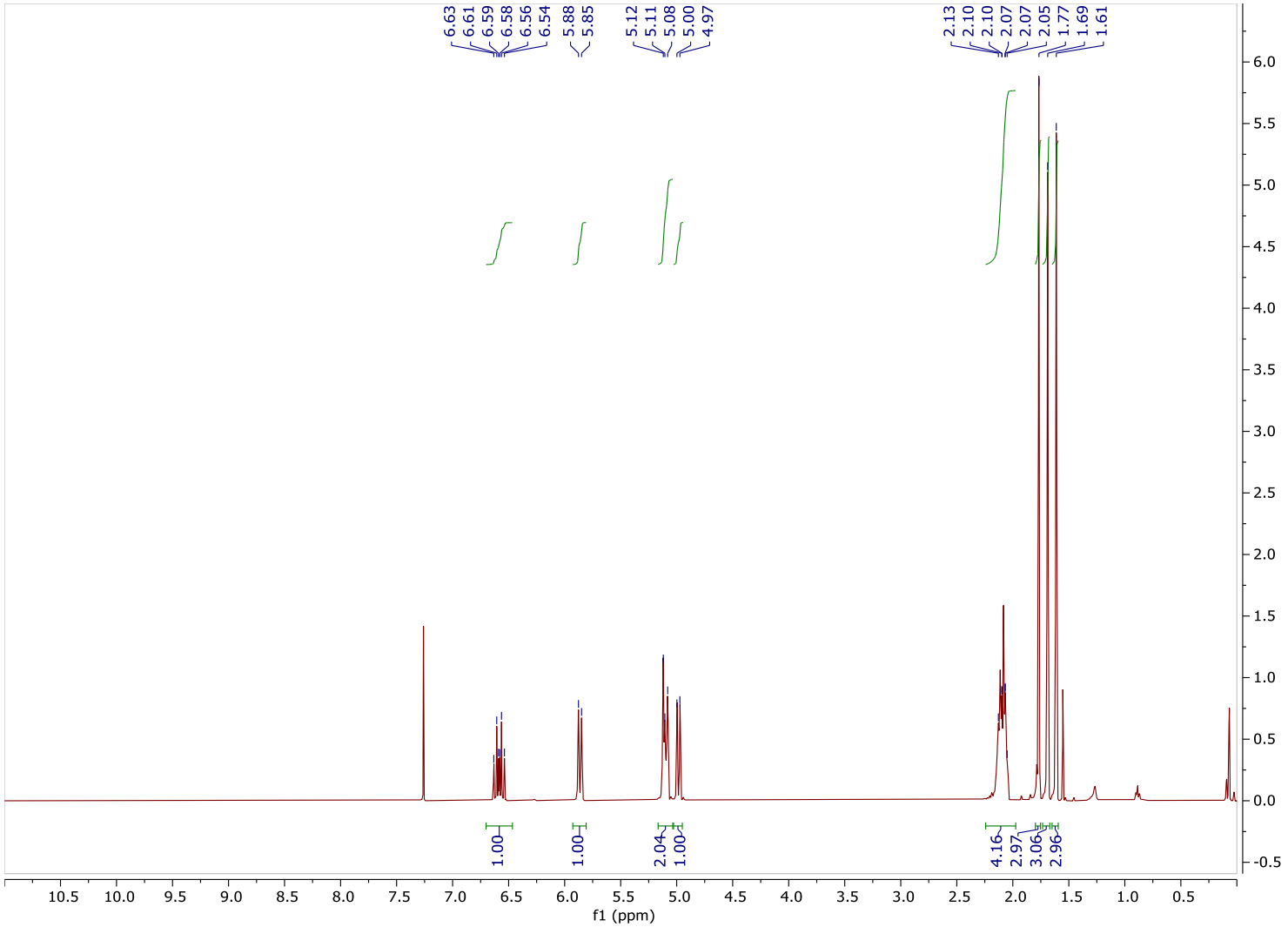

*Figure A.2.2 ^{1}H NMR spectrum of **2.12** in $CDCl_3$.*

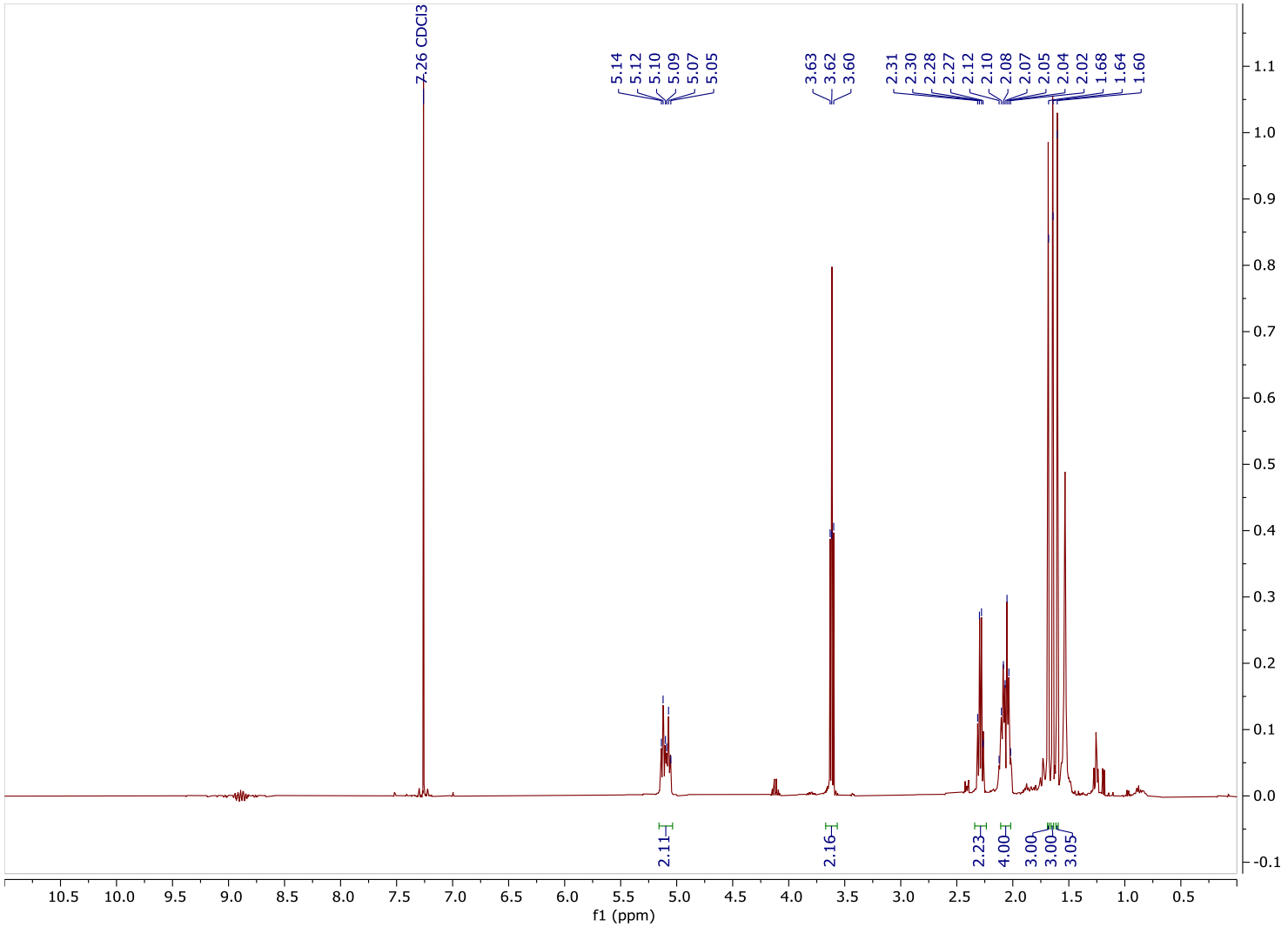

*Figure A.2.3 ^{1}H NMR spectrum of **2.35** in $CDCl_3$.*

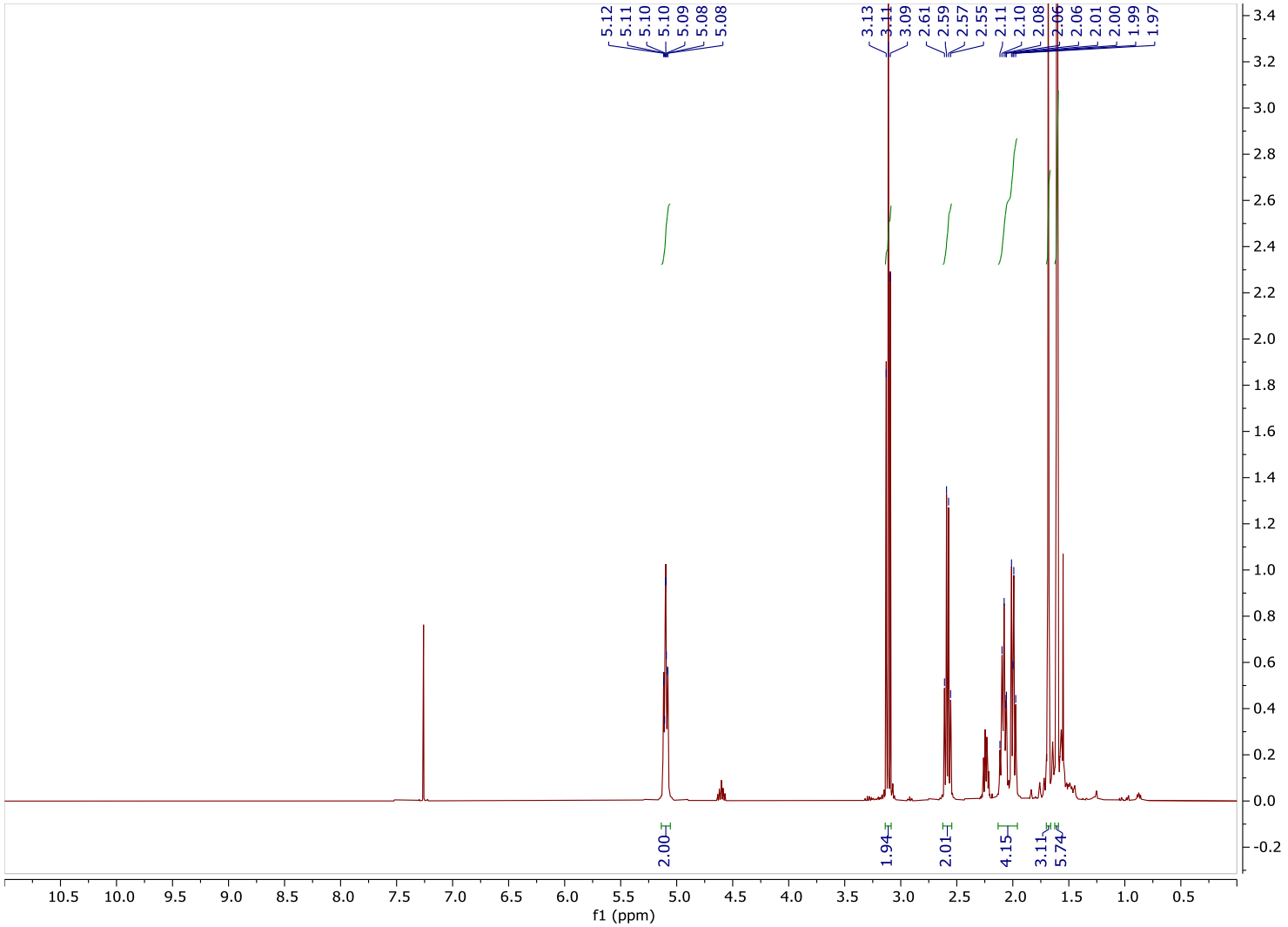

*Figure A.2.4 ^{1}H NMR spectrum of **1.87** in $CDCl_3$.*

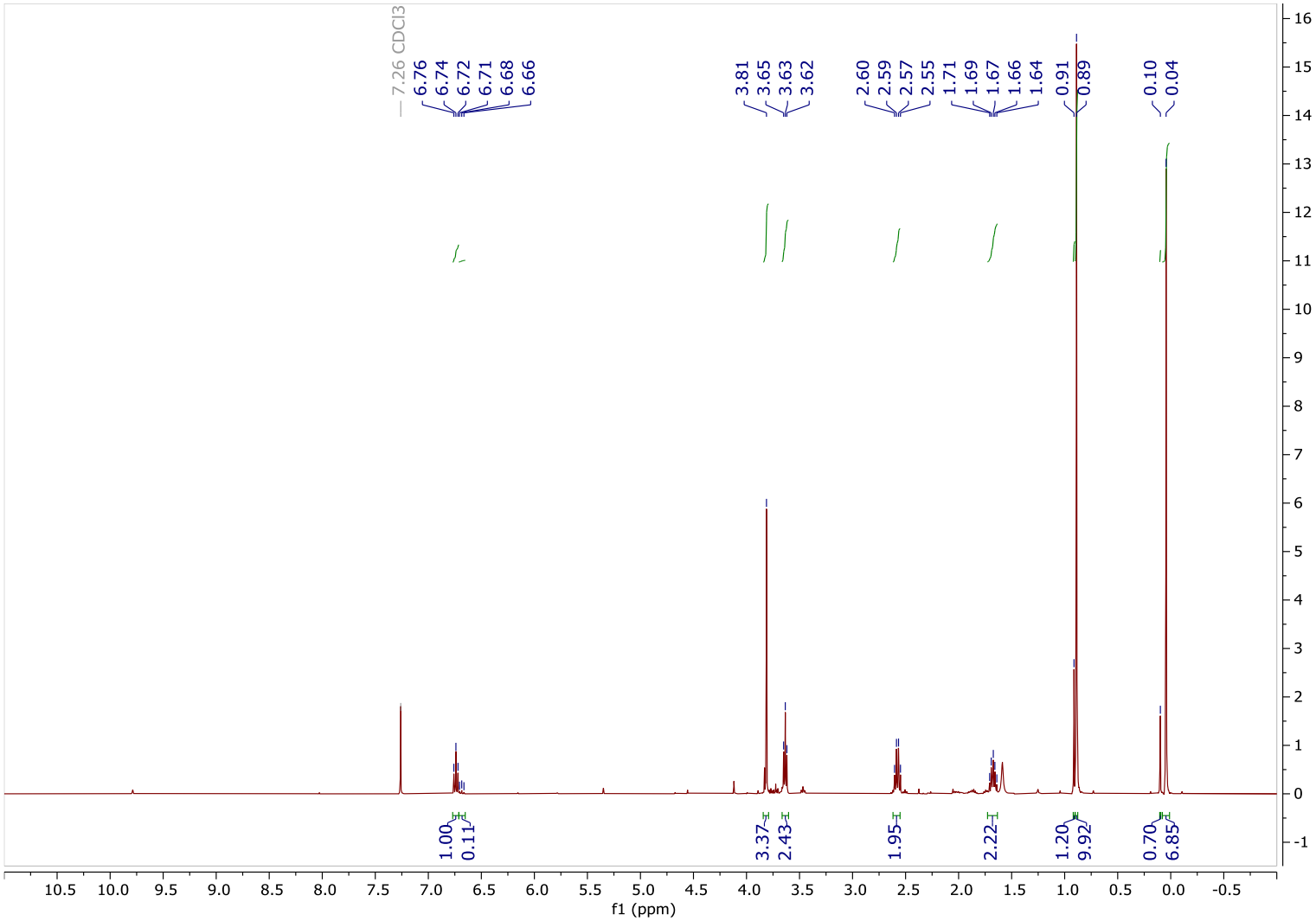

*Figure A.2.5 ^{1}H NMR spectrum of **2.20** in $CDCl_3$.*

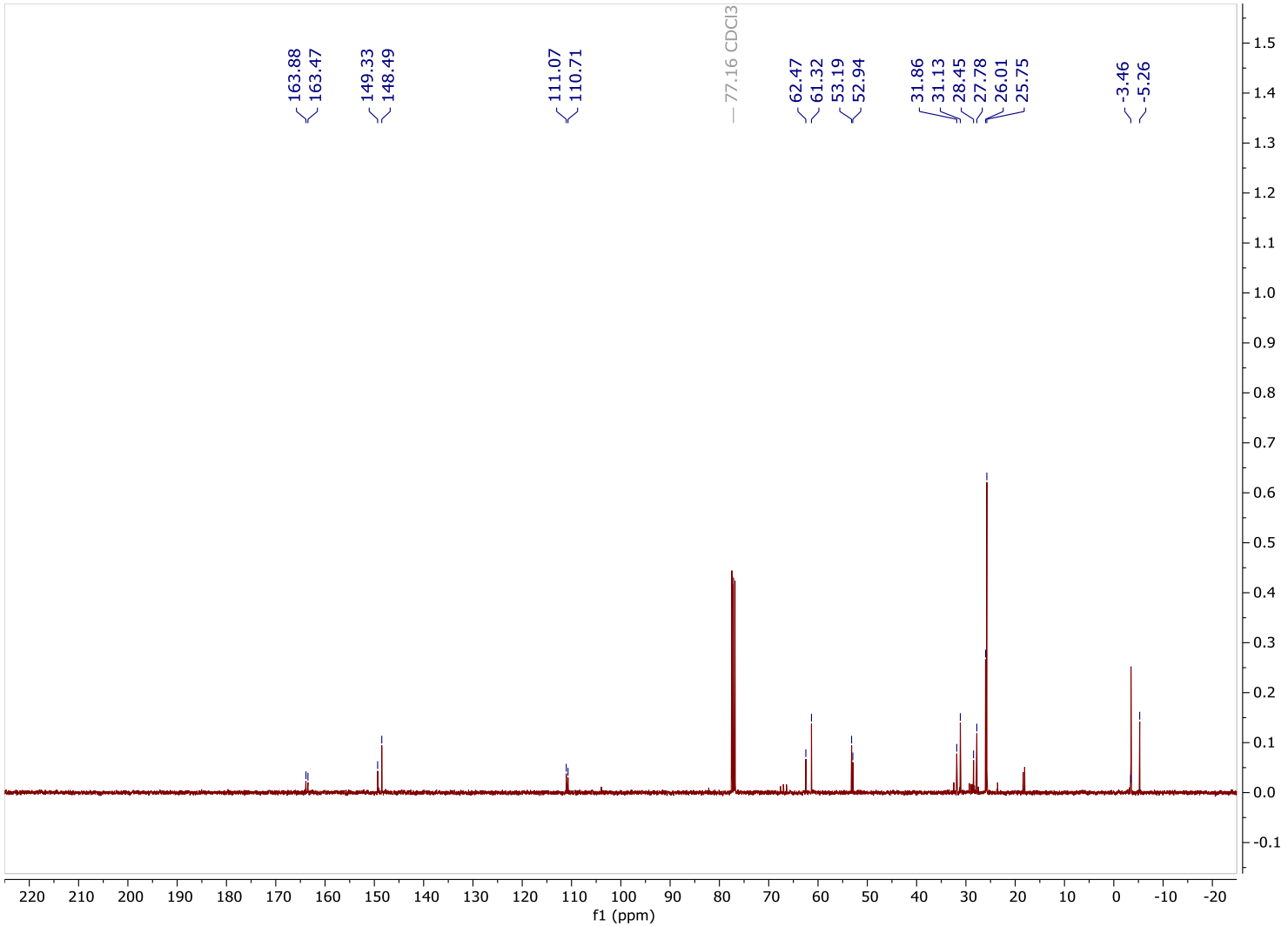

*Figure A.2.6 ^{13}C NMR spectrum of **2.20** in $CDCl_3$.*

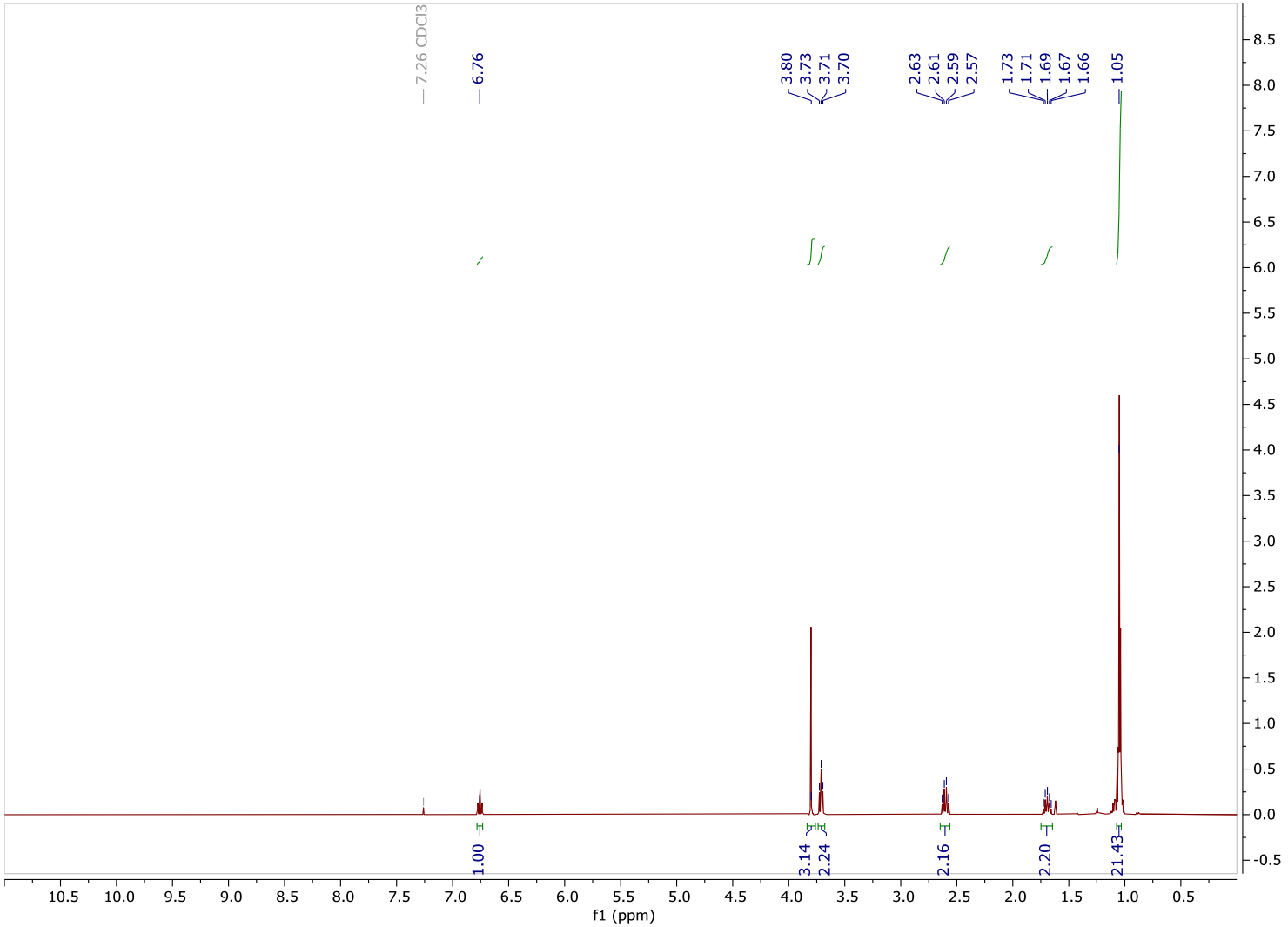

*Figure A.2.7 ^{1}H NMR spectrum of **2.22** in $CDCl_3$.*

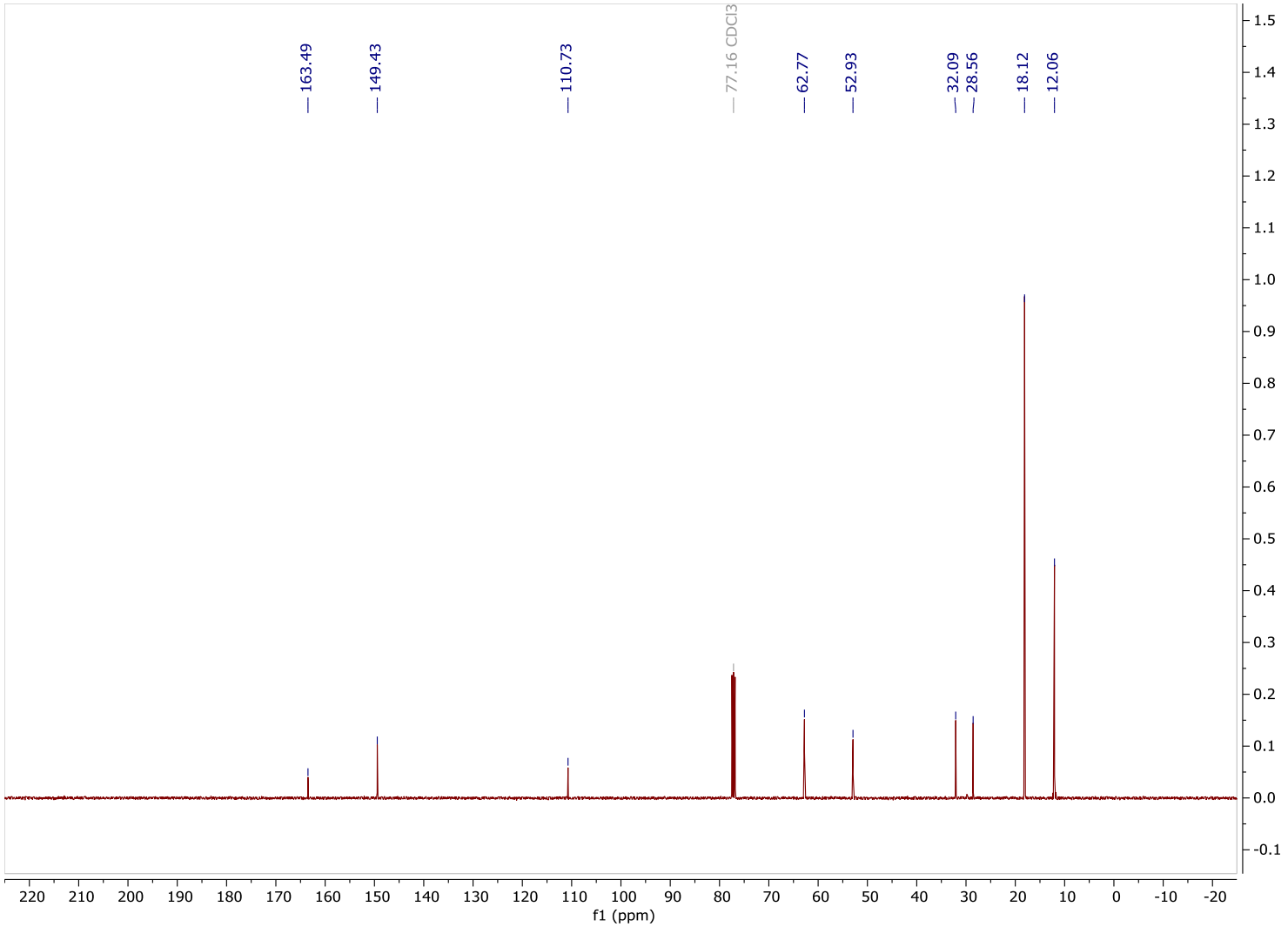

*Figure A.2.8 ^{13}C NMR spectrum of **2.22** in $CDCl_3$.*

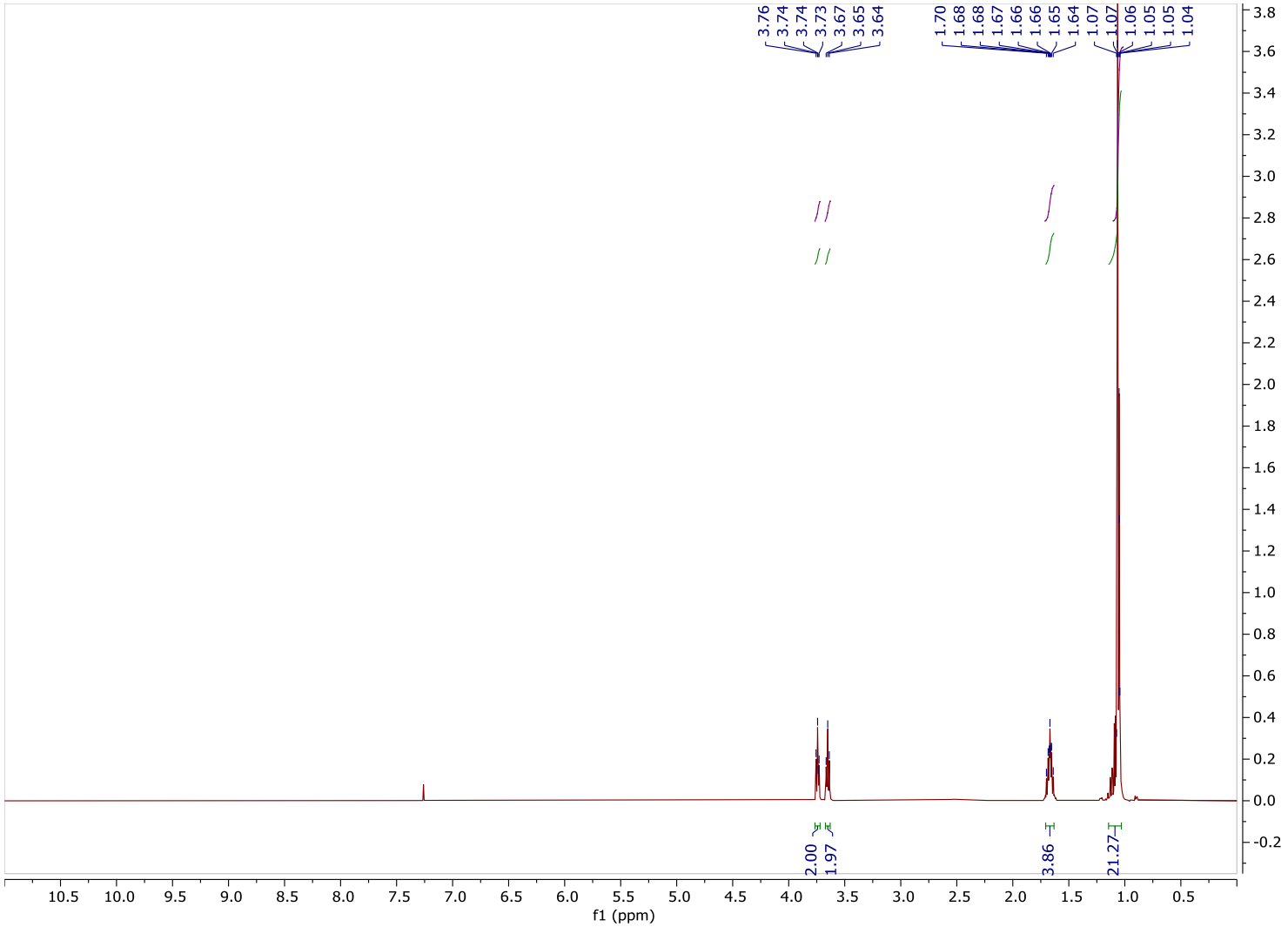

*Figure A.2.9 ^{1}H NMR spectrum of **2.46** in $CDCl_3$.*

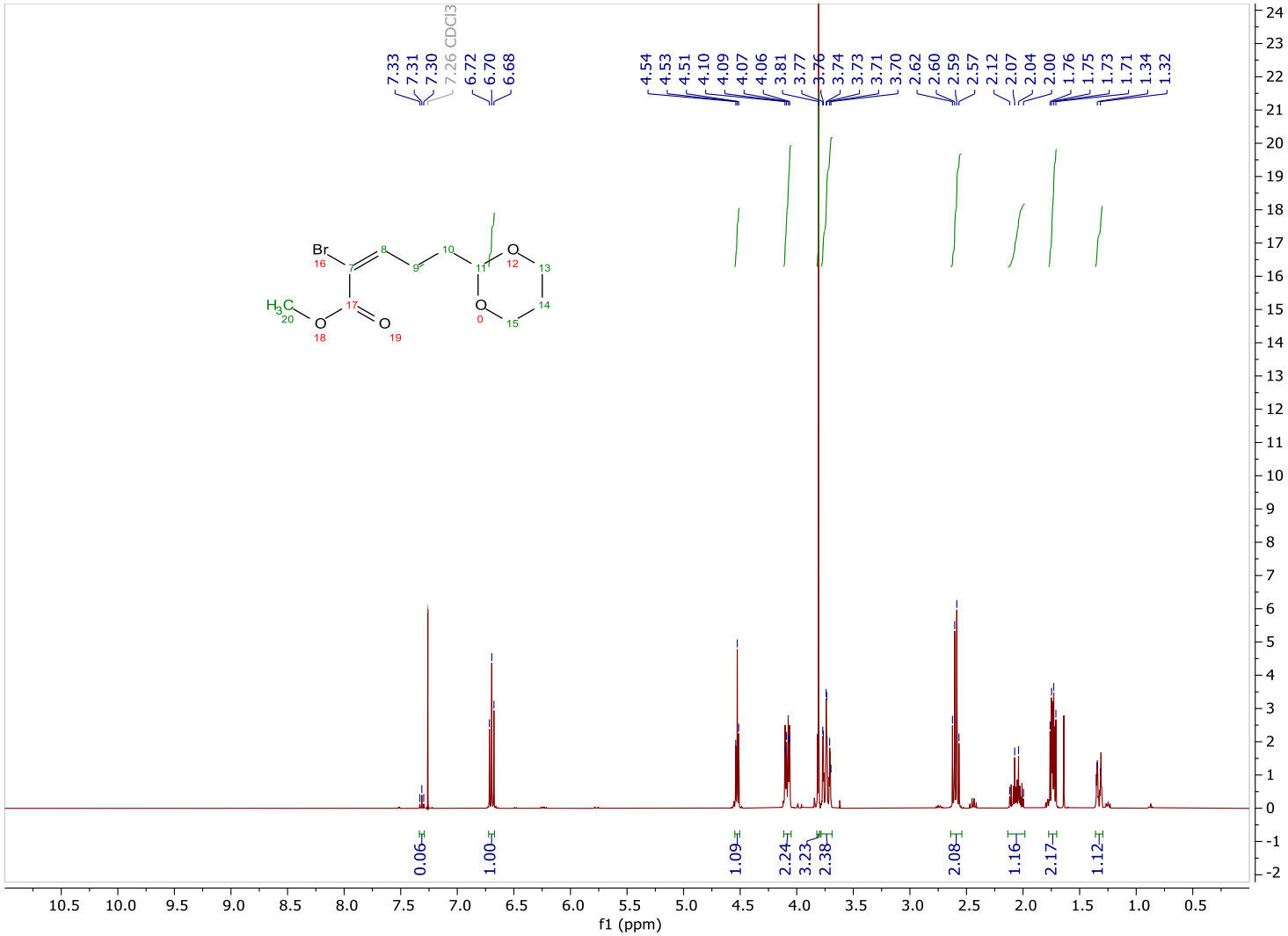

*Figure A.2.10 ^{1}H NMR spectrum of **2.28** in $CDCl_3$.*

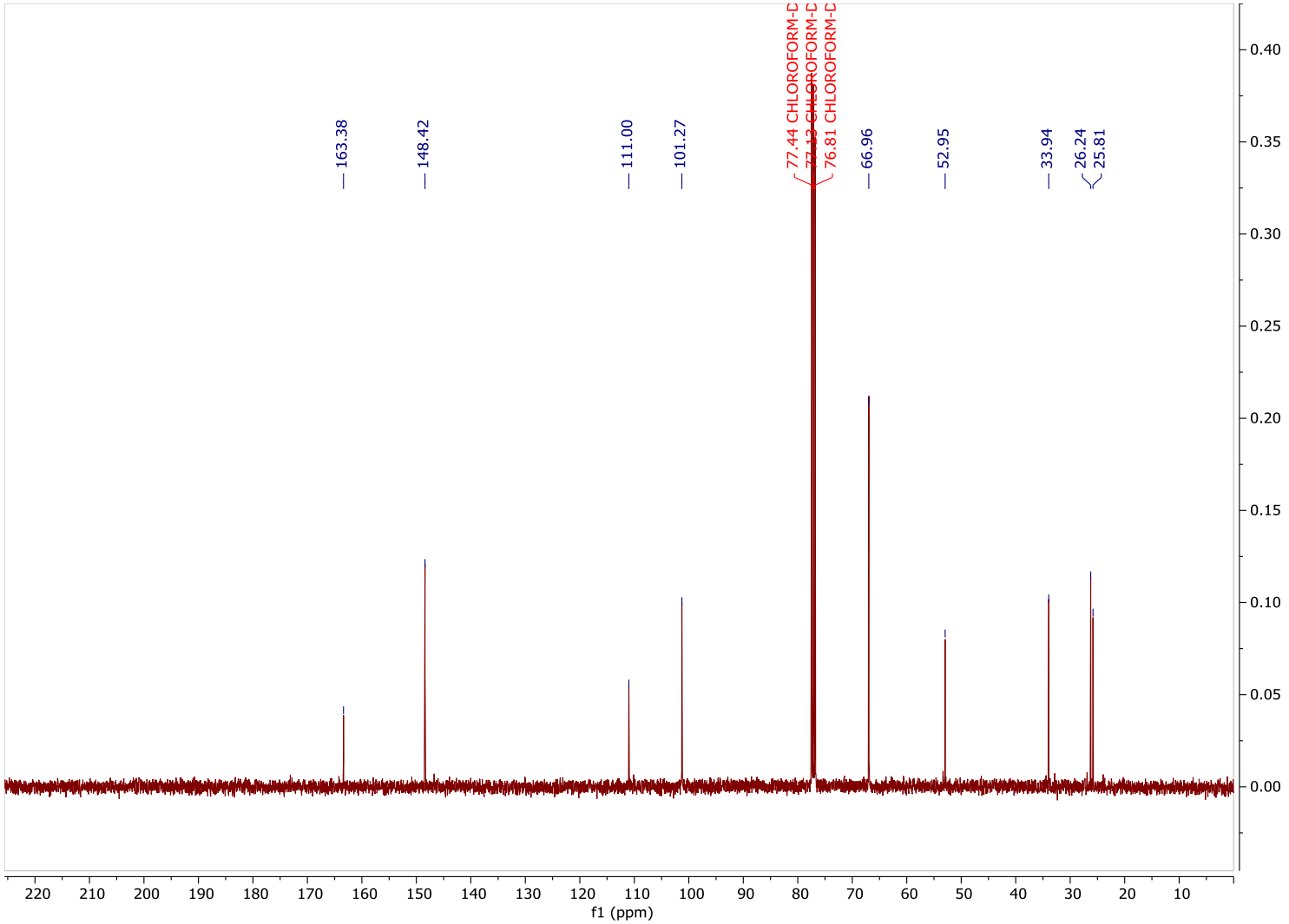

*Figure A.2.11 ^{13}C NMR spectrum of **2.28** in $CDCl_3$.*

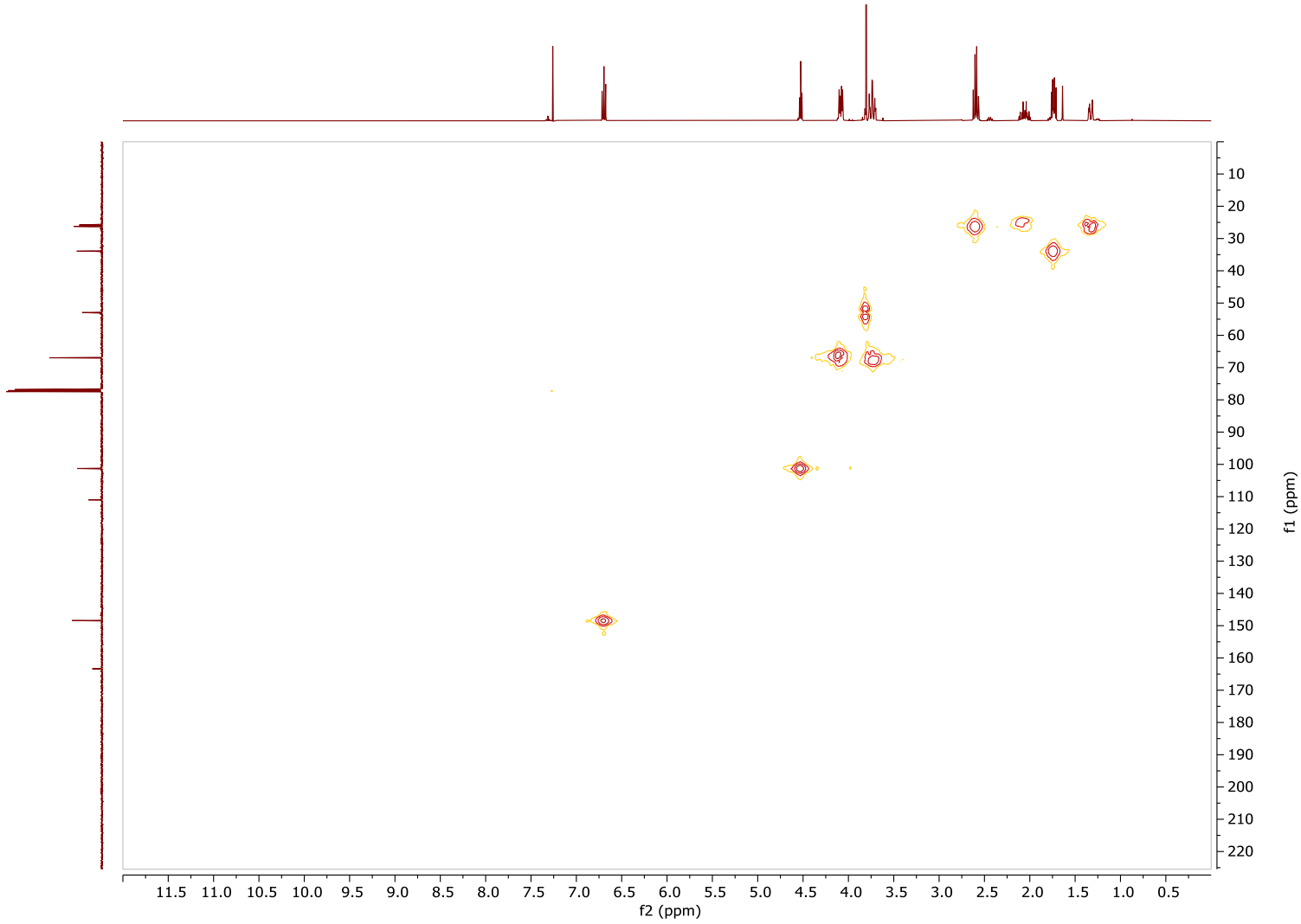

*Figure A.2.12 HMQC NMR spectrum of **2.28** in $CDCl_3$.*

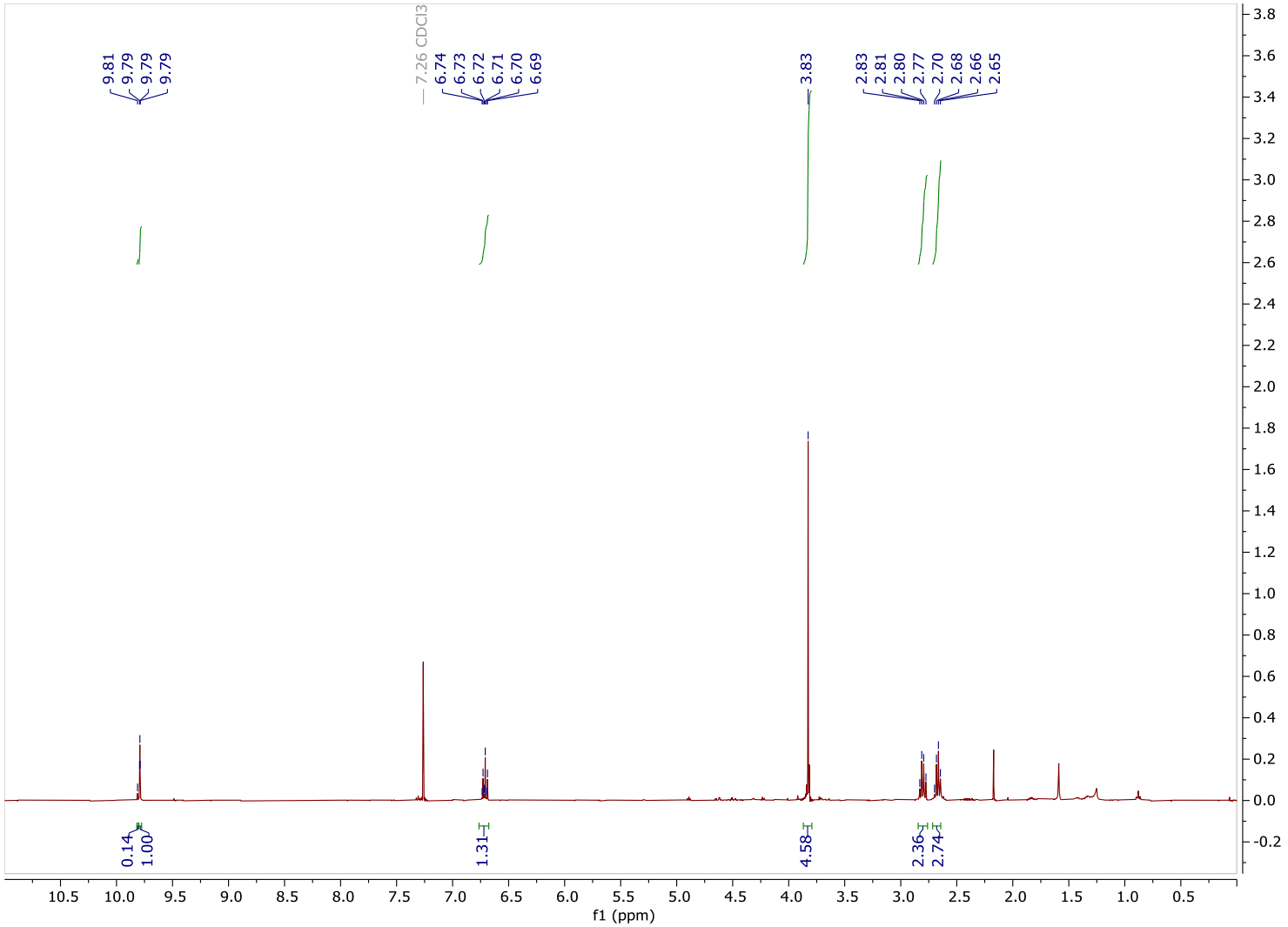

*Figure A.2.13 ^{1}H NMR spectrum of **2.29** in $CDCl_3$.*

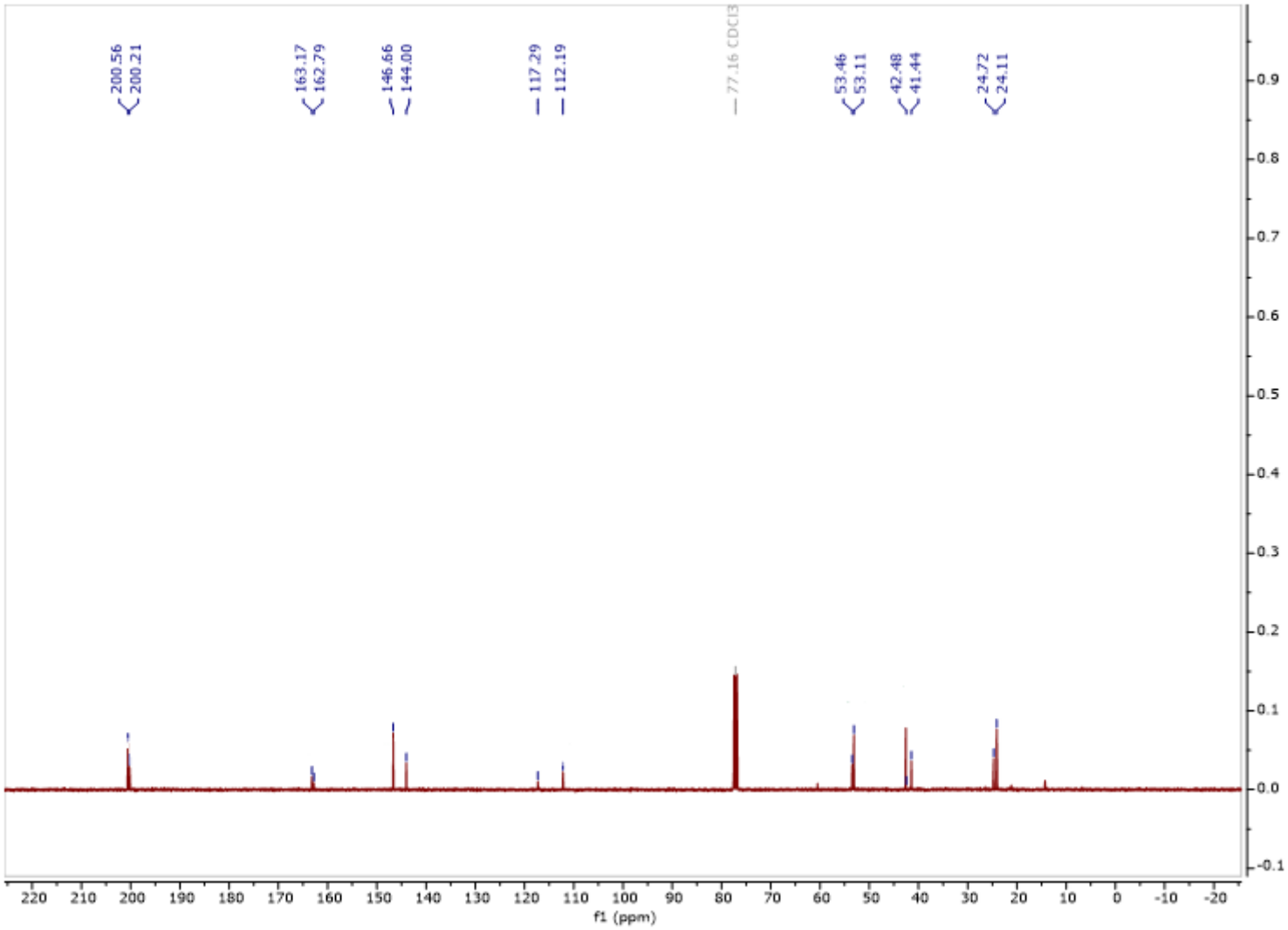

*Figure A.2.14 ^{13}C NMR spectrum of **2.29** in $CDCl_3$.*

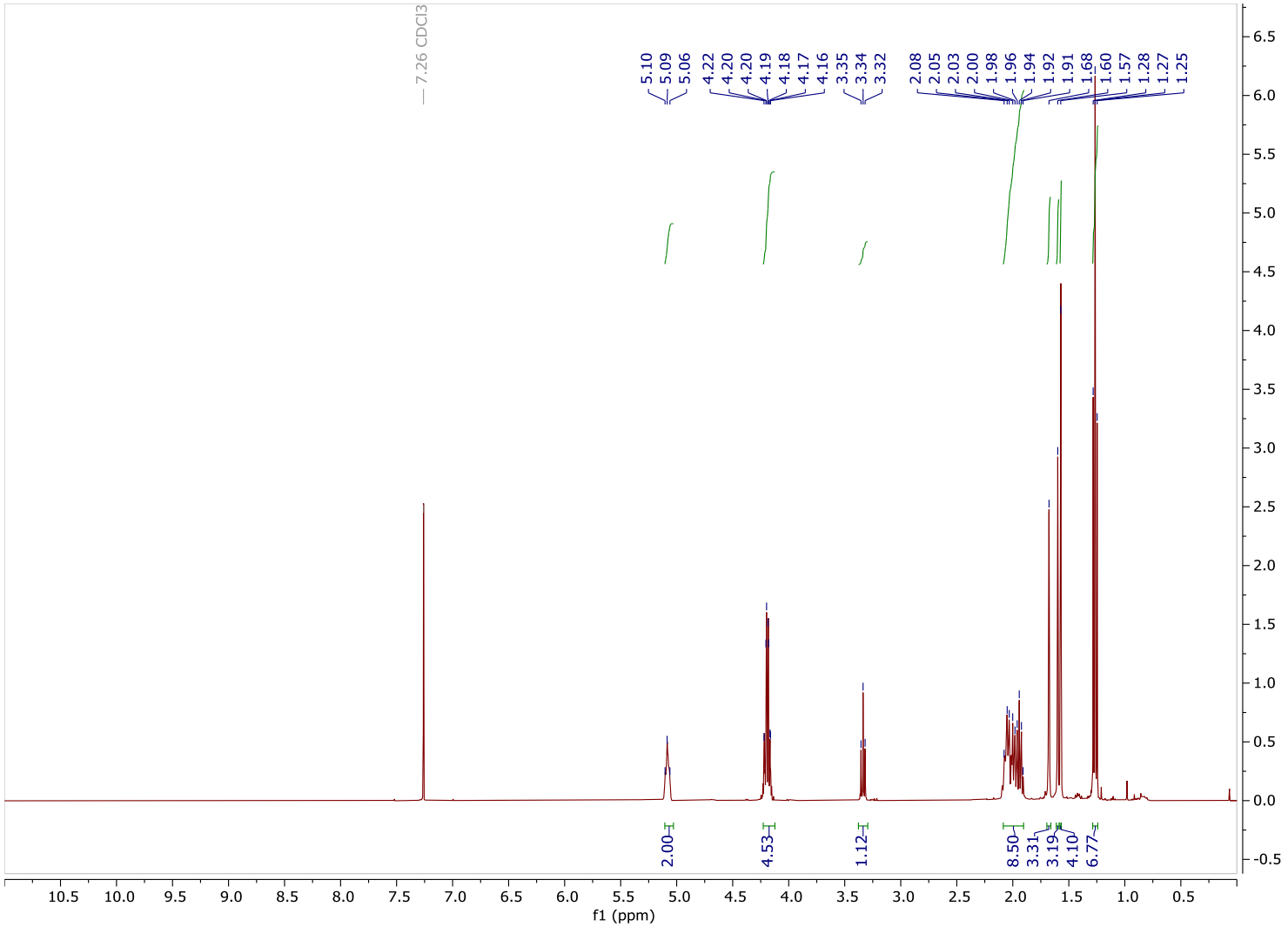

*Figure A.2.15 ^{1}H NMR spectrum of **2.50** in $CDCl_3$.*

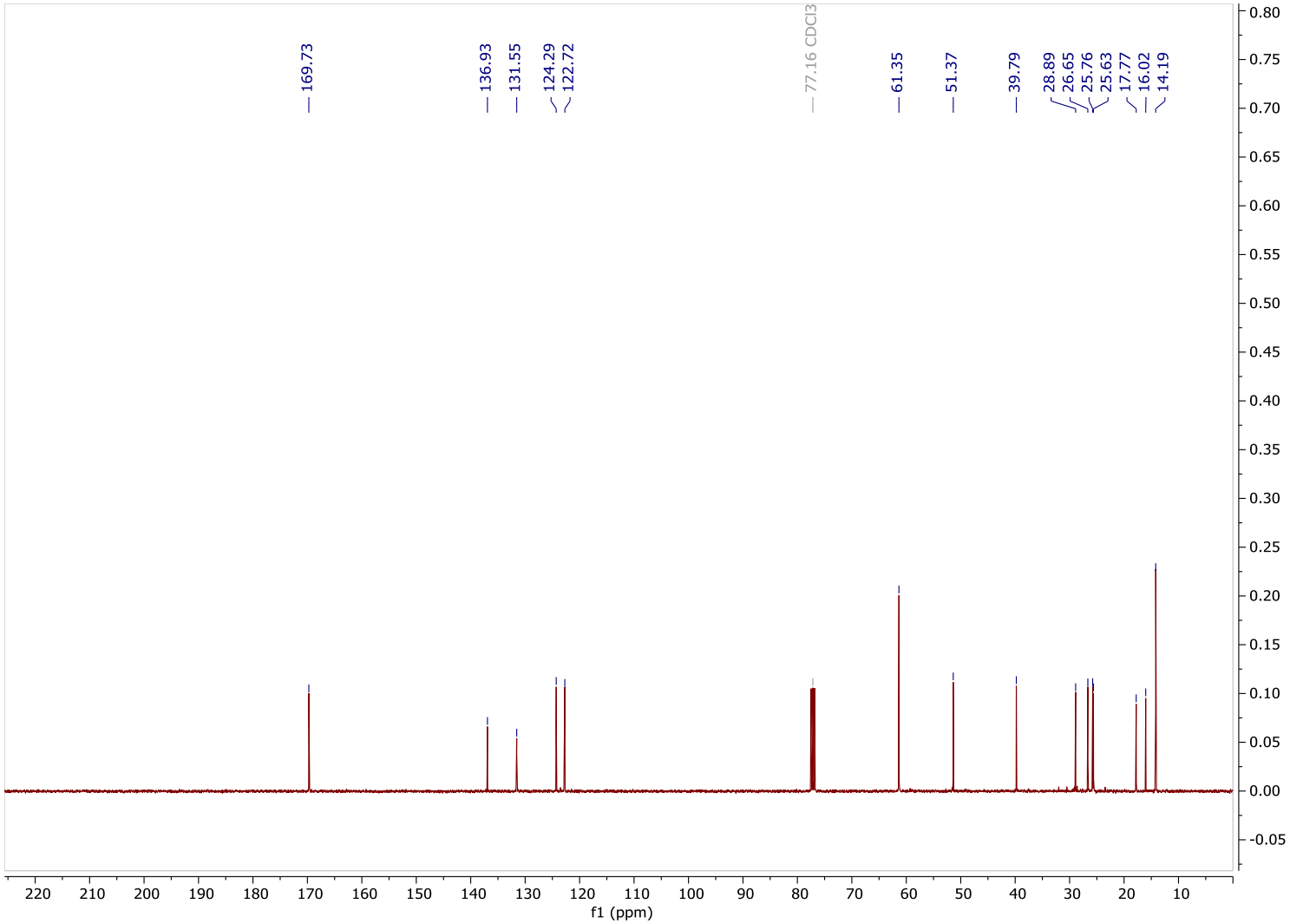

*Figure A.2.16 ^{13}C NMR spectrum of **2.50** in $CDCl_3$.*

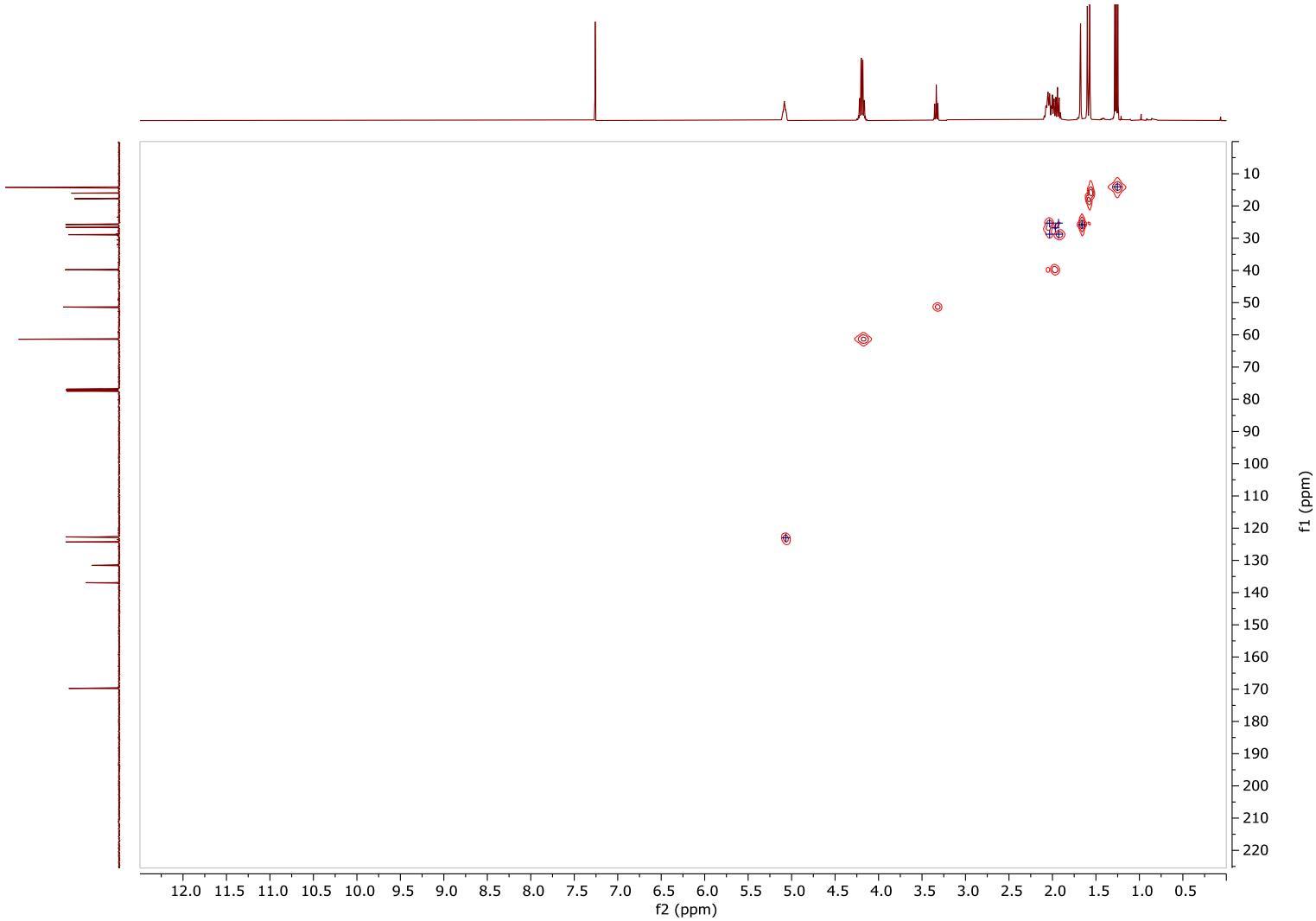

*Figure A.2.17 HMQC NMR spectrum of **2.50** in $CDCl_3$.*

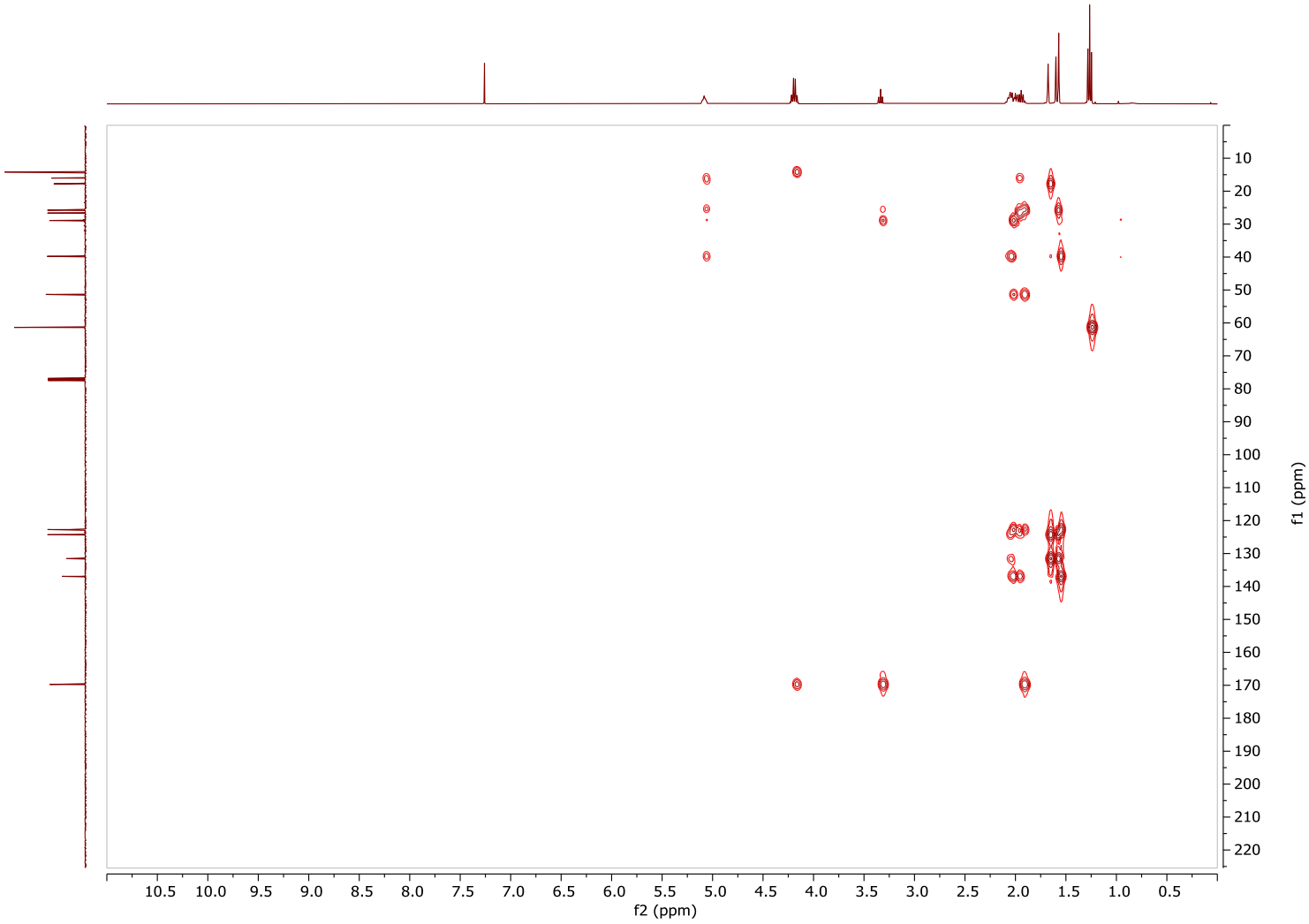

*Figure A.2.18 HMBC NMR spectrum of **2.50** in $CDCl_3$.*

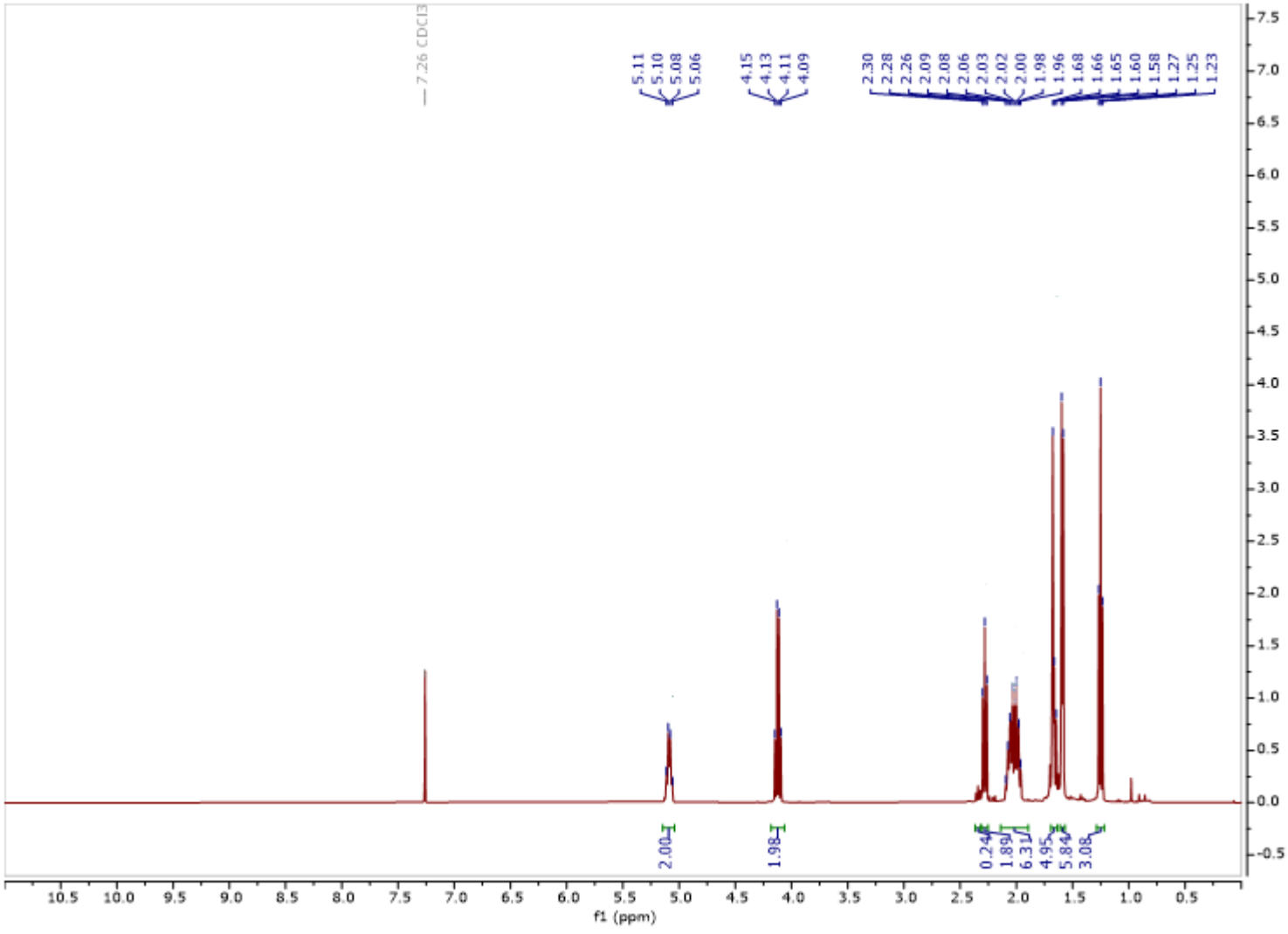

h

*Figure A.2.19 ^{1}H NMR spectrum of **2.39** in $CDCl_3$.*

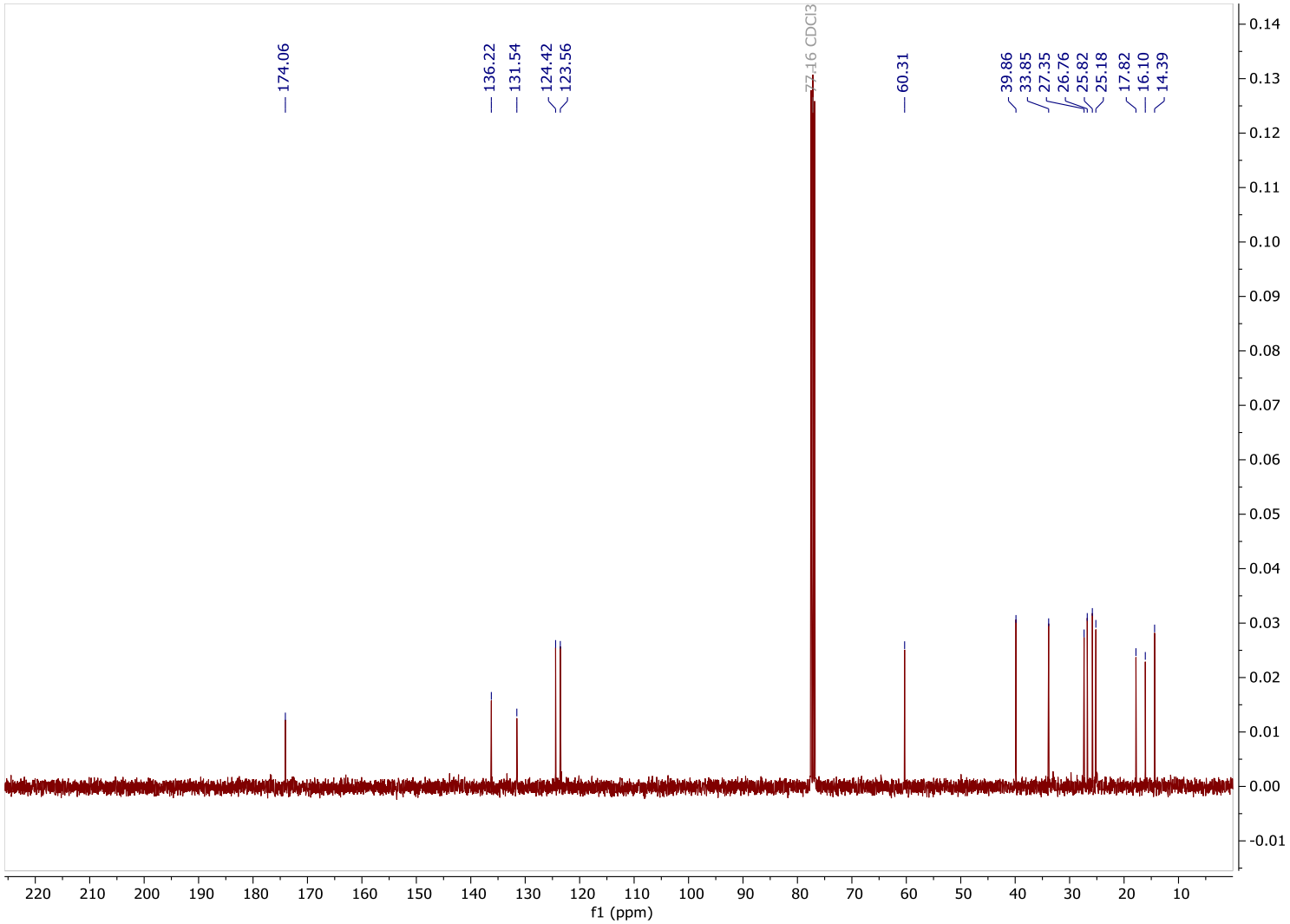

*Figure A.2.20 ^{13}C NMR spectrum of **2.39** in $CDCl_3$.*

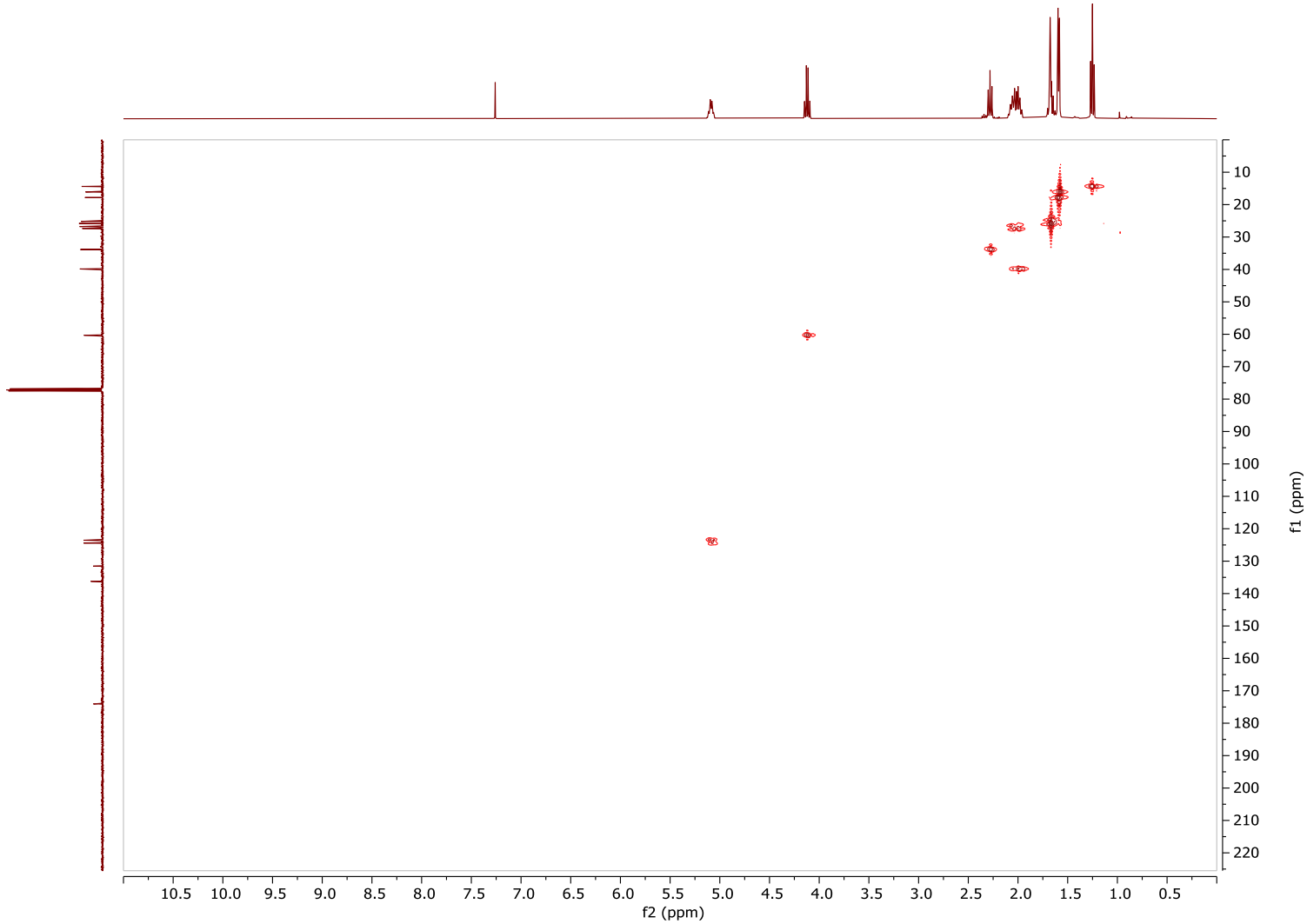

*Figure A.2.21 HMQC NMR spectrum of **2.39** in $CDCl_3$.*

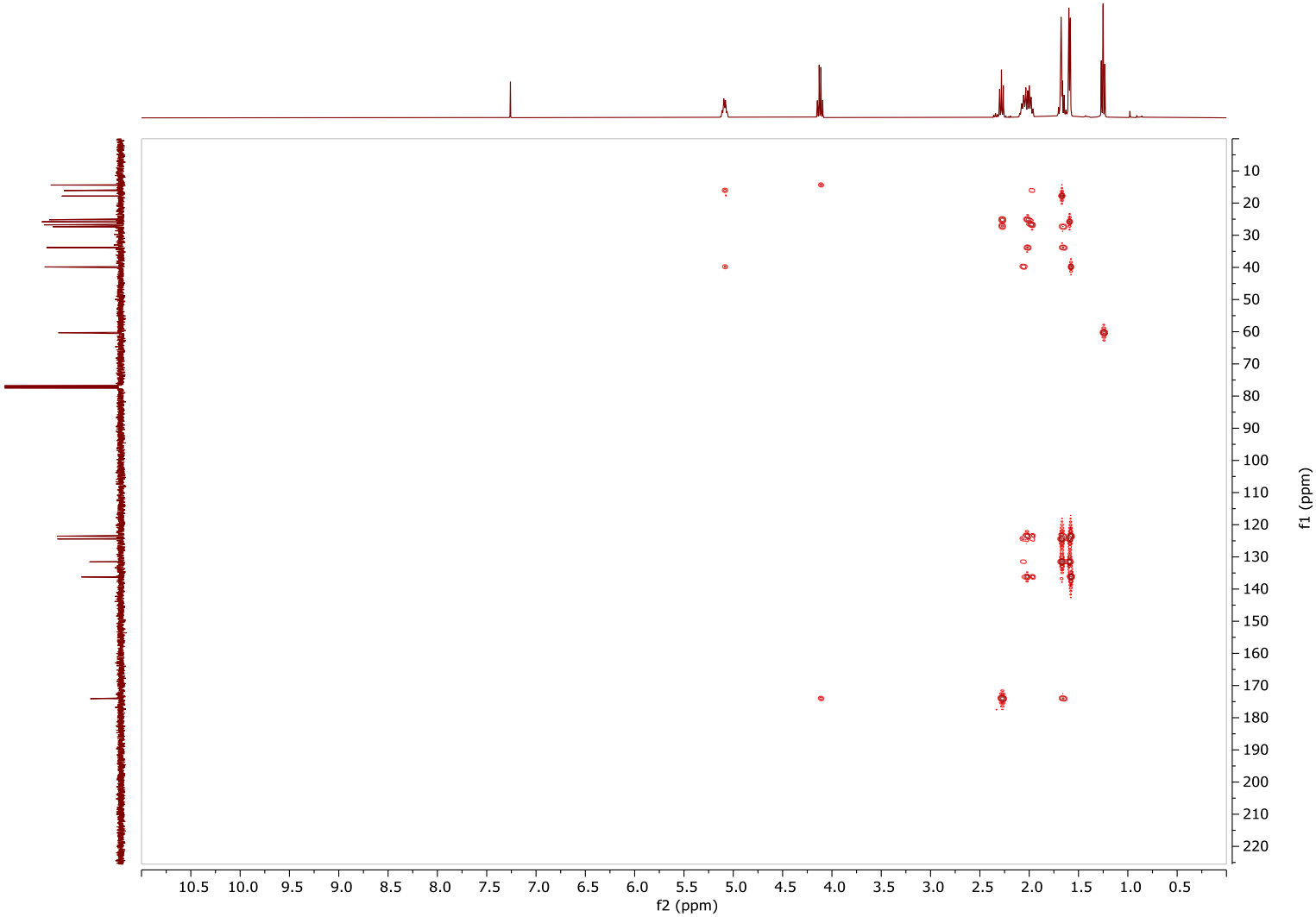

*Figure A.2.22 HMBC NMR spectrum of **2.39** in $CDCl_3$.*

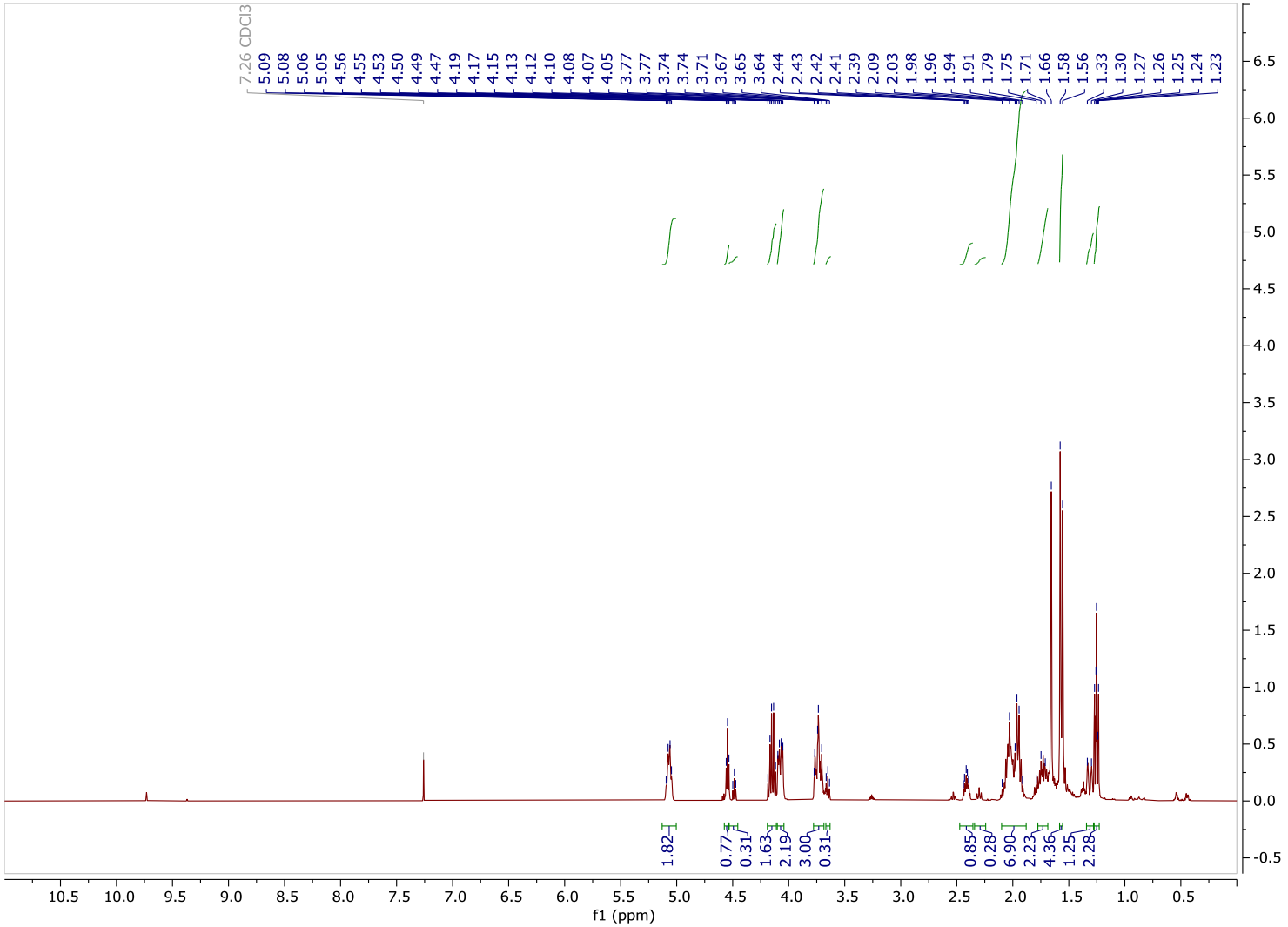

*Figure A.2.23 ^{1}H NMR spectrum of **2.51** in $CDCl_3$.*

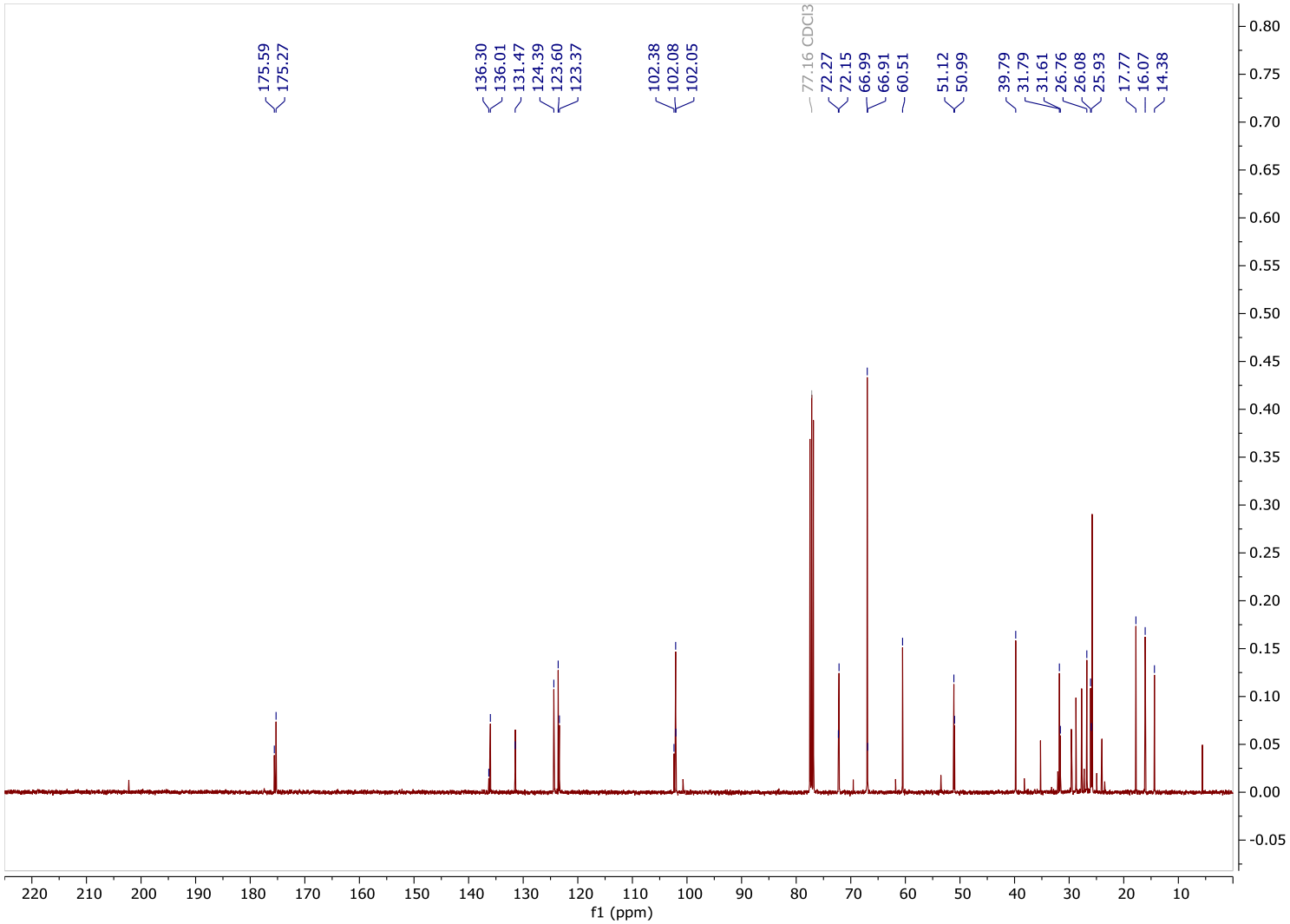

*Figure A.2.24 ^{13}C NMR spectrum of **2.51** in $CDCl_3$.*

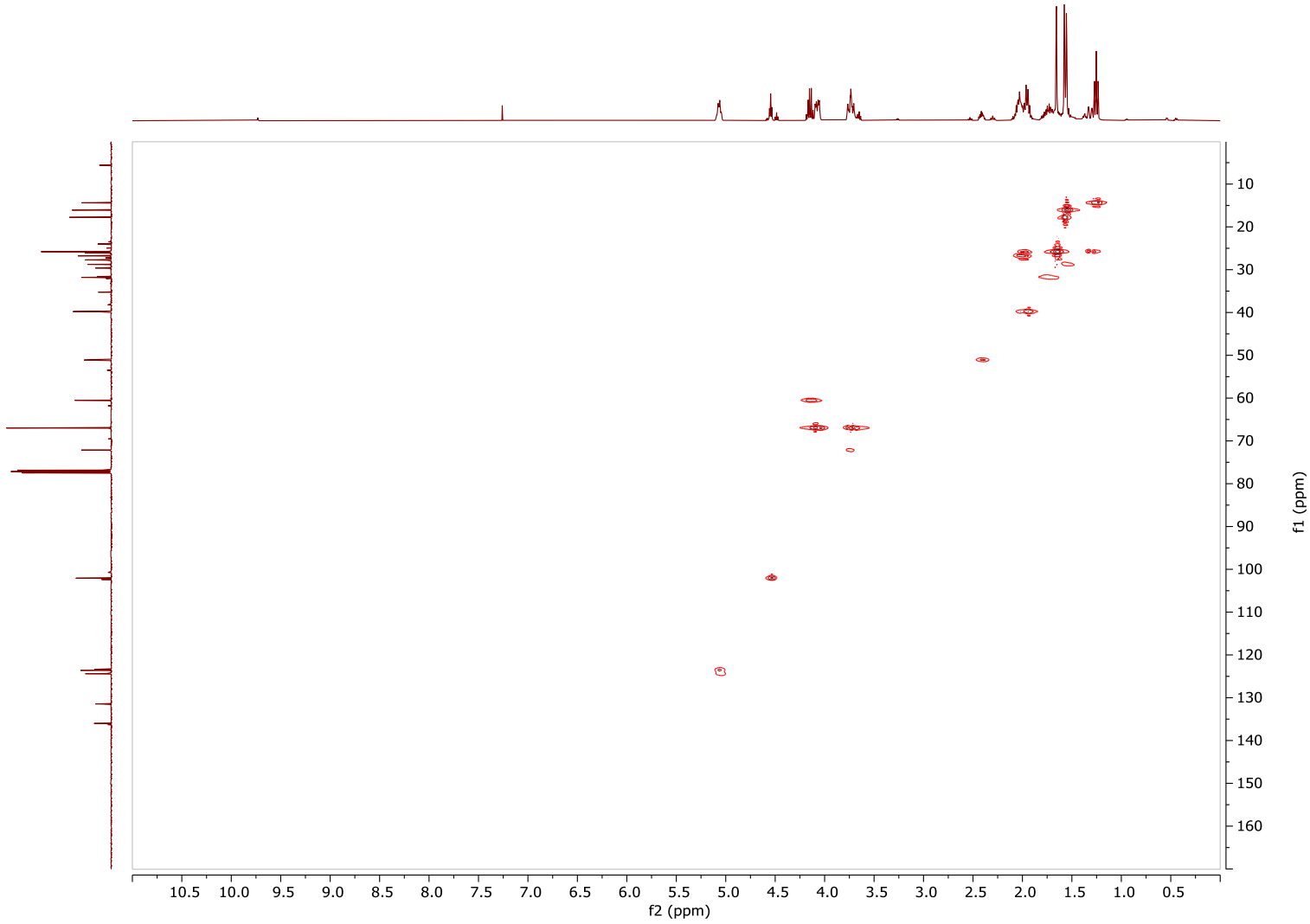

*Figure A.2.25 HMQC NMR spectrum of **2.51** in $CDCl_3$.*

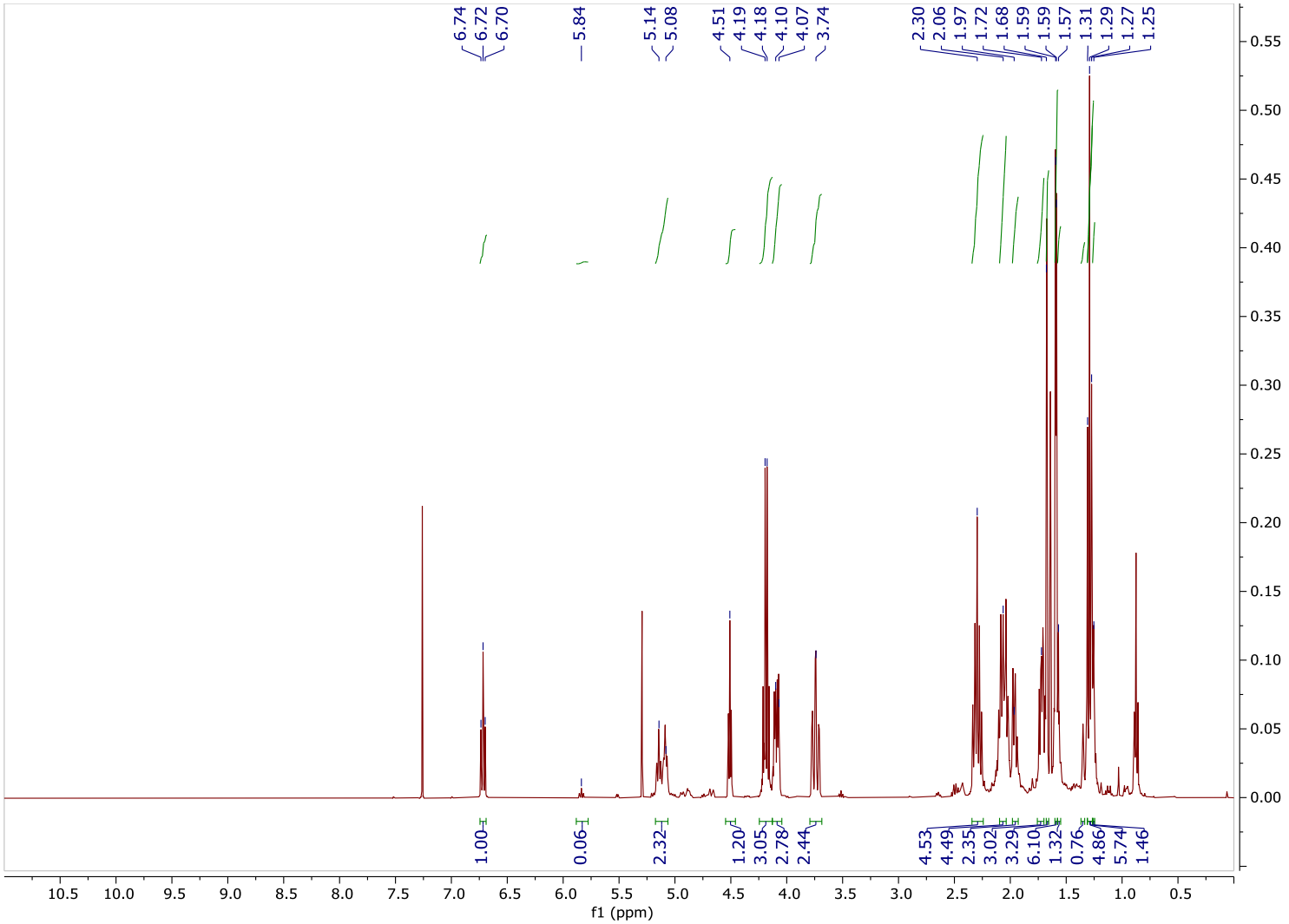

*Figure A.2.26 ^{1}H NMR spectrum of **2.52** in $CDCl_3$.*

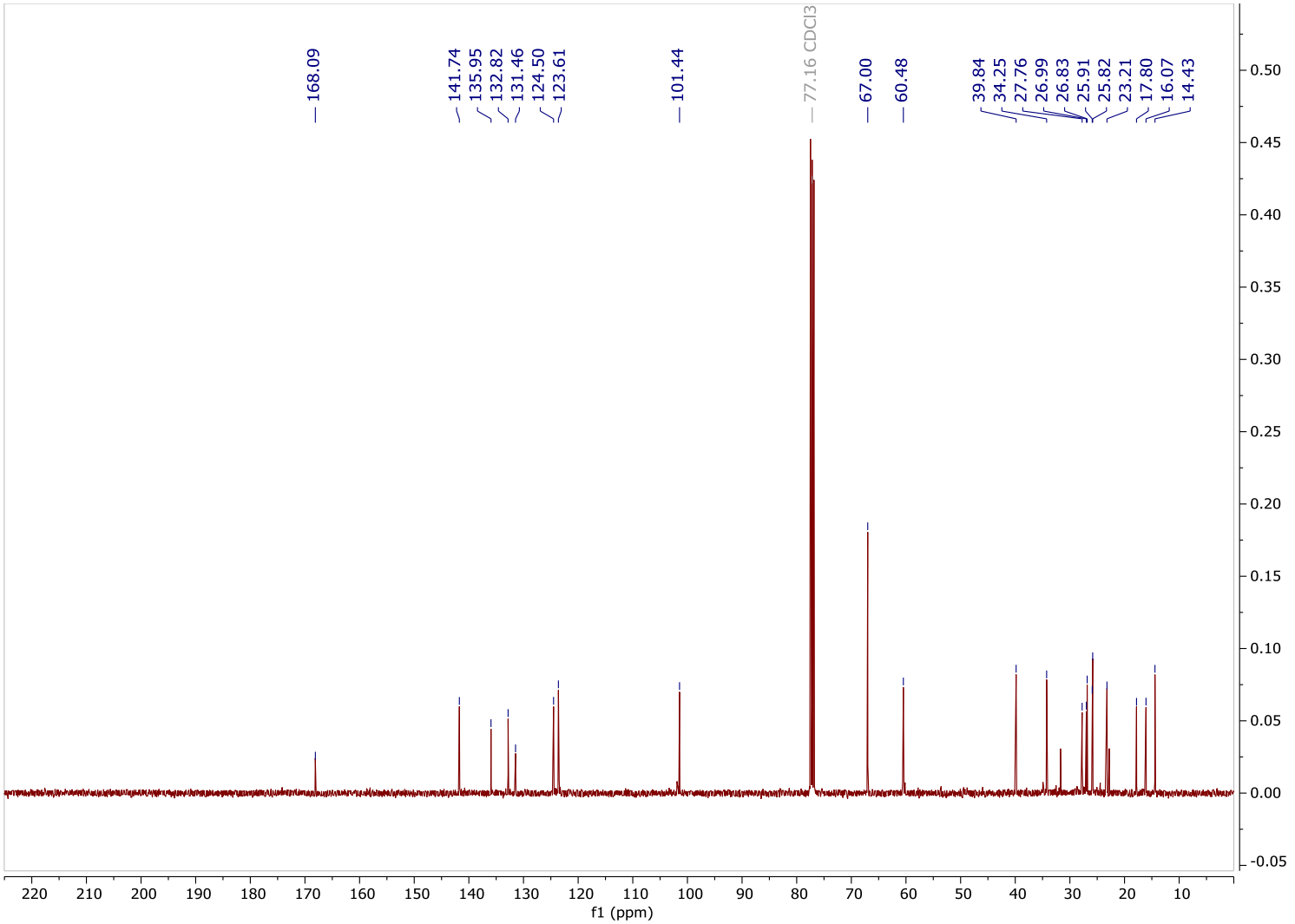

*Figure A.2.27 ^{13}C NMR spectrum of **2.52** in $CDCl_3$.*

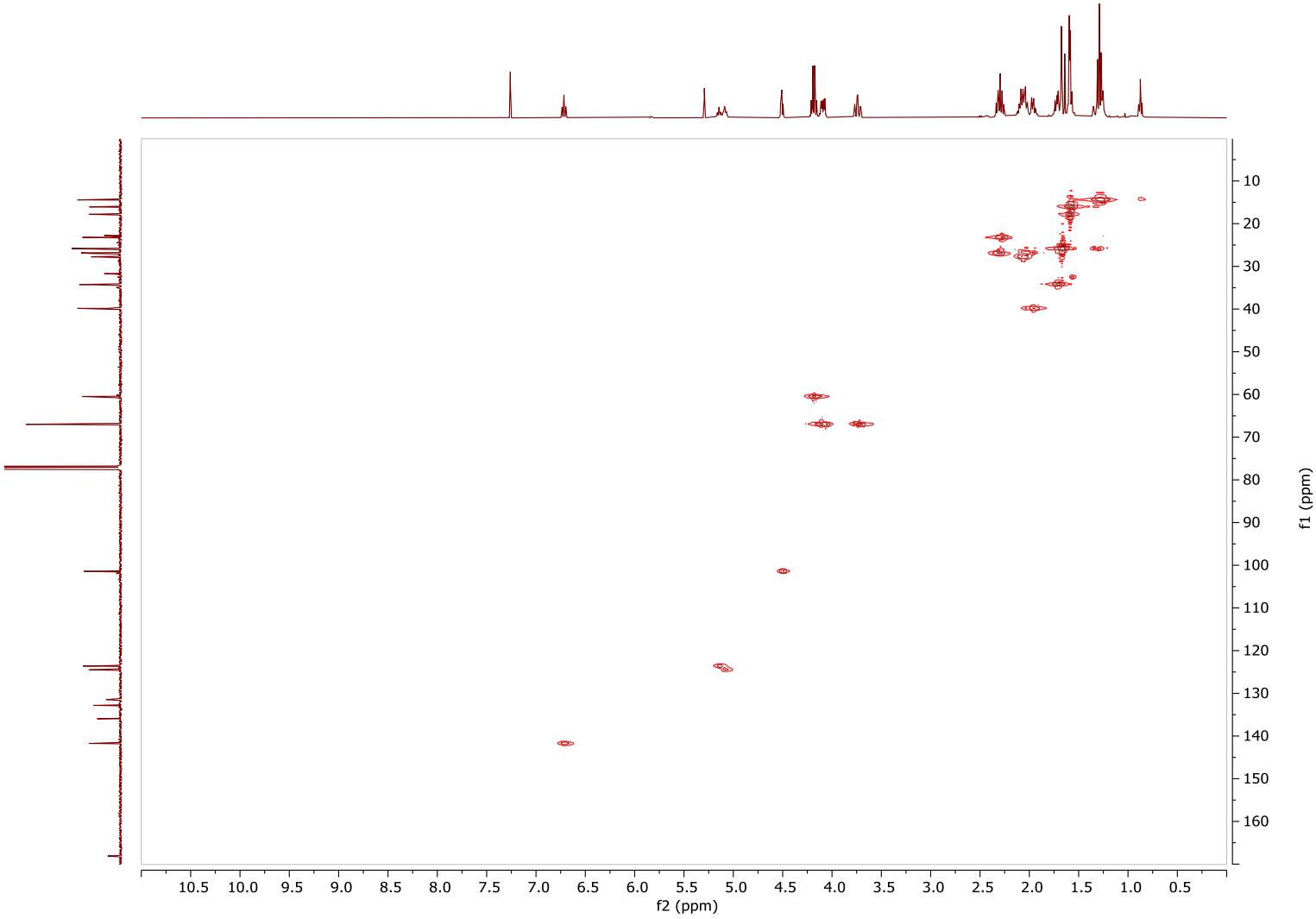

*Figure A.2.28 HMQC NMR spectrum of **2.51** in $CDCl_3$.*

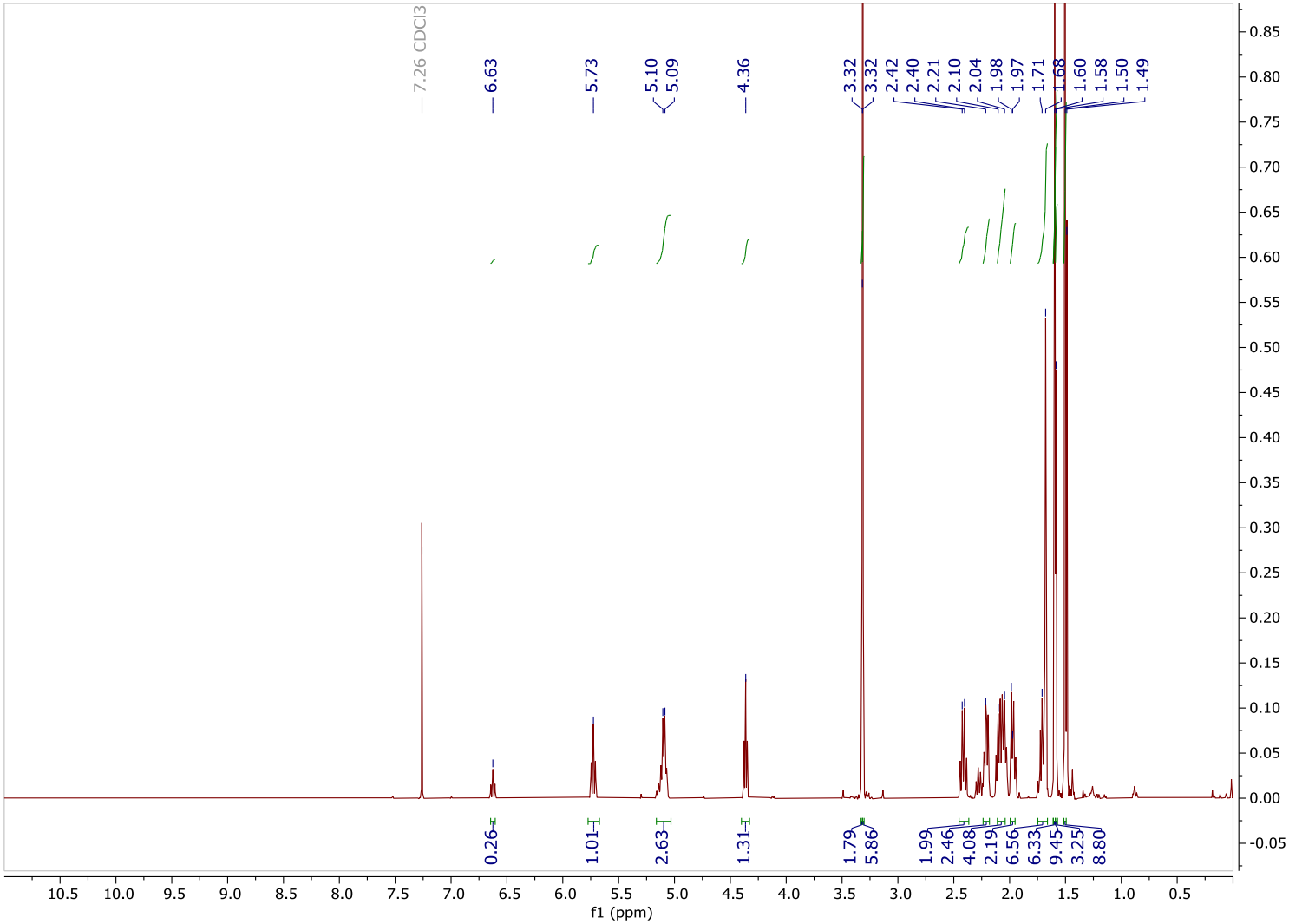

*Figure A.2.29 ^{1}H NMR spectrum of **2.37** in $CDCl_3$.*

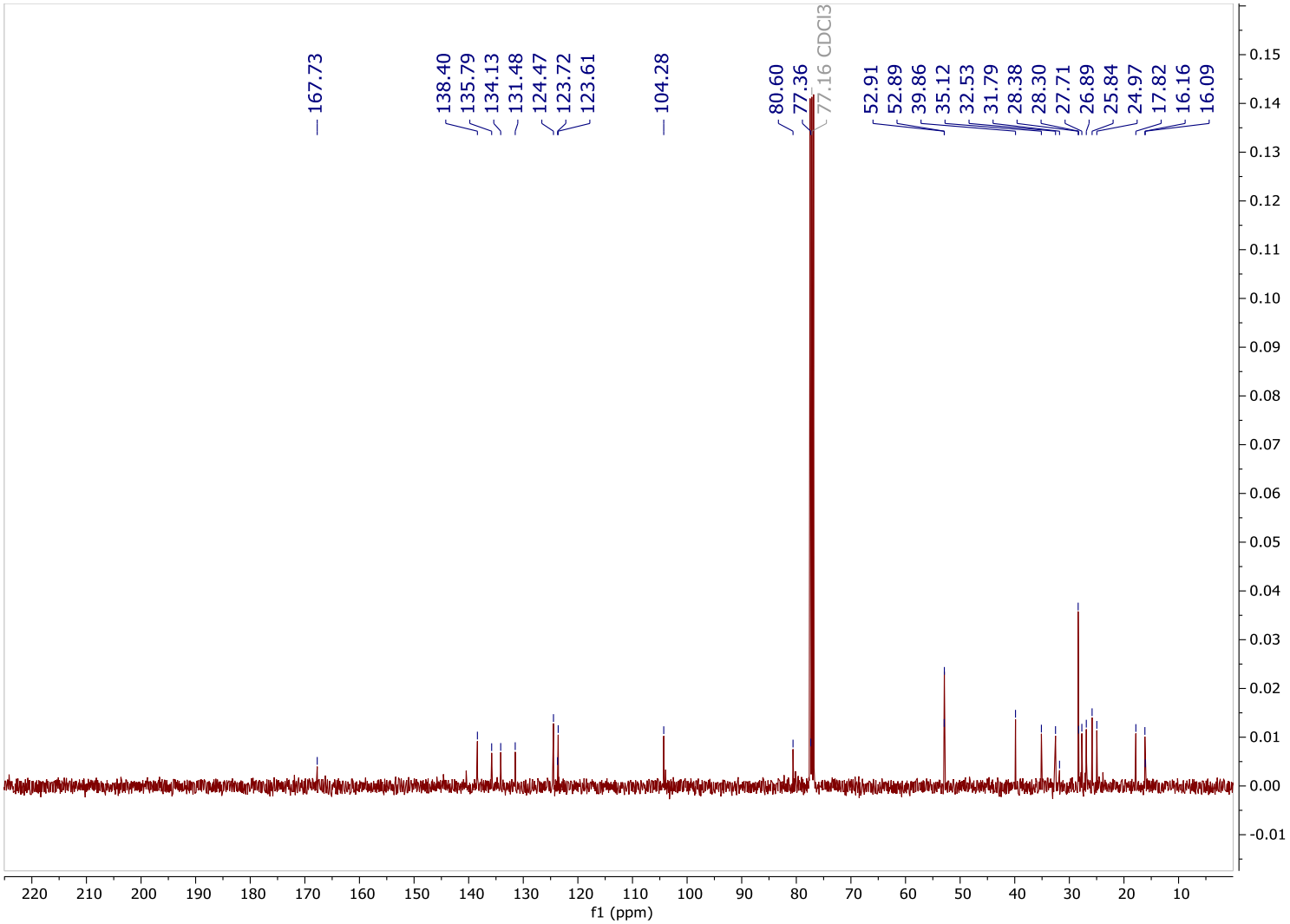

*Figure A.2.30 ^{13}C NMR spectrum of **2.37** in $CDCl_3$.*

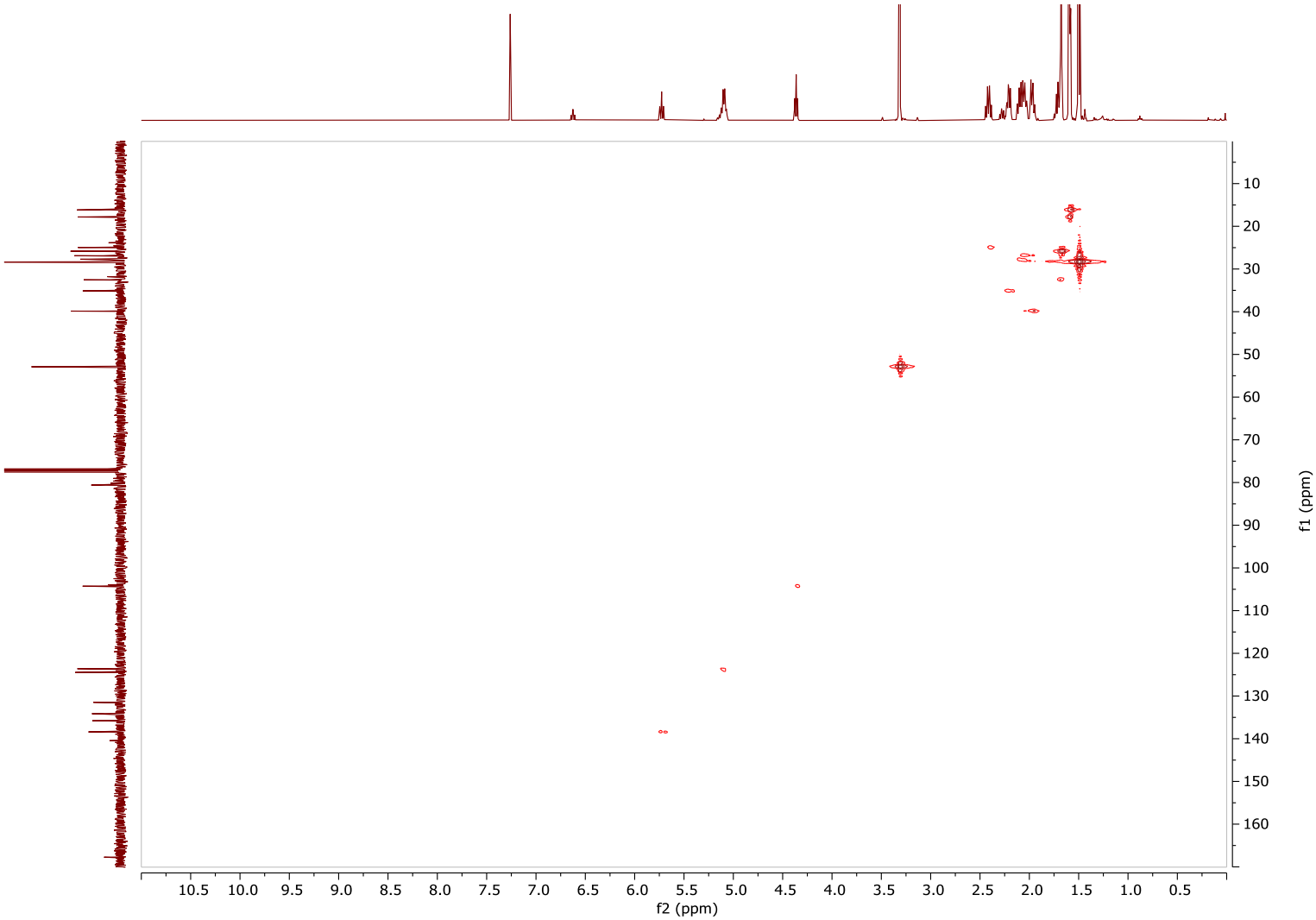

*Figure A.2.31 HMQC NMR spectrum of **2.37** in $CDCl_3$.*

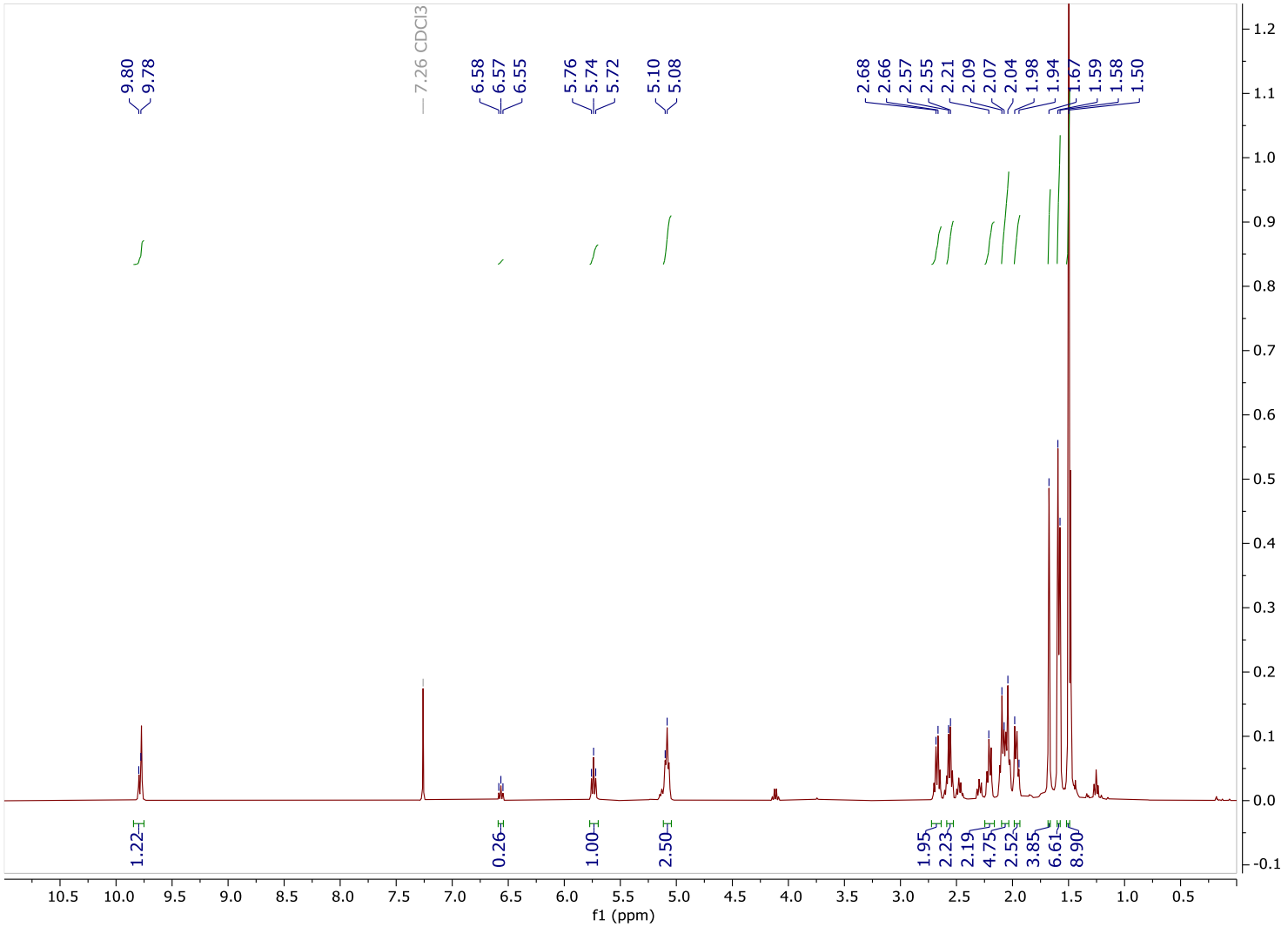

*Figure A.2.32 ^{1}H NMR spectrum of **2.38** in $CDCl_3$.*

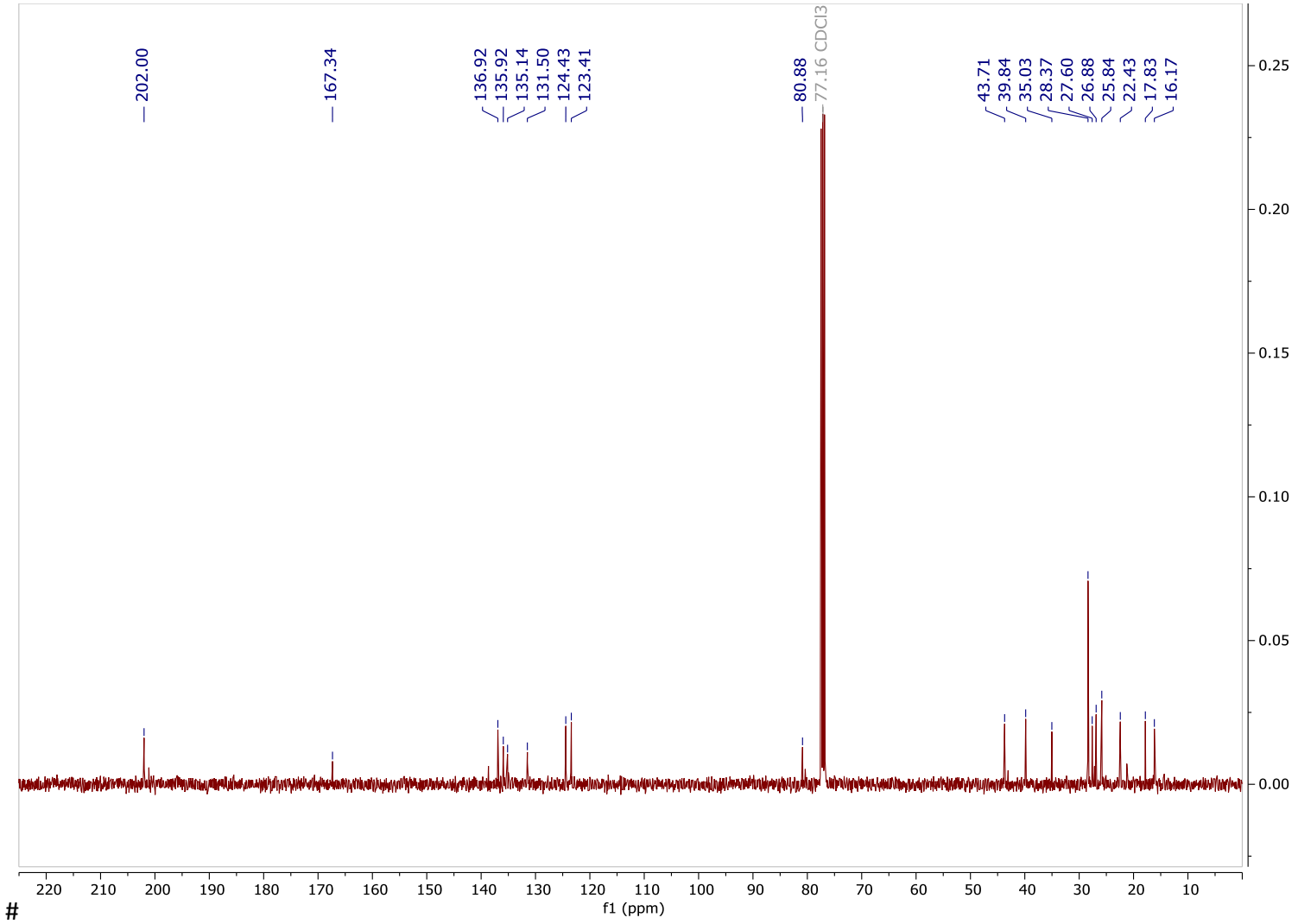

*Figure A.2.33 ^{13}C NMR spectrum of **2.38** in $CDCl_3$.*

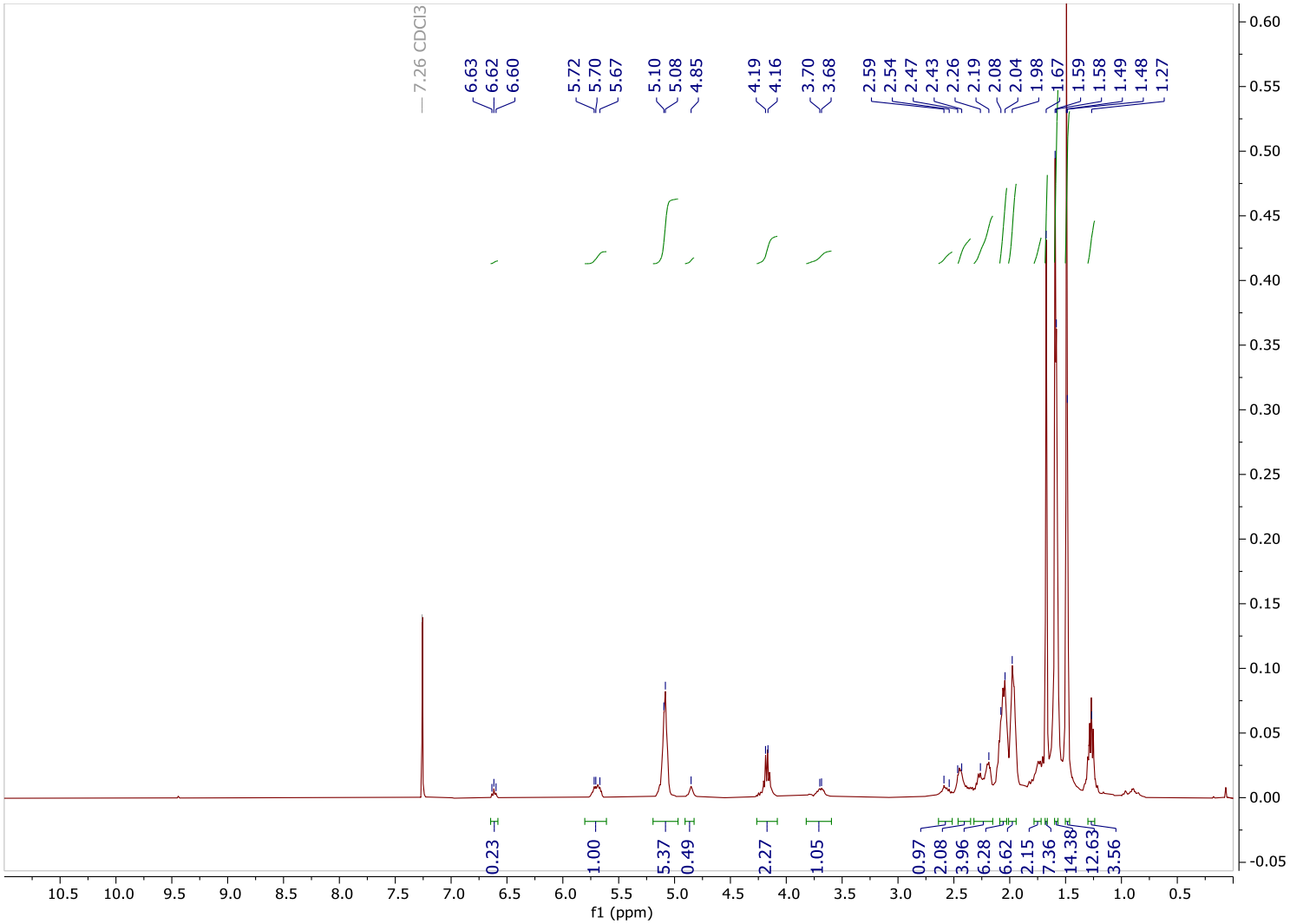

*Figure A.2.34 ^{1}H NMR spectrum of **2.42** in $CDCl_3$.*

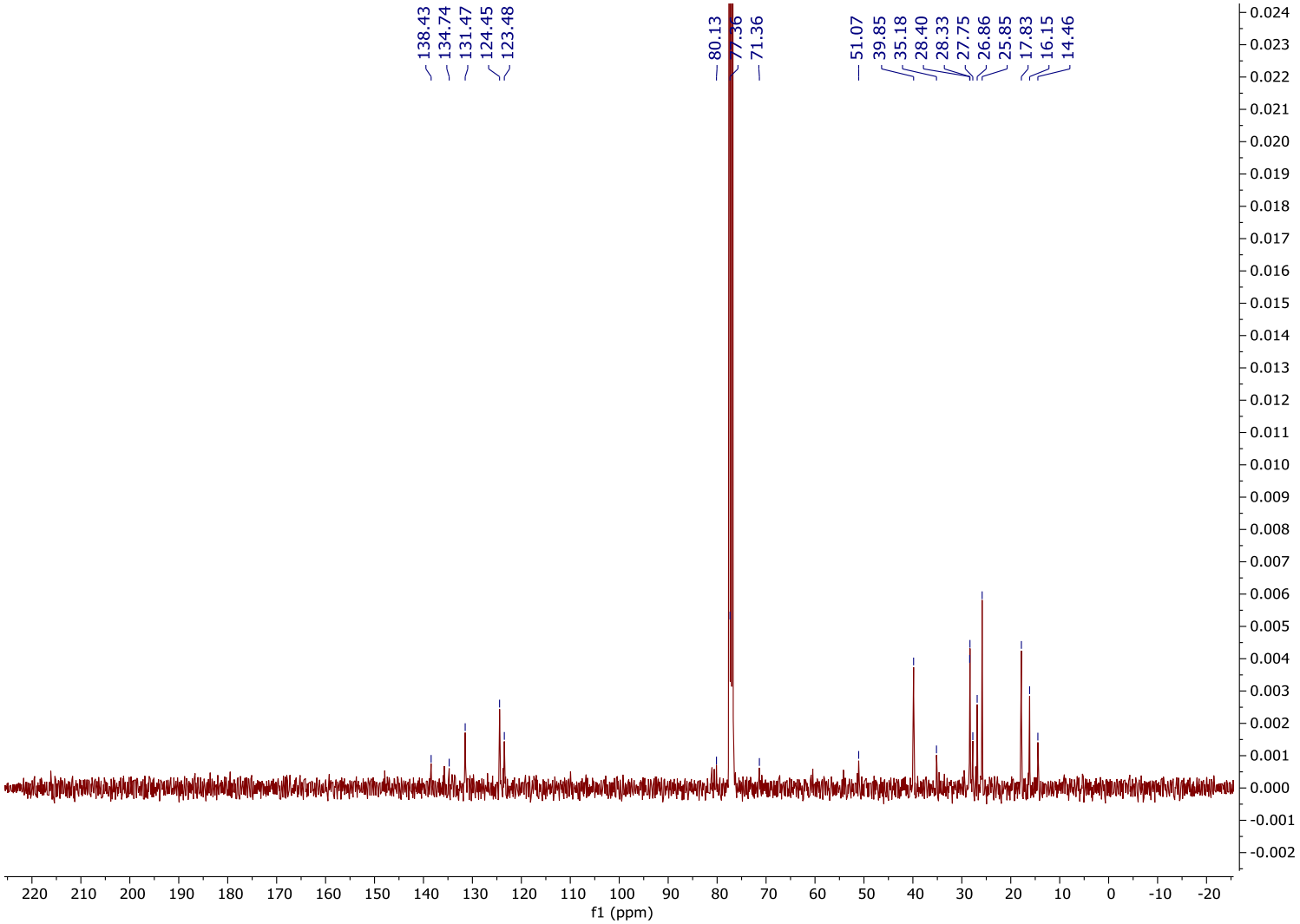

*Figure A.2.35 ^{13}C NMR spectrum of **2.42** in $CDCl_3$.*

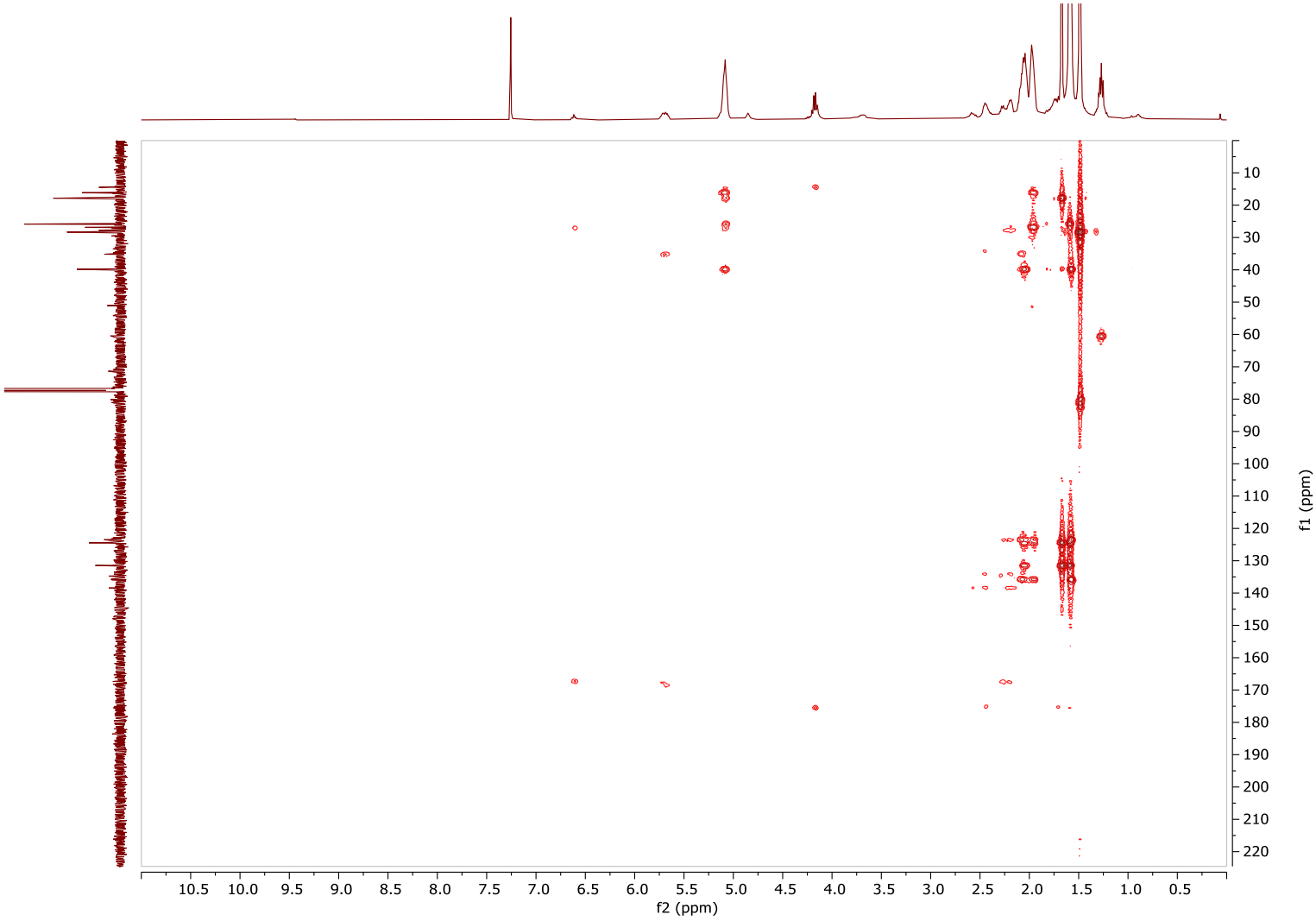

*Figure A.2.36 HMBC NMR spectrum of **2.42** in $CDCl_3$.*

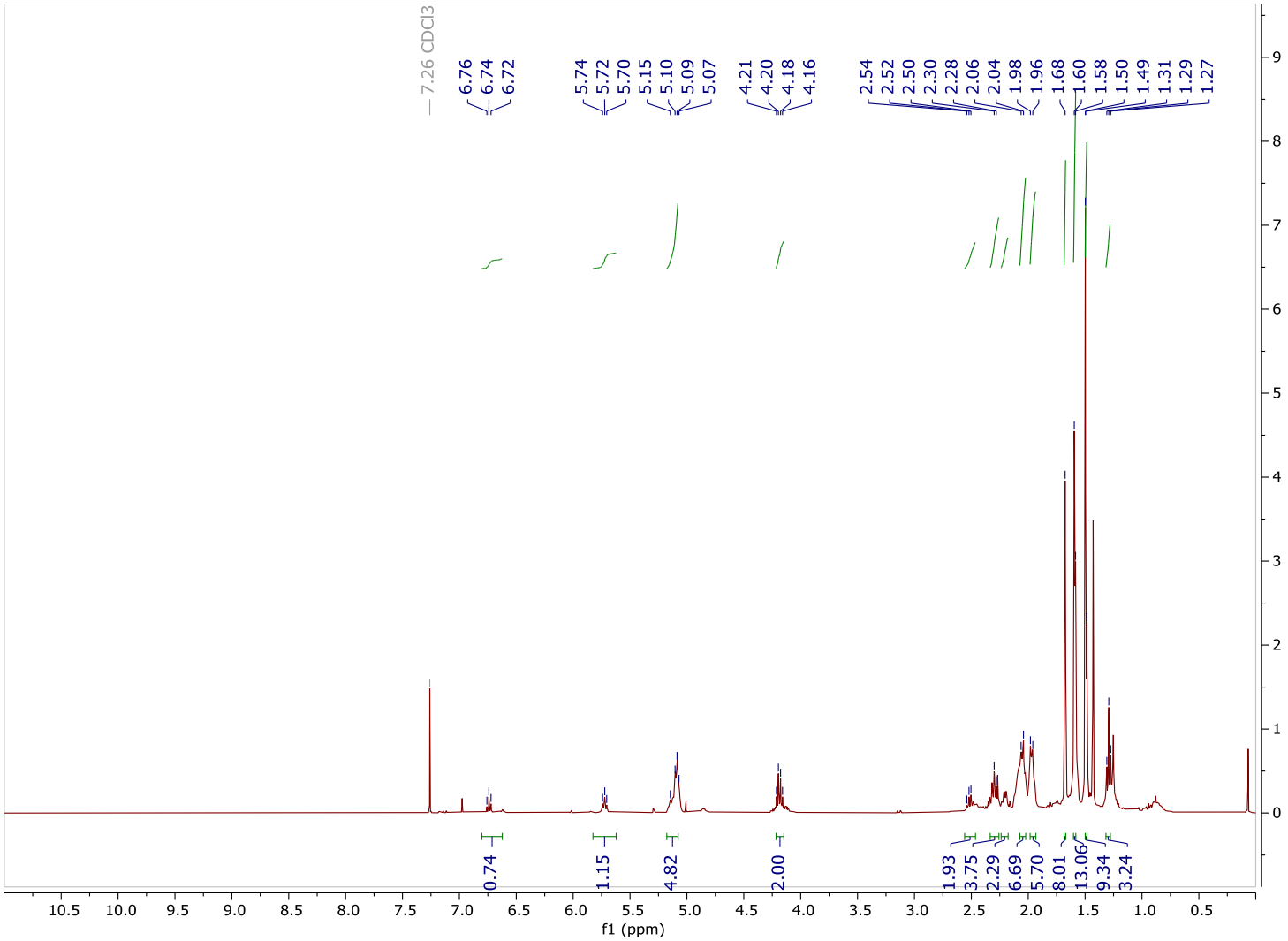

*Figure A.2.37 ^{1}H NMR spectrum of **2.43** in $CDCl_3$.*

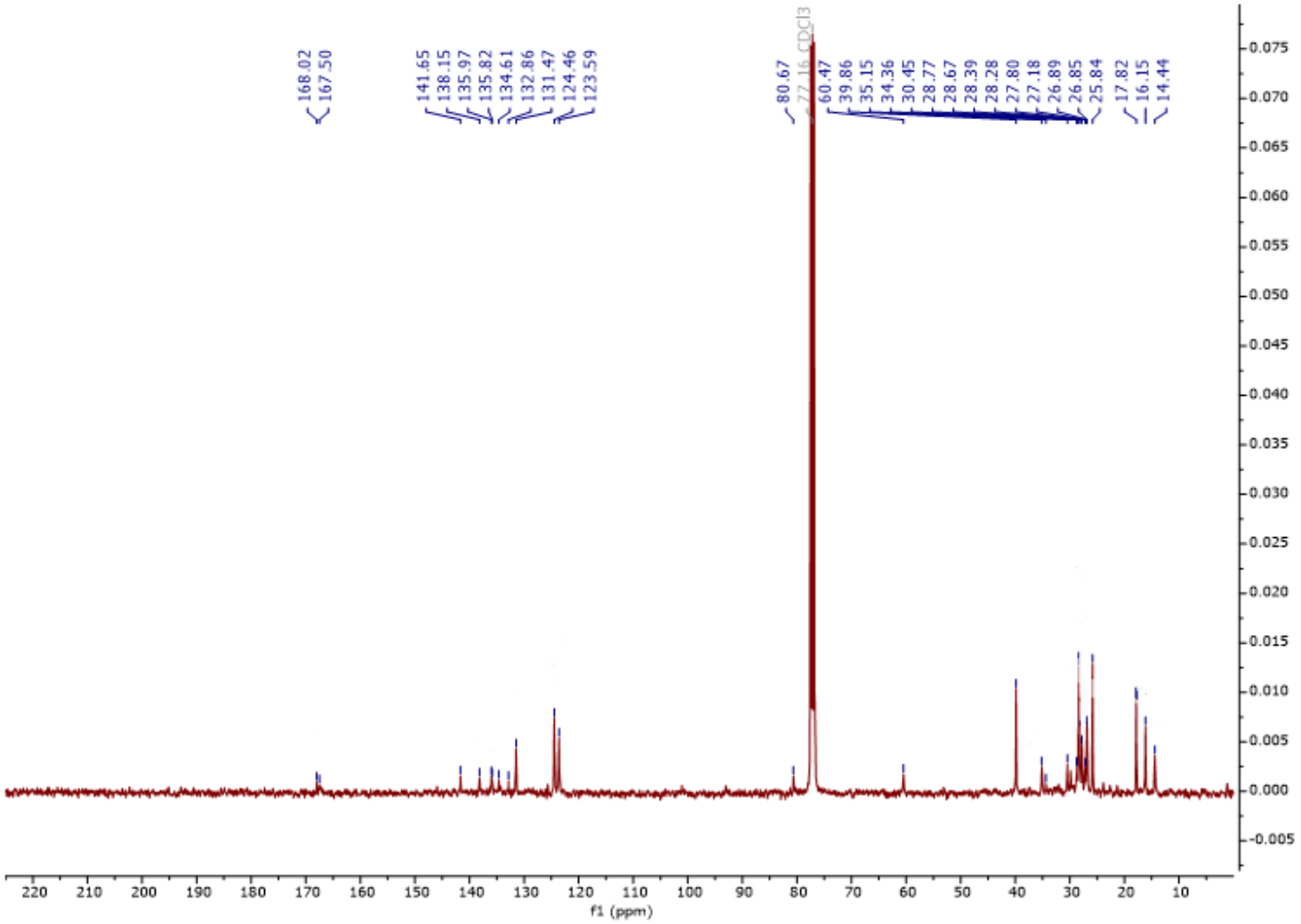

*Figure A.2.38 ^{13}C NMR spectrum of **2.43** in $CDCl_3$.*

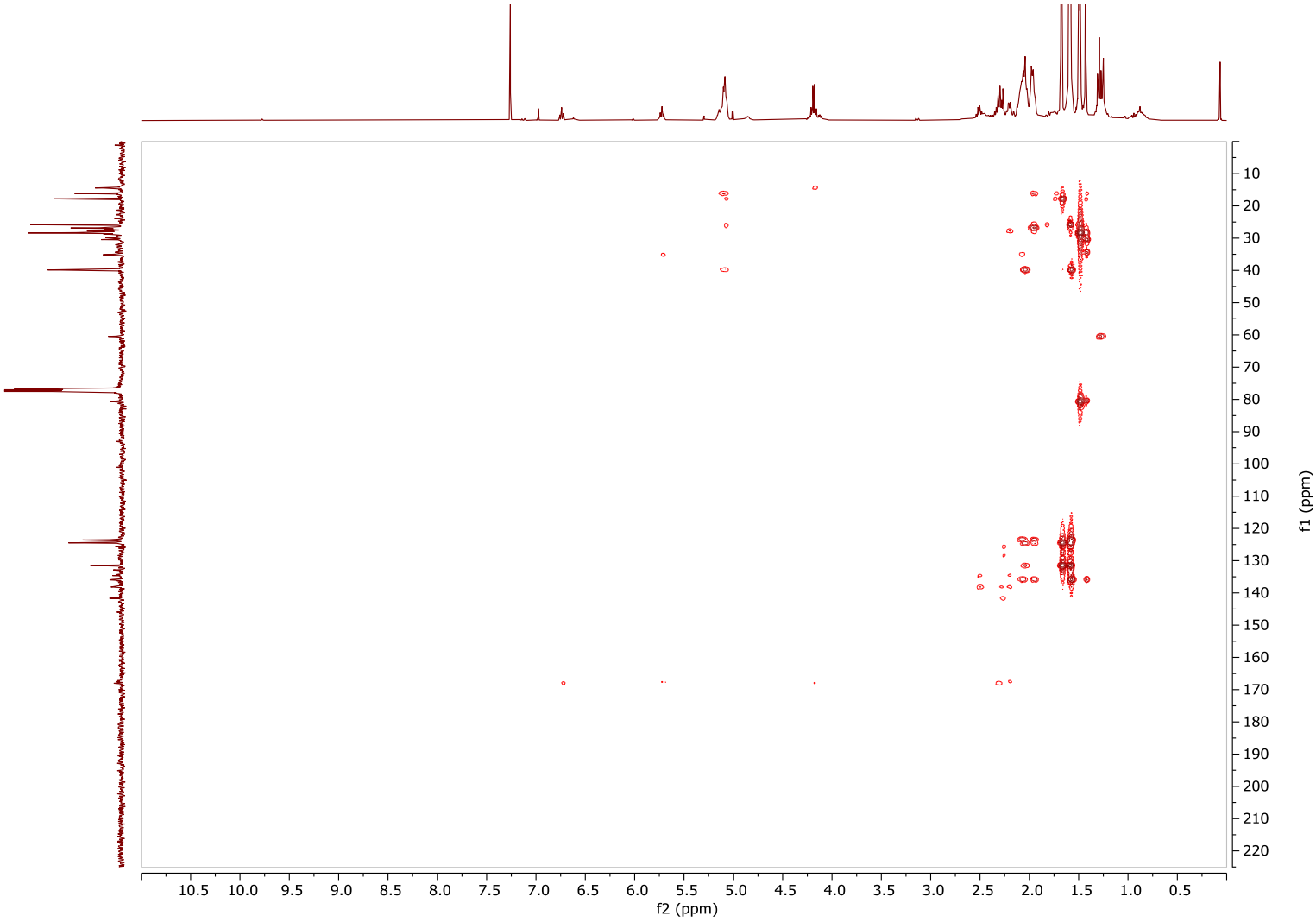

*Figure A.2.39 HMBC NMR spectrum of **2.43** in $CDCl_3$.*

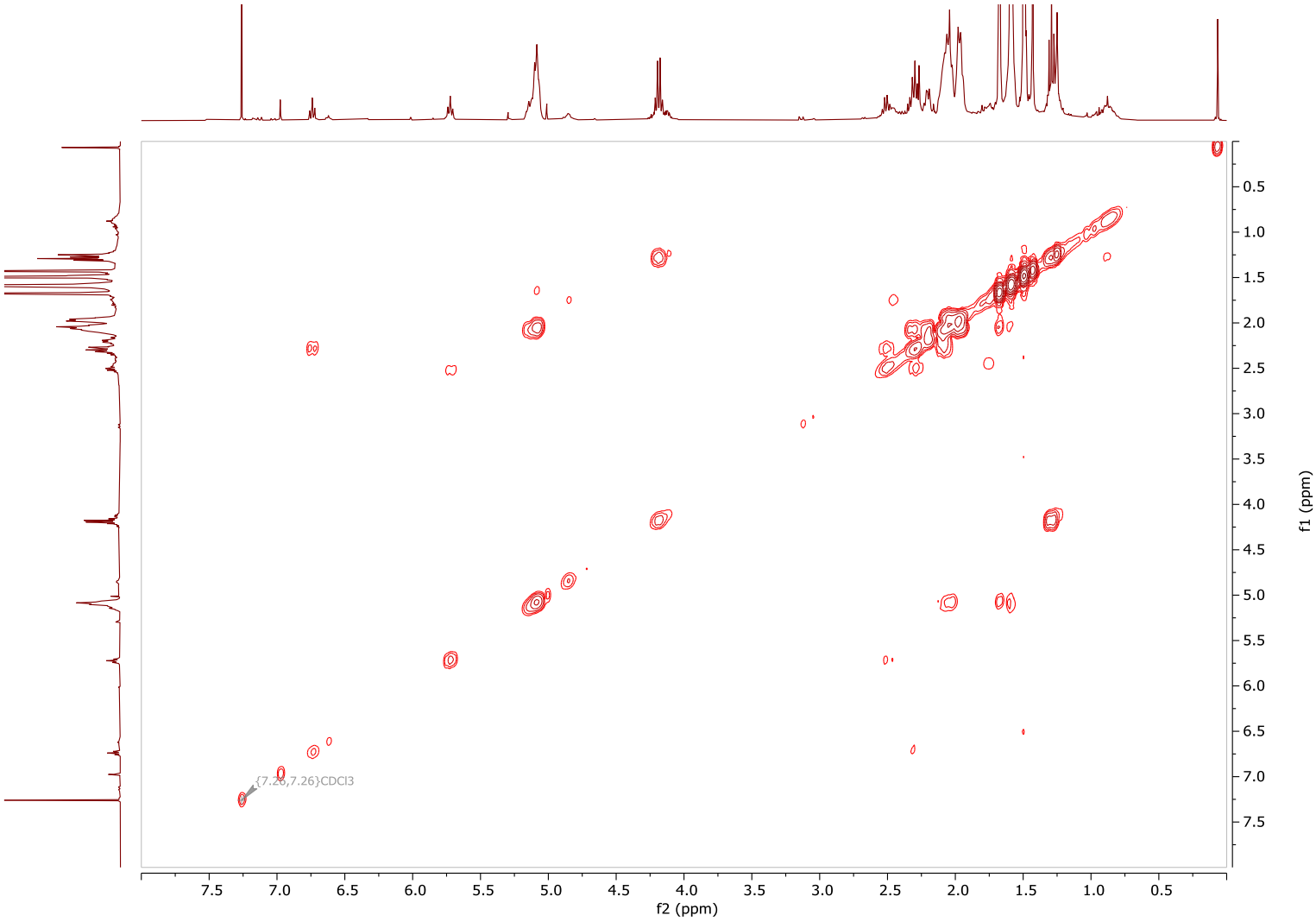

*Figure A.2.40 COSY NMR spectrum of **2.43** in $CDCl_3$.*

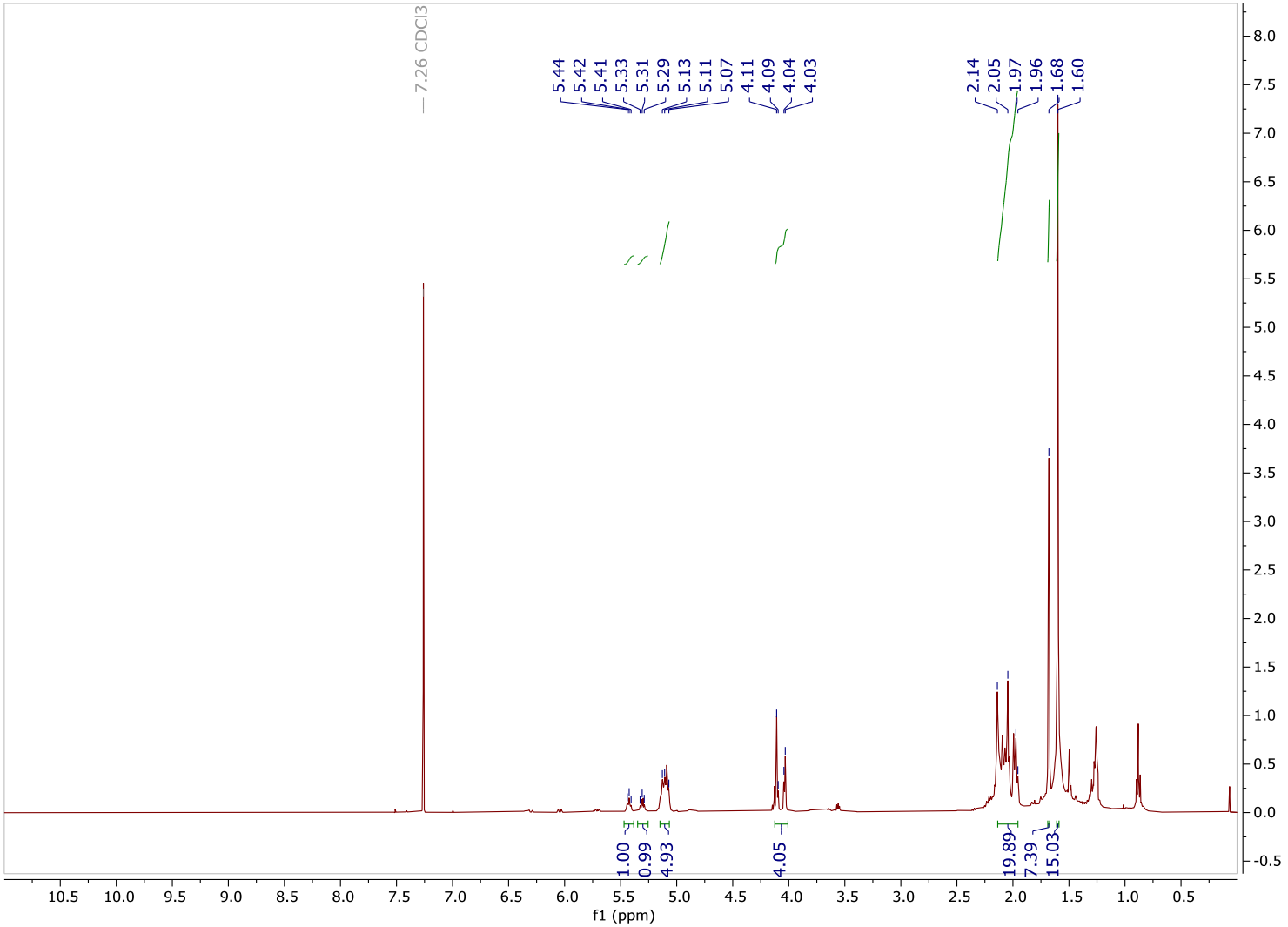

*Figure A.2.41 ^{1}H NMR spectrum of **1.97** in $CDCl_3$.*

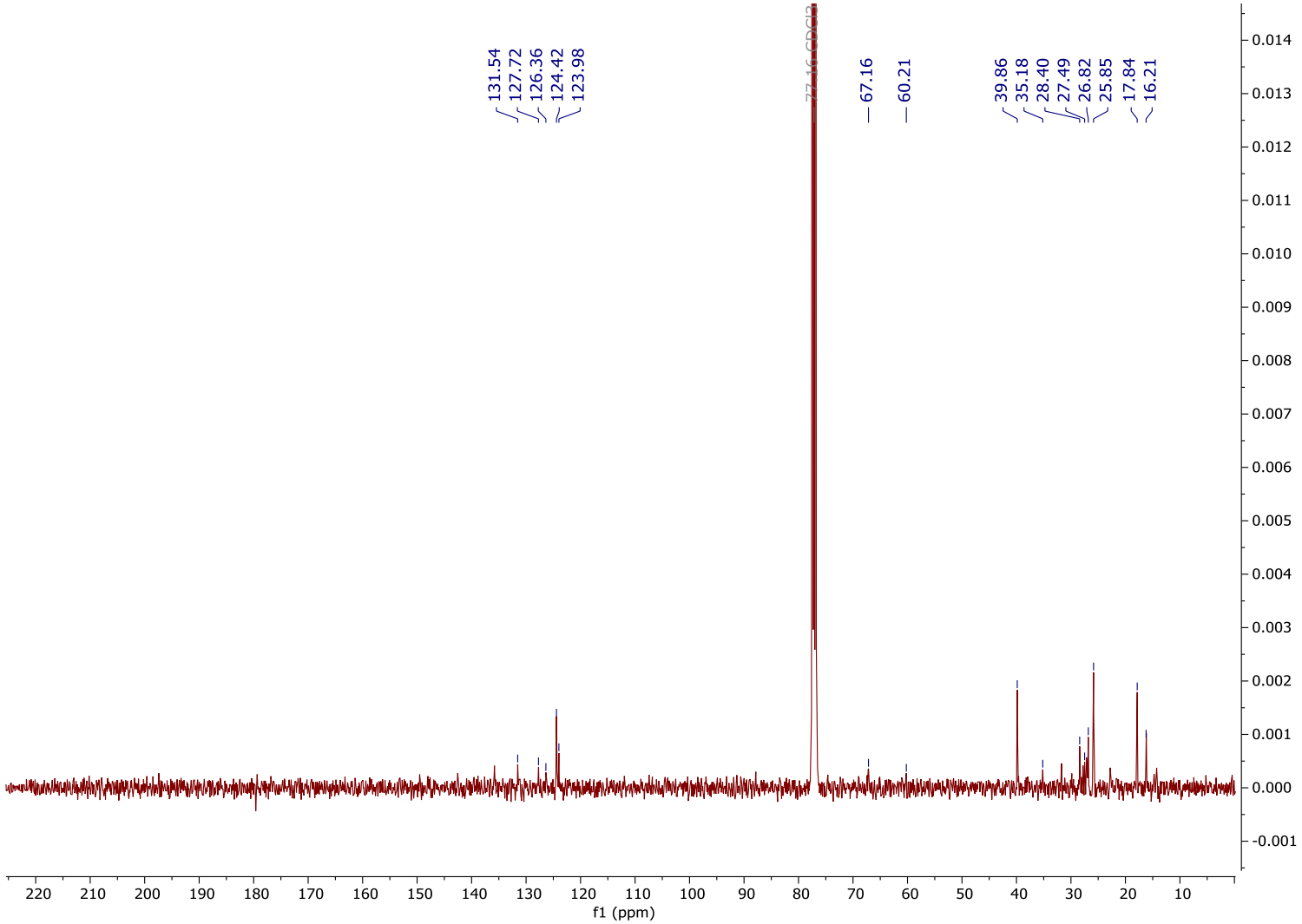

*Figure A.2.42 ^{13}C NMR spectrum of **1.97** in $CDCl_3$.*

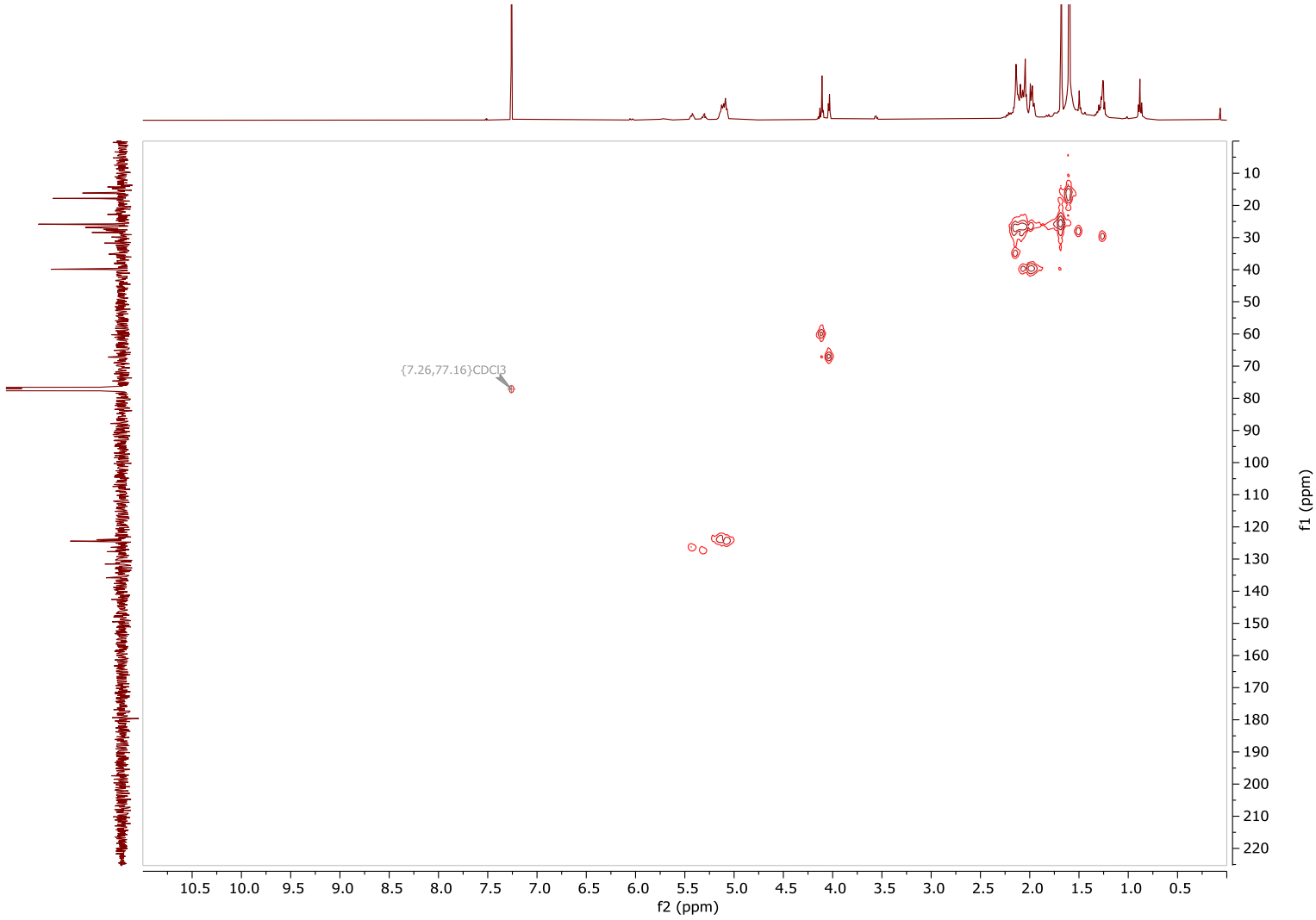

*Figure A.2.43 HSQC NMR spectrum of **1.97** in $CDCl_3$.*

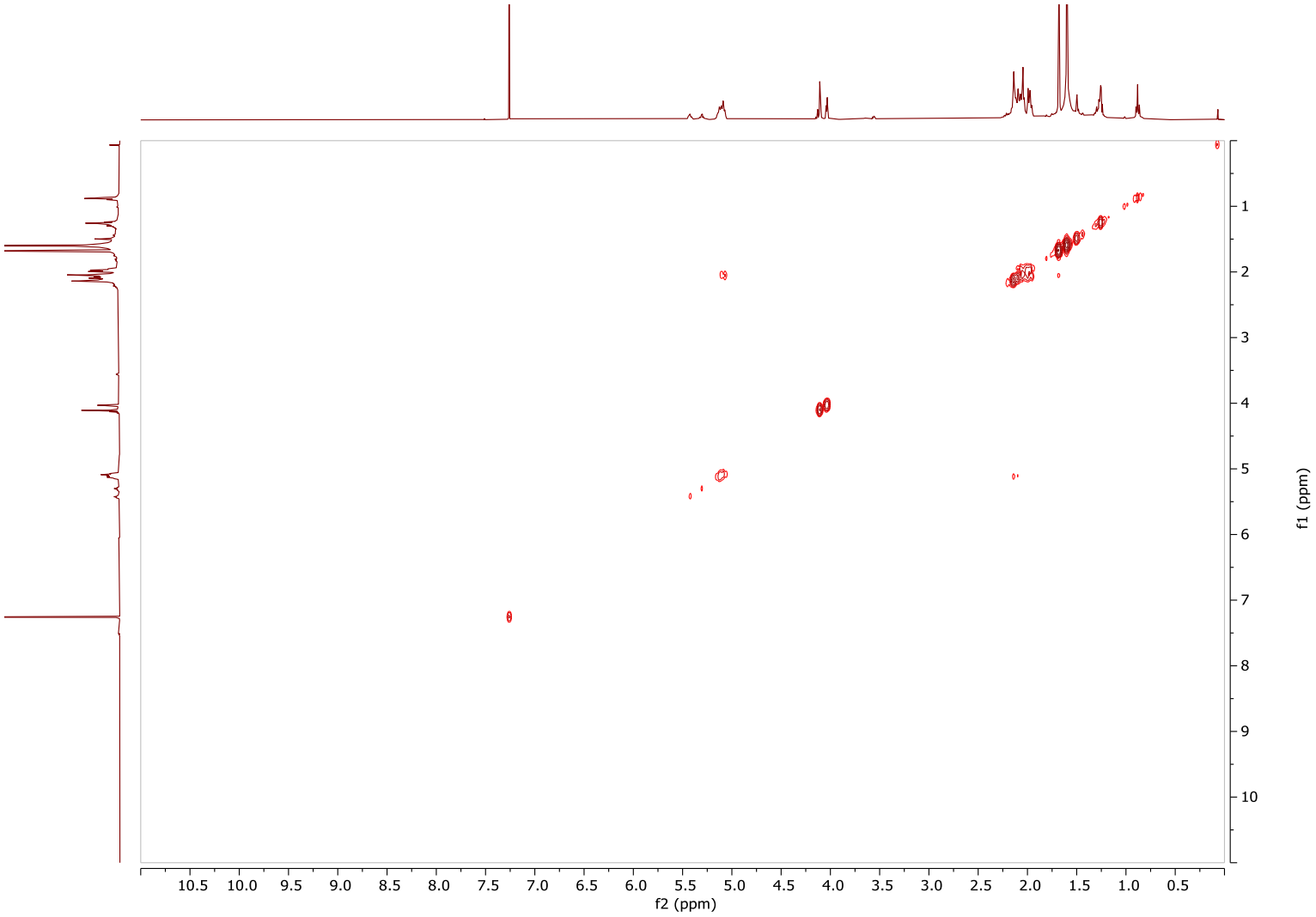

*Figure A.2.44 COSY NMR spectrum of **1.97** in $CDCl_3$.*

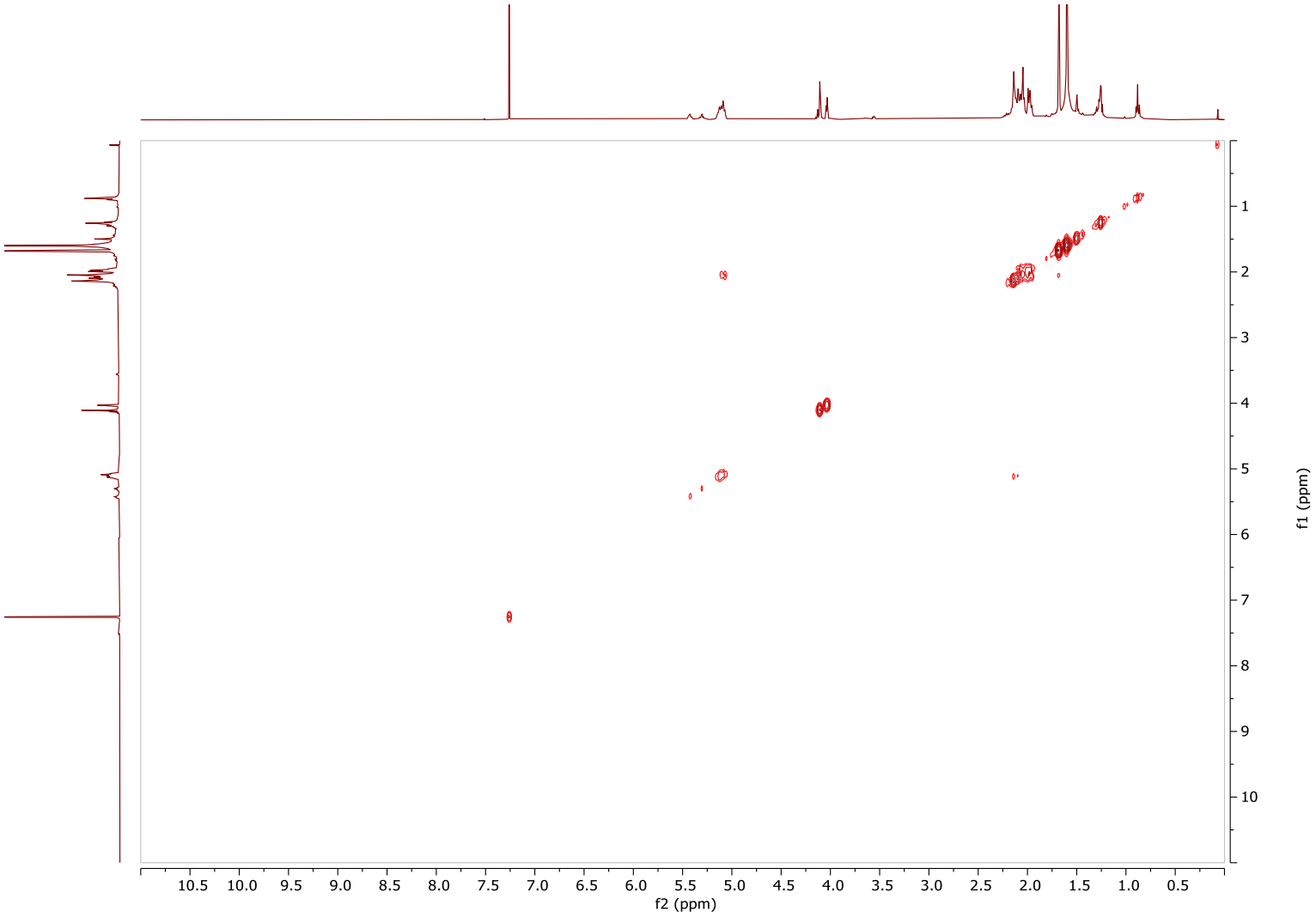

*Figure A.2.45 HMBC NMR spectrum of **1.97** in $CDCl_3$.*

8.2 Chapter 3. Isolation of Daphniphyllum alkaloids

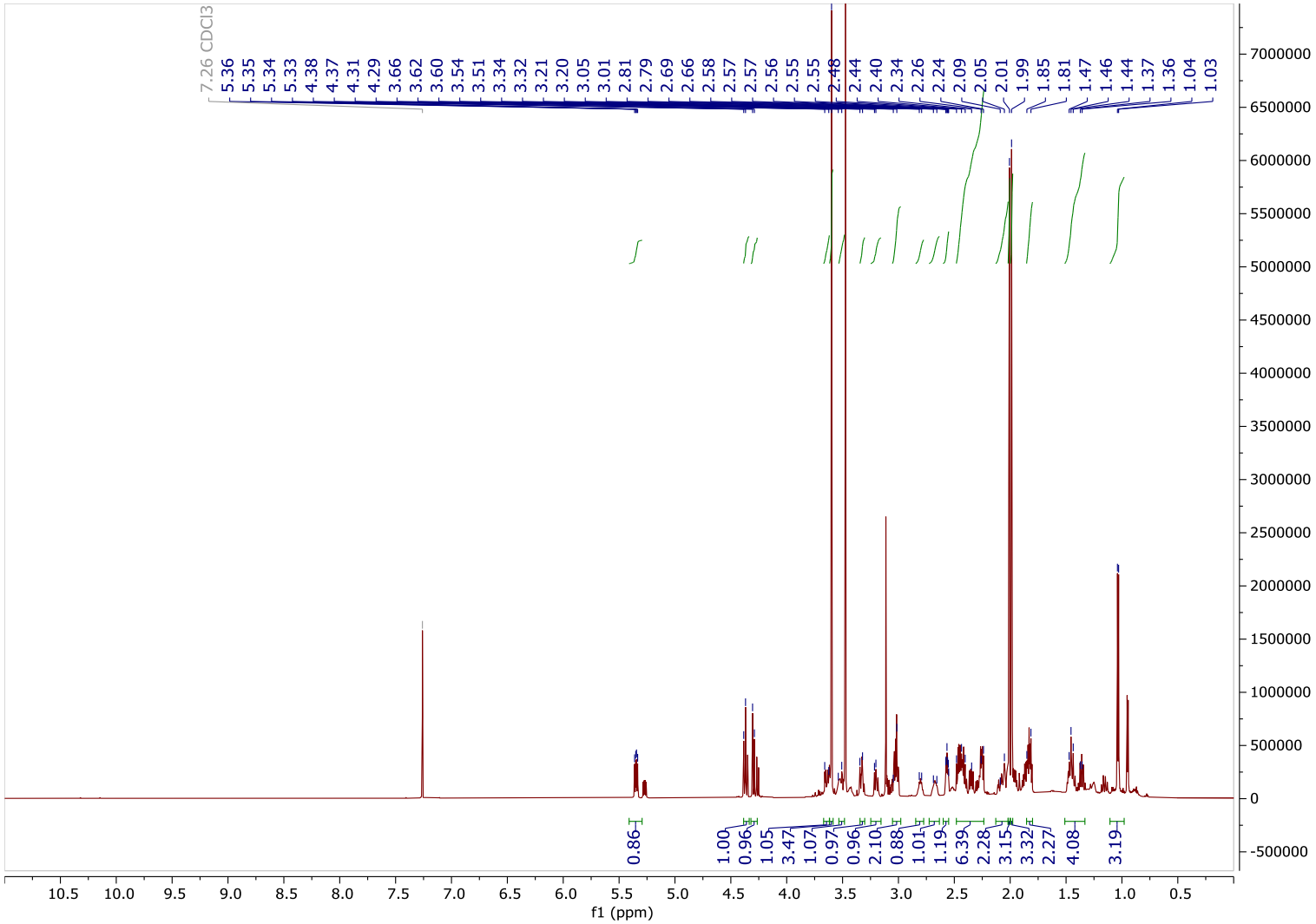

*Figure A.3.1 ^{1}H NMR spectrum of yuzurimine **1.10** in $CDCl_3$.*

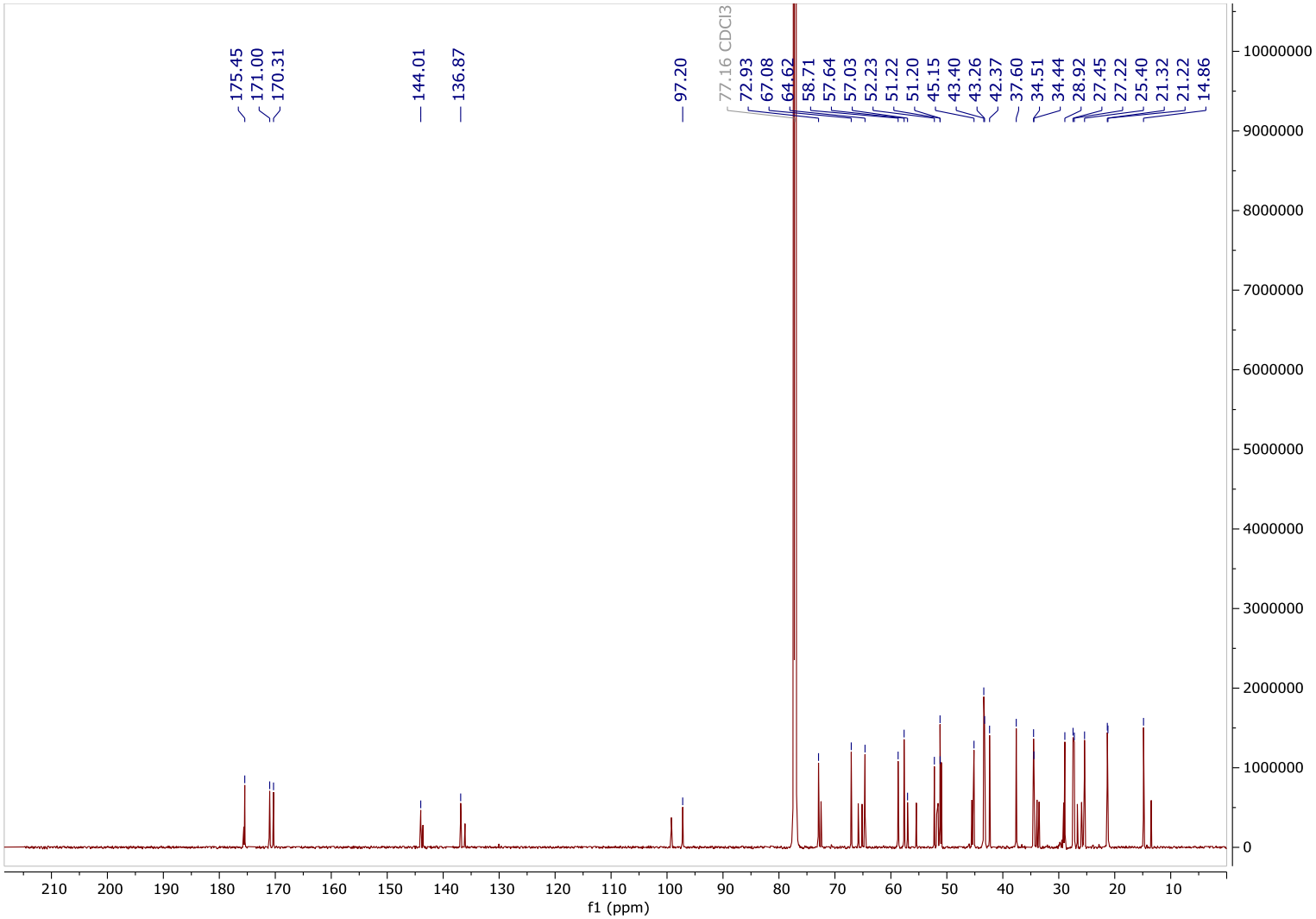

*Figure A.3.2 ^{13}C NMR spectrum of yuzurimine **1.10** in $CDCl_3$.*

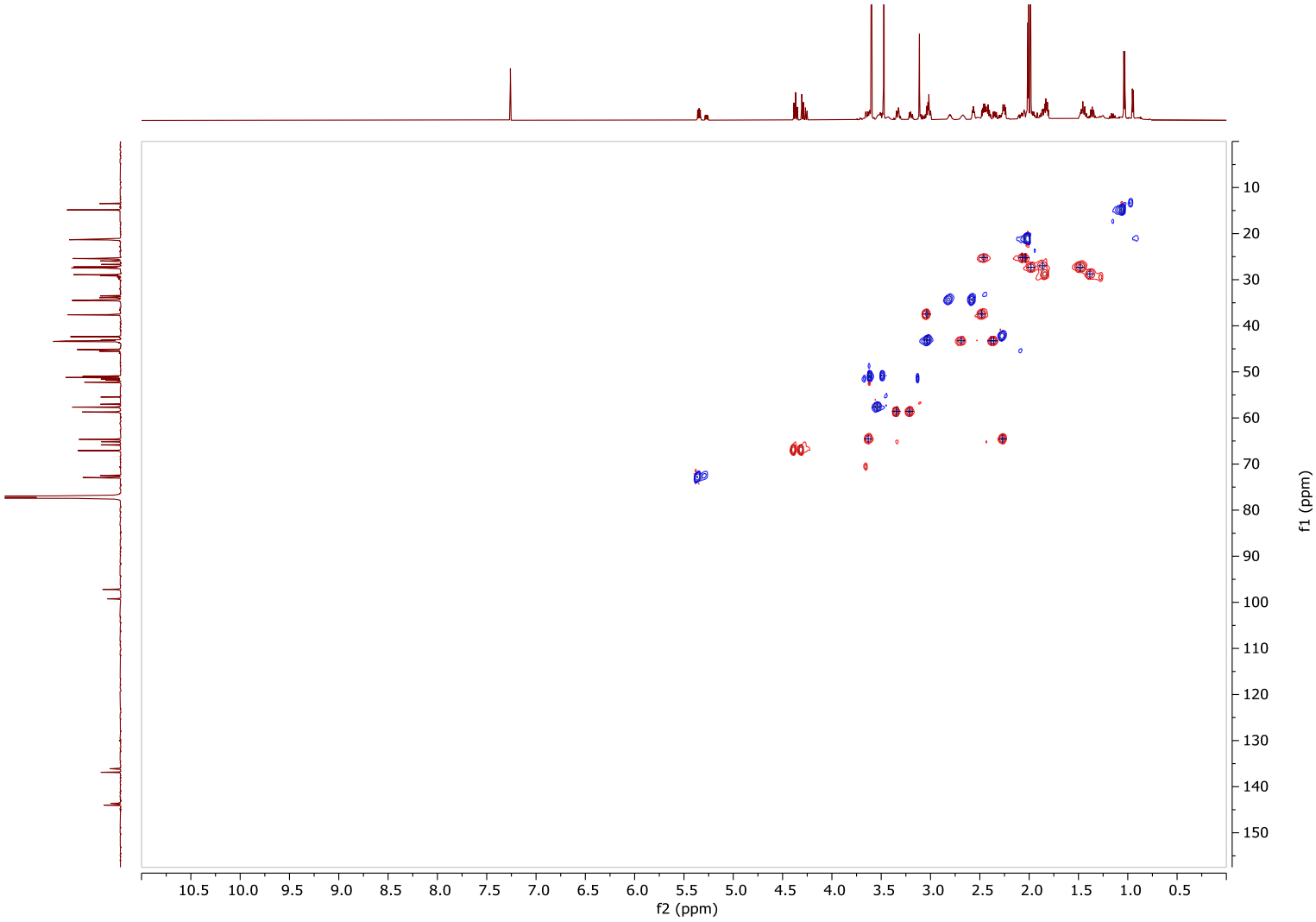

*Figure A.3.3 HMQC NMR spectrum of yuzurimine **1.10** in $CDCl_3$.*

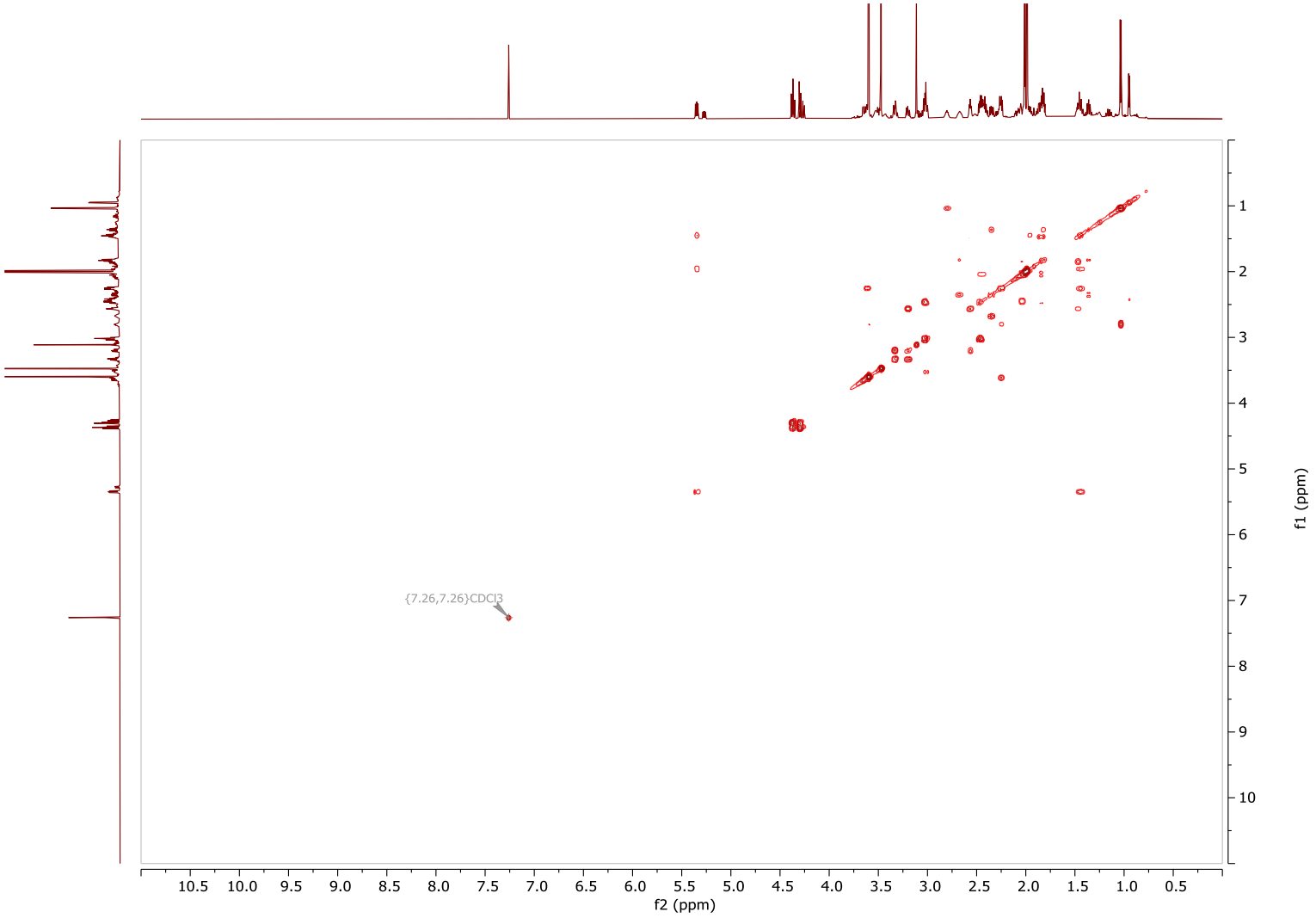

*Figure A.3.4 COSY NMR spectrum of yuzurimine **1.10** in $CDCl_3$.*

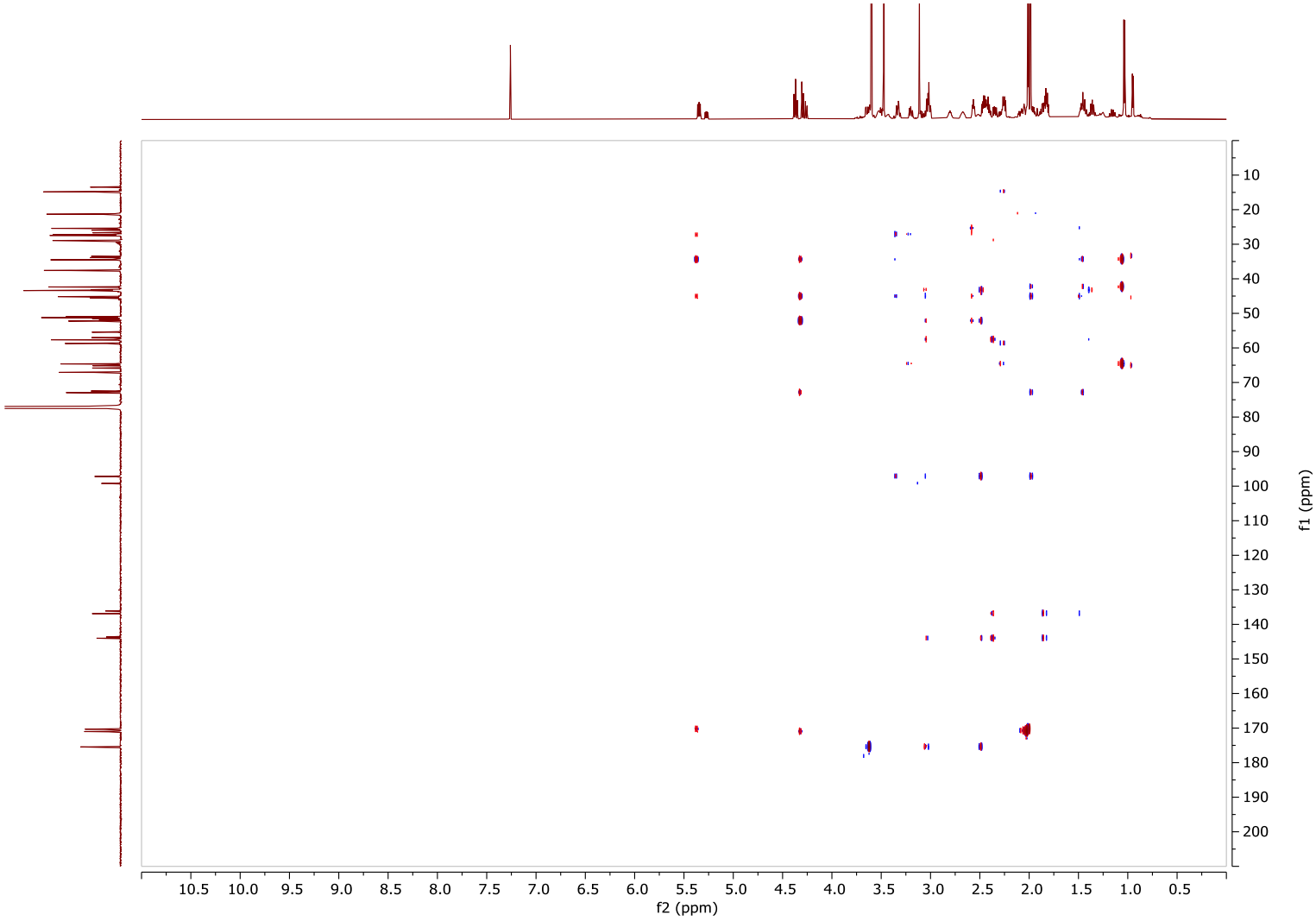

*Figure A.3.5 HBMC NMR spectrum of yuzurimine **1.10** in $CDCl_3$.*

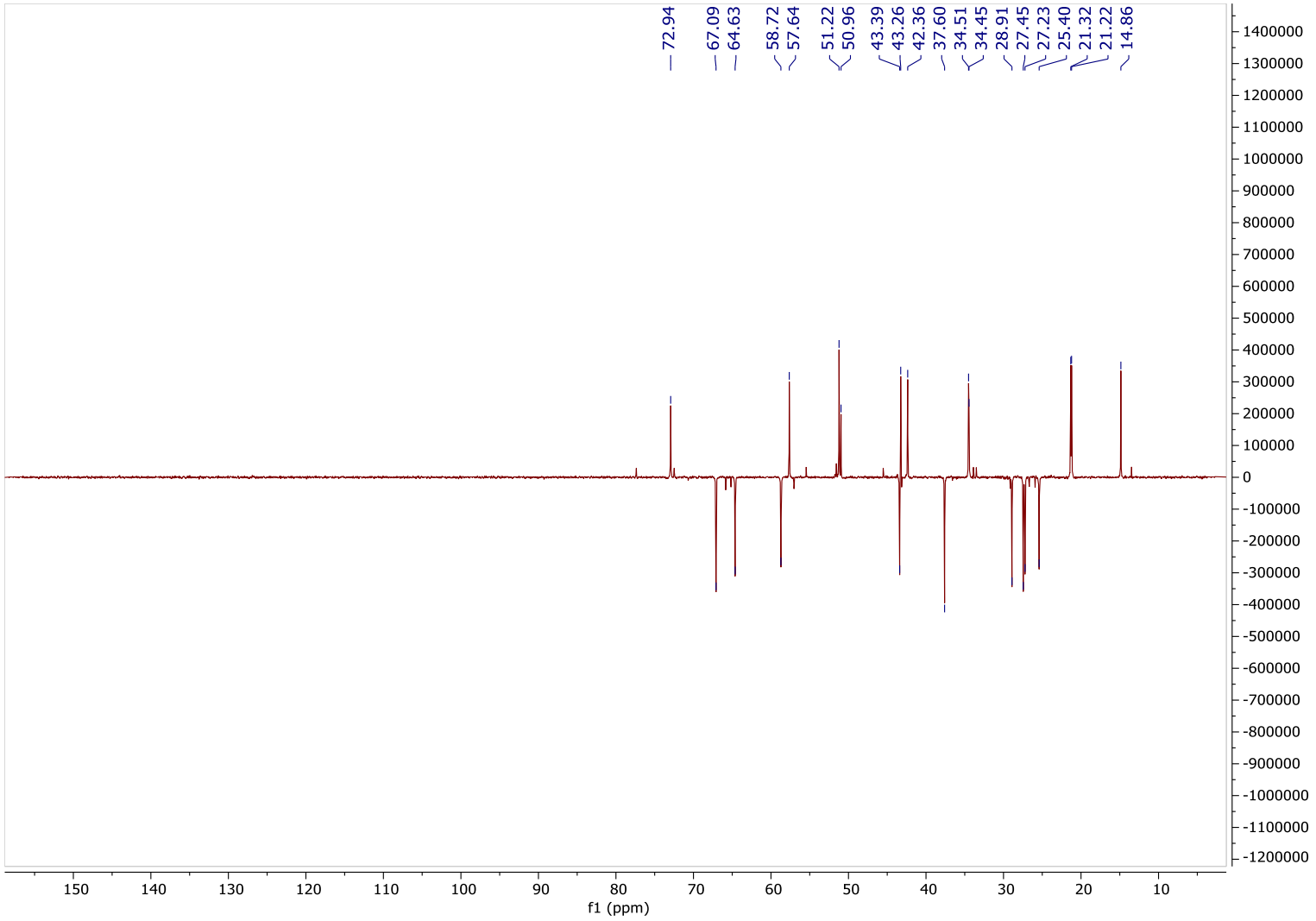

*Figure A.3.6 DEPT NMR spectrum of yuzurimine **1.10** in $CDCl_3$.*

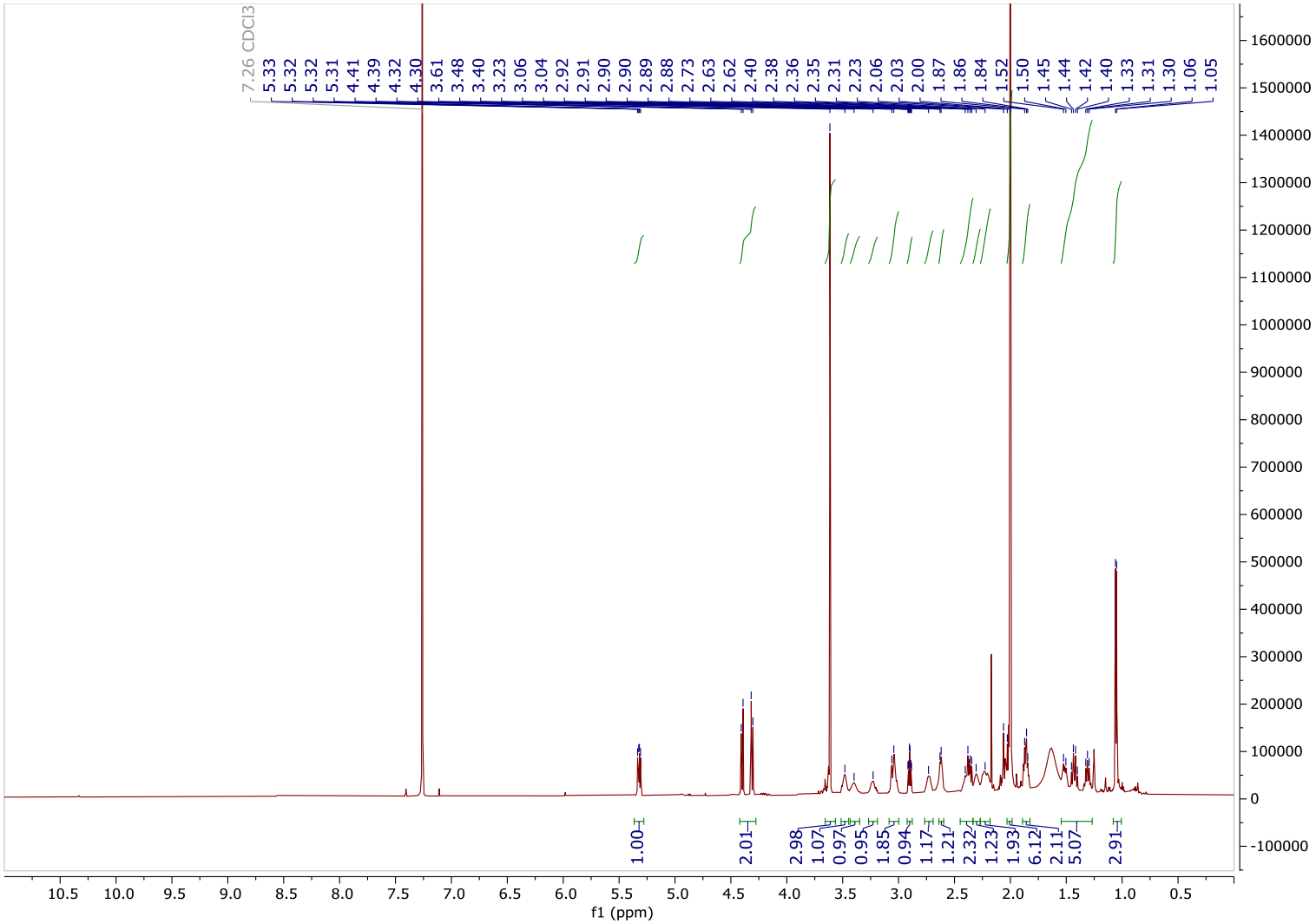

*Figure A.3.7 ^{1}H NMR spectrum of deoxyyuzurimine **1.66** in $CDCl_3$.*

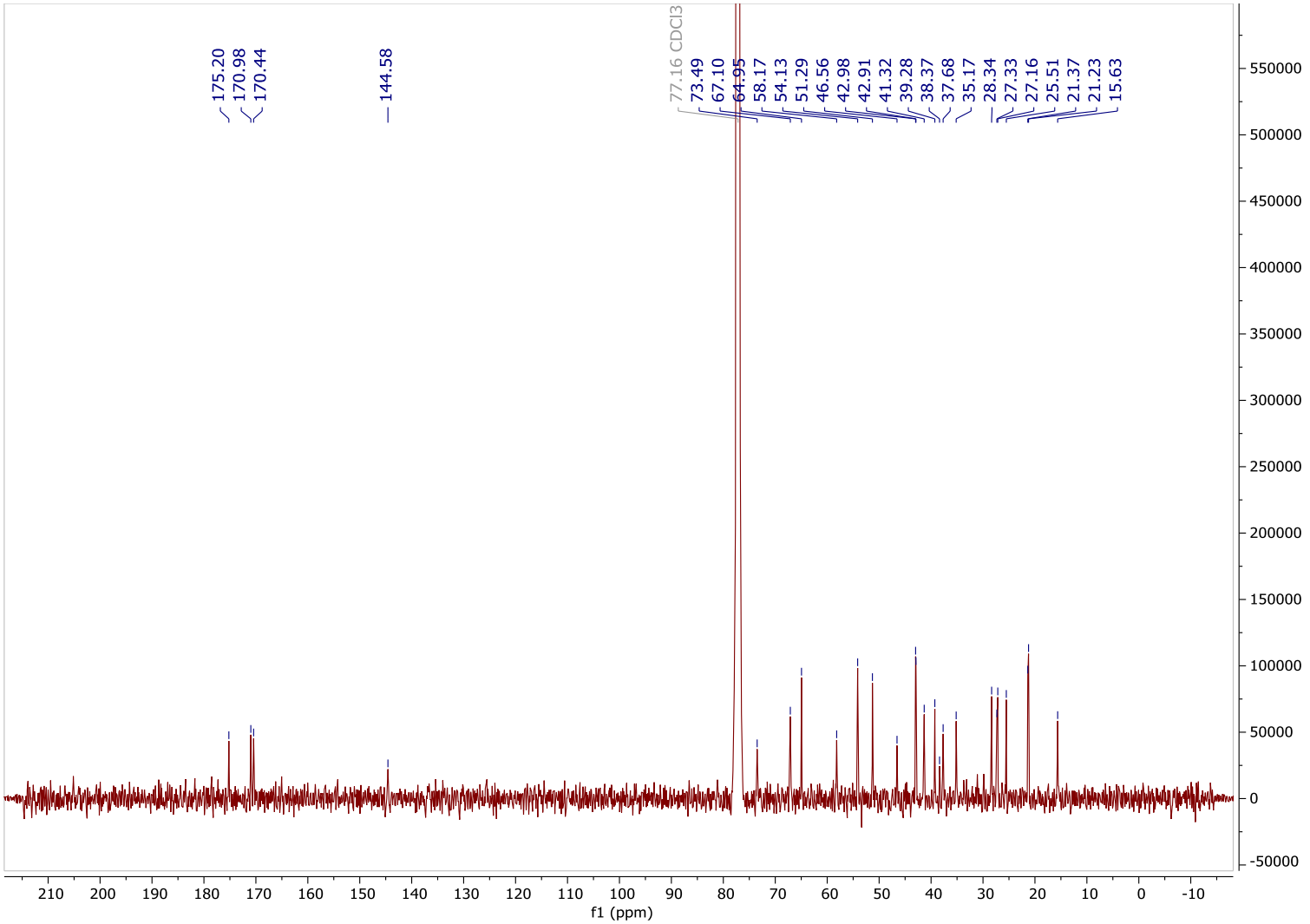

*Figure A.3.8 ^{13}C NMR spectrum of deoxyyuzurimine **1.66** in $CDCl_3$.*

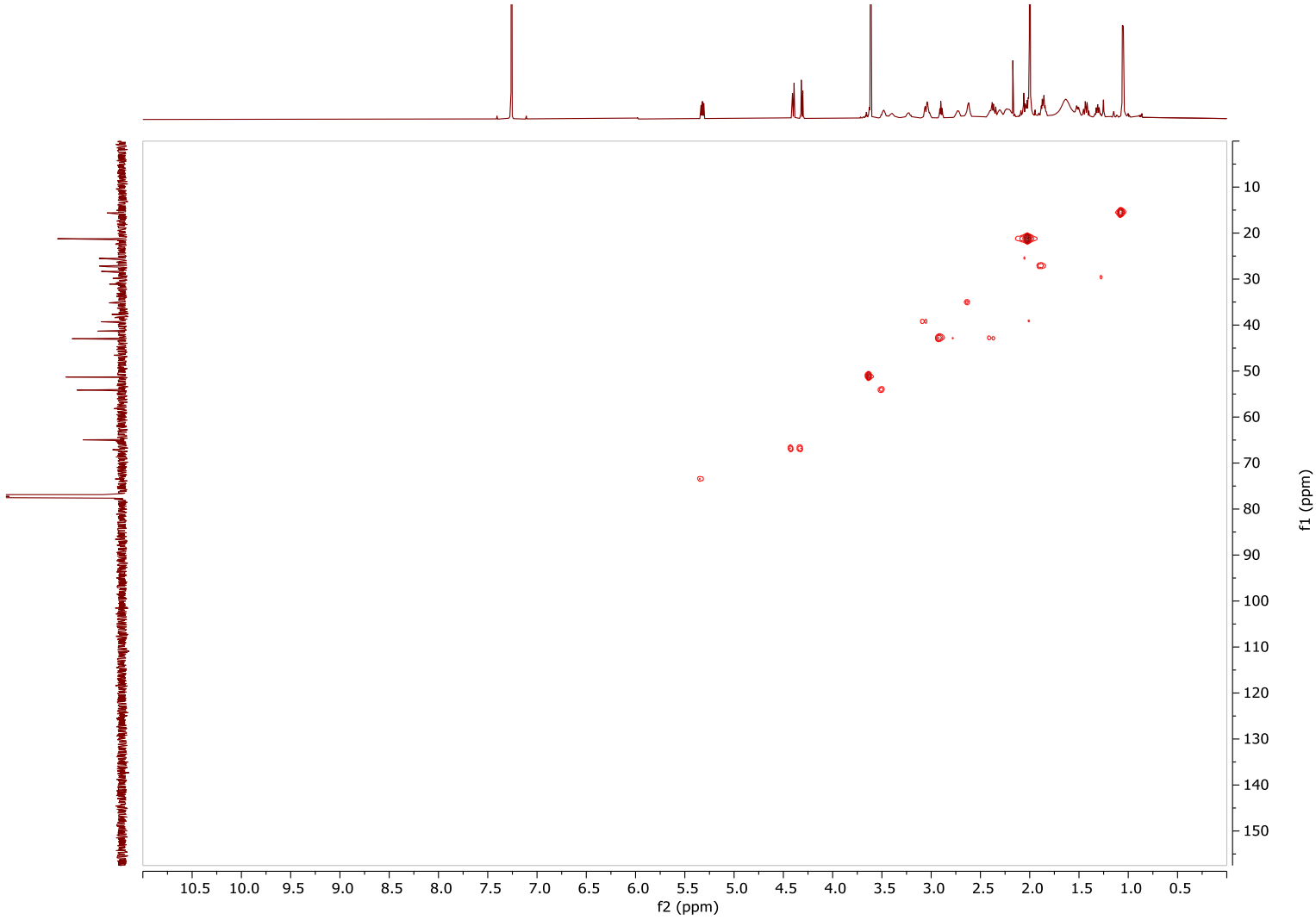

*Figure A.3.9 HMQC NMR spectrum of deoxyyuzurimine **1. 66** in $CDCl_3$.*

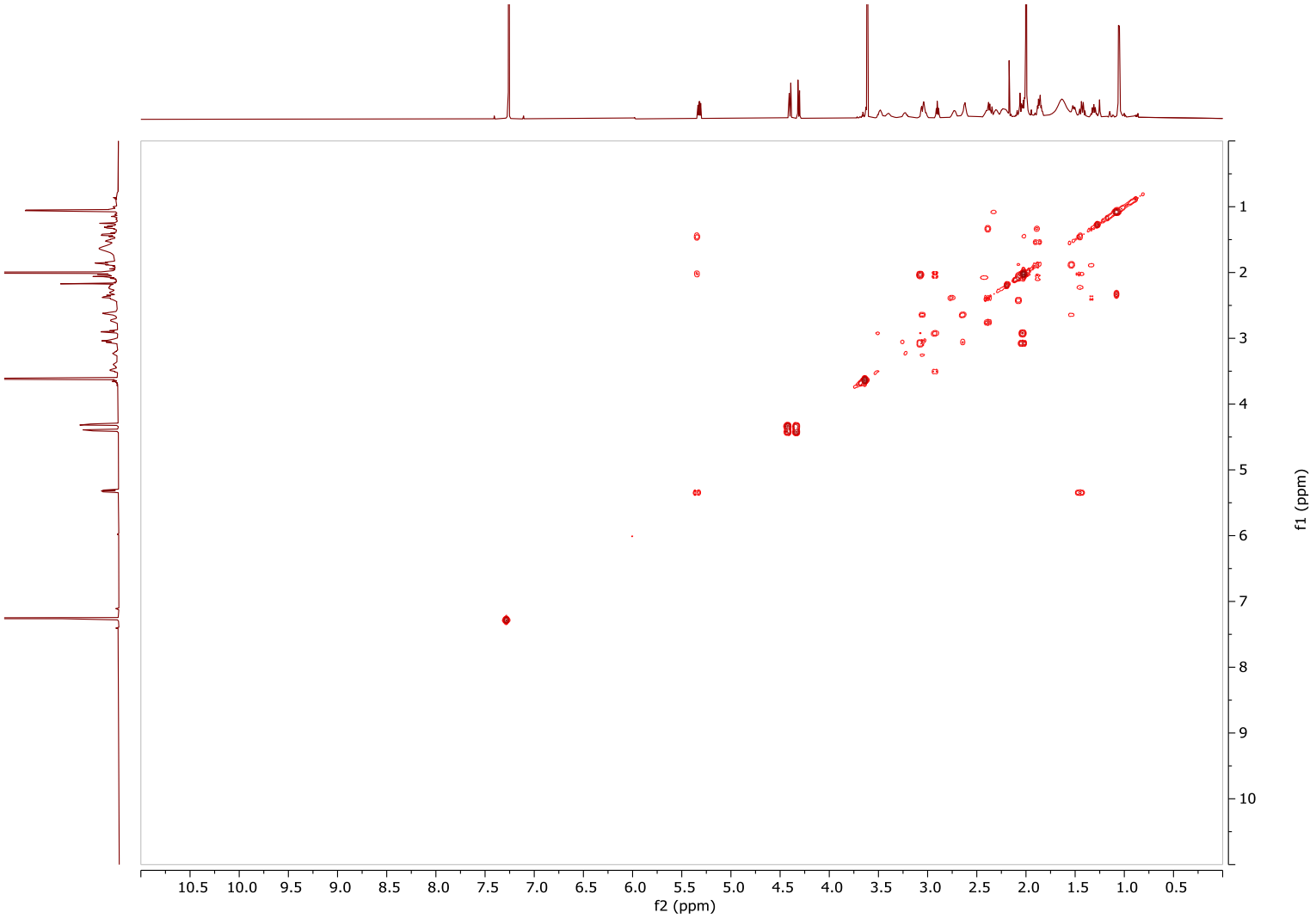

*Figure A.3.10 COSY NMR spectrum of deoxyyuzurimine **1. 66** in $CDCl_3$.*

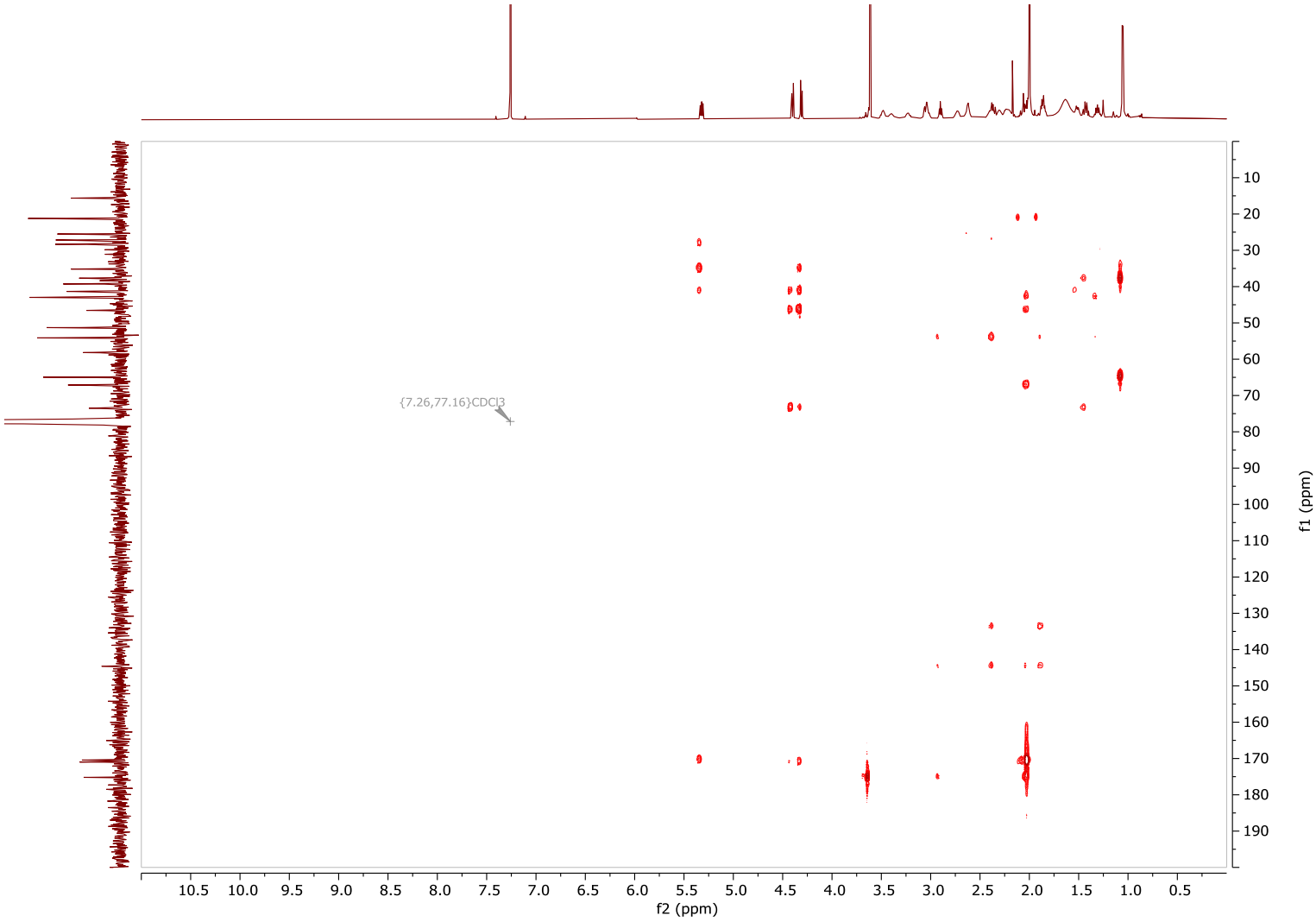

*Figure A.3.11 HBMC NMR spectrum of deoxyyuzurimine **1. 66** in $CDCl_3$.*

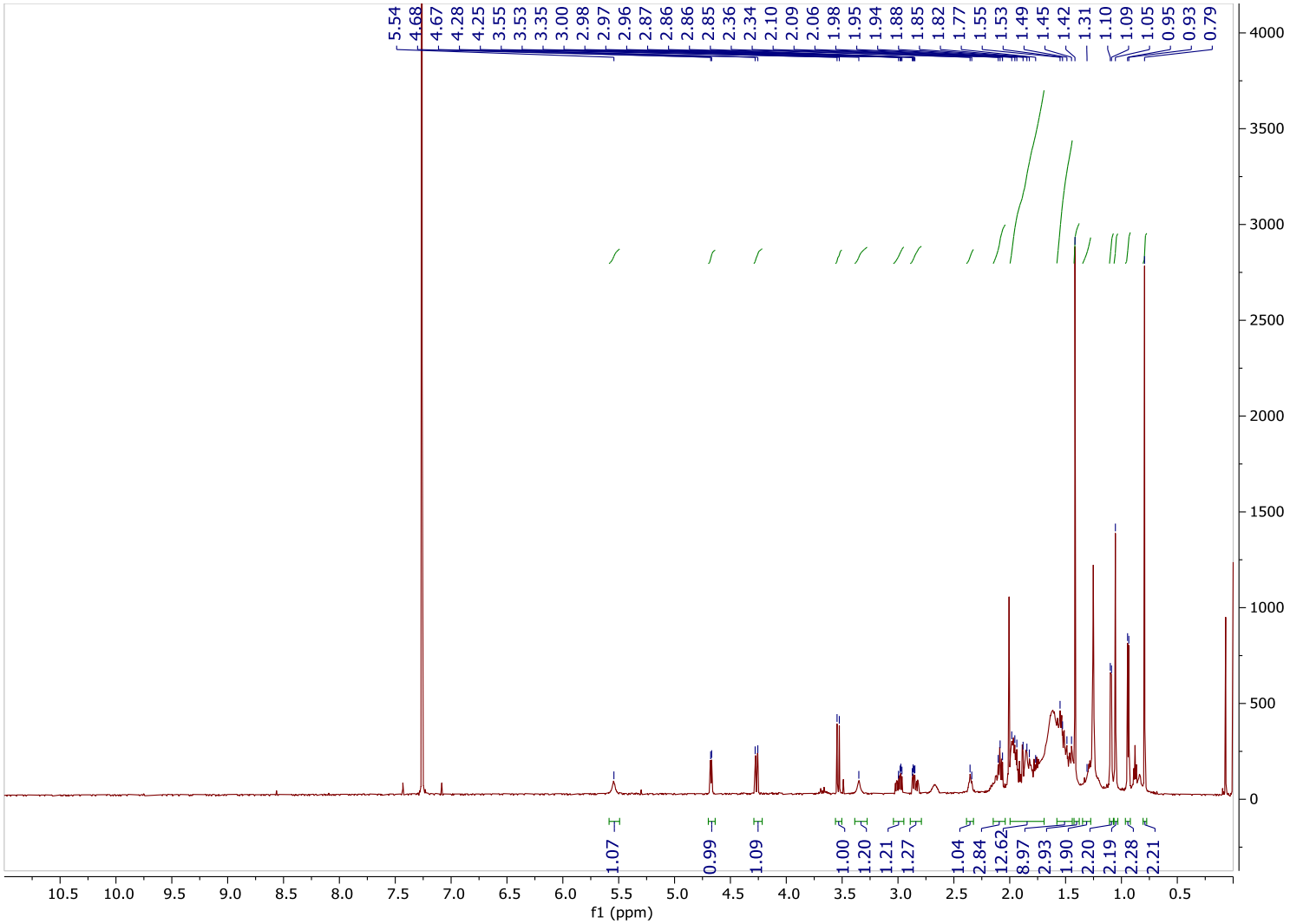

*Figure A.3.12 ^{1}H NMR spectrum of daphnicalycine A **3.1** in $CDCl_3$.*

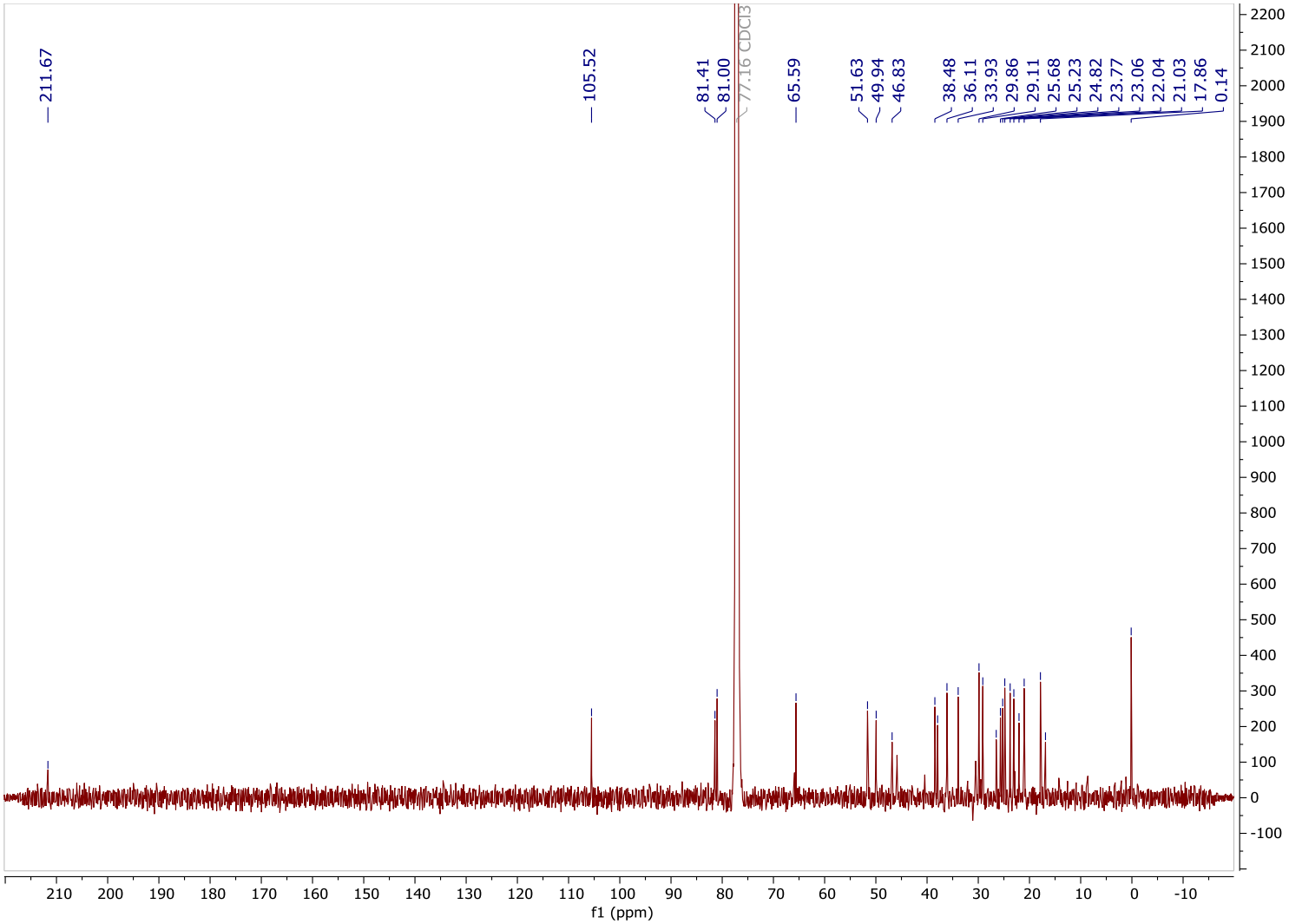

*Figure A.3.13 ^{13}C NMR spectrum of daphnicalycine A **3.1** in $CDCl_3$.*

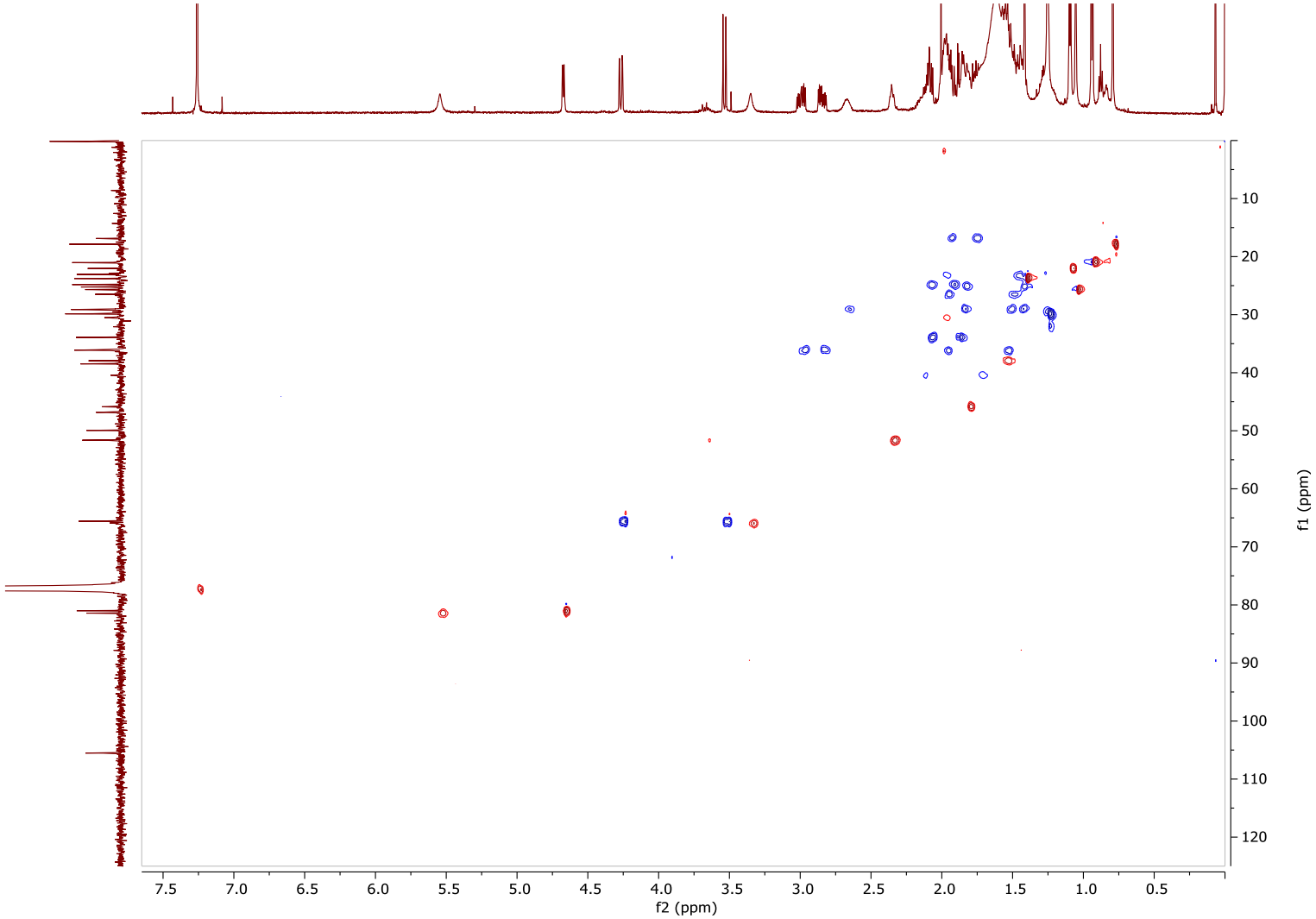

*Figure A.3.14 HMQC NMR spectrum of daphnicalycine A **3.1** in $CDCl_3$.*

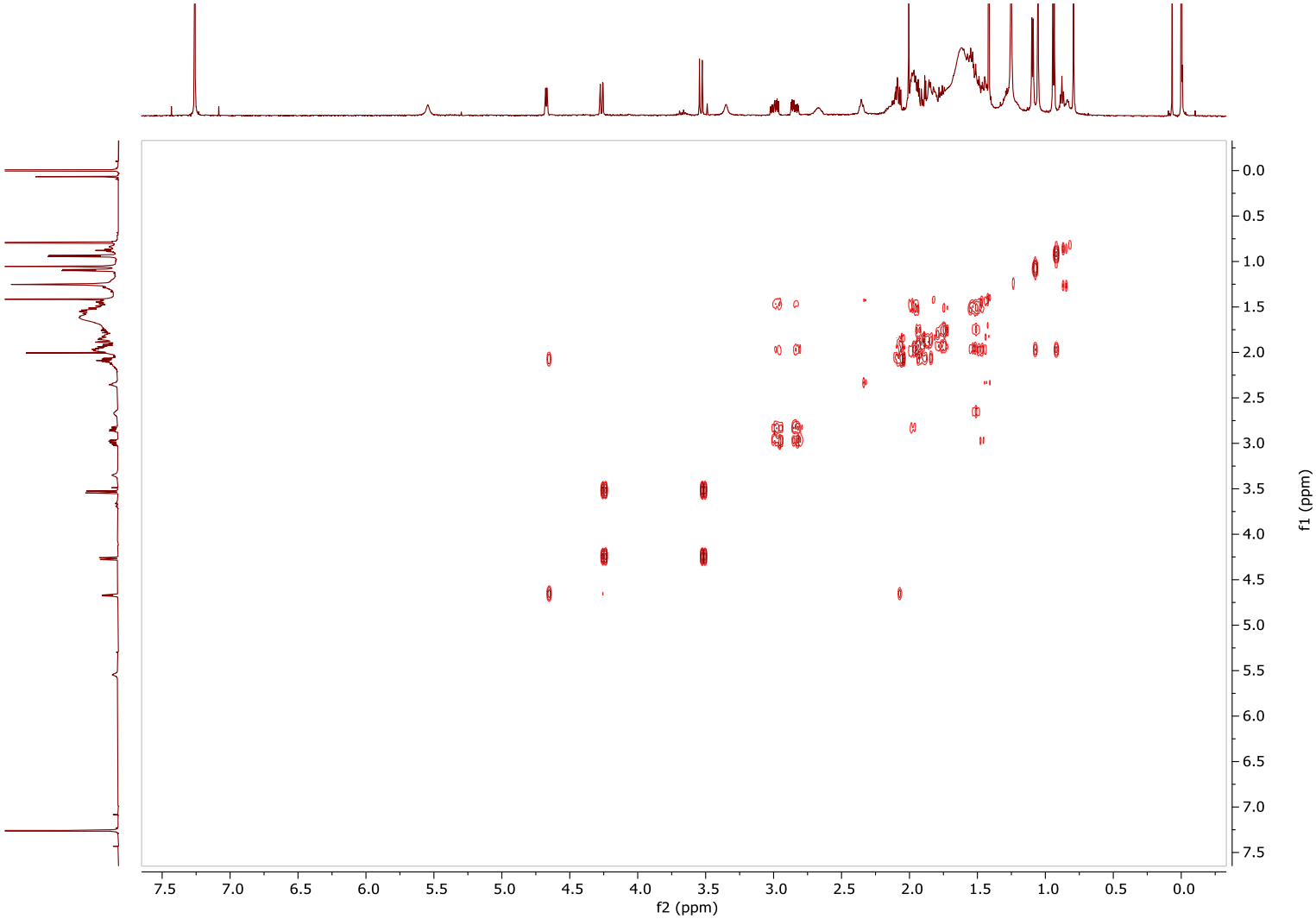

*Figure A.3.15 COSY NMR spectrum of daphnicalycine A **3.1** in $CDCl_3$.*

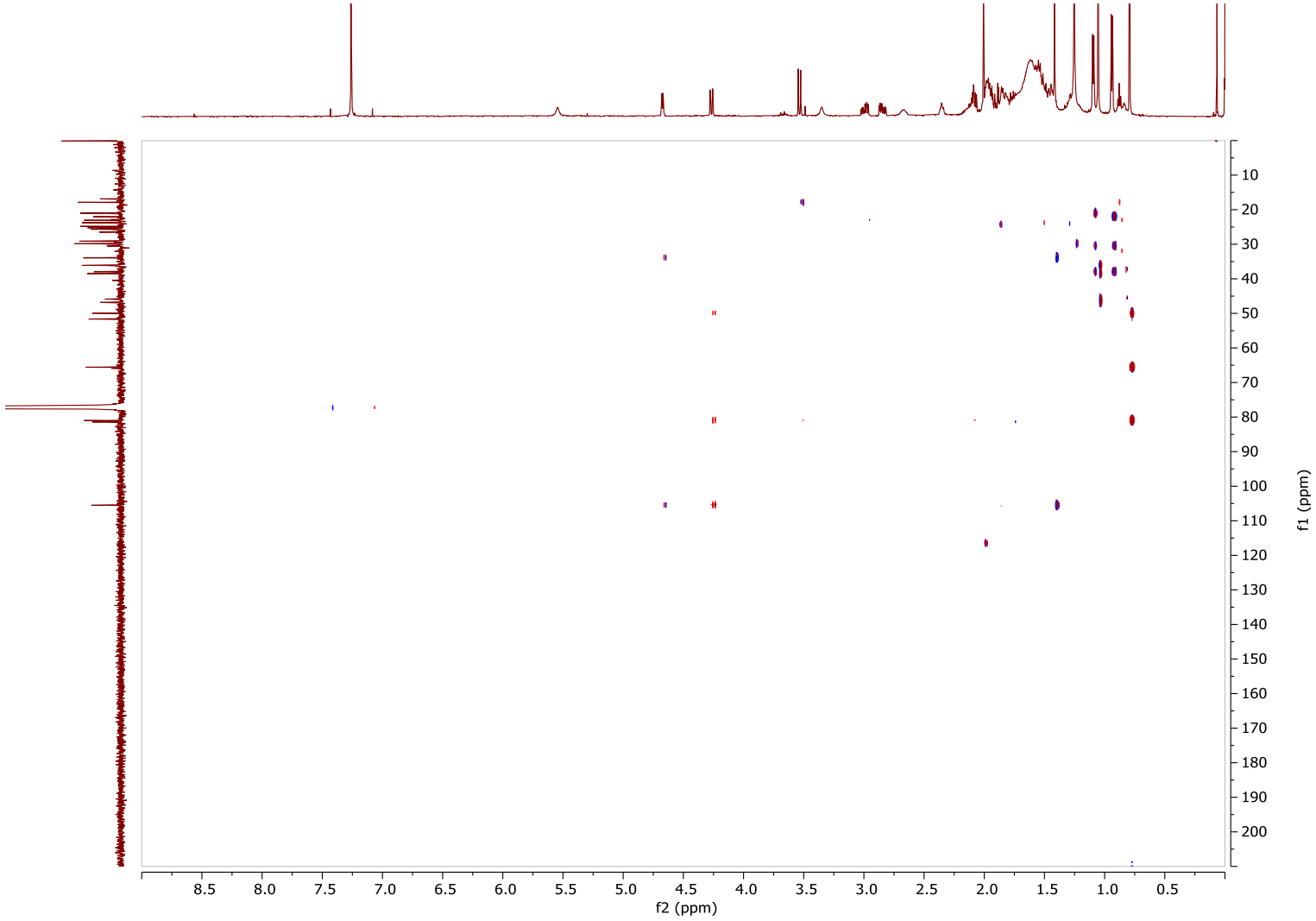

*Figure A.3.16 HBMC NMR spectrum of daphnicalycine A **3.1** in $CDCl_3$.*

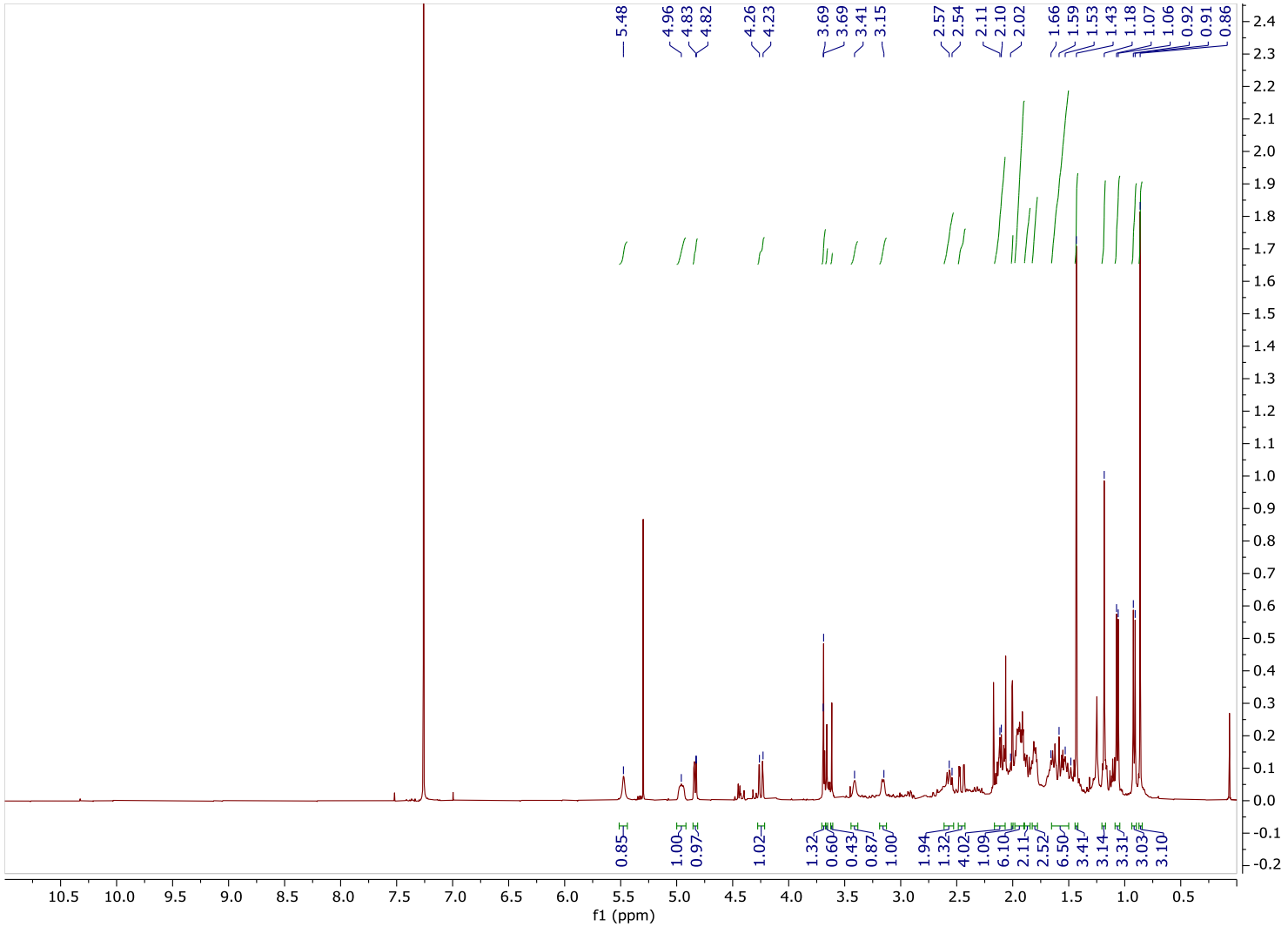

*Figure A.3.17 ^{1}H NMR spectrum of 7-hydroxydaphnilongeranin D **3.4** in $CDCl_3$.*

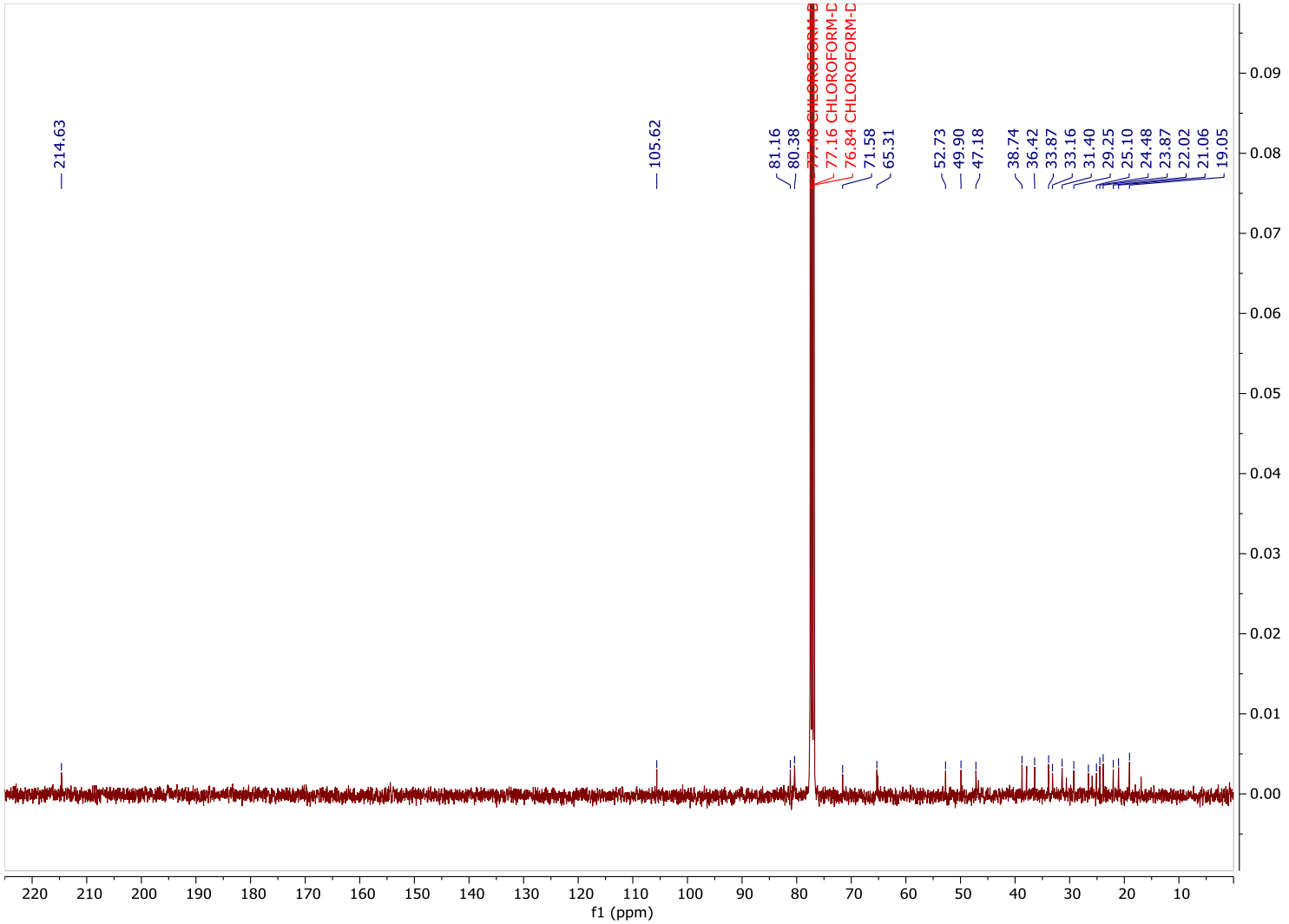

*Figure A.3.18 ^{13}C NMR spectrum of 7-hydroxydaphnilongeranin D **3.4** in $CDCl_3$.*

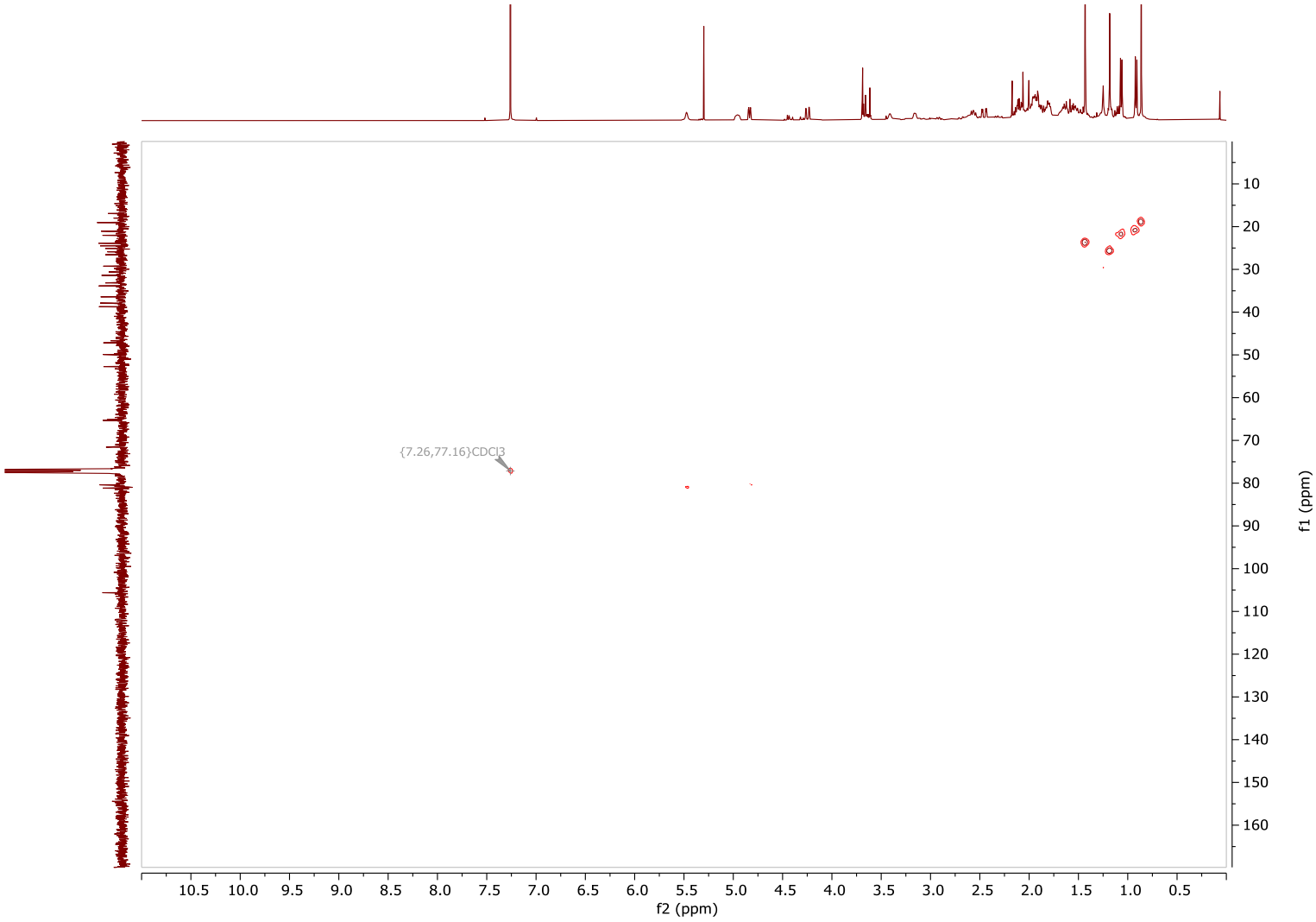

*Figure A.3.19 HMQC NMR spectrum of 7-hydroxydaphnilongeranin D **3.4** in $CDCl_3$.*

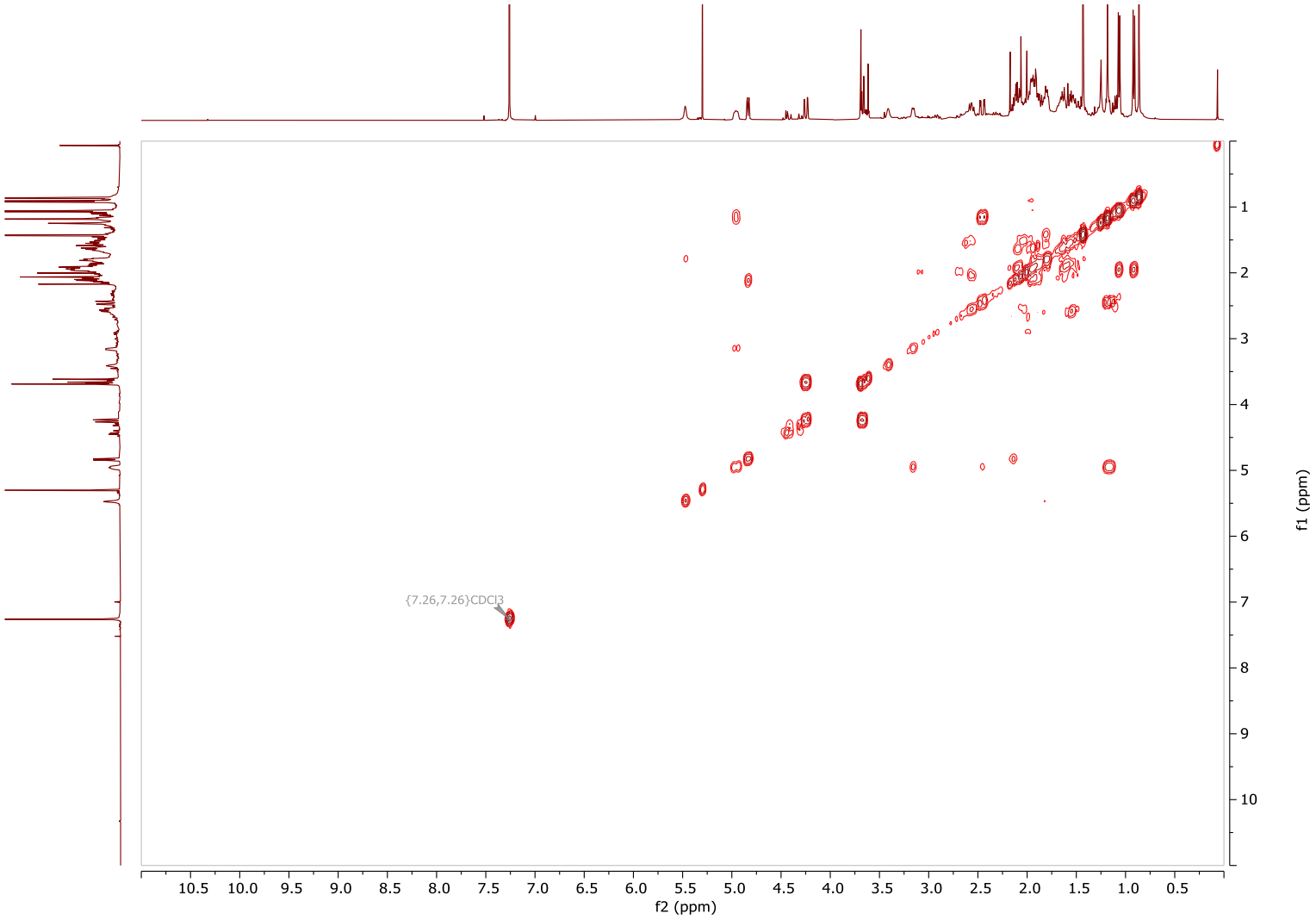

*Figure A.3.20 COSY NMR spectrum of 7-hydroxydaphnilongeranin D **3.4** in $CDCl_3$.*

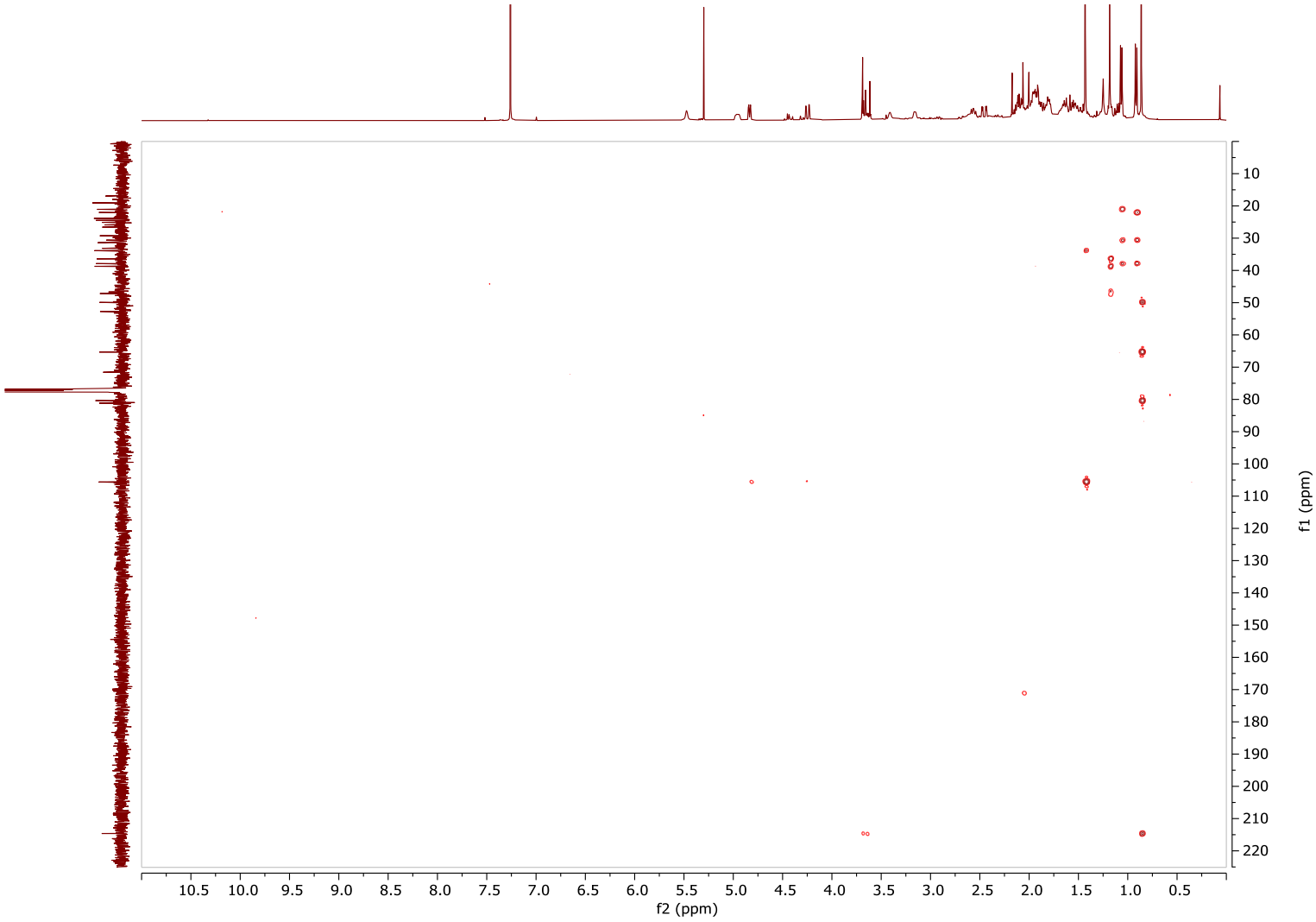

*Figure A.3.21 HBMC NMR spectrum of 7-hydroxydaphnilongeranin D **3.4** in $CDCl_3$.*

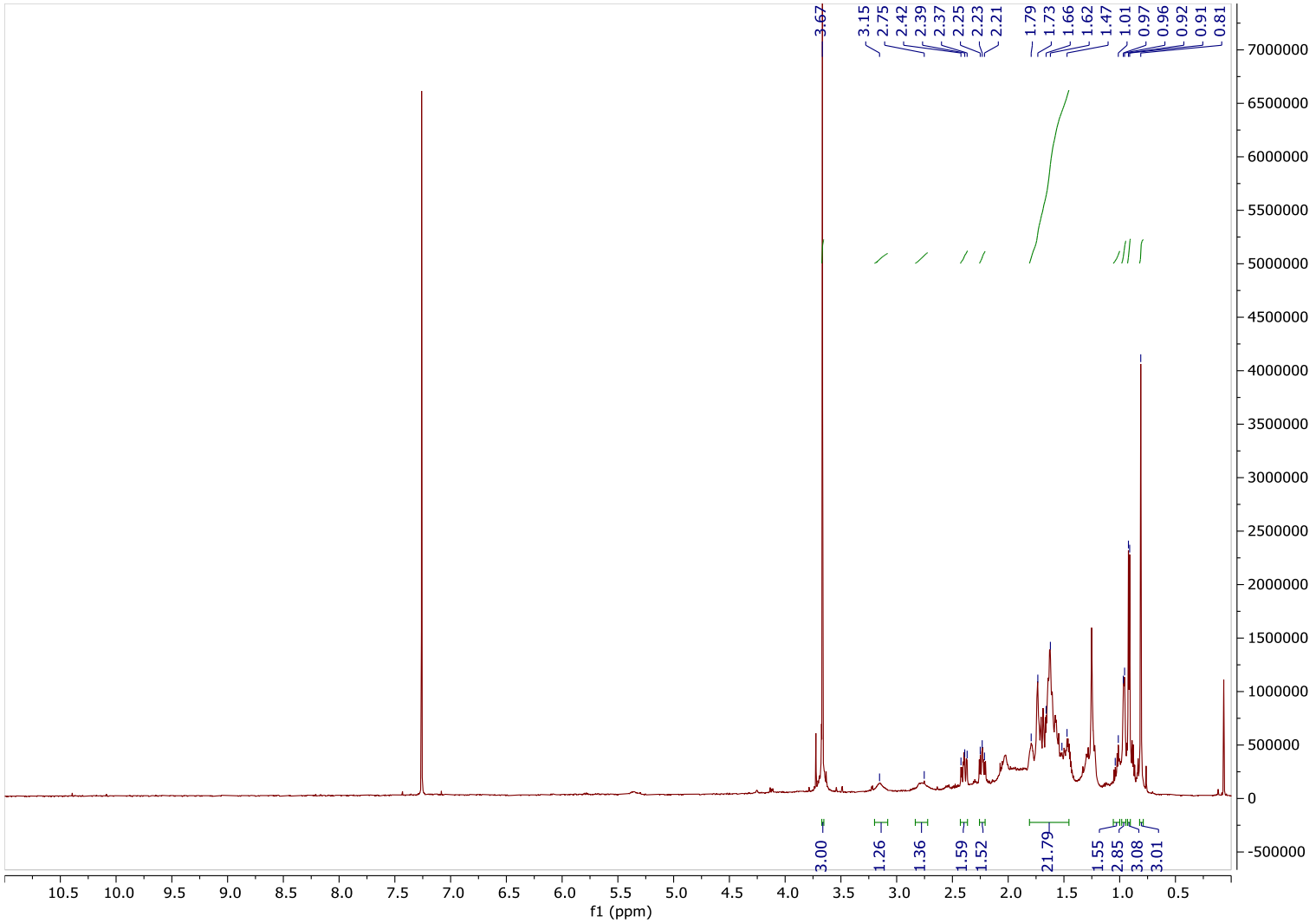

*Figure A.3.22 ^{1}H NMR spectrum of methyl homosecodaphniphyllate **1.52** in $CDCl_3$.*

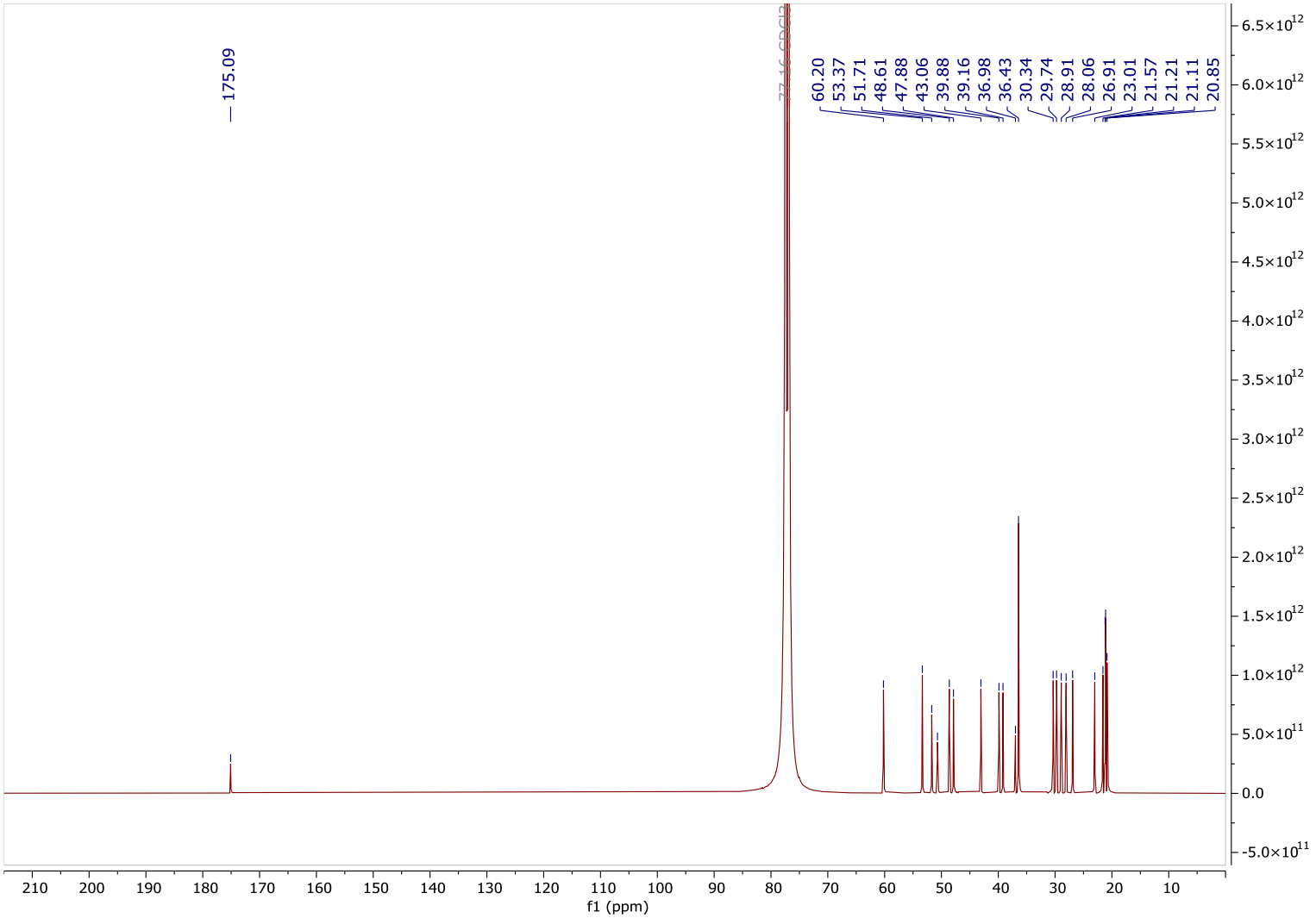

*Figure A.3.23 ^{13}C NMR spectrum of methyl homosecodaphniphyllate **1.52** in $CDCl_3$.*

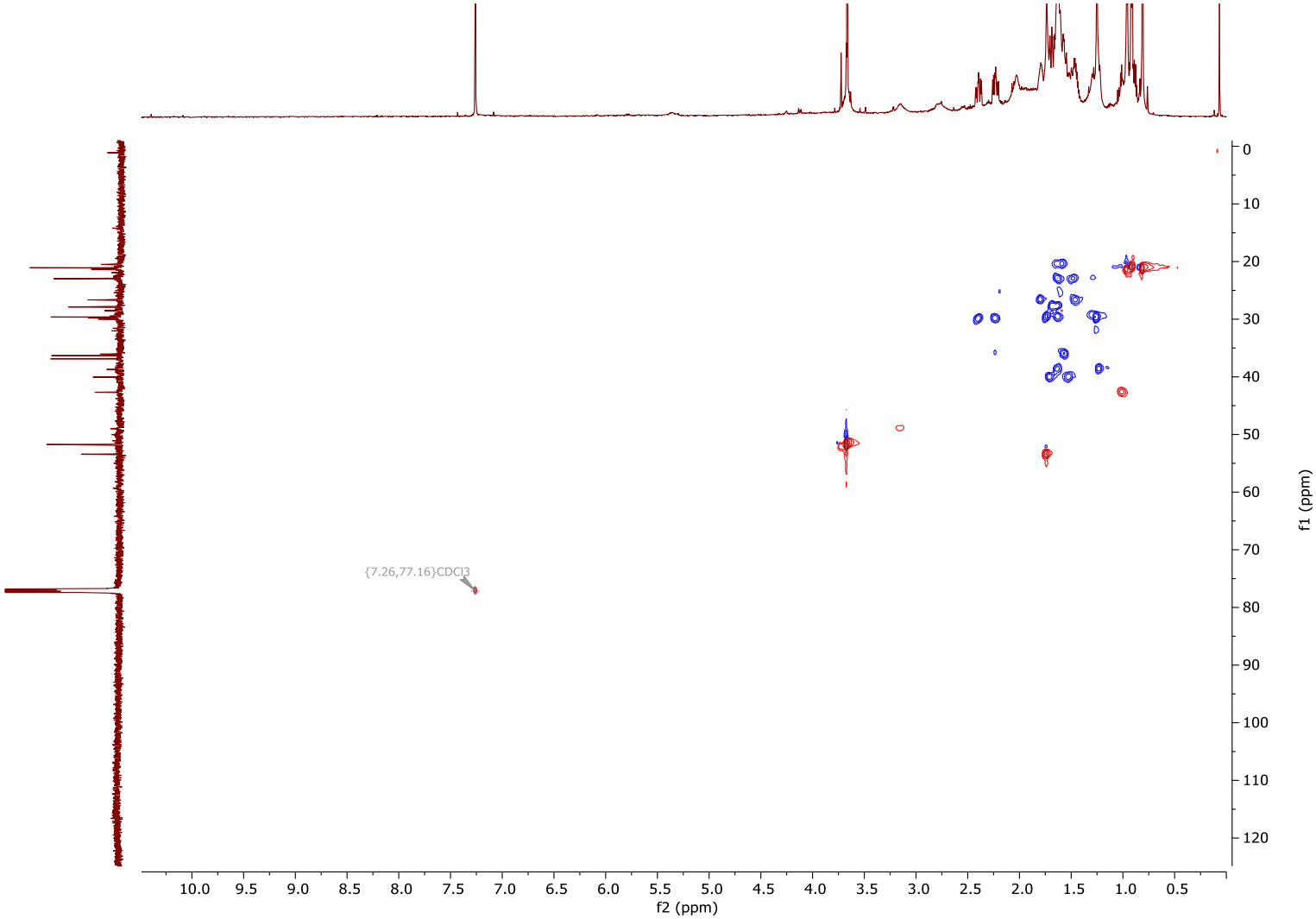

*Figure A.3.24 HMQC NMR spectrum of methyl homosecodaphniphyllate **1.52** in $CDCl_3$.*

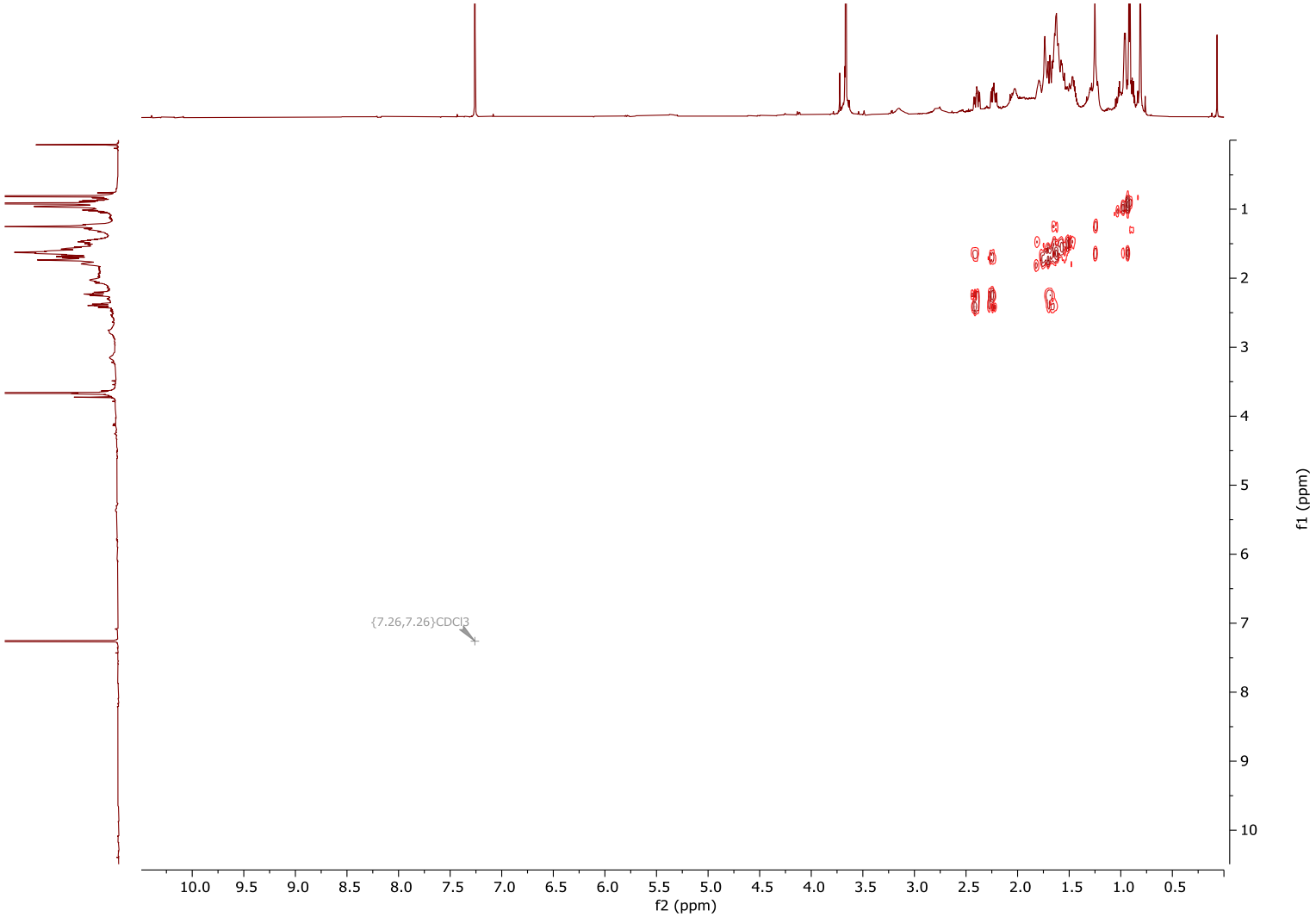

*Figure A.3.25 COSY NMR spectrum of methyl homosecodaphniphyllate **1.52** in $CDCl_3$.*

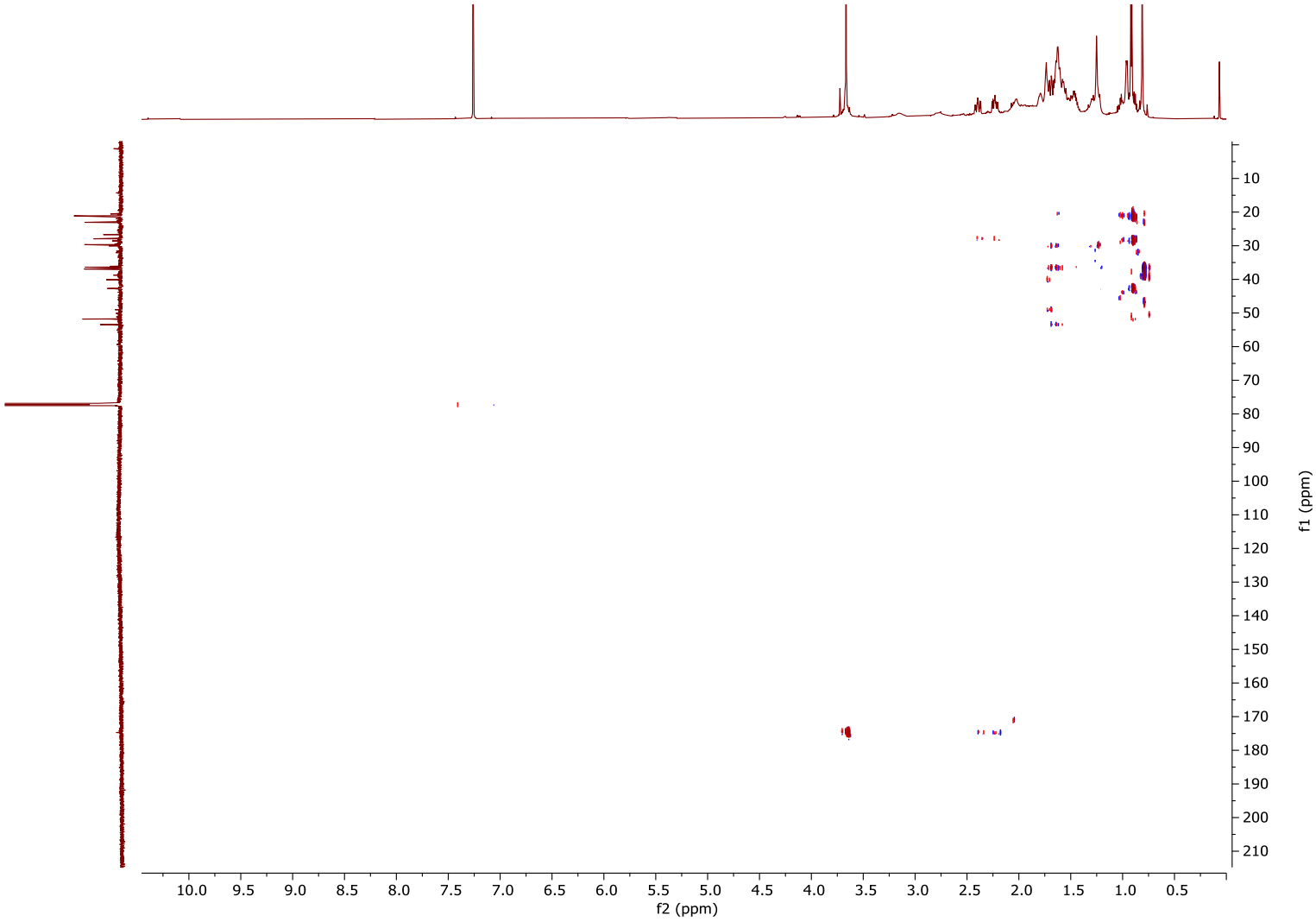

*Figure A.3.26 HBMC NMR spectrum of methyl homosecodaphniphyllate **1.52** in $CDCl_3$.*

8.3 Reported *Daphniphyllum* alkaloids

Table A.1 Table presenting reported Daphniphyllum *alkaloids with their molecular formulas, exact masses, subtypes, species of* Daphniphyllum *and tissues from which they were isolated and reported.*

Exact Mass	$[M+H]^+$	Formula	SubType	Name	*D.* species	Reported from tissue
293.2143	294.2222	C21H27N	Calyciphylline A	daphenylline	longracemosum	fruits
299.1885	300.1964	C19H25NO2	Calyciphylline A	himalensine A	himalense	twigs and leaves
315.2562	316.264	C21H33NO	Daphnilactone B	caldaphnidine G b	calycinum	seeds
317.2719	318.2797	C21H35NO	Seco-daphniphylline	caldaphnidine D	calycinum	leaves
323.1885	324.1964	C21H25NO2	Calyciphylline A	14,15-didehydrodaphnilongeranin B	himalense	twigs and leaves
323.1885	324.1964	C21H25NO2	Daphnicyclidin	2-deoxydaphnicyclidin G	himalense	twigs and leaves
325.2042	326.212	C21H27NO2	Calyciphylline A	10-deoxydaphnipaxianine A	himalense	twigs and leaves
325.2042	326.212	C21H27NO2	Calyciphylline A	15-epidaphnilongeranin B	himalense	twigs and leaves
325.2042	326.212	C21H27NO2	Calyciphylline A	daphlongamine E	longracemosum	leaves
325.2042	326.212	C21H27NO2	Calyciphylline A	daphnilongeranin B	longracemosum	leaves and stems
325.2042	326.212	C21H27NO2	Calyciphylline A	daphniyunnine C	yunnanense	stems and leaves
325.2042	326.212	C21H27NO2	Calyciphylline A	himalenine C	himalense	twigs and leaves

325.2042	326.212	C21H27NO2	Calyciphylline A	longeracinphyllin A	longracemosum	leaves
327.2198	328.2277	C21H29NO2	Calyciphylline A	daphnipaxianine C	paxianum	leaves and fruit
331.2511	332.259	C21H33NO2	Calyciphylline D	caldaphnidine M	calycinum	twigs
331.2511	332.259	C21H33NO2	Daphniphylline	daphnezomine O	humile	stems
339.1834	340.1913	C21H25NO3	Daphnicyclidin	daphnicyclidin G	humile	stems
341.1991	342.2069	C21H27NO3	Calyciphylline A	daphnipaxianine A	paxianum	leaves and fruit
341.1991	342.2069	C21H27NO3	Calyciphylline A	daphnipaxianine B	paxianum	leaves and fruit
341.1991	342.2069	C21H27NO3	Calyciphylline A	daphniyunnine C N-oxide	himalense	twigs and leaves
341.1991	342.2069	C21H27NO3	Calyciphylline A	daphniyunnine D	yunnanense	stems and leaves
341.1991	342.2069	C21H27NO3	Calyciphylline A	daphniyunnine E	yunnanense	stems and leaves
341.1991	342.2069	C21H27NO3	Calyciphylline A	himalenine E	himalense	twigs and leaves
341.2355	342.2433	C22H31NO2	Bukittinggine	bukittinggine	Sapium baccatum	
341.2355	342.2433	C22H31NO2	Calyciphylline B	daphlongamine H	longracemosum	leaves
341.2355	342.2433	C22H31NO2	Calyciphylline B	deoxycalyciphylline B	subverticillatum	stem
341.2355	342.2433	C22H31NO2	Calyciphylline B	deoxyisocalyciphylline B	subverticillatum	stem
341.2355	342.2433	C22H31NO2	Daphnilactone B	daphnilactone B	macropodum	
341.2355	342.2433	C22H31NO2	Daphnilactone B	isodaphnilactone B	humile	leaves
343.2147	344.2226	C21H29NO3	Calyciphylline A	daphniyunnine B	yunnanense	stems and leaves

343.2147	344.2226	C21H29NO3	Calyciphylline A	himalenine D	himalense	twigs and leaves
343.2147	344.2226	C21H29NO3	Paxdaphnine A	daphlongamine B	longracemosum	fruits
343.2147	344.2226	C21H29NO3	Yuzurimine	calycinumine A	calycinum	twigs
343.2511	344.259	C22H33NO2	Daphnezomine L	Daphnezomine L	humile	stems
343.2511	344.259	C22H33NO2	Daphnilactone B	caldaphnidine C	calycinum	leaves
343.2511	344.259	C22H33NO2	Seco-daphniphylline	daphnezomine N	humile	stems
345.2304	346.2382	C21H31NO3	Calyciphylline A	longeracinphyllin B	longracemosum	leaves
345.2304	346.2382	C21H31NO3	Paxdaphnine A	paxdaphnine B	paxianum	seeds
345.2668	346.2746	C22H35NO2	Calyciphylline D	calyciphylline F	calycinum	twigs
345.2668	346.2746	C22H35NO2	Daphnezomine L	paxdaphnidine B	paxianum	stems and leaves
345.2668	346.2746	C22H35NO2	Daphniphylline	homodaphniphyllate	calycinum	leaves and stems
345.2668	346.2746	C22H35NO2	Seco-daphniphylline	daphnezomine M	humile	stems
352.2277	353.2355	C23H30NO2+	Calyciphylline G	calyciphylline G	calycinum	stems
353.1627	354.1705	C21H23NO4	Daphnicyclidin	daphnipaxinin	paxianum	stems
353.1627	354.1705	C21H23NO4	Daphnicyclidin	oldhamine A	oldhami	twigs
353.1991	354.2069	C22H27NO3	Daphhimalenine A	daphhimalenine A	himalense	leaves
355.2147	356.2226	C22H29NO3	Calyciphylline A	daphlongamine G	longracemosum	leaves
355.2147	356.2226	C22H29NO3	Calyciphylline A	daphnilongeranin C	longracemosum	leaves and stems

355.2147	356.2226	C22H29NO3	Calyciphylline C	calyciphylline J	calycinum	leaves and stems
355.2147	356.2226	C22H29NO3	Daphniglaucin AB	daphangustifoline A	angustifolium	whole plant
355.2147	356.2226	C22H29NO3	Daphnilactone B	calycilactone A	calycinum	leaves
355.2511	356.259	C23H33NO2	Yuzurimine	yunnandaphnine D	yunnanense	leaves and twigs
357.194	358.2018	C21H27NO4	Daphnicyclidin	2-deoxymacropodumine A	angustifolium	stem
357.194	358.2018	C21H27NO4	Daphnicyclidin	dehydroxymacropodumine A	macropodum	stems
357.2304	358.2382	C22H31NO3	Bukittinggine	caldaphnidine N	calycinum	twigs
357.2304	358.2382	C22H31NO3	Calyciphylline B	calyciphylline B	calycinum	leaves
357.2304	358.2382	C22H31NO3	Calyciphylline B	daphnioldhanine J	oldhami	leaves
357.2304	358.2382	C22H31NO3	Calyciphylline B	oldhamiphylline A	oldhami	leaves
357.2304	358.2382	C22H31NO3	Daphniglaucin C	daphnimacropodine A	macropodum	fruits
357.2304	358.2382	C22H31NO3	Daphnilactone B	daphnezomine H	humile	leaves
357.2304	358.2382	C22H31NO3	Daphnilactone B	daphnezomine I	humile	stems
357.2304	358.2382	C22H31NO3	Paxdaphnine A	paxdaphnine A	paxianum	seeds
357.2304	358.2382	C22H31NO3	Yuzurimine	yuzurimic acid B	calycinum	seeds
357.2668	358.2746	C23H35NO2	Bukittinggine	caldaphnidine O	calycinum	twigs
357.2668	358.2746	C23H35NO2	Daphnezomine L	caldaphnidine B	calycinum	
357.2668	358.2746	C23H35NO2	Daphnezomine L	paxdaphnidine A	paxianum	stems and leaves

357.2668	358.2746	C23H35NO2	Daphnilactone A	Daphnilactone A	macropodum	
357.2668	358.2746	C23H35NO2	Daphniphylline	calyciphylline L	calycinum	leaves and stems
357.2668	358.2746	C23H35NO2	Yuzurine	daphnezomine L	subverticillatum	leaves
358.262	359.2699	C22H34N2O2	Daphnilactone B	macropodumine I_1	macropodum	leaves
359.2097	360.2175	C21H29NO4	Calyciphylline A	calyciphylline S	macropodum	stem bark
359.2097	360.2175	C21H29NO4	Calyciphylline A	daphhimalenine D	himalense	leaves
359.246	360.2539	C22H33NO3	Bukittinggine	angustimine	angustifolium	
359.246	360.2539	C22H33NO3	Daphnezomine L	calycinumine B	calycinum	twigs
359.246	360.2539	C22H33NO3	Daphnilactone B	daphnilactone B hydrate	teijsmanii	fruits
359.246	360.2539	C22H33NO3	Daphnilactone B	zwitterionic alkaloid	macropodum	leaves
359.246	360.2539	C22H33NO3	Longracemine	Longracemine	longracemosum	fruits
359.246	360.2539	C22H33NO3	Seco-daphniphylline	dapholdamine A	oldhami	leaves
359.246	360.2539	C22H33NO3	Yuzurine	yuzuric acid_1	oldhami	fruits
359.2824	360.2903	C23H37NO2	Daphnezomine L	calyciphylline K	calycinum	leaves
359.2824	360.2903	C23H37NO2	Daphniphylline	methyl homo-daphniphyllate	macropodum	fruit
359.2824	360.2903	C23H37NO2	Seco-daphniphylline	methyl homosecodaphniphyllate	macropodum	
361.2253	362.2331	C21H31NO4	Paxdaphnine A	N-hydroxypaxdaphnine B	macropodum	fresh fruit

361.2617	362.2695	C22H35NO3	Daphnezomine AB	daphnezomine A	humile	leaves
361.2617	362.2695	C22H35NO3	Daphnezomine AB	dapholdhamine B	oldhami	leaves
361.2617	362.2695	C22H35NO3	Daphniphylline	17-hydroxyhomodaphniphyllic acid	calycinum	seeds
363.2773	364.2852	C22H37NO3	Yuzurine	daphnoldine A	oldhami	fruits
365.1627	366.1705	C22H23NO4	Daphnicyclidin	daphmacrodin A	macropodum	leaves and stems
366.1705	367.1784	C22H24NO4+	Daphnicyclidin	daphnicyclidin B	humile	stems
367.1784	368.1862	C22H25NO4	Daphnicyclidin	daphmacrodin B	macropodum	leaves and stems
367.1784	368.1862	C22H25NO4	Daphnicyclidin	daphnicyclidin A	humile	stems
367.2022	368.21	C22H27N2O3+	Daphnicyclidin	daphnicyclidin I	longracemosum	leaves and stems
367.2147	368.2226	C23H29NO3	Calyciphylline A	18,19-didehydrodaphniyunnine A	himalense	twigs and leaves
367.2147	368.2226	C23H29NO3	Calyciphylline A	longistylumphylline A	longistylum	leaves
369.2304	370.2382	C23H31NO3	Calyciphylline A	daphniyunnine A	yunnanense	stems and leaves
369.2304	370.2382	C23H31NO3	Calyciphylline C	calyciphylline C	calycinum	leaves and stems
369.2304	370.2382	C23H31NO3	Daphmanidin A	calyciphylline N	calycinum	leaves
369.2304	370.2382	C23H31NO3	Yuzurimine	calycinine A	calycinum	

369.2304	370.2382	C23H31NO3	Yuzurimine	calyciphylline H	calycinum	leaves
370.2382	371.246	C23H32NO3	Daphniglaucin AB	daphniglaucin A	glaucescens	leaves
371.2097	372.2175	C22H29NO4	Calyciphylline A	demethyl calyciphylline A	longracemosum	fruits
371.2097	372.2175	C22H29NO4	Calyciphylline A	himalenine B	himalense	twigs and leaves
371.2097	372.2175	C22H29NO4	Daphlongeranine AB	daphlongeranine B	longracemosum	fruits
371.2097	372.2175	C22H29NO4	Daphniglaucin C	daphnimacropodine C	macropodum	fruits
371.2097	372.2175	C22H29NO4	Yuzurimine	daphmacromine L	macropodum	leaves and stems
371.2097	372.2175	C22H29NO4	Yuzurimine	daphnezomine T	himalense	leaves
371.246	372.2539	C23H33NO3	Yuzurimine	2-hydroxyyunnandaphnine D	calycinum	leaves and stems
371.246	372.2539	C23H33NO3	Yuzurimine	calyciphylline I	calycinum	leaves
371.246	372.2539	C23H33NO3	Yuzurimine	yunnandaphnine A	yunnanense	leaves and twigs
371.246	372.2539	C23H33NO3	Yuzurimine	yunnandaphnine B	yunnanense	leaves and twigs
371.246	372.2539	C23H33NO3	Yuzurimine	yunnandaphnine C	yunnanense	leaves and twigs
371.246	372.2539	C23H33NO3	Yuzurimine	yuzurimine B	macropodum	
371.246	372.2539	C23H33NO3	Yuzurine	dehydrodaphnigraciline	oldhami	fruits
371.246	372.2539	C23H33NO3	Yuzurine	longistylumphylline B	longistylum	stems and leaves
371.2824	372.2903	C24H37NO2	Daphnilactone A	daphtenidine B	teijsmanii	leaves
373.1889	374.1967	C21H27NO5	Daphnicyclidin	macropodumine A	macropodum	stems

373.2253	374.2331	C22H31NO4	Yuzurimine	4,21-deacetyl-23-demethyldeoxyyuzurimine	macropodum	bark
373.2617	374.2695	C23H35NO3	Bukittinggine	caldaphnidine P	calycinum	twigs
373.2617	374.2695	C23H35NO3	Calyciphylline B	caldphnidine R	calycinum	twigs
373.2617	374.2695	C23H35NO3	Calyciphylline B	longstylumphylline C	longistylum	leaves and stems
373.2617	374.2695	C23H35NO3	Daphnezomine L	caldaphnidine K	calycinum	twigs
373.2617	374.2695	C23H35NO3	Daphnilactone B	daphnimacropodine D	macropodum	fruits
375.241	376.2488	C22H33NO4	Daphnilactone B	daphnezomine S	humile	fruits
375.241	376.2488	C22H33NO4	Daphnilactone B	daphnioldhanin C	oldhami	aerial tissues
375.2773	376.2852	C23H37NO3	Daphnezomine L	caldaphnidine L	calycinum	twigs
375.2773	376.2852	C23H37NO3	Daphniphylline	caldaphnidine Q	calycinum	twigs
375.2773	376.2852	C23H37NO3	Daphniphylline	methyl 17-hydroxyhomodaphniphyllic acid	macropodum	fresh fruit
375.2773	376.2852	C23H37NO3	Daphniphylline	Methyl 7-hydroxyhomodaphniphyllate	calycinum	leaves and stems
375.2773	376.2852	C23H37NO3	Seco-daphniphylline	calyciphylline O	calycinum	leaves
376.2852	377.293	C23H38NO3+	Daphnezomine AB	daphnezomine B	humile	leaves
379.2147	380.2226	C24H29NO3	Calyciphylline A	calyciphylline Q	macropodum	stem bark

380.1862	381.194	C23H26NO4+	Daphnicyclidin	daphnicyclidin E	humile	stems
381.194	382.2018	C23H27NO4	Calyciphylline A	17-oxolongistylumphylline A	himalense	twigs and leaves
381.194	382.2018	C23H27NO4	Daphnicyclidin	daphnicyclidin D	humile	stems
383.1733	384.1811	C22H25NO5	Daphnicyclidin	daphnicyclidin C	humile	stems
383.2097	384.2175	C23H29NO4	Calyciphylline A	17-epi-daphlongamine F	himalense	twigs and leaves
383.2097	384.2175	C23H29NO4	Calyciphylline A	4B-hydroxylongistylumphylline A	himalense	twigs and leaves
383.2097	384.2175	C23H29NO4	Calyciphylline A	daphlongamine F	longracemosum	leaves
383.2097	384.2175	C23H29NO4	Calyciphylline A	daphnilongeranin A	longracemosum	leaves and stems
383.2097	384.2175	C23H29NO4	Calyciphylline A	paxiphylline D	paxianum	twigs and leaves
383.2097	384.2175	C23H29NO4	Daphnicyclidin	daphnicyclidin Mb	paxianum	stems and leaves
383.2097	384.2175	C23H29NO4	Yuzurimine	caldaphnidine A	calycinum	twigs
383.2097	384.2175	C23H29NO4	Yuzurimine	daphhimalenine B	himalense	leaves
383.2097	384.2175	C23H29NO4	Yuzurimine	daphmacromine K	macropodum	leaves and stems
383.246	384.2539	C24H33NO3	Calyciphylline A	daphnilongeranin C ethyl ester	himalense	twigs and leaves
385.2253	386.2331	C23H31NO4	Calyciphylline A	11a-hydroxydaphniyunnine A	himalense	twigs and leaves
385.2253	386.2331	C23H31NO4	Calyciphylline A	11b-hydroxydaphniyunnine A	himalense	twigs and leaves
385.2253	386.2331	C23H31NO4	Calyciphylline A	12a-hydroxydaphniyunnine A	himalense	twigs and leaves

385.2253	386.2331	C23H31NO4	Calyciphylline A	12b-hydroxydaphniyunnine A	himalense	twigs and leaves
385.2253	386.2331	C23H31NO4	Calyciphylline A	17B-hydroxydaphniyunnine A	himalense	twigs and leaves
385.2253	386.2331	C23H31NO4	Calyciphylline A	17-O-acetyldaphniyunnine B	himalense	twigs and leaves
385.2253	386.2331	C23H31NO4	Calyciphylline A	21-deoxymacropodumine D	himalense	twigs and leaves
385.2253	386.2331	C23H31NO4	Calyciphylline A	calyciphylline A	calycinum	leaves
385.2253	386.2331	C23H31NO4	Calyciphylline A	daphniglaucin D	glaucescens	leaves
385.2253	386.2331	C23H31NO4	Calyciphylline C	calydaphninone	calycillum	leaves and twigs
385.2253	386.2331	C23H31NO4	Yuzurimine	caldaphnidine G a	calycinum	twigs
385.2253	386.2331	C23H31NO4	Yuzurimine	caldaphnidine H	calycinum	twigs
385.2253	386.2331	C23H31NO4	Yuzurimine	caldaphnidine I	calycinum	twigs
385.2253	386.2331	C23H31NO4	Yuzurimine	calyciphylline E	calycinum	leaves
385.2253	386.2331	C23H31NO4	Yuzurimine	daphmacromine N	macropodum	leaves and stems
385.2253	386.2331	C23H31NO4	Yuzurimine	pordamacrine B	macropodum	leaves
385.2253	386.2331	C23H31NO4	Yuzurimine	yunnandaphnine E	yunnanense	leaves and twigs
385.2253	386.2331	C23H31NO4	Yuzurine	daphmacromine I	macropodum	leaves and stems
385.2617	386.2695	C24H35NO3	Yuzurine	dehydrodaphnigracine	longracemosum	fruits
387.241	388.2488	C23H33NO4	Paxdaphnine A	12-O-acetylpaxdaphnine B	macropodum	fresh fruit
387.241	388.2488	C23H33NO4	Paxdaphnine A	21-O-acetyl-paxdaphnine B	macropodum	fruits

387.241	388.2488	C23H33NO4	Yuzurimine	daphlongamine C	longracemosum	fruits
387.241	388.2488	C23H33NO4	Yuzurimine	daphniglaucin K	glaucescens	leaves
387.241	388.2488	C23H33NO4	Yuzurimine	deacetyl yuzurimine A	macropodum	
387.241	388.2488	C23H33NO4	Yuzurine	daphgraciline	gracile	bark
387.241	388.2488	C23H33NO4	Yuzurine	daphnilongertone	longracemosum	fruits
387.241	388.2488	C23H33NO4	Yuzurine	daphnioldhanine K	oldhami	fruits
389.2202	390.228	C22H31NO5	Calyciphylline A	himalenine A	himalense	twigs and leaves
389.2202	390.228	C22H31NO5	Daphniglaucin C	daphnimacropodine B	macropodum	fruits
389.2566	390.2644	C23H35NO4	Daphnezomine L	daphnezomine W	angustifolium	stems
389.2566	390.2644	C23H35NO4	Yuzurimine	daphnioldhanin A	oldhami	aerial tissues
389.2566	390.2644	C23H35NO4	Yuzurine	daphnigraciline	gracile	leaves
389.2566	390.2644	C23H35NO4	Yuzurine	yuzuric acid_2	oldhami	fruits
391.2723	392.2801	C23H37NO4	Yuzurine	daphnoldine B	oldhami	fruits
393.194	394.2018	C24H27NO4	Daphnicyclidin	paxiphylline A	paxianum	twigs and leaves
395.1733	396.1811	C23H25NO5	Daphnicyclidin	caldaphnidine H (2009)	calycinum	leaves and stems
395.1733	396.1811	C23H25NO5	Daphnicyclidin	daphnicyclidin J	humile	stems
395.1733	396.1811	C23H25NO5	Daphnicyclidin	daphnicyclidin M	macropodum	stem bark
395.1733	396.1811	C23H25NO5	Daphnicyclidin	paxiphylline B	paxianum	twigs and leaves

397.1889	398.1967	C23H27NO5	Daphnicyclidin	daphnicyclidin F	humile	stems
397.1889	398.1967	C23H27NO5	Daphnicyclidin	macropodumine B	macropodum	stems
399.2046	400.2124	C23H29NO5	Calyciphylline A	calyciphylline R	macropodum	stem bark
399.2046	400.2124	C23H29NO5	Calyciphylline A	paxiphylline E	paxianum	twigs and leaves
399.2046	400.2124	C23H29NO5	Daphnezomine F	daphnezomine U new	humile	leaves and branches
399.2046	400.2124	C23H29NO5	Daphnicyclidin	daphnicyclidin H	humile	stems
399.2046	400.2124	C23H29NO5	Yuzurimine	macropodumine G	macropodum	leaves
399.2046	400.2124	C23H29NO5	Yuzurimine	yuzurimine C	macropodum	
399.241	400.2488	C24H33NO4	Yuzurine	daphmacromine J	macropodum	leaves and stems
400.2488	401.2566	C24H34NO4+	Daphniglaucin AB	daphniglaucin B	glaucescens	leaves
401.1838	402.1917	C22H27NO6	Daphnicyclidin	daphnicyclidin L	macropodum	stem bark
401.2202	402.228	C23H31NO5	Calyciphylline A	daphniglaucin E	glaucescens	leaves
401.2202	402.228	C23H31NO5	Calyciphylline A	daphniglaucin G	glaucescens	leaves
401.2202	402.228	C23H31NO5	Calyciphylline A	macropodumine D	macropodum	leaves and bark
401.2202	402.228	C23H31NO5	Yuzurimine	caldaphnidine J	calycinum	twigs
401.2202	402.228	C23H31NO5	Yuzurimine	deacetyl daphnijsmine	teijsmanii	seeds
401.2202	402.228	C23H31NO5	Yuzurimine	macropodumine F	macropodum	leaves
401.2202	402.228	C23H31NO5	Yuzurimine	pordamacrine A	macropodum	leaves

401.2566	402.2644	C24H35NO4	Paxdaphnine A	daphlongamine A	longracemosum	fruits
401.2566	402.2644	C24H35NO4	Yuzurine	daphgracine	gracile	bark
401.2566	402.2644	C24H35NO4	Yuzurine	daphnilongerine	longracemosum	fruits
403.2359	404.2437	C23H33NO5	Daphnezomine F	daphlongeranine C	longracemosum	fruits
403.2359	404.2437	C23H33NO5	Daphniglaucin C	daphniglaucin C	glaucescens	leaves
403.2359	404.2437	C23H33NO5	Himalensine B	himalensine B	himalense	twigs and leaves
403.2359	404.2437	C23H33NO5	Yuzurimine	daphnezomine K	humile	fruits
403.2359	404.2437	C23H33NO5	Yuzurine	daphnioldhamine A	oldhami	fruits
403.2359	404.2437	C23H33NO5	Yuzurine	epioxodaphnigraciline	gracile	leaves
403.2359	404.2437	C23H33NO5	Yuzurine	hydroxydaphgraciline	gracile	bark
403.2359	404.2437	C23H33NO5	yuzurine	macrodumine A	macropodum	leaves and twigs
403.2359	404.2437	C23H33NO5	Yuzurine	oxodaphnigraciline	gracile	leaves
403.2723	404.2801	C24H37NO4	Yuzurine	daphnezomic acid	oldhami	fruits
403.2723	404.2801	C24H37NO4	Yuzurine	daphnezomic acid	oldhami	fruits
403.2723	404.2801	C24H37NO4	Yuzurine	yuzurine	macropodum	bark and leaves
405.2515	406.2593	C23H35NO5	Yuzurimine	daphlongamine D	longracemosum	fruits
411.1682	412.176	C23H25NO6	Daphnicyclidin	dapholdhamine C	oldhami	leaves
413.1838	414.1917	C23H27NO6	Daphnicyclidin	daphnicyclidin K	humile	stems

413.2202	414.228	C24H31NO5	Daphlongeranine AB	daphlongeranine A	longracemosum	fruits
413.2566	414.2644	C25H35NO4	Yuzurimine	acetyl yuzurimine B	macropodum	
413.2566	414.2644	C25H35NO4	Yuzurimine	daphmacromine M	macropodum	leaves and stems
415.1995	416.2073	C23H29NO6	Daphnicyclidin	macropodumine C	macropodum	stems
415.2359	416.2437	C24H33NO5	Yuzurimine	daphcalycic acid	calycinum	seeds
415.2723	416.2801	C25H37NO4	Yuzurine	daphlongeranine E	longracemosum	fruits
417.2515	418.2593	C24H35NO5	Yuzurine	daphlongamine J	longracemosum	fruits
417.2515	418.2593	C24H35NO5	Yuzurine	daphmacromine E	macropodum	leaves and stems
417.2515	418.2593	C24H35NO5	Yuzurine	daphmacromine F	macropodum	leaves and stems
417.2515	418.2593	C24H35NO5	Yuzurine	daphmacromine G	macropodum	leaves and stems
417.2515	418.2593	C24H35NO5	Yuzurine	daphmacromine H	macropodum	leaves and stems
417.2515	418.2593	C24H35NO5	yuzurine	macrodumine B	macropodum	leaves and twigs
417.2515	418.2593	C24H35NO5	yuzurine	macrodumine C	macropodum	leaves and twigs
417.2515	418.2593	C24H35NO5	Yuzurine	oxodaphnigracine	gracile	leaves
417.2879	418.2957	C25H39NO4	Yuzurine	daphnezomine R	humile	fruits
417.2879	418.2957	C25H39NO4	Yuzurine	daphnigracine	gracile	leaves
419.2308	420.2386	C23H33NO6	Yuzurine	daphmalenine A	himalense	leaves
419.2672	420.275	C24H37NO5	Yuzurine	11-hydroxydaphnigracine	longracemosum	fruits

419.2672	420.275	C24H37NO5	Yuzurine	daphlongamine I	longracemosum	fruits
425.1838	426.1917	C24H27NO6	Daphnicyclidin	daphnicyclidin N	macropodum	stem bark
425.2202	426.228	C25H31NO5	Daphhimalenine A	glaulactam C	glaucescens	leaves
425.2202	426.228	C25H31NO5	Daphmanidin A	daphmanidin E	teijsmanii	leaves
426.2519	427.2597	C25H34N2O4	Daphnicyclidin	angustifolimine	angustifolium	?
427.2359	428.2437	C25H33NO5	Calyciphylline A	subdaphnidine A	subverticillatum	leaves
427.2359	428.2437	C25H33NO5	Daphmanidin A	daphmanidin A	teijsmanii/oldhani	leaves
428.2437	429.2515	C25H34NO5+	Yuzurimine	daphnezomine J	humile	fruits
429.2515	430.2593	C25H35NO5	Yuzurimine	daphcalycine	calycinum	seeds
429.2515	430.2593	C25H35NO5	Yuzurimine	daphniglaucin J	glaucescens	leaves
429.2515	430.2593	C25H35NO5	Yuzurimine	yuzurimine A	macropodum	
429.2515	430.2593	C25H35NO5	Yuzurimine	yuzurimine E	calycinum	seeds
431.2672	432.275	C25H37NO5	Yuzurine	daphlongeranine D	longracemosum	fruits
431.2672	432.275	C25H37NO5	Yuzurine	daphmacromine A	macropodum	leaves and stems
431.2672	432.275	C25H37NO5	Yuzurine	daphmacromine B	macropodum	leaves and stems
431.2672	432.275	C25H37NO5	Yuzurine	daphmacromine D	macropodum	leaves and stems
431.2672	432.275	C25H37NO5	Yuzurine	dapmacromine C	macropodum	leaves and stems
432.3114	433.3192	C26H42NO4	Yuzurine	daphnipaxianine D	paxianum	leaves and fruit

441.2151	442.223	C25H31NO6	Daphmanidin A	daphmanidin F	teijsmanii	leaves
443.2308	444.2386	C25H33NO6	Calyciphylline A	daphniglacuin F	glaucescens	leaves
443.2308	444.2386	C25H33NO6	Calyciphylline A	daphniglaucin H	glaucescens	leaves
443.2308	444.2386	C25H33NO6	Daphhimalenine A	glaulactam B	glaucescens	leaves
443.2308	444.2386	C25H33NO6	Yuzurimine	daphnijsmine	teijsmanii	seeds
445.2464	446.2543	C25H35NO6	Daphnezomine F	daphmanidin B	teijsmanii	leaves
447.2621	448.2699	C25H37NO6	Yuzurimine	daphnioldhanin B	oldhami	aerial tissues
449.2413	450.2492	C24H35NO7	Yuzurine	daphmalenine B	himalense	leaves
451.1995	452.2073	C26H29NO6	Daphnicyclidin	dapholdhamine D	oldhami	leaves
453.2515	454.2593	C27H35NO5	Paxdaphnine A	daphlongeramin A	longracemosum	fruits
455.3399	456.3478	C29H45NO3	Calyciphylline D	calyciphylline D	calycinum	leaves
457.21	458.2179	C25H31NO7	Daphnicyclidin	paxphylline C	paxianum	twigs and leaves
457.2464	458.2543	C26H35NO6	Yuzurimine	macropodumine H	macropodum	leaves
459.2257	460.2335	C25H33NO7	Daphmanidin CD	daphmanidin C	teijsmanii	leaves
459.2257	460.2335	C25H33NO7	Daphnezomine F	daphnezomine F	humile	stems
469.3556	470.3634	C30H47NO3	Daphniphylline	codaphniphylline	macropodum	
469.3556	470.3634	C30H47NO3	Daphniphylline	daphnioldhanine H	oldhami	leaves
469.3556	470.3634	C30H47NO3	Daphniphylline	yunnandaphninine G	yunnanense	leaves and stems

469.3556	470.3634	C30H47NO3	Seco-daphniphylline	daphnioldhanin D	oldhami	roots
469.3556	470.3634	C30H47NO3	Seco-daphniphylline	secodaphniphylline	macropodum	
471.2621	472.2699	C27H37NO6	Yuzurimine	deoxyyuzurimine	humile	
471.2621	472.2699	C27H37NO6	Yuzurimine	macropodumine I_2	macropodum	leaves
471.3712	472.3791	C30H49NO3	Daphniphylline	yunnandaphninine H	yunnanense	leaves and stems
471.3712	472.3791	C30H49NO3	Seco-daphniphylline	caldaphnidine E	calycinum	leaves
471.3712	472.3791	C30H49NO3	Seco-daphniphylline	daphnioldhanin F	oldhami	roots
471.3712	472.3791	C30H49NO3	Seco-daphniphylline	daphniteijsmanine	teijsmanii	fruits
473.205	474.2128	C25H31NO8	Daphmanidin CD	daphmanidin D	teijsmanii	leaves
473.2413	474.2492	C26H35NO7	Yuzurimine	macropodumine K	macropodum	bark
475.2723	476.2801	C30H37NO4	Yuzurimine	daphangustifoline B	angustifolium	whole plant
483.3349	484.3427	C30H45NO4	Daphnilactone A	daphtenidine A	teijsmanii	leaves
483.3349	484.3427	C30H45NO4	Seco-daphniphylline	daphnezomine C	humile	stems
485.2413	486.2492	C27H35NO7	Daphhimalenine A	glaulactam A	glaucescens	leaves
485.2413	486.2492	C27H35NO7	Daphmanidin A	daphtenidine C	teijsmanii	leaves
485.2413	486.2492	C27H35NO7	Daphnezomine F	daphnezomine G	humile	stems
485.2413	486.2492	C27H35NO7	Yuzurimine	7-oxo-deoxyyuzurimine	macropodum	bark
485.2413	486.2492	C27H35NO7	Yuzurimine	daphtenidine D	teijsmanii	leaves

485.3505	486.3583	C30H47NO4	Daphniphylline	11-hydroxycodaphniphylline	subverticillatum	
485.3505	486.3583	C30H47NO4	Daphniphylline	daphnilongeranin D	longracemosum	leaves and stems
485.3505	486.3583	C30H47NO4	Daphniphylline	daphniphyllidine	macropodum	bark and leaves
485.3505	486.3583	C30H47NO4	Daphniphylline	yunnandaphninine F	yunnanense	leaves and stems
487.257	488.2648	C27H37NO7	Yuzurimine	yuzurimine	macropodum	
487.3662	488.374	C30H49NO4	Daphniphylline	calyciphylline P	calycinum	leaves and stems
489.2726	490.2805	C27H39NO7	Yuzurimine	macrodaphnine	macropodum	
496.2573	497.2652	C28H36N2O6	Yuzurimine	macropodumine J	macropodum	bark
501.2363	502.2441	C27H35NO8	Daphniglaucin C	macropodumine E	macropodum	leaves and bark
501.2363	502.2441	C27H35NO8	Yuzurimine	17-oxoyuzurimine	macropodum	leaves
501.2363	502.2441	C27H35NO8	Yuzurimine	daphmacromine O	macropodum	leaves and stems
501.3454	502.3532	C30H47NO5	Daphniphylline	daphnezomine V	humile	leaves and branches
509.3505	510.3583	C32H47NO4	Seco-daphniphylline	daphnioldhanin I	oldhami	roots
511.3662	512.374	C32H49NO4	Daphniphylline	daphmacrine	macropodum	bark
511.3662	512.374	C32H49NO4	Seco-daphniphylline	daphnioldhanin E	oldhami	roots
513.3818	514.3896	C32H51NO4	Daphniphylline	daphmacropodine	longracemosum	leaves and stems
513.3818	514.3896	C32H51NO4	Seco-daphniphylline	daphnilongeridine	longracemosum	leaves and stems

513.3818	514.3896	C32H51NO4	Seco-daphniphylline	daphnioldhanin D (Fengliao-Changweikang)	calycinum	Fengliao-Changweikang TCM
513.3818	514.3896	C32H51NO4	Seco-daphniphylline	daphnioldhanin G	calycinum	leaves and stems
527.3611	528.3689	C32H49NO5	Daphniphylline	calyciphylline M	calycinum	leaves and stems
527.3611	528.3689	C32H49NO5	Daphniphylline	daphniphylline	macropodum	
527.3611	528.3689	C32H49NO5	Seco-daphniphylline	daphnezomine D	humile	stems
527.3611	528.3689	C32H49NO5	Seco-daphniphylline	daphniteijsmine	teijsmanii	fruits
543.356	544.3638	C32H49NO6	Daphniphylline	daphnezomine E	humile	stems
543.356	544.3638	C32H49NO6	Daphniphylline	daphnipmacropine	macropodum	bark
618.4185	619.4264	C42H54N2O2	Calyciphylline A	logeracemin A	longracemosum	
681.3149	682.3227	C37H47NO11	Calyciphylline A	hybridaphniphylline A	longracemosum	stems and leaves
681.3149	682.3227	C37H47NO11	Calyciphylline A	hybridaphniphylline B	longracemosum	stems and leaves
697.3098	698.3176	C37H47NO12	Calyciphylline A	longphyllineside A	longracemosum	leaves
697.3098	698.3176	C37H47NO12	Calyciphylline A	longphyllineside B	longracemosum	leaves
727.3204	728.3282	C38H49NO13	Daphniglaucin AB	daphcalycinosidine C	calycinum	
727.3568	728.3646	C39H53NO12	Yuzurine	daphmacropodosidine B	macropodum	fruits
745.3673	746.3752	C39H55NO13	Yuzurine	caldaphnidine F	calycinum	leaves
745.3673	746.3752	C39H55NO13	Yuzurine	daphenzomine Q	humile	fruits

745.3673	746.3752	C39H55NO13	Yuzurine	daphnezomine Q	humile	fruits
759.383	760.3908	C40H57NO13	Yuzurine	daphcalycinosidine B	calycinum	seeds
759.383	760.3908	C40H57NO13	Yuzurine	daphmacropodosidine A	macropodum	fruits
759.383	760.3908	C40H57NO13	Yuzurine	daphnezomine P	humile	fruits
771.3466	772.3544	C40H53NO14	Yuzurimine	daphcalycinosidine	calycinum	seeds